Vascular Calcification in Rat Cultured Smooth Muscle Cells: a Role for Nitric Oxide

Nimer Fehaid N Alsabeelah

February 2016

Submitted to the University of Hertfordshire in partial fulfilment of the requirements of the degree of Doctor of Philosophy

Abstract

The underlying inflammatory storm in renal or diabetic disease may induce expression of inducible nitric oxide synthase (iNOS). Similarly, expression of iNOS or nitric oxide (NO) production in vascular smooth muscle cells (VSMCs) in a calcifying environment, may promote vascular calcification (VC) (Zaragoza *et al.*, 2006). However, emerging data suggests that NO generated by either endothelial nitric oxide synthase (eNOS) or iNOS may protect VSMCs from VC (Kanno *et al.*, 2008). Thus, the role of NO and its associated enzymes in the development of VC is unclear. The aim of this study was to identify whether NO produced by iNOS regulates calcification in VSMCs, and to further understanding of potential mechanisms that may mediate the actions of NO/iNOS.

A significant and sustained production of NO by iNOS, which peaked at day 3 and declined thereafter was found in rat aortic smooth muscle cells (RASMCs) that were preactivated with lipopolysaccharide (LPS; 100µg ml^{-1}) and interferon gamma (IFN-γ;100U ml^{-1}) in the presence of calcification buffer (CB) containing calcium chloride (CaCl$_2$; 7mM) and *β*-glycerophosphate (*β*-GP; 7mM). This was associated with formation of hydroxyapatite crystals (HA) or calcification plaques, observed via alizarin red staining (ARS) and/or fourier transform infrared (FT-IR) analysis. However, when RASMCs were incubated with the iNOS inhibitor GW274150 at 10 µM, together with LPS + IFN-γ + CB, HA crystal formation was abolished. When RASMCs were pretreated with diethylenetriamine/nitric oxide adduct (NOC 18) at either 30 or 50 µM for an hour prior to addition of CB, to generate NO; calcium levels were elevated leading to form HA crystals. However, the elevation of calcium caused by the presence of NO generated via iNOS, did not result in phosphorylation of mitogen activated protein kinases (p38 MAPK), extracellular signal-regulated kinases (Erks), and protein kinase B. Furthermore, there was a reduction of Runx2 levels (pro-calcific factor) which could be another pro-calcific factor involved in this mechanism.
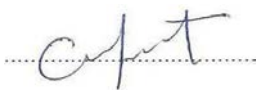
These findings suggest that NO may indeed play a fundamental role in calcification, enhancing mineralisation of smooth muscle cells. Furthermore, the expression of iNOS/ NO appears to be enhanced under conditions that favour calcification and these together may contribute to enhanced calcification with potential detrimental consequences in *vivo*.

Keywords: Vascular calcification, Nitric oxide, Inducible nitric oxide, Vascular smooth muscle cells, Runt-related transcription factor 2

Declaration

I, Nimer Alsabeelah, hereby declare that this Ph. D. thesis entitled "Vascular Calcification of Rat Aortic Smooth Muscle Cells: Role of Nitric Oxide" was prepared me for the degree of doctor of philosophy. The work presented within it is my own, and was produced by me from my original research. I declare that all the information provided in this document adheres to the academic rules and ethical conduct of the University of Hertfordshire. The contribution of my supervisors and others to the research, and to this thesis, are in keeping with normal supervisory practice.

I certify that this work has not been previously submitted to any university or institution for the award of any other degree, or for a diploma in my name. This work contains no previously published material, or any work written by another person to the best of my knowledge and belief, other than where referenced in the text. Further, I certify that no part of this work will in the future be used in a submission in my name for any other degree or diploma, to any university or institution, without the approval of the University of Hertfordshire.

Signature

Date: …………February 2016……….

Acknowledgement

I wish to express gratitude first to my principal supervisor, Prof Anwar Baydoun, for supporting, motivating, and encouraging me in my research. I am also immensely grateful for his patience with continually offering valuable advice and guidance, as well as greatly appreciate his spending so many hours generating constructive, applicable ideas toward making my thesis as incisive and intriguing as possible. I will never forget the invaluable knowledge and knowhow that I gained from him, which I will certainly apply in my future work and research.

I also wish to express thanks to my second supervisor, Dr Shori Thakur, for her constant efforts toward developing and deepening the knowledge and skills that proved essential to my PhD work. I have highly appreciated her advice and suggestions, even from the very beginning of my PhD study. I have learned so much from her, especially when she tracked and questioned participants about their projects to make their coursework toward earning their degrees thorough and meaningful.

I additionally wish to express my appreciation of my colleagues for all of their assistance. I have truly cherished working with these friends, who came to form a second family as I worked toward completing my project: Hema Pramod, Nasima Chowdary, Ashish Patidar, Praveen Bingi, Pablo Zardoya, Mahdi Alsugoor, Gagan Maan, and Adem Nasraddin, as well as all of the other laboratory technicians.

"An expert is one who knows more and more about less and less until he knows absolutely everything about nothing"

-William Shakespeare

1582-1616

"Hold a picture of yourself long and steadily enough in your mind's eye, and you will be drawn toward it"

-Napoleon Hill

1883-1970

TABLE of CONTENTS

Table of Contents

LIST of FIGURES

List of Figures:

Chapter III- Results:

Regulation of vascular calcification and induced nitric oxide synthesis by calcification buffer and/or inflammatory mediators:

Chapter IV- Results:

Effects of LPS and/or IFN-γ on iNOS expression. NO synthesis and vascular calcification in the absence and presence of calcification indcuers.

Chapter V- Results:

Effects of nitric donors and of the selective iNOS inhibitor, GW274150, on calcification of smooth muscle cells

Chapter VI-Results:

Signal transduction mechanisms that regulate iNOS expression, NO production and calcification in cultured RASMCs

LIST of TABLES

List of Tables:

Chapter V- Results:

Effects of nitric donors and of the selective iNOS inhibitor, GW274150, on calcification of smooth muscle cells

Chapter VII- Results:

General discussion, Conclusion, and Limitations & future work

ABBREVIATIONS

ADMA	Asymmetric Dimethylarginine
AKT	A Serine/Threonine Kinase And Named As Protein Kinase B
ALP	Alkaline Phosphatase
ANOVA	Analysis of Variance
AP-1	Activating Protein-1
ATP	Adenosine Triphosphate
BCA	Bicinchoninic Acid
β-GP	β- Glycerophosphate
β-actin	Beta Actin
BH4	Tetrahydrobiopterin
BMP 2	Bone Morphogenetic Proteins 2
BMP4	Bone Morphogenetic Proteins 4
BSP	Bone Sialo Protein
BSA	Bovine Serum Albumin
CaCl$_2$	Calcium Chloride
CB	Calcification Buffer
Cbfa-1	Core Binding Factor Alpha -1
CKD	Chronic Kidney Disease
CCr or CrCl	Creatinine Clearance Rate
Cu^{+1}	Cuprous
Cu^{+2}	Copper
CVC	Calcifying Vascular Cells
D1, D3, D5, and D7	Day1, Day3, Day5 And Day 7
DDW	Double Distil Water
DMEM	Dulbecco's Modified Eagle Medium
ECM	Extra Cellular Matrix
EDRF	Endothelium Drive Relaxation Factor
eNOS	Endothelial Nitric Oxide Synthase
ERK	Extracellular Signal-Regulated Kinase
ESRD	End Stage Renal Disease
FAD	Flavin Adenine Dinucleotide
FBS	Foetal Bovine Serum
FGF-23	Fibroblast Growth Factor 23

H_2O_2	Hydrogen Peroxide
IL6 or 1	Interleukin 6 or 1
IFN-γ	Interferon Gamma
IFNR1	Interferon Receptor 1
IFNR2	Interferon Receptor 2
iNOS	Inducible Nitric Oxide Synthase
IRF 1	Interferon Response Factor-1
GFR	Glomerular Filtration Rate
GW	GW274150
LBP	LPS Binding Protein
LDL	Low Density Lipoprotein
LPS	Lipopolysaccharide
MAPKs	Mitogen Activated Protein Kinases
MGP	Matrix Gla Protein
mM	Mill Molar
μM	Micro Molar
mRNA	Messenger Ribonucleic Acid
Msx2	Msh homeobox 2
MTT	3-(4, 5-dimethylthiazol-2-yl)-2, 5-diphenyltetrazolium bromide
MyD88	Myeloid Differentiation Primary Response Gene-88
NAD	Nicotinamide-Adenine-Dinucleotide
NADPH	Nicotinamide Adenine Dinucleotide Phosphate
$NaNO_2$	Sodium Nitrite
NF-kB	Nuclear Factor kappa B
nNOS	Neuronal Nitric Oxide Synthase
NO_2^-	Nitrite
NO_3^-	Nitrate
NO	Nitric Oxide
NO donor	Nitric Oxide Donor
O_2	Molecular Oxygen
O_2^-	Superoxide Anion
OC	Osteocalcin
OPG	Osteoprotegerin

OPN	Osteopontin
OS	Oxidative Stress
oxLDL	Oxidized LDL
PBS	Phosphate Buffered Saline
PCR	Polymerase Chain Reaction
PI3K	Phosphatidyl Inositide 3 Kinases
PTH	Parathyroid Hormone
PPi	Pyrophosphate
RANKL	Receptor Activator of Nuclear Factor Kappa-B Ligand
RASMCs	Rat Aorta Smooth Muscle Cells
PKC	Protein Kinase C
PVDF	Polyvinylidene Fluoride
RNS	Reactive Nitrogen Species
ROS	Reactive Oxidative Species
Runx2	Runt-Related Transcription Factor 2
S.E.M	Standard Error Mean
SDS-PAGE	PAGE Sodium Dodecyl Sulphate Polyacrylamide Gel
SDS	Sodium Dodecyl Sulphate
Tak 1	Transforming Growth Factor-B-Activated Kinase 1
TCA cycle	Tricarboxylic Acid Cycle
TGF-β	Tumor Necrosis Factor- B
TLR 2/4	Toll Like Receptor 2/4
TNFα	Tumor Necrosis Factor- alpha
VSMCs or ECs	Vascular Smooth Muscle Cells Or Endothelial Cells
VC	Vascular Calcification
1,25(OH)2D$_3$	1,25-Dihydroxyvitamin D$_3$
1 α OH	1α Hydroxylvitamin

CHAPTER I

INTRODUCTION

1.Introduction:

Vascular calcification is a common complication of several pathologies including coronary artery disease, renal disease and bone disorders such as osteoporosis and/or adynamic bone disease. Its co-existence accounts for increased mortality in 3 out of 4 individuals (Aslam *et al.*, 2010; Collins *et al.*, 2005). Indeed, the risk of death is 10-50 fold higher in renal subjects with VC even after adjustment for age, gender, ethnicity and other underlying pathologies (Collins *et al*, 2005). An understanding of the regulation of this process, especially by other co-existing factors, is therefore of importance if progress is to be made in controlling its initiation and progression.

1.1-Vascular calcification:

Vascular calcification is an active well-controlled process involving the orchestrated trans-differentiation of smooth muscle cells into bone-like cells (Byon *et al.*, 2008). It is associated with the pathological deposition of calcium and phosphate products in the arterial wall resulting in calcification of the affected vessel. Calcification is however not restricted to the vasculature, and can indeed occur in other extra-skeletal soft tissues such as connective, cartilage, tendons and epithelial tissues. There are therefore different classifications of calcification depending on its anatomical location and pattern which will be discussed later in section 1.3.

Physiologically, serum levels of calcium and phosphate are tightly regulated by the digestive (gastrointestinal tract), endocrine (parathyroid gland), skeletal (bone) and urinary (kidney) systems. Absorption of calcium and phosphate occurs in the small intestine and is sequestered either into bones, cartilages, teeth, or other parts of the body. The skeletal system acts as a major reservoir of calcium and phosphate, utilising and generating free calcium and

phosphate through the process of active bone turnover via osteoblastic (bone formation) and osteoclastic (bone resorption) activities respectively.

The kidneys also play a major role in the regulation of serum calcium and phosphate via active reabsorption or secretion (Brini *et al.*, 2013; Nordin, 1997). Additionally, serum levels of calcium and phosphate are also tightly regulated through hormonal regulation by parathyroid hormone (PTH) and cholecalciferol (active vitamin D) produced by chief cells in the parathyroid gland and proximal convoluted tubules of the kidneys (Jono *et al.*, 1997; Irving, 2012).

Dys-regulation of calcium and phosphate leads to an increase in the deposition of these ions on the extracellular matrix, forming HA crystals with further consequences including cells undergoing a phenotypic alteration by losing smooth muscle markers such as the smooth muscle lineage protein SM22α and expressing osteogenic or chondrogenic markers (Moe and Chen, 2008). More importantly, it has been shown that phosphate ions act as a trigger to initiate these changes in the gene transcription level and result in the mineralisation of VSMCs (Steitz *et al.*, 2001). Similarly, elevated calcium levels alone can also induce the mineralisation process through changing the phenotype of VSMCs (Byon *et al.*, 2008). It does this by regulating levels of phosphate, increasing its binding by changing the sensitivity of VSMCs to phosphate (Proudfoot *et al.*, 1998).

In the investigations the concentrations of the calcium in the calcifying agents and the concentration of phosphate for our model was kept quit smiliar to that used as previous studies (Byon *et al.*,2008; Kanno et al., 2008) as well as from our group (Patidar *et al.*,2013), in order to allow a comparison of effects. Furthermore, exploration of concentrations of calcium or phosphate in plasma and tissue would be vary. For example, the normal range of human plasma and tissue fluid calcium concentration is 2.2 - 2.6mM (Ihmoda, 2005), while

in rats the level is 2.5mM (Lewin *et al*., 2002). Thus, 3mM concentration of extracellular calcium is considered to be hypercalcemic, whereas the concentration used in these studies was more than 2x higher, at 7mM. Furthermore, the levels of *β*-GP could also be varied, as this too had the fixed concentration of 7mM. Therefore, the methods used could be modified to explore a wider variety of concentrations of calcium, phosphate, etc.

It is interesting to note that in VSMCs free calcium concentrations vary, and intracellular signalling is partly achieved by waves of elevated calcium (Hill-Eubank *et al.,* 2011). Altering extracellular calcium levels could disrupt the intracellular signalling as calcium enters the cell, for example through voltage gated channels. This is itself may contribute to cytotoxicity, and thus promote vascular calcification.

1.2-Calcium and Phosphate induced calcification:

Calcium is a prominent cation with major cellular actions that includes regulating cardiac contraction, controlling nerve impulse transmission, cell permeability, and even memory. However, calcium may also exert deleterious effects including cell death if uncontrolled and sustained higher intracellular concentrations are present (Berridge, 1998). More importantly, elevated calcium in the presence of phosphate results in apatite nucleation, and calcium can also increase phosphate levels by changing the sensitivity of VSMCs to phosphate (Proudfoot *et al.*, 2001; Proudfoot *et al.*, 1998). Additionally, calcium itself may also lead to extracellular matrix degradation, induction of apoptosis and osteogenic differentiation which all lead to calcification as summarised in Figure 1.1. Furthermore, *in vitro* cellular studies have suggested that calcium induces more calcification when compared to phosphate due to its direct and more potent adverse effect on the cytoskeleton (Steitz *et al.*, 2001). This does not however mean that phosphate is not important in calcification. In fact phosphate is a more

potent inducer of the cellular signalling events such as expression of osteo/chondrogenic transcription factors that may regulate calcification (Jono *et al.*, 2000). In addition, in clinical settings such as chronic kidney disease (CKD), phosphate levels are chronically elevated (sometime two fold higher than physiological phosphate levels), while serum calcium levels are only moderately increased (10-20%) (Adeney *et al.*, 2009). The proposed mechanisms through which phosphate induce calcification are summarised in Figure 1.2 and reflect parallel similarities with those reported for calcium; see Figure 1.3 for overview of pathways initiated by elevated calcium and phosphate in VSMCs. Further detailed description of these mechanisms is given in sections 1.4.2.
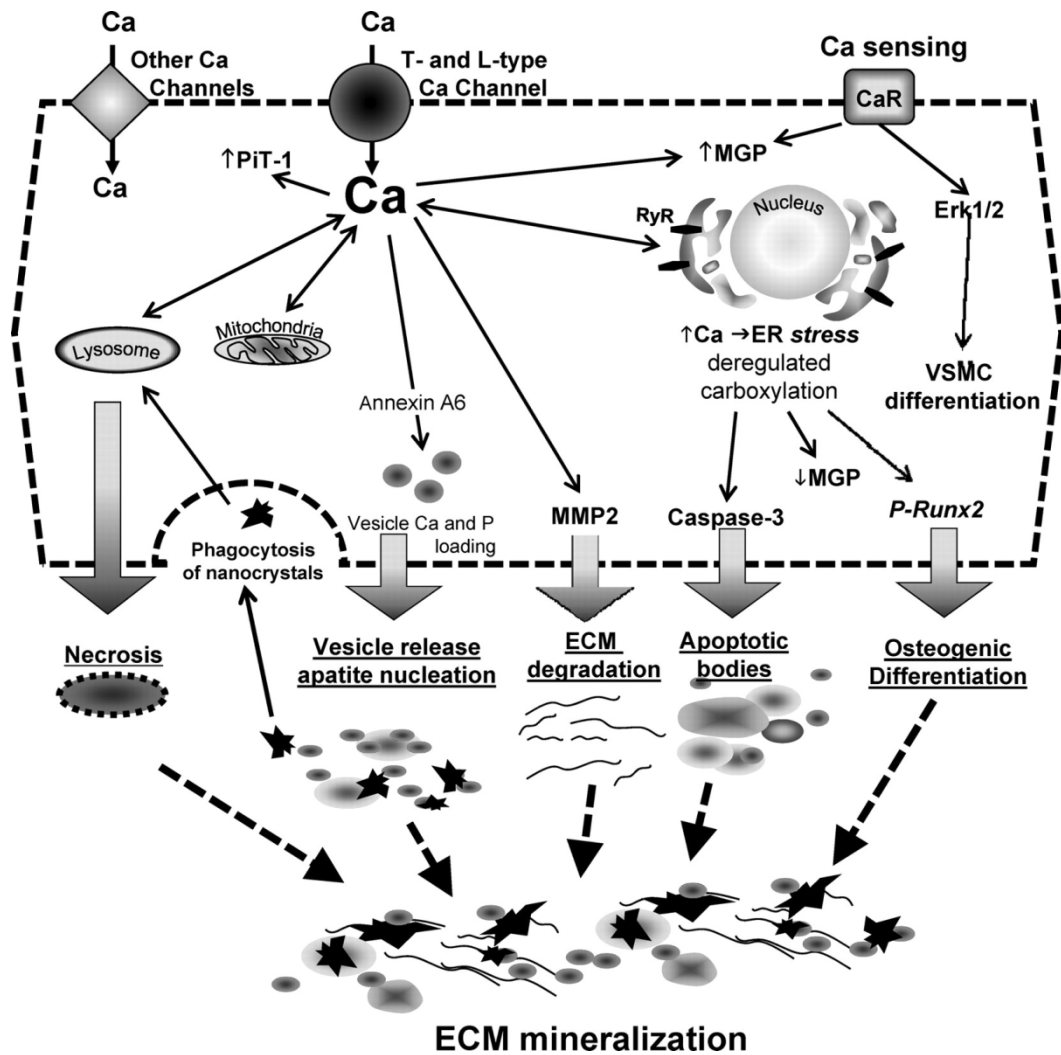
Figure 1.1: Role of calcium in VSMCs calcification. (Taken from: Shanahan *et al*., 2011).

Calcium elevation induces vesicle production and can lead to cell apoptosis and necrosis. High local levels of calcium trigger mineral nucleation in matrix vesicles and also triggers formation of apoptotic bodies. Accumulation of mineralised matrix vesicles and apoptotic bodies, and their uptake accelerate cell death and facilitate further crystal growth. Degradation of extracellular matrix (ECM) and nucleation of calcium apatite induces ECM protein mineralization. Runt-related transcription factor2 (Runx2), calcium sensing receptor (Ca R sensing), matrix gla protein (MGP), endoplasmic reticulum stress (ER stress), Erk1/2,
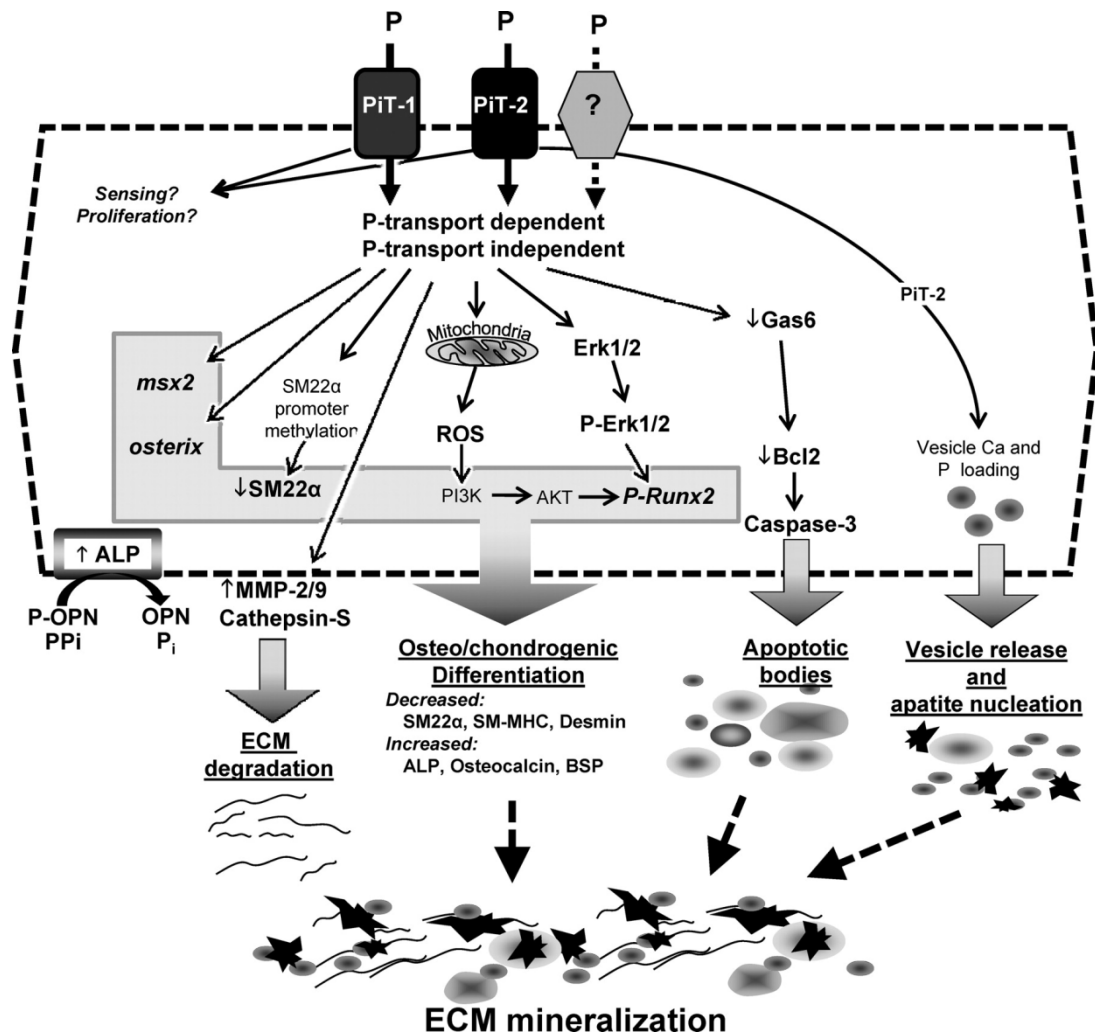
Figure 1.2: Role of phosphate in VSMCs calcification. **(Taken from: Shanahan *et al*., 2011)**

Elevated extracellular phosphate affects multiple signalling pathways that increase the susceptibility of VSMC to calcification, including decreased calcification inhibitors, increased ECM degradation, osteogenic/chondrogenic differentiation, apoptosis, and vesicle release. Some of the effects of phosphate are mediated through sodium-dependent phosphate co-transporters, Pit-1 and Pit-2, potentially via phosphate transport-dependent and phosphate transport-independent activities. Whether other receptors exist that mediate specific downstream signalling pathways in response to phosphate is not yet known but cannot be excluded. Msh homeobox 2 (Msx2), alkaline phosphatase (ALP), reactive oxygen species (ROS), matrix metallopeptidase 2/ 9 (MMP-2/9), phosphoinositide 3-kinase (PI3K). B-cell lymphoma 2 (Bcl2), Growth arrest specific 6 (Gas 6), bone sialoprotein (BSP)

↑ Phosphate **↑Calcium**

↑ MMP-9
↑ Cathepsin-S
↑ Msx2
↑ Osterix
↑ ALP
↑ ROS
↓ SM22α

↑ Erk1/2
↑ P-Runx2
↑ Vesicle loading
↑ Caspase-3
↑ MMP-2

↑ ER stress
↑ PiT-1
↓ MGP
↓ ALP
↑ Lysosomal loading
CaR sensing
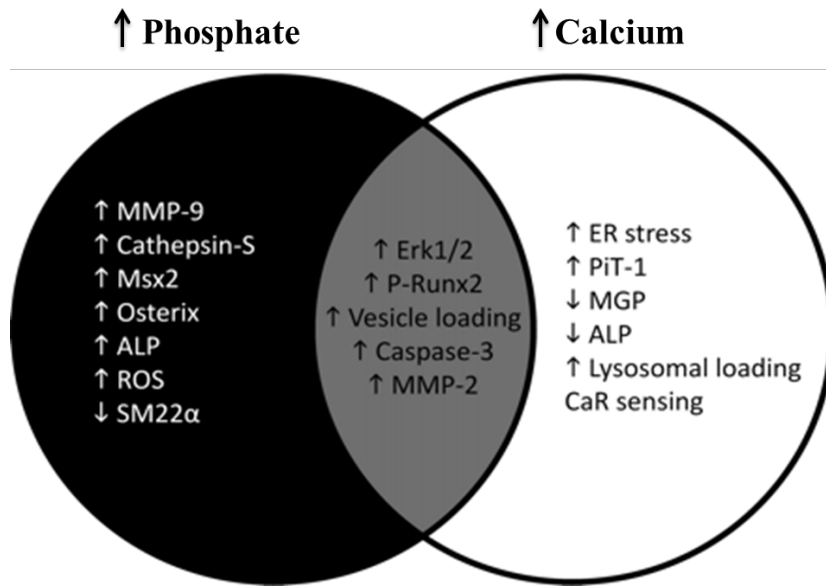
Figure 1.3: Overview of distinct and overlapping pathways initiated by elevated calcium and phosphate in VSMCs. (Taken From: Shanahan *et al*., 2011).

1.3- Type of vascular calcification and associated co-pathologies:

Vascular calcification is classified further depending on the site of calcification.

Clinically, calcification of the blood vessels as well as cardiac tissues is classified into four different categories:

➢ Atherosclerotic or intimal calcification is initiated by the development of the atheromatous plaque (Sage *et al.*, 2010) and as explained in section 1.3.1 with an example given in Figure 1.4 A.

➢ Medial artery calcification (Figure 1.4B), also known as Mönckeberg's sclerosis, is linked to the stiffening of the vascular wall as a consequence of either diabetes or CKD and this sometimes involves both pathologies (Amann, 2008;Leopold, 2014). The smooth muscle cells are located in the medial artery layer along with elastic tissue, whereas endothelium is located in the intimal layer. Therefore, the current study uses an experimental medial model for calcification, as the calcification of VSMCs rather than endothelial cells is the focus of the investigation.

➢ Cardiac valve calcification (Figure 1.4C) occurs when calcium deposits in the valves of the heart (Wirrig *et al.*, 2014).

➢ Calciphylaxis or calcific uraemic arteriolopathy is associated with extraskeletal calcification and extensive medial calcification (Brandenburg *et al.*, 2014). It is characterised by extensive necrosis of skin with highest mortality in subjects with end stage of renal disease (ESRD) (Blacher *et al.*, 2001; Floege and Ketteler, 2004) and causes non-healing wounds (Figure 1.4D).
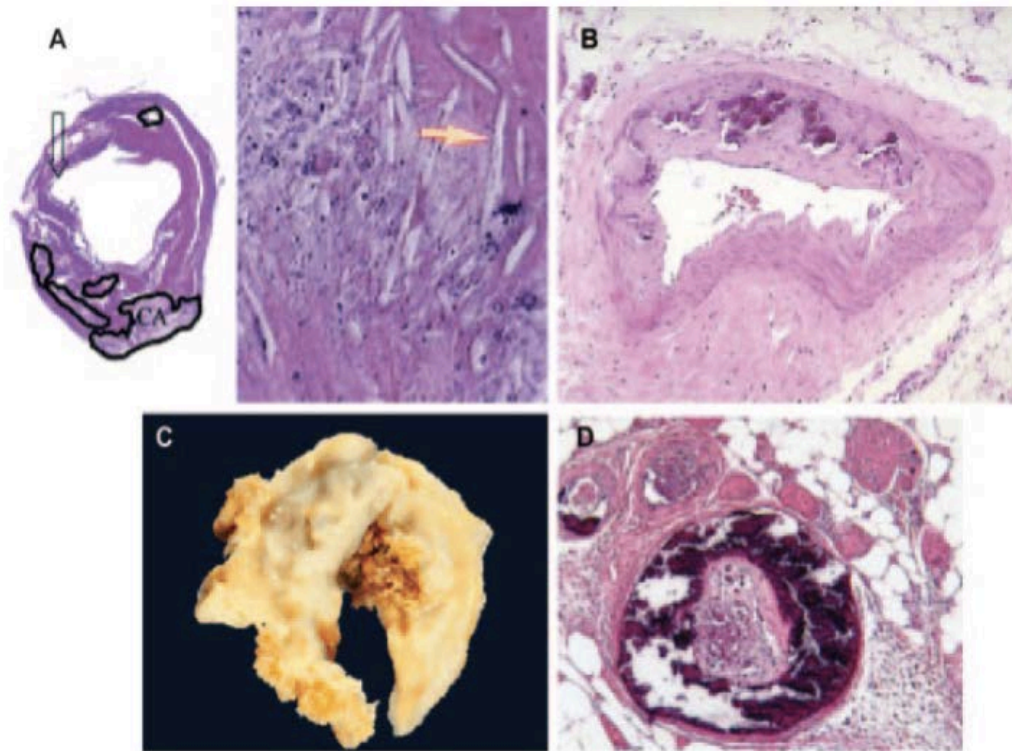
Figure 1.4: Types of calcification within the cardiovascular system (Johnson *et al*, 2006).

A: atherosclerotic (Intimal) calcification. Diagram on the left hand side of Figure A, shows a the atherosclerotic plaque and the figure on the right hand side of Figure B shows a magnified image of a ruptured atherosclerotic plaque (hematoxylin and eosin stain, H&E stain). Cholesterol crystals are indicated by the arrow. Calcification or areas of concentration of calcium is represented by the blue spherules. **B**: medial calcification: abundant calcification as indicated by the dark purple staining. **C**: valvular calcification in excised stenotic bicuspid aortic valve. **D**: calciphylaxis: extensive medial calcification is noted in this subcutaneous vessel isolated from the thigh of a patient with calciphylaxis.

Vascular calcification is an aging process; however it progress rapidly in pathologies such as diabetes, atherosclerosis and CKD. Disease specific factors will be discussed in the following sections:

1.3.1 Atherosclerotic calcification (Intimal calcification):

Atherosclerosis is a chronic inflammatory, fibro proliferative disease of large and medium sized arteries, fuelled by the build-up of low density lipoproteins. The process summarised in Figure 1.5 involves modification of low density lipoprotein (LDL), infiltration of monocytes that transform to macrophages and form lipid laden macrophages or foam cells (Aviram,1995; Simon *et al.*, 1993). Simultaneously, VSMCs migrate to and proliferate in the intima. This ultimately leads to the formation of fibrous plaque which is composed of necrotised VSMCs (Wever *et al.*, 1998), macrophage, foam cells and calcium-phosphate crystals. The stability of the plaque is of prime importance in determining the severity of atherosclerosis (Zhu *et al.*, 2001) and this may in turn be determined by the development of calcification in the plaque. Furthermore, atherosclerotic calcification may be linked to necrosis of VSMCs caused by reactive nitrogen species (RNS) or modified oxidised LDL. In addition, the development of atherosclerosis is critically associated with oxidative stress which may play a critical role not only for atheroma development but also to the subsequent calcification (Katakami *et al.*, 2009). Furthermore, macrophages in the atherosclerotic milieu can secrete inflammatory cytokines which accelerates plaque formation and promote calcification (Riemer, 2003).

A characteristic feature of atherosclerotic calcification is the aggregation of calcium crystals, which can further coalesce with lipid laden matrix to produce crystals of a larger size (Schiffrin *et al.*, 2007). This eventually reduces vascular compliance and can contribute in the dislodgement of the plaque and precipitation of subsequent adverse cardiac events. The co-localisation of the atheroma and calcified plaques occurs mostly due to increased deposition

11

of calcium and phosphate on the apoptotic bodies and necrotised cells in the vascular wall. The process of intimal calcification renders the vessel with characteristics similar to bone (Shanahan *et al.*, 1998) by expressing factors such as Runx2, Msx2 and also the dedifferentiation of VSMCs into secretory a phenotype by releasing bone morphogenetic protein 2/4 (BMP2/4). Once cells around the atheroma are dedifferentiated into bone like cells; active recruitment of more calcium and phosphate from the circulation occurs and is deposited within or around the atheroma.

Clinical studies have indicated that intimal calcification increases in the elderly, especially in subjects with diabetes (Creager *et al.*, 2003) and dyslipidaemia (Goodman, 2001). In addition, in CKD at least 50% of subjects show a presence of VC at the initiation of haemodialysis that progress rapidly with dialysis vintage and is responsible for the cardiovascular related mortality in these patients (Eddington *et al.*, 2009). However, there are conflicting reports as to whether calcification provides plaque stabilisation or causes plaque to rupture in these settings (van der Wal *et al.*, 1999; Wong *et al.*, 2012).

1.3.2- Medial vascular calcification (Monckeberg's Sclerosis):

Medial calcification was identified by Johann Georg Mönckeberg in 1903 as deposition of calcium and phosphate minerals along the elastic lamellae, suggesting that elastin may be the primary site for initiating medial calcification (Luo *et al*., 1997).

Clinically, medial calcification is considered a less serious pathology when compared to intimal calcification as it does not pose a direct threat to blocking the smaller arterioles but it is still clinically relevant because in the long term it can lead to left ventricular hypertrophy (LVH) and cardiovascular related events (Nitta *et al.*, 2004). Medial calcification is most common in subject with diabetes (Chen *et al.*, 2003).

Recent evidence suggests that VSMCs in diabetic patients express elevated levels of bone matrix proteins such as osteocalcin (OC) (Al-Aly *et al.*, 2007) and peroxynitrite (ONOO $^-$) (Deedwania *et al.*, 2008) which may contribute to VC.

In addition, *in vitro* cultured VSMCs expressed less MGP, a local inhibitor of VC, upon incubation in high glucose medium (Proudfoot *et al.*, 1998). Furthermore, persistent hyperglycaemia leads to endothelial dysfunction and glucose induced oxidative stress, impairing coupling of endothelial nitric oxide synthase (eNOS) and therefore vascular tone. Chronic hyperglycaemia also produces free radicals via the activation of protein kinase C (PKC), a strong regulator of superoxide anion (O_2^-) generation by mitochondria which reduces the bioavailability of NO not only by converting it to ONOO $^-$ but also by inhibiting its de novo production (Félétou, 2011). Furthermore, peroxynitrite could upregulate the osteogenic protein, such as Runx2, which is responsible for the differentiation of cells into osteoblast-like-cells resulting in extracellular matrix degradation. There is also evidence demonstrating that incubation of murine osteoblasts and rat-derived primary osteoblast precursors with ONOO $^-$ resulted in the activation of the apoptosis pathway and this could lead to apoptotic bodies and matrix vesicles. This action could enlarge the nucleation site of extracellular matrix allowing more calcium and phosphate products to accumulate at the site of crystal formation (Kelpke *et al.*, 2001).

Brownlee hypothesis suggests that hyperglycemia initiates microvascular disease due to the excess generation of superoxide ions via the mitochondrial electron-transport chain (Brownlee, 2001). Increased glucose provides greater pyruvate concentrations, resulting in a higher turnover of the tricarboxylic acid cycle (TCA) cycle, and consequential flow of nicotinamide adenine dinucleotide phosphate (NADH) and flavin adenine dinucleotide (FADH$_2$) into the electron transport chain. The increase causes a "critical threshold" potential to be reached which results in complex III of the electron transport chain being prevented

from allowing the passage of electrons further along the chain. The resulting excess electrons flow backward towards coenzyme Q, where superoxide ions form due to the reaction of the electrons with molecular oxygen.

Damage caused by hyperglycemia can be eliminated by reducing the amount of superoxide ions present, as this reduces the rates of several biochemical pathways including activation of protein kinase C isoforms; glycation of cell proteins, the polyol pathway (Giacco and Brownlee, 2010), the aldose reductase pathway (Nishikawa *et al*. 2000), and the hexosamine pathway (Du *et al*. 2000).

Additionally, incubation of smooth muscle cells with uraemic serum upregulated Runx2/core binding factor alpha 1 (Cbfa1), an osteoblastic transcription factor. This indicates that high glucose and uraemic serum factors may transform VSMCs into osteoblast-like cells (Chen *et al.*, 2003). As with CKD (Hayashino *et al.*, 2012), calcification caused in diabetics may be related to the inflammatory response in the disease state. The disease vintage and factors such as gender, age and ethnicity may however also contribute to the elevated mineralisation process seen in diabetic patients (Singh *et al.*, 2012).
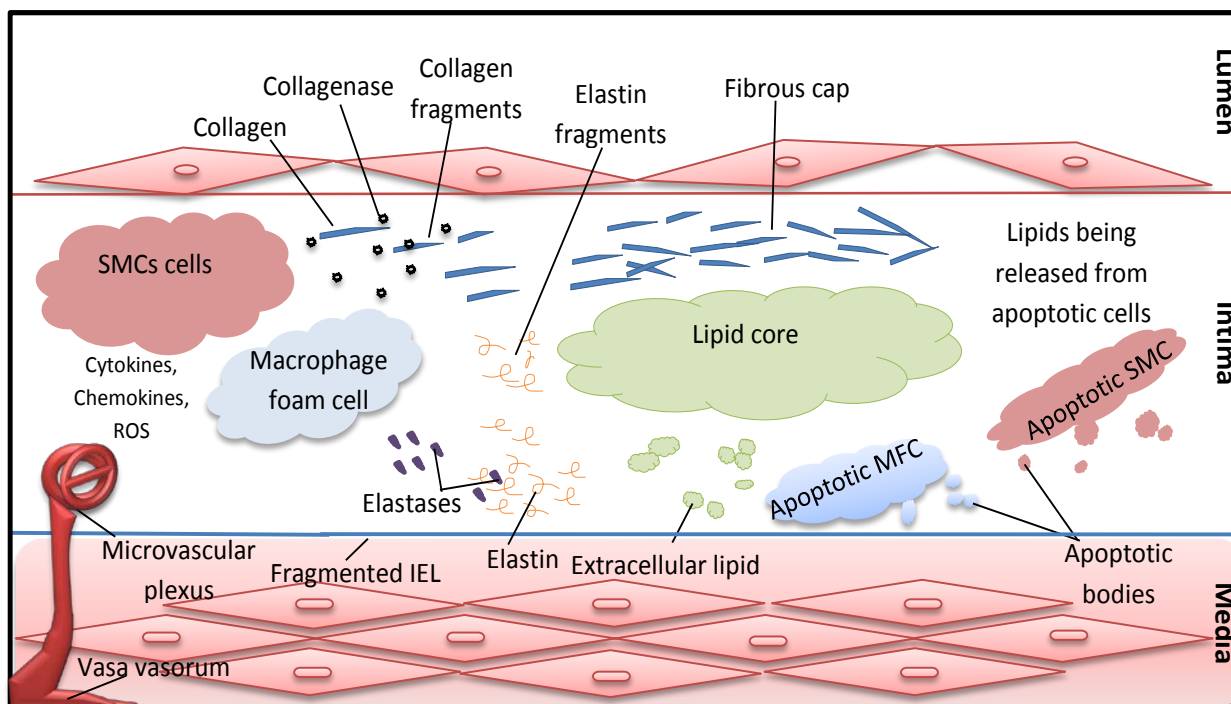
Figure 1.5: The process of atherosclerosis plaque formation (Adapted from Libby *et al.*, 2006).

Maturation of the atherosclerotic plaque, the fibrous cap, macrophages, dead macrophages, cellular debris including apoptotic bodies, and extracellular lipid accumulations, and proinflammatory mediators develop plaques leading to extracellular matrix degradation which causes vascular calcification.

1.3.3 Cardiac valve calcification:

Compared to intimal and medial calcification, cardiac valve calcification is an unstructured and disordered process (Gross *et al.*, 2007). An amalgamation of mechanical stress in the valve and local/systemic inflammation is the primary cause of valvular calcification. In response to an injury or inflammation, there is infiltration of macrophages and T cells to the valves. This is followed by the expression of BMP2 and BMP4 by the myofibroblasts (Mohler III *et al.*, 2001). Moreover, OC and Cbfa1 are also expressed by valvular cells confirming osteoblastic differentiation (Rajamannan *et al.*, 2003). Oxidised cholesterol may also be present within the nodules of calcification, calcified gallstones and atherosclerotic vessels, strongly suggesting oxidative stress and lipid oxidation (Sarig *et al.*, 1994).

1.3.4 Vascular calciphylaxis:

Calciphylaxis, otherwise known as calcific uraemic arteriolopathy (CUA) of vessels, is another systematic process characterised by extensive calcification of subcutaneous arterioles and arteries of small to medium size. It is also associated with intimal hyperplasia and tissue necrosis (Angelis *et al.*, 1997). Elevated serum calcium and phosphate resulting from chronic renal failure and hyperparathyroidism is considered to be the primary cause of widespread calcification of the subcutaneous soft tissue (Saifan, 2013 a). Additionally thrombosis, calcification of adipocytes, dedifferentiation of VSMCs, production of bone matrix proteins like osteopontin (OPN) and infiltration of inflammatory cells have also been shown to cause vascular calciphylaxis (Ahmed *et al*., 2001). However, calciphylaxis is relatively rare in renal population, and it is not very well understood why some patient develops this deadly skin necrotising form of calcification. Recent research suggests its association with warfarin therapy and a link to inhibition of the activation of MGP (Saifan *et al*., 2013 b). Table 1.1 below summaries the different types of calcification and their characteristics features.

Table 1.1: Overview of the different types of vascular calcification

Type of calcification	Site of location	Primary inducer	Associated disease	Citations
Intimal calcification	Intimal layer of the arteries	Generation of matrix vesicles and apoptotic bodies from VSMCs, down-regulation of calcification inhibitory proteins.	Atherosclerosis, aging, genetic disorders, dyslipidaemia, diseases related to disturbed mineral homeostasis	(Johnson *et al*, 2006)
Medial calcification	Medial layer of the arteries	Deterioration of elastin fibres and generation of apoptotic cells	Diabetes and chronic kidney disease. Singleton-Merton syndrome and chronic renal disease	(Al-Aly *et al.*, 2007; Proudfoot *et al.*, 2001)
Cardiac valve calcification	Cells present in cardiac valves (bicuspid, tricuspid, atrio-ventricular valve and others)	Infiltration of T cells and macrophages in valves, in response to inflammation	Chronic kidney disease, dyslipidaemia, and diseases related to disturbance in calcium metabolism	(Sarig *et al.*, 1994)
Vascular calciphylaxis	Medial layer of small to medium sized arteries and arterioles	Increase in the threshold of calcium phosphate solubility due to conditions like hyperparathyroidism or chronic renal failure	Warfarin therapy, chronic renal failure, significant weight loss immunosuppressive drugs, diabetes, obesity, and hypercoagulable states	(Ahmed *et al.*, 2001)

1.4-Molecular mechanism of vascular calcification:

Vascular calcification is a significant predictor of mortality in subjects with renal disease, and may occur very early in the disease cycle, contributing at least in part to increased cardiovascular mortality in this population. This is indeed true even in young children. A landmark paper by Foley *et al* (1998) highlighted that VC was present in children with CKD and contributed to the increased risk of cardiovascular diseases (Foley *et al*, 1998).

For most of the 20th century, physicians believed that VC was a passive process of deposition of calcium phosphate products due to higher levels in circulation. However, researches in past 30 years lead a new consensus that VC is in fact an actively orchestrated biological process. Also, recent research confirms that VC can occur at physiological serum levels of calcium and phosphate in subjects with diabetes (Singh *et al.*, 2012), CKD (Reynolds *et al.*, 2004) and/or atherosclerosis (McCullough *et al.*, 2008). However, very little is known about the events that lead to calcification under these conditions. It is also not clear what fraction of calcium and phosphate are un-ionised or ionised and whether these change in the disease states; which may be responsible for initiation of calcification. Growing evidence from clinical and basic study however suggest that there could potentially be four non-mutually exclusive mechanisms of calcification which may include: 1) loss in inhibitory protein and/or gain of promoters of calcification, 2) differentiation of VSMCs in to bone like cells, 3) circulating nucleating complexes and 4) apoptosis. These mechanisms are summarised in Figure 1.6 and discussed in more details below.
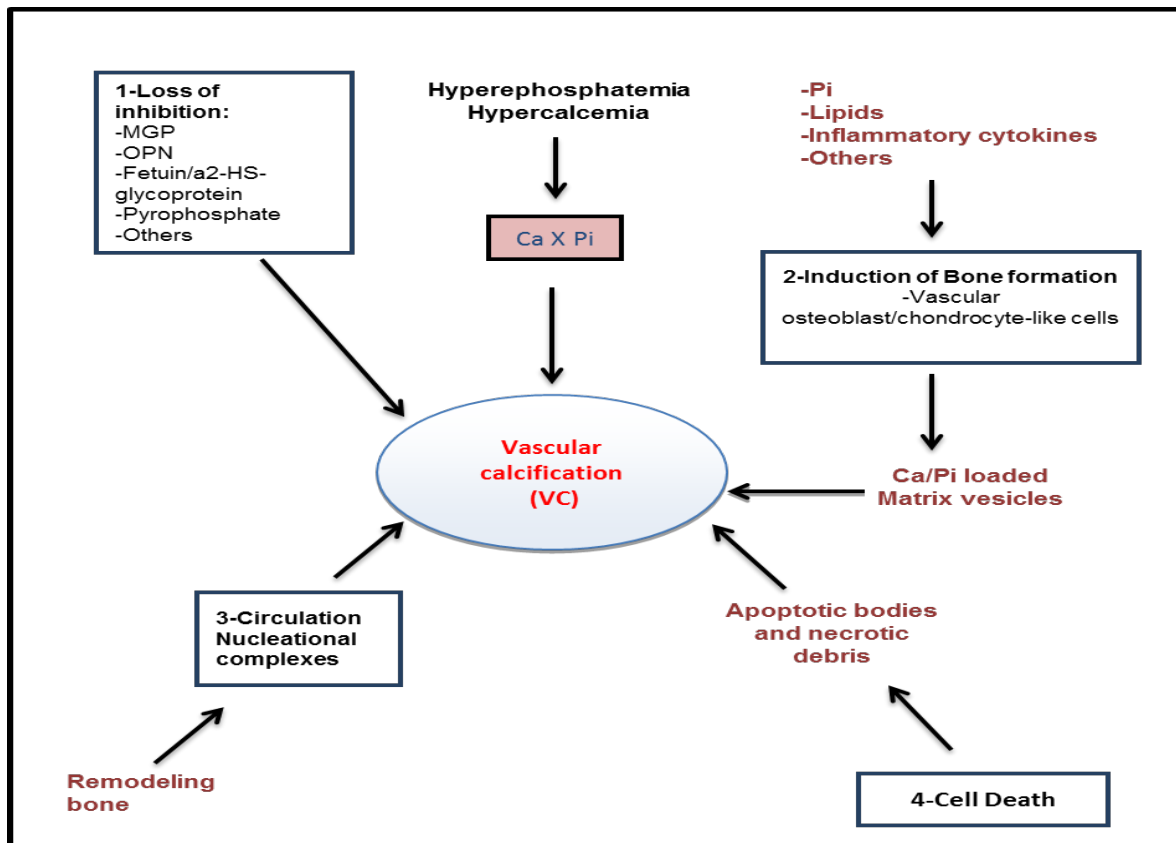
Figure 1.6: Four non-mutually exclusive mechanism of vascular calcification. (Adapted from; Giachelli, 2004).

1.4.1: Mechanism 1: Down-regulation of inhibitors of calcification:

Some of the key proteins reported to inhibit the process of calcification are listed in Table 1.2 and include MGP, OPN and pyrophosphates (Saifan *et al*, 2013 b). Other molecules that have been implicated are Fetuin-A and albumin. It is reported that even a minutes decrease in circulatory Fetuin-A in inflammation in CKD (Westenfeld *et al*., 1998) or albumin due to proteinuria in diabetes (Rees *et al*., 2004) will increases the possibility of mineralisation by forming micro crystals of calcium-phosphate which will eventually deposit in the arterial wall where necrotic or apoptotic cells are presented (Giachelli, 2004).

A role for Fetuin-A was further confirmed by Valdivielso *et al* (2011) who reported that circulatory Fetuin-A levels were decreased in haemodialysis subjects due to inflammation and this was associated with increased free calcium and phosphate as well as the rapid progression of calcification (Valdivielso *et al.,*2011).

With regards to MGP and osteoprotegerin (OPG) (Browner *et al.*, 2001)they may regulate calcium and apatite binding and may each serve a number of functions including regulation of apatite, crystal nucleation and growth (Giachelli, 2004). Low levels of OPG may exert its protective effect on calcification by a) acting as a decoy receptor for receptor activator of nuclear factor kappa-B ligand (RANKL) protein, b) inhibiting BMP2 signalling, and c) binding with calcium and phosphate crystals and inhibiting their seeding (Boyace and Xing, 2007). Furthermore, knock out models of both OPG and MGP produced extensive VC in mice models (Boyace and Xing, 2007; Johnson *et al*., 2006). However, elevated levels of OPG and MGP have been seen in patients with diabetes (Dalmeijer *et al*, 2013) and CKD (O'N, 2005) which questions whether these elevated levels are due to the underlying pathology as a defence mechanism or actively taking part in the progression of calcification. Interestingly, in *in vitro* studies, supra-physiological concentrations of OPG have been shown to enhance calcification via insulin-like growth factor receptor (IGF-1R) signalling (Di Bartolo *et al*, 2011). This would suggest a dual role for OPG with the effects produced determined by the concentrations present locally at the tissue level.

Table 1.2: Inhibitors of calcification

Marker of Inhibited Calcification	Main action	Molecular weight of Protein	Citations
MGP	Prevent calcification in cartilage, bone matrix and the arterial wall by a phosphorylated and γ-carboxylated protein the HA crystals formed.	10 KDa	(Proudfoot *et al.*, 1998)
Pyrophosphate	Directly inhibits HA through physiochemical mechanism by reducing binding site of calcium and phosphate	90 KDa	(Addison *et al.*, 2007; Persy *et al.*, 2011)
Fetuin-A	Prevents the mineralisation process by inhibiting the growth of HA crystals.	59 KDa	(Giachelli, 2004)
OPG	Binds to a decoy receptor for RANKL and this inhibits HA crystals.	60 KDa	(Giachelli, 2004; Naschberger *et al.*, 2004)

1.4.2 Mechanism 2: Induction of bone formation – promoters of calcification:

In addition to the inhibitors, VSMCs also express other proteins such as OC, osteonectin, ALP, BSP (Hunter *et al.*, 1993), and BMP2 that promote calcification (Shao *et al.*, 2007). These proteins play a very critical role in regulating nucleating sites of calcification and also regulate the process of mineralisation and crystal growth (Shanahan *et al*., 1998).

The mechanisms that lead to the expression of these proteins by VSMCs, and eventually to VC, are yet to be fully understood. It is however hypothised that VSMCs along with macrophages express low levels of these bone associated proteins which become elevated in disease states and may eventually lead to their osteogenic differentiation causing VC. They do this by being able to cause cells to recruit more calcium and phosphate intracellular and finally excreting this out in the form of apoptotic bodies to deposit within the extracellular matrix (Kockx *et al.*, 1998).

In relation to medial calcification, it is proposed that there may be a down regulation of MGP expression intracellularly leading to a decrease it its expression. In parallel, other proteins mentioned above (OC), which are not expressed under normal circumstances, become over-expressed (Kanazawa *et al.*, 2011). These changes eventually lead to calcification. Indeed, Luo *et al* (1997) have demonstrated using MGP knockout mice that down-regulation of this protein which inhibit the process of calcification results in deterioration of elastic fibres and generation of apoptotic bodies, which act as nucleating sites leading to extensive medial calcification and subsequent death (Luo *et al.,* 1997).

Studies using human atherosclerotic plaque have also demonstrated the presence of BMP2 (Mohler III *et al.*, 2001) which together with other factors such as Runx2 are elevated at the sites of early calcification and these protein are activated by inflammatory cytokines such as IFN-γ contributing to an elevated level of local concentration of 1,25-dihydroxycholecalciferol or 1,25-dihydroxyvitamin D_3 [$1,25(OH)_2D_3$] that causes progression of VC (Adams *et al.*, 2012: Jono *et al*., 1998).

Furthermore, activation of toll like receptor 4 (TLR4) in VSMCs by bacterial endotoxin such as LPS plays a significant role in enhanced progression of mineralised plaques (Lin *et al.*, 2006; Ortolani *et al*, 2010). This occurs because LPS stimulates its receptor resulting in the release of inflammatory cytokines such as interlukin-8 (IL-8) (Heo *et al.*, 2008) and also BMP2 (Yang *et al*, 2009). Lipopolysaccharide and tumour necrosis factor (TNF-α) contribute to the accumulation of lipid in the artery wall in atherosclerotic plaques which in turn promote calcium and phosphate crystallisation to form HA crystals (Alò *et al.*, 2009). Under the influence of calcium and phosphate VSMCs undergo differentiation into a cartilage and a bone like phenotype, which in turn enhances the process of calcification (Lu *et al.*, 2014). Inflammatory cells, such as macrophages and T lymphocytes are known to interact with VSMCs, endothelial cells and extracellular matrix to result in calcification by increasing expression of BMP2 and loss of MGP when VSMCs are exposed to macrophages incubated condition medium containing TNF-α (Tintut *et al.*, 2002;Ikeda *et al*, 2012). In addition, in CKD, secondary parathyroidism is prevalent and can induce 1-alpha hydroxylase (1alpha-OHase) expression in VSMCs and thereby the local production of vitamin-D (Somjen *et al*, 2005). However, it is not clear whether this is protective against calcification as the concentration of vitamin-D produced by PTH stimulus is not known. Similarly, proinflmmatory cytokines such as IFN-γ is also known to induce vitamin-D production in VSMCs and macrophages (Shioi *et al*., 2000). Expression of vitamin D receptor has been

found in endothelial cells, VSMCs and macrophages (Norman and Powell, 2014). The vitamin D receptor has transient fast effects on the levels of intracellular calcium, (Norman, 2006), possibly by inducing the opening of cell membrane calcium channels. It achieves this via the proposed ability of the receptor to achieve different conformations depending on configuration of the flexible vitamin D_3 molecule 1alpha,25(OH)$_2$D$_3$ (Norman, 2006). The accumulation *in vitro* of vitamin D_3 and its receptor has been observed in caveolae , which are sphingolipids and cholesterol rich invaginator membrane region (Huhtakangas, *et al*., 2004). Thus, different receptor-ligand conformations locate to different targets either the nucleus to function as transcription regulators; or caveolae at the cell membrane- where it modulates secondary messenger signalling.

Furthermore, when overexpressed, the vitamin D receptor can cause changes further down-stream at the nuclear level producing osteogenic proteins, activate MAPKs signalling and induce proinflammatory cytokine (Norman and Powell, 2014). These effects are however only induced when vitamin D concentrations are high. A high dosage of 1,25-dihydroxyvitamin D_3 was equated to be 0.25 μg kg^{-1} day^{-1} in the studies conducted by Lamawansa et al. (1996) and Zebger-Gong et al. (2011).

At low concentrations, vitamin-D protects against calcification by protecting the expression of vascular anti-aging protein Klotho (Lim *et al*., 2012). See table 1.3 showing an example of protein induced calcification.

Table 1.3: Inducers of calcification

Marker of calcification	Main action	Molecular weight of Protein	Citations
(Runx2)/Cbfa1	Runx2/Cbfa1 is a key transcription factor which induces osteogenic differentiation by elevating calcium and phosphate. This works cooperatively with the ligand bound vitamin D_3 nuclear receptor to cooperatively regulate the expression of multiple genes.	60-90 KDa	(Ho *et al.*, 2009; Stephens and Morrison, 2014)
BMP2	BMP2 belongs to the TGF-beta superfamily, and is thus a regulatory peptide/growth factor. BMP2 binds BMP receptor I, initiating the linked signal transduction cascade and also activates BMP receptor II (BMPRII) by phosphorylation. Activated BMPRII phosphorylates R-SMAD which acts as a transcription factor after translocation to the nucleus. A dose dependent phosphate uptake and induced calcification with BMP2 is observed in VSMCs. BMP2 enhances osteoblast differentiation.	44KDa	(Li *et al.*, 2008;Shao *et al.*, 2007, Wang *et al.* 2014)
OC	OC is secreted by osteoblasts and is the most plentiful non-collagenous protein in bone and dentin. It is expressed in both osteoblasts and VSMCs which are undergoing calcification. It circulates in the blood in an uncarboxylated form. However, it is modified post-translationally at 3 glutamic acid (Gla) residues by vitamin K. After γ-carboxylation it binds calcium and phosphate. OC is required for HA formation.OC increases the rate of HA nucleation.	37.4KDa	(Covic *et al.*, 2010; Kapustin & Shanahan, 2011; Gundberg, Lian & Booth, 2012 ;Flade *et al.* 2001)
ALP	ALP enzyme is homodimeric and found in all body tissues. Several isoenzymes are produced, with serum ALP being derived mostly from skeletal muscle and liver. The ALP isoenzyme in bone is the same as that in the liver and kidney, where it is membrane bound; and is termed tissue non-specific ALP. In the bone matrix ALP is found in vesicles where it hydrolyses pyrophosphate into monophosphate ions, which is used for HA nucleation. Lack of this enzyme leads to defective bone mineralisation in mice**.** Mis-sense mutations in humans are linked to hypophosphatasia and bone mineralisation deficiency.	49 KDa	(Schutte *et al.*, 2013; Anderson *et al.*, 2004)

1.4.3: Mechanism 3: Circulating nucleational complexes:

Subject with CKD and osteoporosis (Abedin *et al.*, 2004) often have increased concentration of nucleational complexes compared to normal healthy individuals. These nucleational complexes are released into the blood stream from bone and can act as nucleating sited for extra calcium and phosphate i.e. already present in the circulation (Giachelli, 2004). This process accelerates even more when serum levels of proteins such as albumin, Fetuin-A are reduced. Postmenopausal woman with osteoporosis have been shown to reduce the rapid progression of calcification when treated with bisphosphonates (Price *et al.*, 2001).

1.4.4: Mechanism 4: Apoptosis:

Studies have also shown that the medial VSMCs undergo apoptosis and the apoptotic bodies formed act as nucleating sites for calcium crystal (Figure 1.7). This has been confirmed by showing that inhibition of apoptosis reduces calcification (Giachelli, 2004) while increased apoptosis resulted in increased levels of VC (Giachelli, 2004). Furthermore, studies conducted on patients with atherosclerosis show that vesicles are shed when VSMCs undergo apoptosis and these vesicles are rich in calcium and phosphate (Ewence *et al.*, 2008; Kapustin *et al.*, 2011; Otsuka *et al.*, 2014). The characteristics of the vesicles are similar to those of the matrix vesicles which are formed in the bone by biogenesis and budding and pinching-off of the osteoblasts, odontoblasts and chondrocytes (Trion *et al.*, 2004; Trion *et al.*, 2008). In other words, these matrix vesicles are usually seen at the initial stage of calcification of bone in which the matrix vesicle acts as a submicroscopic extracellular membrane-invested particle that serves as the initial site of calcification in all skeletal tissues (Trion *et al.*, 2008). The crystals formed grow along the length of elastin fibres (Kim, 1995; Kim *et al.*, 2002). The anatomy of elastin fibres consists of an elastin core, which is surrounded by micro-fibrils. Any alterations in the structure of these fibres can enhance the process of calcification (Giachelli, 2004). Pereira *et al* (1999) demonstrated that there was a higher rate of medial

calcification in aorta in mice which were genetically modified to under-express micro-fibrils (Pereira *et al.*, 1999). Additionally, with aging, the levels of free elastin peptides in the circulation increase due to the degradation of the elastin itself. These elastin peptides have been shown to encourage the process of intimal as well as medial calcification (Faury *et al.*, 1998).
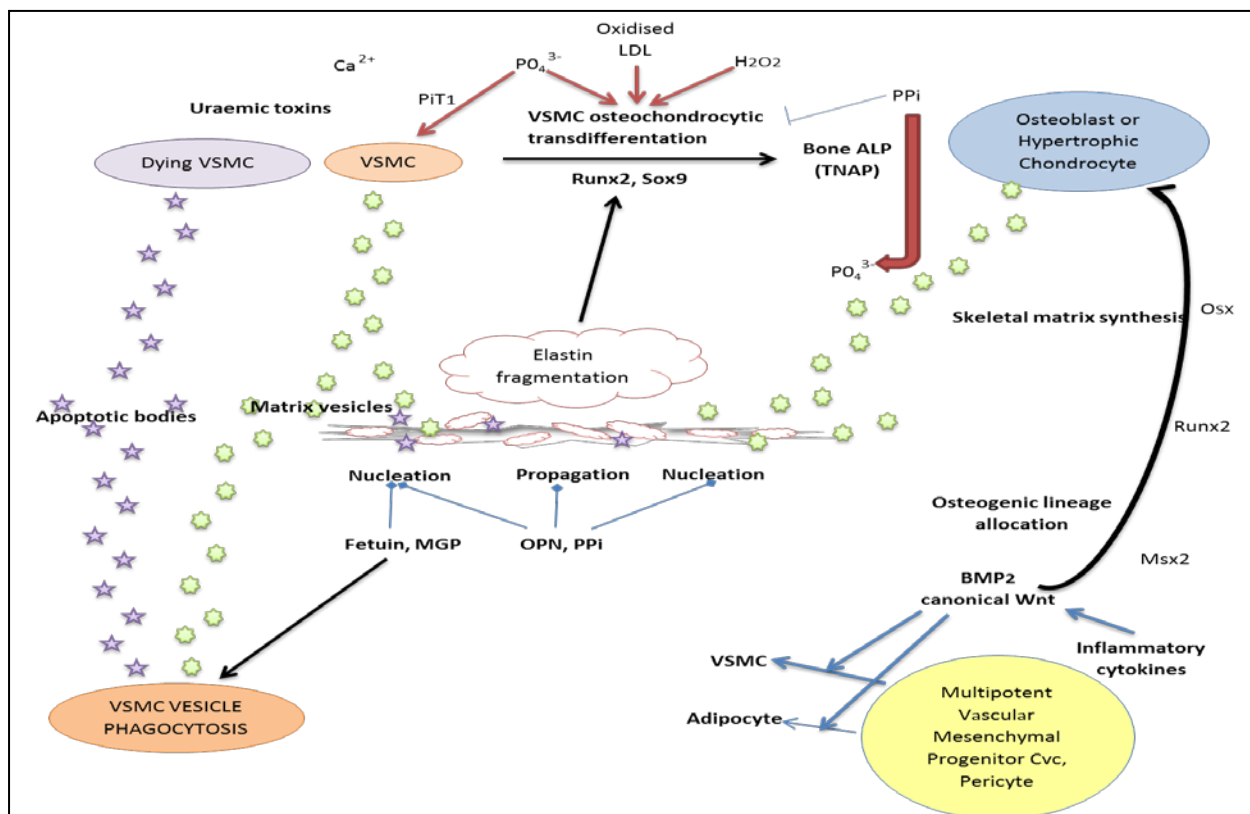
Figure 1.7: Cell fate, function, and phenotype in vascular calcification (Mizobuchi *et al.*, 2009).

Under the influence of an elevation of calcium and phosphate levels or uraemic toxins, VSMCs generate apoptotic bodies and matrix vesicles. These apoptotic bodies and matrix vesicles are able to concentrate calcium and phosphate at the nucleating sites and initiate the formation of calcium crystals.

1.5 Inflammation and vascular calcification:

It has already been indicated before that inflammation may play a critical role in the development of calcification. For instance, cytokines such as IFN-γ may elevate the expression of promoters of calcification such as the transcription factors Runx2. Interferon-γ may additionally cause over production of vitamin D which in turn induces osteogenic proteins including BMP2. Other inflammatory mediators such as LPS may also stimulate BMP2 production (Yang *et al*, 2009) thereby potentiate calcification. Similarly, *in vivo* administration of LPS in rat fed on high phosphate resulted in enhanced inflammatory cytokines such as TNF-α and IL-1 and in calcification (Guerrero *et al*., 2011; Pan *et al*., 2007). It has also been shown that inflammation can lead to free radical generation and the reactive oxygen species generated regulates the inflammatory cascade (Pacher *et al.*, 2007) which in turn leads to the progression of calcification (Byon *et al.*, 2008). A study has also demonstrated that the transcription factor Runx2 is involved in oxidative stress in VSMCs incubated with hydrogen peroxide (H_2O_2) and high phosphate media thus inducing calcification (Liu *et al.*, 2010). This process may have occurred through the activation of inflammatory mediators such as transforming growth factor-β (TGF-β) or LPS.

The actions of inflammatory mediators may not be restricted to the discussions above but may extend to other molecules and pathways of which that associated with the induction of NO production may be of key importance.

1.6 Nitric Oxide and nitric oxide synthases:

Physiologically NO , known as endothelium drive relaxation factor, is formed via cleavage of the amino-terminal nitrogen of L-arginine producing L-citrulline by a product (Moncada *et al.*, 1991). This reaction is catalysed by the family of nitric oxide synthase (NOS) enzymes which exist as three distinct isoforms. These include eNOS and neuronal NOS (nNOS) which are constitutive while the third isoform is iNOS in response to inflammatory mediators (Napoli and Ignarro, 2001; Förstermann *et al*., 1998). All three isoforms of NOS only function to produces NO whilst in the dimer form. Dimerization of NOS not only activates the enzyme but also increase its affinity for L-arginine and a critical co-factor, tetrahydrobiopterin (BH_4).

This enzymatic reaction is also dependent on binding of calmodulin in eNOS and nNOS but not in case of iNOS as calmodulin is already tightly bound with the NOS enzyme (Alderton *et al*., 2001; Napoli and Ignarro, 2001). Nitric oxide is a well known and studied molecule that has either beneficial effects under physiological conditions or damaging effects in several pathologies. Whether NO/iNOS is good or bad primarily depends upon the underling pathologies and organ systems involved.

Nitric oxide itself is a free radical which can exist in several forms depending on the oxido-reductive state of the cells such as nitroxyl ions (NO^-), NO free radicals (NO•), nitrosonium cations (NO^+), nitrite ions (NO_2^-) and nitrate ions (NO_3^-) (Ischiropoulos and Gow, 2001). Nitric oxide also reacts with the superoxide ions to form $ONOO^-$ which is a very potent oxidant of lipids and proteins. In addition, NO can react with thiol cysteine residues on proteins leading to compromised protein function. Also, binding of NO to cytochrome c oxidase causes irreversible nitrosation of mitochondrial complex-I which can activate uncontrolled leakage of protons, dysfunction of permeability transition pore and cellular apoptosis (Brown, 2001).

Inducible nitric oxide synthase protein is highly conserved in different species however its promoter regions are different in different cells and species. Due to this, iNOS activation of rat smooth muscle cells can be achieved by LPS, IFN-γ or cytokines such as IL-1/6 or TNF α but not necessarily in human aortic smooth muscle cells (Vallance and Charles, 1998). It has been very well postulated that iNOS expression in immune cells is critical for host defences mechanisms (Bogdan, 2001). However, iNOS can also be induced in other cells such as aortic smooth muscle cells where its expression has been implicated in pathologies such as septic shock and, of relevance to this thesis, in VC. Its role in relation to the latter is however inconclusive.   Figure 1.8 & 1.9 below shows relaxation of vascular smooth muscle cells by NO generation via endothelial cells or within smooth muscle cells

1-Acetylcholine binds Ach-G-protein linked receptor on endothelial cell surface, the endothelial cell is stimulated by shearing forces or inflammatory mediators

10-The muscle cell relaxes

2-G-protein activates phospholipase C at the inner face of the membrane

9-Decrease in smooth muscle calcium ion inhibits the enzyme myosin light chain (MLC) kinase, so that dephosphorylated MLC increases in the cell.

3-inositol trisphosphate (IP3) diffused to the endoplasmic reticulum and opens IP3 gated calcium channels in the endoplasmic reticulum membrane.

8-cGMP activates protein kinase G which phosphorylates muscle proteins at maxi-potassium channels, causing opening of K^+ channels, resulting in hyperpolarisation of the cell, which leads to inhibition of voltage-dependent calcium channels.

4-Calcium-calmodulin complex activates eNOS or iNOS or nNOS in the endothelial cell. These synthesise NO from L-arginine.

7-NO activates guanylyl cyclase in smooth muscle cell to synthesise a cyclic guanosine monophosphate (cGMP)

5-Calcium ions bind calmodulin in the endothelial cytoplasm.

6-NO diffuses from endothelial cells into adjacent vascular smooth muscle cells.

Figure 1.8: Relaxation of vascular smooth muscle cells by NO generation via endothelial cells.

1-LPS, TNF-a, IL-1b bind G-protein coupled receptors on the surface of the smooth muscle cell. The G-proteins activates phospholipase C

2-Phospholipase C generates diacylglycerol (DAG) and IP3

3-DAG and calcium activate PKC

4-PKC activates transcription factor nuclear factor kappa B (NF-kB). NF-kB acts as a transcription activator for the iNOS gene.

5-iNOS is produced in the cell and this synthesises NO from l-arginine

6-NO activates guanylyl cyclase in smooth muscle cell to synthesise cGMP

7-cGMP activates protein kinase G which phosphorylates muscle proteins at maxi-potassium channels, causing opening of K^+ channels, resulting in hyperpolarisation of the cell, which leads to inhibition of voltage-dependent calcium channels.

8-Decrease in smooth muscle calcium ion inhibits the enzyme myosin light chain (MLC) kinase, so that dephosphorylated MLC increases in the cell.

9-The muscle cell relaxes

Figure 1.9: Relaxation of vascular smooth muscle cells by NO generation within smooth muscle.

1.7: Nitric oxide and vascular calcification:

Low levels of NO have generally been reported in chronic renal failure (Baylis, 2006) and this has been suggested to contribute to the development of hypertension as well as the subsequent cardiovascular related events observed. This however, contradicts other reports of elevated production of NO and iNOS expression in subjects with renal dysfunction (Schmidt *et al*., 1999; Schmidt *et al*., 2000; Qiu *et al.*, 2004) which would indicate otherwise. Moreover, there is no conclusive evidence about the role of NO in the regulation of calcification in this high risk renal population. Indeed it is not clear whether NO is an active player in the regulation of calcification or an innocent bystander due to renal failure.

Low levels of vitamin K are evident in CKD population and especially on haemodialysis (El Asmar *et al*., 2014). The reduction in vitamin K (especially K2 isoforms) may be linked to the progression of VC and may lead to reduced gamma carboxylation or MGP (local intracellular inhibitor of calcification) and its activation (Asmar *et al*., 2014). Furthermore, incubation of vitamin K2 (menatetrenone) with cultured bovine vascular smooth muscle cells (BVSMCs) induced iNOS and NO production in a time dependent manner over 24 to 72 hours (Sano *et al*., 1999). It is however not known whether these changes are linked to the suppression of MGP or contribute to the actions of vitamin K on calcification. Worth noting however is the observation that NOC 18, an NO donor see table 1.6 summarised the half- life , inhibited the expression of MMP-2 in endothelium (Chen and Wang, 2004, Milkiewicz *et al*., 2006). Also inhibition of iNOS resulted in increased expression of MMP-9 (Knipp *et al*., 2004) in aortic smooth muscle cells. MMP-9 is known to regulate VC with elevated levels found in the arterial wall calcification (Chen *et al*., 2011). Additionally, SNP, another NO donor see table 1.6 summarised the half- life, has also been shown to inhibit calcification (Huitema *et al*., 2006a). Furthermore, Kanno *et al* (2008) have demonstrated that NO could prevent differentiation of VSMCs into osteoblastic cells by inhibiting TGF-β signalling

through cGMP dependent pathway. They showed that inhibiting guanylate cyclase reversed the inhibitory characteristics of NO on VC by inhibiting the osteoblastic differentiation of VSMCs (Kanno *et al.,* 2008). Any notion that NO may suppress calcification would however contradict observations that it accumulates in VC and in chondrocytes. In turn this inhibits mitochondrial respiration leading to modulation of matrix loss which is associated with mineralisation of the chondrocytes (Johnson *et al.*, 2000; Johnson *et al.*, 2006). Furthermore, production of NO may lead to elevations in ONOO ⁻ induced oxidative stress and apoptosis in osteoblast cells, again contributing to calcification. Other studies have however shown that incubation of cells with FGF-1 exposed to ONOO ⁻ reversed apoptosis and oxidative stress (Kelpke *et al.*, 2001) inducing calcification. In one other study, incubation of cells with calcium phosphate activated iNOS and produced NO in *in vitro* cultured articular chondrocytes in a dose dependent manner (Ea *et al.,*2005). These observations are again contradictory with those reported above and throws further confusion as to whether NO inhibits or promotes calcification. This clearly needs further investigation and has been explored in this thesis.

Nitric oxide has many roles in cells and tissues. It is a potent inflammatory mediator, vasodilator, neurotransmitter, free radical and secondary messenger. The evidence suggests that the mode of NO promoting calcification of blood vessels of is via its S-nitrosylation reactions with respiratory enzymes, primarily the complex enzymes in the mitochondrial electron transport chain. Loss of mitochondrial function promotes apopotosis by clearly identified pathways (Estaquier *et al*., 2012). This means that NO is cytotoxic at certain levels, which need further characterisation. However, NO also functions to protect cells from death, which includes the inhibition of calcification in VSMCs. Here evidence suggests its mode of action involves vasodilation, inhibition of tissue remodelling after injury, as well as inhibition of vascular disease pathology.

Table 1.4 & 1.5 below summarised primary evidence to support the functioning of NO as an inhibitor or a promoter of vascular calcification

Table 1.4: Primary evidence to support the functioning of NO as an inhibitor of vascular calcification

Action	Effect	Cell / tissue / organelle / enzyme effect observed in	Citation
L-arginine transport reduced	Reduced NO contributes to hypertension	Vascular endothelial cells using uremic plasma from end-stage renal disease patients	(Xiao *et al.,* 2001)
Urea inhibits L-arginine transport	Elevated blood urea nitrogen may lead to endothelial L-arginine deficiency *in vivo*, chronic kidney disease leads to hypertension	Bovine aortic endothelial cells	(Wagner *et al.,* 2002)
Inhibition of arginase slows the progression of renal failure. Arginase limits NO production	Increase of NO production protects against endothelial cell damage	Rat with kidney ablation	(Sabbatini *et al.,* 2003)
NO-mediated dilation of coronary arterioles is inhibited in hypertension by an increase in arginase activity in endothelium, which limits l-arginine availability to e/iNOS for NO production.	NO production and NO mediated blood vessel dilation reduced in hypertension	Pig coronary arterioles	(Zhang *et al.,* 2004)
Inhibiting arginase or supplementing with L-arginine restored endothelial vasodilation	Enhanced vascular arginase activity contributes to endothelial dysfunction	Arteriole endothelium from rats with salt-induced hypertension	(Johnson *et al.,* 2005)
Chronic renal disease patients had low excretion of NO	Hypertension is linked to reduced NO production	Human renal disease patients	(Schmidt & Baylis, 2000)
Patients with end-stage renal disease have low NO production	NO production contributes to increased blood pressure in end-stage renal disease	Human renal disease patients	(Schmidt *et al.,* 1999)
NO inhibits transcription of matrix metalloproteases in a dose dependent way	NO acts as a negative regulator in endothelial migration and tissue remodelling	Endothelial Cells	(Chen & Wang, 2004)

NO donors significantly reduced MMP-2 production	NO reduces tissue remodelling	Microvascular endothelial cells	(Milkiewicz *et al*., 2006)
iNOS inhibition resulted in increased expression of MMP-9	Reduced NO levels promote tissue remodelling	Rat aorta smooth muscle cells	(Knipp *et al*., 2004)
MMP inhibitors decreased calcification of aorta rings from normal and chronic kidney diseased rats.	MMP-2 and MMP-9 promote aorta calcification. NO inhibits calcification due to MMP downregulation noted in (Milkiewicz *et al*., 2006 and Knipp *et al*., 2004)	Rat aorta rings	(Chen *et al*., 2011)
NO prevents differentiation of VSMCs into osteoblastic cells by inhibiting TGF-beta signalling through a cGMP-dependent pathway	NO limits vascular calcification	Murine vascular smooth muscle cells	(Kanno *et al*., 2008)
NO inhibits angiotensin II-induced migration of smooth muscle cells	NO limits artherosclerosis pathology	Rat aortic smooth muscle cells	(Dubey *et al*., 1995)
NO generating vasodilators inhibit mitogenesis and proliferation of smooth muscle cells	NO limits artherosclerosis pathology	Rat vascular smooth muscle cells	(Garg & Hassid, 1989)

Table 1.5: Primary evidence to support the functioning of NO as a promoter of vascular calcification

Action	Effect	Cell / tissue / organelle / enzyme effect observed in	Citation
Nitrosation of mitochondrial complex-I	Protons leakage, increased permeability and apoptosis	Macrophage targeting tumour cells	(Lancaster & Hibbs 1990)
Nitrosation of mitochondrial complex-I	Cytotoxicity	Macrophage targeting tumour cells	(Hibbs *et al.,* 1988)
Inhibition of mitochondrial iron-sulphur	Cytotoxicity	Macrophage targeting tumour cells	(Drapier & Hibbs, 1988)
Cytostasis and respiratory inhibition	Cytotoxicity	Macrophage targeting tumour cells	(Stuehr & Nathan, 1989)
Inhibition of mitochondrial electron transport	Cytotoxicity	Macrophage targeting tumour cells	(Granger & Lehninger, 1989)
NO targets enzymes	Enzyme damage	Not tested in cells – enzyme only	(Henry *et al.,* 1993)
NO targets ubiquinol-cytochrome c reductase activity	Enzyme damage	Not tested in cells – enzyme only	(Welter, Yu & Yu, 1996)
NO damages mitochondrial cytochrome oxidase	Enzyme damage	Not tested in cells – enzyme only	(Sharpe & Cooper, 1998)
S-nitrosylation of mitochondrial enzyme complex I	Inhibition of respiration, cytotoxicity	Macrophage	(Clementi *et al.,* 1998)
Inhibition of complex I activity and S-nitrosylation of glyceraldehyde-3-phosphate dehydrogenase and glutathione reductase	inhibition of respiration	Human fibroblast cell lines	(Beltran *et al.,* 1998)
Inhibition of respiration	Oxygen consumption reduced, hypoxia, cytotoxicity	Macrophage	(Orsi *et al.,* 2000)
NO reacts with cytochrome c oxidase	Enzyme damage	Not tested in cells – enzyme only	(Boelens *et al.,* 1983)

NO reacts with Fe2+ oxidase	Enzyme damage	Not tested in cells – enzyme only	(Blackmore, Greenwood &. Gibson.,1991)
NO inhibits cytochrome oxidase	Inhibition of respiration	Rat skeletal muscle mitochondria	(Cleeter *et al.,* 1994)
NO deenergizes mitochondria	Inhibition of respiration	Liver and brain mitochondria	(Schweizer & Richter., 1994)
Reversible inhibition of respiration by competition with cytochrome c oxidase	Inhibition of respiration	Rat heart mitochondria	(Borutaité & Brown., 1996)
Cytochrome oxidase activity inhibited, increased production of O^{2-} and H_2O_2	Inhibition of respiration	Rat heart mitochondria	(Poderoso *et al.,* 1996)
Inhibition of electron transport chain, regulation of mitochondrial oxygen uptake and superoxide anion, peroxynitrite formation	Inhibition of respiration	Rat heart	(Poderoso *et al.,* 1998)
Mitochondrial proton leakage increased	Irreversible inhibition of respiration	Rat brain mitochondria	(Brookes *et al.,* 1998)
iNOS induced in damaged tubules in late-stage kidney disease	Apoptosis may increase in kidney tubules due to increased NO	Human kidney	(Qiu, Sinniah & Hsu., 2004)
NO accumulates in vascular cells	NO-induced depression of chondrocyte respiration, which may lead to mineralization	Human chondrocytes	(Johnson *et al*., 2000)
A dose dependent delayed cell death occurred in osteoblasts subjected to peroxynitrite	Superoxide and nitric oxide react to produce peroxynitrite.	Murine osteoblasts	(Kelpke *et al*., 200)
Calcium phosphate activated iNOS generating NO in a dose dependent manner *in vitro*	NO production increases in calcifying environment	Cultured chondrocytes	(Ea *et al.,*2005)

Table below summarised biological half-life for different releasing NO donors

Table 1.6: the biological half-life for different NO donors

Nitric oxide donor	Biological half-life
SNP	115-119 seconds (Resting circulatory half- life) (Desoky, Derendorf & Klotz, 2006)
(DETA NONOate/NOC-18)	20–22 hours (Chen and Wang, 2004, Milkiewicz *et al*., 2006).

1.8- Aims and objectives:

The main aim of this PhD programme is to determine whether NO production contributes to the calcification process *in vitro* (VSMCs) and establish whether excessive NO production exacerbates VC. Thus this study aims to investigate the relationship between NO/ iNOS expression and VC in VSMCs cultures. Selective pharmacological inhibitors of iNOS, such as GW274150, will be used in studies to block NO production. In addition, NO donors with defined NO releasing profiles will be used in parallel studies to establish whether the profile and/or levels released determine either the inhibition or development and degree of calcification. It is possible that modulators of NO levels may have an impact on VC.

Confirmation of HA crystals formed by calcification inducers alone, or with/ without inflammatory mediators, NOC 18 and SNP will be investigated using ARS. Further characterisation of HA crystals will be conducted by FT-IR spectroscopy through determination of specific spectrum/wave number (cm^{-1}) characteristic of HA crystals. Where calcification is enhanced, we will aim to establish whether known pro-calcific markers such as Runx2 are induced. It is also intended that signalling pathways such as those involving kinases (p38 MAPK) known to regulate iNOS expression will be investigated.

CHAPTER II

MATERIALS AND METHODS

2.Materials and Methods:

2.1- Drugs and Reagents:

Materials used in cell culture were Dulbecco's Modified Eagles Medium (all ingredients of DMEM see page 342), foetal bovine serum (FBS; containing growth factors, low gamma globulin (immunoglobulin), penicillin (100U ml^{-1}) and streptomycin (100 µg ml^{-1}), and Trypsin-EDTA (10X), liquid (0.5% Trypsin in 5.3 mM EDTA). All these reagents were purchased form (GIBCO, Loughborough, UK). Primary smooth muscle-22 alpha actin (SM22α) anti-SM22 alpha antibody rabbit polyclonal, anti-Runx2 antibody, phospho-p38 MAPK rabbit mAb, phospho-Akt rabbit mAb, and phospho-p44/42 MAPK (Erk1/2) rabbit mAb were purchased from (Abcam PLC, Cambridge, UK). Furthermore, iNOS mouse monoclonal antibody was purchased from BD (Biosciences, Oxford, UK). Other standard laboratory reagents such as calcium chloride dihydrate for cell culture use, *β*-glycerophosphate disodium salt hydrate, lipopolysaccharides from Escherichia coli, diethylenediamine/nitric oxide adduct, sodium nitroprusside dehydrate , phosphatase inhibitor cocktail 2, protease inhibitor cocktail, SB203580, LY294002, ARS, horse radish peroxidase (HRP) conjugated β-actin antibody, and 3-(4, 5-dimethyl-2-thiazolyl)-2, 5-diphenyl-2H-tetrazolium bromide (MTT) for cytotoxicity use were purchased from Sigma Aldrich (Dorset, UK). Inducible nitric oxide synthase inhibitor GW274150 was a gift from GlaxoSmithKline. Recombinant rat – interferon-gamma (IFN-γ) was purchased from Merck Chemicals (Nottingham, UK).

2.1.1- Preparation of complete cell culture medium, phosphate buffer saline (PBS) and trypsin:

Dulbecco's Modified Eagles Medium (89%) was used in all the studies and was supplemented with 10% FBS, penicillin (100U ml^{-1}) and streptomycin (100 µg ml^{-1}). This solution will be referred to as complete culture medium from here on. Working stock PBS

was prepared by a 1:10 dilution of 10X stock with autoclaved double distilled water (DDW). Trypsin-EDTA (10X) was diluted 1:10 to give a 1X working solution using 1X PBS solution. All solutions were stored at 4^0C and used within 6 weeks of preparation except complete culture medium was used only for 15 days.

2.1.2 Isolation of rat aortic smooth muscle cells:

Male Sprague-Dawley rat were euthanized in a carbon monoxide chamber as per schedule 1 following the University and home office guidelines. The aorta was isolated into complete culture medium as followed from Wileman *et al*., (1995). Each aorta was then stripped of fat and connective tissues using sterile scalpel blades in a class II tissue cabinet. The tissues were then cut longitudinally to expose the endothelial layer, which was removed by gentle scraping. Each aorta was then cut into approximate sizes of 2-4mm and 4 to 6 explants placed into a T-25 tissue culture flask with the luminal surface against the flask surface. 5 ml of complete culture medium was placed into each flask, avoiding dislodging the explants called passage 0 (P0). The flasks were kept standing upright in a cell culture incubator maintained at 37^oC for approximately 4 hours to ensure firm attachment of the tissues. The flasks were subsequently inverted ensuring that all the aortic explants were submerged in medium and left for 7 to 14 days to allow cells to migrate from the explants onto the flask surface (Figure 2.1). The culture medium was changed every 72 hours to ensure adequate nutrient supplementation. Cells were eventually subcultured as explained in section 2.1.3, transferred to T-75 flask and labelled as P1 (Figure 2.2). Subcultured was repeated to two times and labelled as P2 and P3 to make sure the majority of cells were used smooth muscle cells. Isolated cells were also characterised routinely by immunostaining against SM22α as explained is section 2.2 to confirm the phenotypic lineage. A representative photograph of cells migrating from a tissue explants and growing in culture is shown in Figure 2.1 and a partially confluent flask of cells in culture is shown in Figure 2.2.
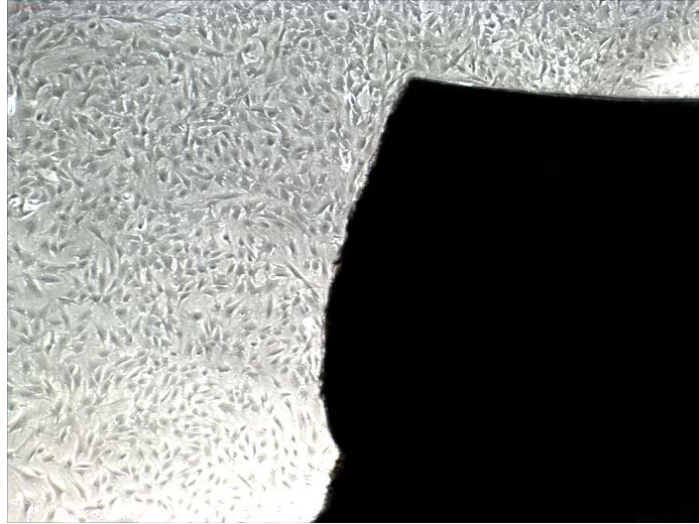
Figure 2.1: Migration of smooth muscle cells from aortic explants in a T-25 cell culture flask at passage 0. Images were captured at 40X magnification using an Olympus inverted light microscope with a GX capture software.
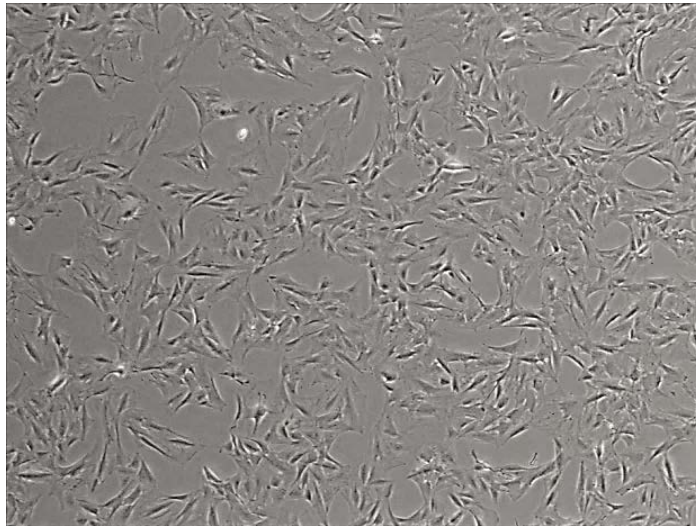
Figure 2.2: Rat aortic smooth muscle cells growing in a T-75 cell culture flask at passage 1.

2.1.3- Subculture of rat aortic smooth muscle cells:

Cells were routinely subcultured at 80-90% confluency to avoid an over-confluent and overgrown state. Tissue culture flasks were routinely subcultured (P3- P6) and plated either in 12 or 24 well cell culture plates for further experimentation as required. The cell culture medium was aspirated from the flasks and the cells washed three times in excess of 1X PBS (5ml) followed by the addition of 3 ml of 1X trypsin. Excess of trypsin was removed within 30 second after addition, leaving about 0.5 ml in the flasks which were incubated for 3-5 minutes at room temperature. Flasks were swirled occasionally to ensure that the trypsin was in direct contact with cells. At the end of the incubation period, each flask was gently tapped on the sides to lift monolayers of cells and 2.66 ml complete cell culture added to inactivate the trypsin. Suspend monolayers were dispersed into single cells using a Pasteur pipette. A further 12.34 ml of medium was added and cell counting performed as explained in section 2.1.4 prior to plating in tissue culture plates for further experimentation or into culture flasks to generate further stocks.

2.1.4-Cell counting and plating for experimentation:

Following trypsinisation cells were centrifuged at 4^0C at 1100 rpm for 5 minutes. The cell pellet was re-suspended in 2 ml of fresh cell culture medium. 10 µl of the cell suspension was mixed with 10 µl of trypan blue (0.08 %) in an eppendorf tube before loading into a cell counting chamber for counting on a Countess™. The total cell count was determined as following:

Total cells in chamber A = 5.8 x10^5 / ml   (living cell: 4.5 x10^5 /ml, viability of cells: 79%)

Total cells in chamber B = 7.3 x10^5 /ml (living cells: 6.3 x10^5 /ml, viability of cells: 86%).

Average total cell number per ml = 5.4 x10^5 cells

To plate the cells needed per well (A) the volume containing the required cell number was determined as follows:

Total cells / ml determined from above = 5.4 x10^5 cell /ml

Cells needed per 24 well = 60,000

Thus, if 1 ml of stock cell suspension contains 5.4 x10^5 cell, then to get 60,000 cells we will need 60,000 x 1000/5.4 x10^5 = 111.1 µl

For a full 24-well plate the volume of cell suspension required = 111.1 x 24 = 2.67 ml.

This volume was then made up to 24 ml with complete DMEM and plated into the wells.

2.2- Identification of smooth muscle cells isolated from rat aorta:

Isolated and subcultured cells were stained for the expression of the smooth muscle cell marker SM22α by immunostaining. Cells were plated in Lab-Tek wells and allowed to grow to ~40-50% confluency, before washing 3times (five minutes each) with 1X PBS and fixed with ice cold 100% methanol for 20 minutes. After fixing, cells were then incubated with 5% bovine serum albumin (BSA) consisting of 100mM Tris–Base (pH 7.5), 100mM NaCl, Tween-20 (0.1 % equivalent to 100μl) to block nonspecific binding of primary SM22α antibody. Cells were then incubated with the primary antibody at 1:200 dilution into 5% BSA in PBS for 1 hour at room temperature on an orbital shaker. Cells were washed 3times with 1X PBS and incubated at room temperature for an hour with goat an anti-rabbit IgG secondary antibody (Alexa Fluor® 488) at a dilution of 1:1000 in 5 % BSA. Excess of secondary antibody was removed and the cells washed 3X with 1X PBS before being visualised using a Nikon Confocal Microscope TE-2000U at a magnification of 100x. A representative photograph of positively SM22α stained cells is shown in Figure 2.3.
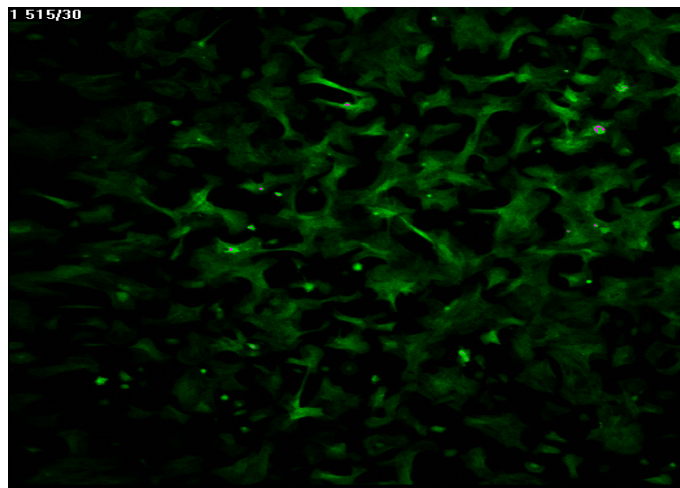
Figure 2.3: Stained smooth muscle cells isolated from rat aorta.

Smooth muscle cells were plated in LabTek wells at passage 3, and allowed to grow to 40-50% confluency. Cells were then incubated with the primary antibody (SM22α antibody) for 1 hour and washed 3 times. This was followed by incubation with goat anti-rabbit IgG secondary antibody for an hour. The cells were then washed 3 times with 1x PBS before being visualised using a Nikon Confocal Microscope TE-2000U at a magnification of 100x. The photograph is representative of cultures routinely obtained, and confirms the presence of smooth muscle cells which are predominantly positively stained.

2.3-Griess assay:

The Griess assay was used to quantify nitrite in culture medium collected from cells following different experimental conditions. The Griess assay reagents consisted of reagent I which contained 0.2% N-1-naphthylethylenediamine dihydrochloride and reagent II containing 2% sulfalinamide +10% H_3PO_4. The reaction of nitrite with 2% sulfalinamide +10% H_3PO_4 results in the formation of a diazonium salt which in turn reacts with 0.2% naphthylethylenediamine dihydrochloride producing chromophoric azo-derivative (Pink colour) (Green *et al*, 1982). This reaction is summarised in Figure 2.4.
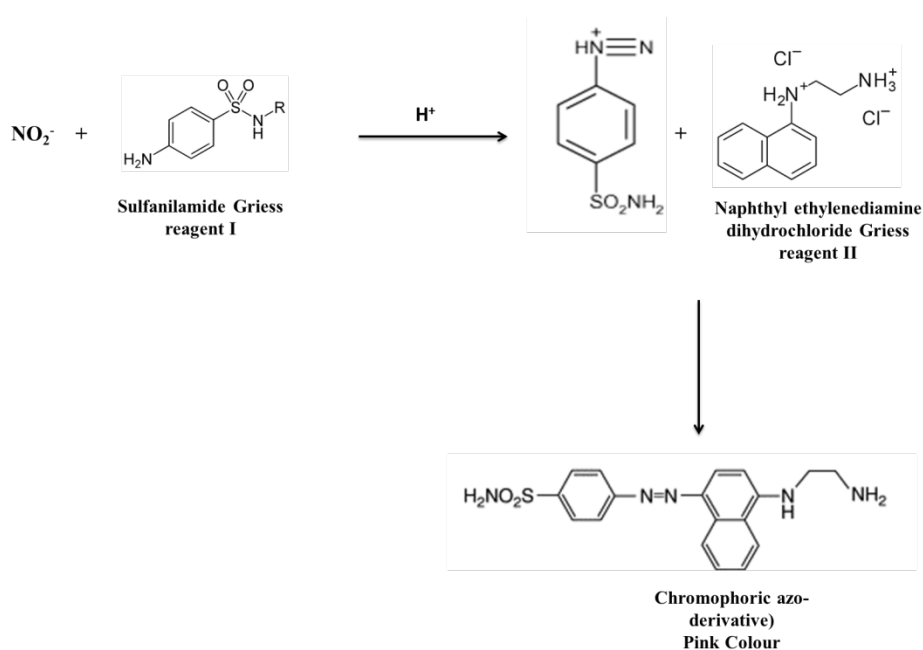
Figure 2.4: Detection of nitrite by the Griess assay.

For the reaction, reagent I and reagent II were mixed in equal ratio. Nitrite standards were prepared by dissolving 0.0345g of sodium nitrite ($NaNO_2$) in 5 ml of complete culture medium to give a 100mM stock solution which was further diluted to 1mM and used to construct the standard curve as shown in the Table 2.1.

Table 2.1: Preparation of a nitrite standard curve.

Concentration of standard NaNO$_2$ (mM) required	NaNO$_2$ (1mM) in (µl)	Complete Culture Medium (µl)	Final Concentration in 100µl added to each well (nmole/100µl)
0.1	100	900	10
0.05	50	950	5
0.04	40	960	4
0.03	30	970	3
0.02	20	980	2
0.01	10	990	1
0	0	1000	0

100 µl of each standard solutions and unknown samples were added in triplicates in 96 well plate followed by the addition of 100 µl of the Griess reagent mix. The plate was incubated at room temperature for 15 minutes and absorbance values read at 540nm using a MultiSkan Ascent Plate Reader (Labsystem). A representative standard curve is shown in Figure 2.5. A regression equation was used to quantify the amount of nitrite present in samples.

$$y = 0.0995x$$
$$R^2 = 0.9954$$

Figure 2.5: Nitrite standard curve.

The nitrite standard curve was constructed as described above. The average absorbance measurement of the blank was subtracted from the absorbance values of each standard used. The average of triplicates was plotted against the $NaNO_2$ concentrations used. This standard curve is the representative of several Griess assays carried out during the course of the studies.

2.4- Cell Lysis:

10X lysis buffer was prepared using 10 % of sodium dodecyl sulfate (SDS) + 10 mM of Tris-Base at (pH 7.5) and stored at room temperature. When required, the stock was diluted with DDW by ten folds to get the working solution. The lysis buffer was then pre heated to 95^0C prior to addition to cell monolayer kept on ice. Cell lysates were then collected in eppendorf tubes and subjected to sonication for 30 second with 30 second interval for 5 times. Lysates were reheated and centrifuged using a bench-top microfuge at 10000 rpm for 5 minutes. The supernatant was collected for analysis and the cellular debries discarded.

2.5- Protein Assay:

Total proteins were quantified using the bicinchoninic acid assay (BCA). Its principle is bases on the reduction of cupric ions (Cu^{+2}) to cuprous ions (Cu^{+1}) by proteins in an alkaline medium which is a selective and sensitive colorimetric detection of the cuprous ions. Chelation of one Cu^{+1} ion by two molecules of BCA results in purple colour formation. The intensity of the colour is proportional to the amount of protein in the lysate sample. The reaction is shown in Figure 2.6 (Smith *et al.*, 1985). A serial dilution of BSA stock solution (10mg/ml) in water was used to construct a protein standard graph within a concentration ranging of 0.2-6 µg/µl as shown in Table 2.2.

Protein + Cu^{2+} $\xrightarrow{\quad OH^- \quad}$ Protein +Cu^+

Cu^{2+} + 2

Bicinchoninic acid

BCA Cu^+ complex
Purple colour
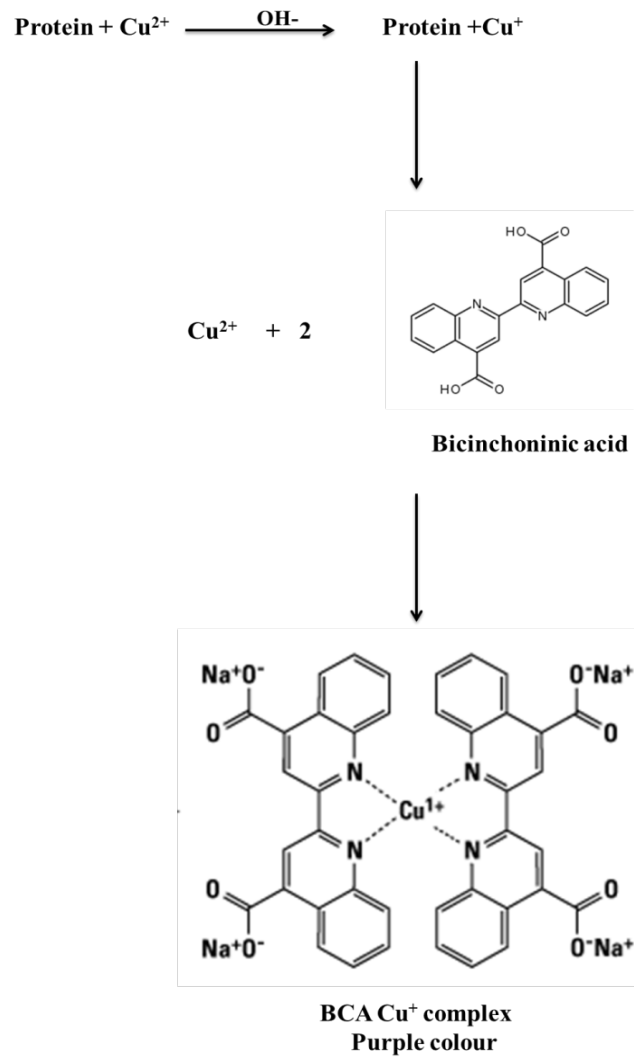
Figure 2.6: Detection of protein by BCA reagents.

Table 2.2: Preparation of protein standard graph using BSA.

No.	Protein per well (µg)	10mg/ml BSA (µl)	DDW (µl)	Final concentration (µg/µl)
1.	0	0	1000	0
2.	1	20	980	0.2
3.	2	40	960	0.4
4.	3	60	940	0.6
5.	5	100	900	1
6.	10	200	800	2
7.	15	300	700	3
8.	20	400	600	4
9.	25	500	500	5
10.	30	600	400	6

The BCA reagent was prepared by mixing reagent B and A in a 1:50 ratio. A non-sterile 96 well plate was then set up as follows:

BSA Standards: 5µl standard solution + 5µl 1X lysis buffer + 100µl (BCA Reagent Mix)

Samples: 5µl DDW +5µl lysate sample + 100µl BCA.

The plate was then incubated at room temperature for 40-45 minutes on a shaker before reading the absorbance at 620 nm. The absorbance readings of the standards were used to construct the standard curve (Figure 2.7) and regression equation was used to calculate protein in unknown samples.

$y = 0.0063x$
$R^2 = 0.9985$
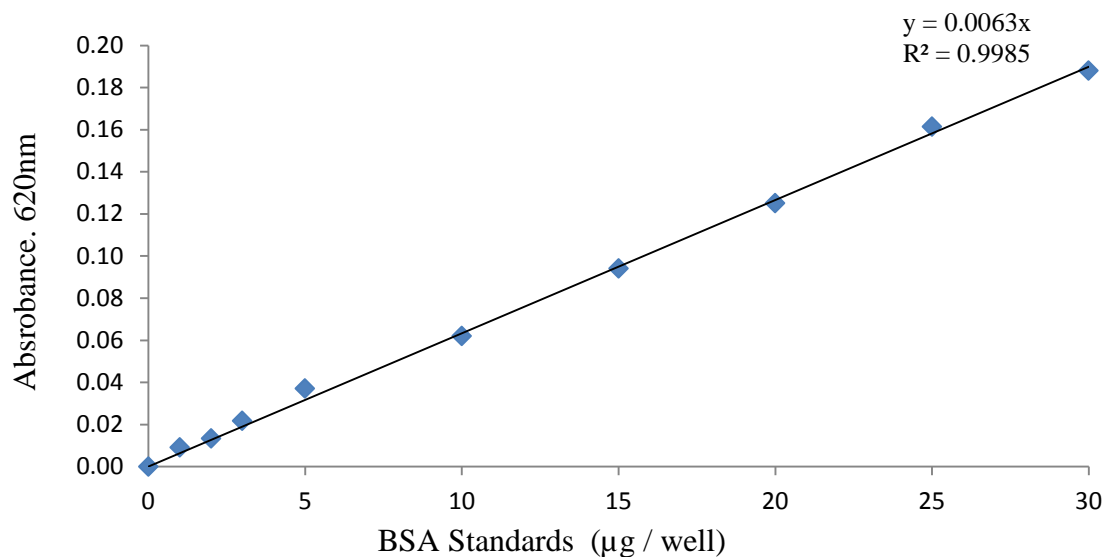
Figure 2.7: Protein standards curve.

The protein standard curve was constructed as described above. The average absorbance measurement of the blank was subtracted from the absorbance values of each standard used. The average of triplicates was plotted against the BSA concentrations used. This standard curve is representative of the protein assays carried out during the course of the studies.

2.6- Calcium assay using the QuantiChrom™ calcium assay kit (DICA-500 ™):

In parallel to the BCA assay, cell lysates were subjected to calcium quantification using the QuantiChrom™ calcium assay kit (DICA-500). A phenolsulphonephthalein dye in the kit forms a very stable blue coloured complex specifically with free calcium. The intensity of the colour, measured at 620 nm, is directly proportional to the calcium concentration in the sample. The concentration of calcium can be quantified by comparing the intensity of the cell lysate sample a standard curve/line of best fit. The standard curve is obtained from reactions of the phenolsulphonephthalein dye with known serial dilutions of free calcium, as shown in Table 2.3. The equation of the graph for the line of best fit was used to determine the concentration of free calcium in the cell lysates.

Calculation calcium concentration in nanomoles (nM):

20 mg in 100ml of calcium is equivalent to 5mM according to the protocol

5000 μmoles in 1000 ml   (As concentration is always in 1liter)

Then in 1 ml is 50μM,   therefore, 5000μM in 1 litre   or 5μM in 1ml   or 5nM in 1μl

Therefore, for 20 mg/dl is equivalent to 5nM/μl. So we use 5μl of standards which hence 25nM for 20mg/dl concentration of calcium.

Table 2.3: Preparation of a calcium standard graph:

No.	Volume of calcium standard solution (5mM or 20mg/dl) (µl)	Volume of DDW in (µl)	Final concertation (mM)
1.	100	0	5
2.	80	20	4
3.	60	40	3
4.	40	60	2
5.	30	70	1.5
6.	20	80	1
7.	10	90	0.5
8.	0	100	0

5µl of standards or cell lysates were added in triplicate into 96 well plates. Equal proportions of reagent A and B were mixed and 200µl added to each well. The plates were then incubated for 5 minutes at room temperature and absorbance values were recorded at 620 nm as per manufacturer guidelines using a MultiSkan Ascent Plate Reader (Labsystem). An example of a standard curve routinely produced is shown in Figure 2.8.
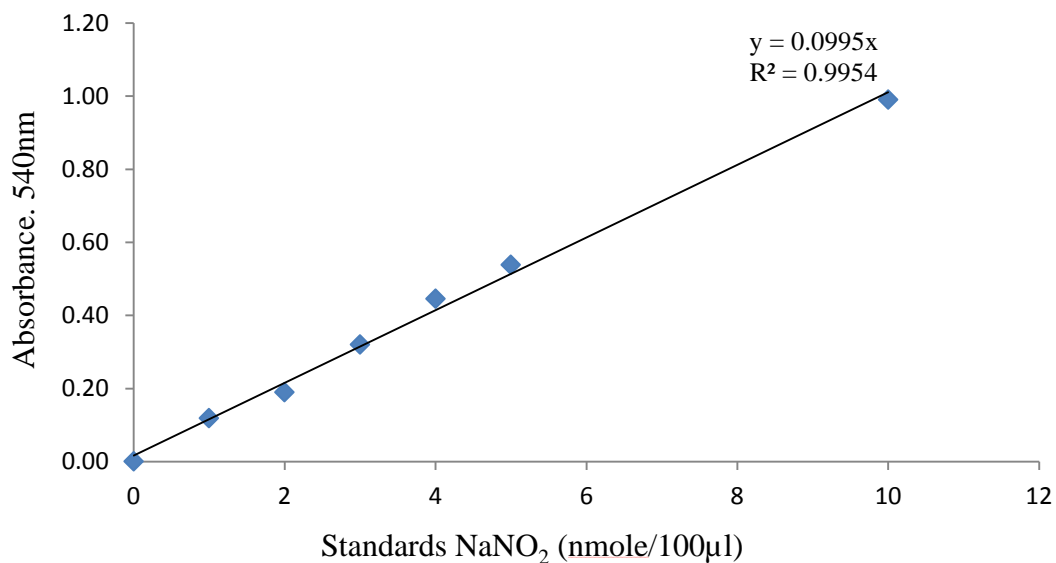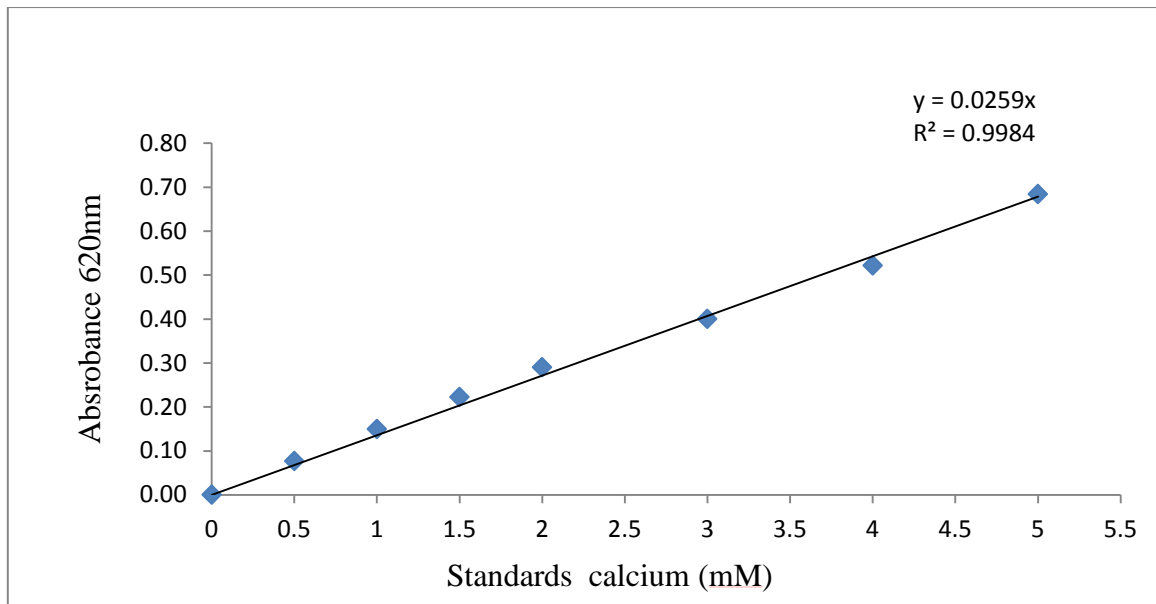
Figure 2.8: Calcium standard curve.

The Calcium standard curve was constructed as described above. The average absorbance measurement for the blank was subtracted from the absorbance values of each standard used. The average of the triplicates was plotted against the calcium concentration used. This standard curve is representative of several calcium standards constructed during the course of the studies. The equation of the graph for the line of best fit was used to determine the concentration of free calcium in the cell lysates.

2.7- Determination of cytotoxicity by MTT assay:

This assay was used to determine the relative cytotoxicity of various treatment conditions on cells by monitoring the metabolism of 3-(4, 5-dimethyl-2-thiazolyl)-2, 5-diphenyl-2H-tetrazolium bromide (yellow colour) to form formazan (purple colour) which is formed by viable cells as shown in Figure 2.9. The intensity of the colour is directly proportional to the viability of the cells (Mosmann, 1983).

Tetrazolium salts (Yellow colour)   Formazan (Purple colour)
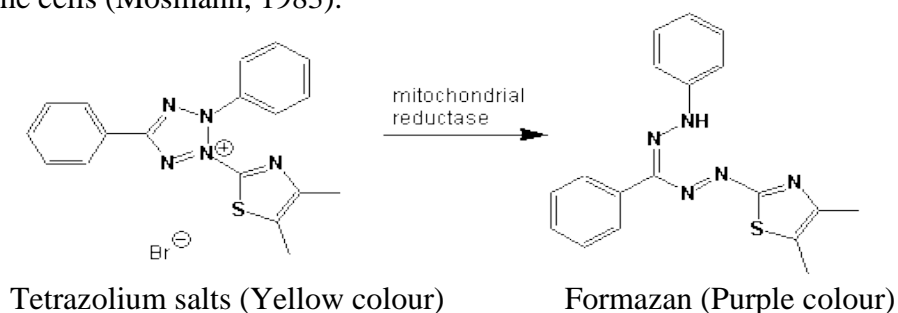
Figure 2.9: The formation of formazan from MTT metabolism.

A 5mg/ml stock of MTT solution was prepared in 1X PBS, which was diluted 1:10 in complete cell culture medium to achieve a final concentration of 0.5 mg/ml. Cells incubated under different experimental condition were then incubated with MTT (0.5 mg/ml) in fresh culture medium for 4 hours. Cellular supernatant were discarded and formazan complexes dissolved using 200µl of iso-propanol. 200µl of purple coloured isopropanol were then transferred into a 96 well plate and read at 540 nm. Absorbance of control cells (without any treatment) were used a 100% to calculate relative cellular viability.

2.8- Alizarin Red Staining for mineralised plaques:

Alizarin Red Staining or 1, 2-dihydroxyanthraquinone is one of the dihydroxyanthraquinone which exchanges hydrogen for hydroxyl (OH) resulting in the formation of 1, 2-dihydroxyanthraquinone. 2g of alizarin red staining was dissolved in 100 ml DDW and the pH was adjusted to between 4.1 - 4.3. 1X of ARS was prepared from the stock by diluting in DDW. For each experiment, RASMCs were incubated in the presence of CB (consisting of 7 mM $CaCl_2$ and 7 mM β-GP) with or without LPS, IFN-γ or both. Cells were fixed at the end of the relevant incubation periods and incubated with 10% formaldehyde for 15 minutes at room temperature. After fixing, cells were washed three times (two minutes each) using DDW. The dye solution was added and incubated with the RASMCs for 20-30 minutes at room temperature. After this period, the ARS was removed and 1 ml of DDW was added to the wells. The amount of ARS added was dependent on the type of plate used. For instance, with 24 wells plate 500µl/well ARS was added. Stained cells were observed using the Olympus inverted microscope at 10x magnifications and captured using the GX capture programme and software. A representative photograph of ARS stained plaques is shown in Figure 2.10.
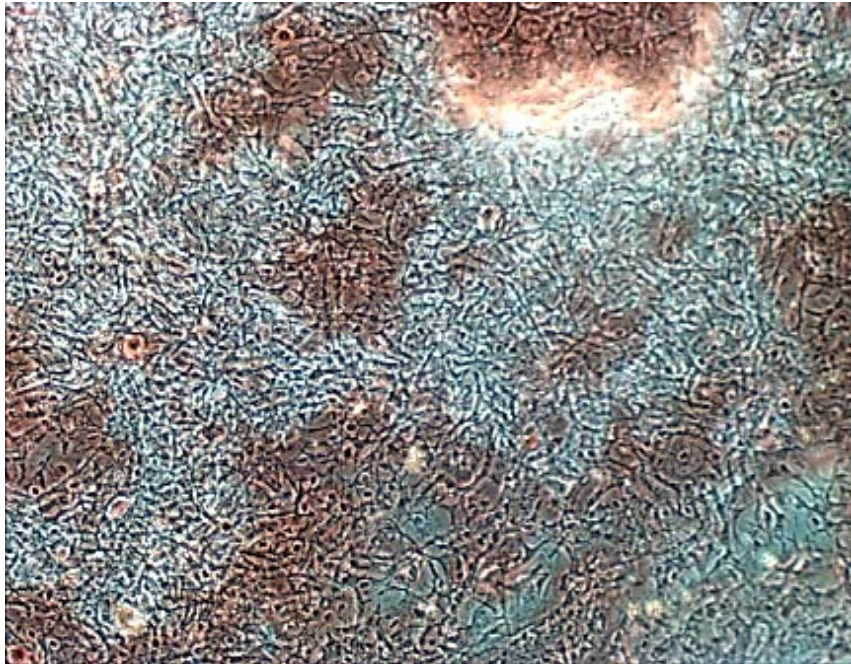
Figure 2.10: Staining of calcific plaques by ARS on rat cultured smooth muscle cells.

Rat aortic smooth muscle cells cultured to ~90% confluency were incubated with a combination of 7 mM $CaCl_2$ and 7 mM β-GP for 5 days. Cells were treated with ARS at the end of the treatment period. The images are representative of 3 individual experiments which were taken with an Olympus inverted microscope at 10x magnification and captured using the GX programme.

2.9. Identification of HA crystal [Ca$_{10}$ (PO$_4$)$_6$(OH)$_2$] by FT-IR:

Fourier Transform Infrared Spectroscopy was used in parallel to investigate the chemical nature of deposited minerals on cellular monolayers. Chemical bonds within any molecule give particular vibrational frequencies upon exposure to infra-red beam which can be used to identify the molecule or complex. Thus, using FT-IR allows for the detection of HA crystals formed when cells calcify following incubation with calcification buffer.

Cells were plated in T-25 flasks and incubated under different experimental conditions. At the end of the incubation period, the medium was aspirated and the cells washed gently in absolute ethanol. Cellular monolayers were then scrapped in methanol using a rubber policeman cell scrapper and centrifuged at 2000rpm for 2 minute to make a pellet. The pellet was left to dry out completely at room temperature prior to FT-IR analysis. A Perkin Elmer FT-IR spectrometer-Frontier was used to analyse the chemical characteristics of mineral plaques including HA complex which was identified at a wavenumber of 1080 -1089 (Figure 2.11). Obtained spectra were then analyse using Thermo scientific *Omnic* software. Other molecules identified include amide I (-CON) at wavenumber 1620-1632 cm^{-1}, calcium carbonate (-CO$_3^{2-}$) at wavenumber 1400-1480 cm^{-1} and phosphate at wavenumber 1154, 1075,1046, and 1010 cm^{-1}(Figure 2.11).

Identifying peaks:

The wavenumbers identifying a compound by the presence of a specific peak in the FT-IR output were based on the literature review listed in the table 2.4. For example, the asymmetric stretching of phosphate groups (PO$_4^{3-}$) is observed by a peak of absorption (1075 cm^{-1}) (Destainville, *et al*., 2003) while HA crystals are observed at wavenumber (1085 cm^{-1}) (Alò *et al.*, 2009; kwon *et al*., 2003).

Table 2.4: Spectrum of molecules detected by FT-IR in cell cultures/ tissues

Data from Literature review		
Stretch or bend of chemical compound	**wave number (cm^{-1})**	**Citation**
Amide I-(CON stretch), Amide II (NOH bend), Amide III (COH stretch, NOH bend)	1620-1632, 1515-1540, 1216-1290	(Alò *et al.*, 2009; Dritsa, 2012; Lin *et al.*, 2007)
Calcium Carbonate (Calcite -CO_3^{2-})	1430-1480	(Raynaud, *et al.*, 2002)
Tricalcium phosphate (TCP), β-Tricalcium phosphate (β- TCP)	700-750, 690	(Destainville, *et al.*, 2003)
Phosphate (PO_4^{3-})	1154, 1075,1046, 1010 & 1020 or 975	(Destainville, *et al.*, 2003; Han J-K., *et al.*, 2006; Mobasherpour and Heshajin,2007; Raynaud, *et al.*, 2002)
HA crystal $C_{10}(PO_4)_6(OH)_2$	1080 - 1089	(Alò *et al.*, 2009; Kwon, *et al.*,2003)
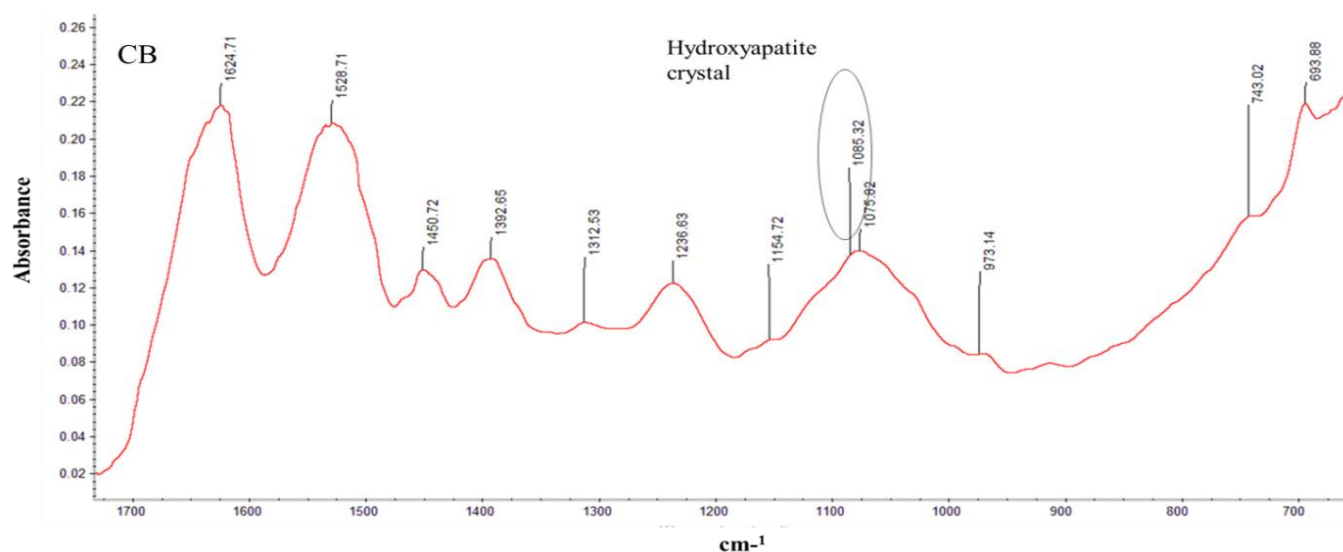
Figure 2.11: Spectrum of HA crystal formed in RASMCs.

RASMCs cultured to approximately 90% confluency were incubated with a CB for 5 days (containing 7 mM $CaCl_2$ and 7 mM β-GP). Thereafter these were scraped from the plate, washed with 100% ethanol and a cell pellet prepared by centrifugation, before being subjected to FT-IR analysis. The cell pellet was scanned using a Perkin Elmer FT-IR spectrometer-Frontier. Infra-red absorption by the pellet was measured, and the peak at 1080-1089 cm-[1], confirming the presence of HA crystals detected by *Omnic* software. The trace is representative of 3 individual experiments.

2.10- Western blot:

In western blotting, polyacrylamide gel (SDS-PAGE) is used to separate specific proteins that are transferred to a polyvinylidene fluoride (PVDF) membrane, making it easy for the antigen to bind to the antibody (Lee *et al*., 2000). There are normally two antibodies (primary and secondary) used for detecting the specific protein, as depicted in Figure 2.12.
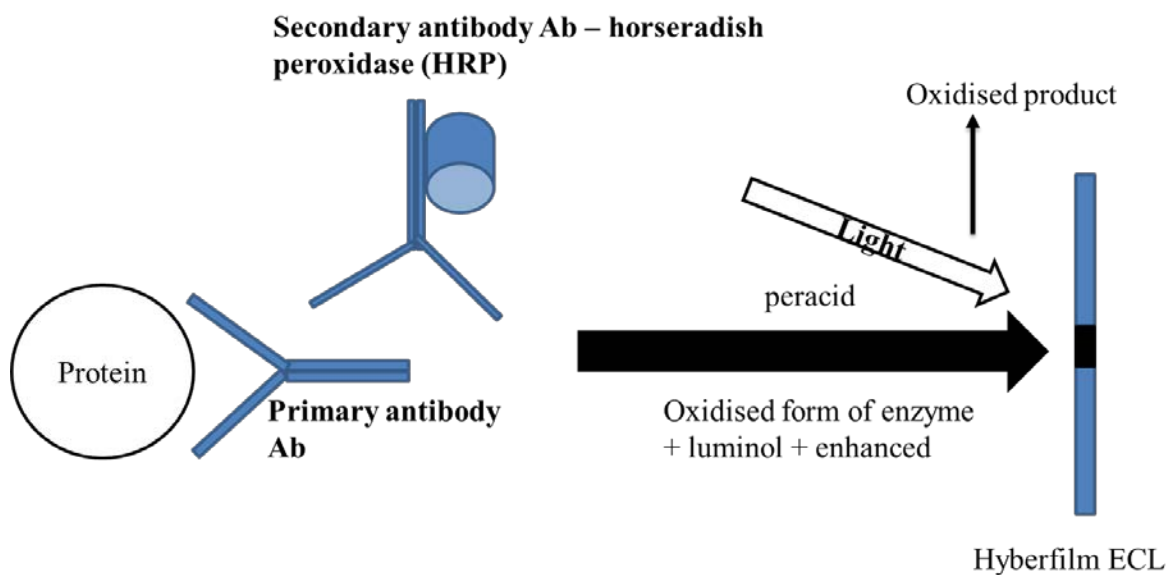
Figure 2.12: Detection of proteins by western blotting

Glass plates were set up for the gel apparatus and the gel cast starting with the resolving gel using: DDW (2.32ml/gel), 30% acrylamide (1.33ml/gel), resolving buffer (1.25 ml/gel) (1.5M Tris-HCl, pH8.8), 10% SDS (50µl/gel), 10% ammonium per sulphate (APS) (50µl/gel) and tetramethylethylenediamine (TEMED; 3µl/gel). The stacking gel was prepared next using DDW (1.22ml/gel), 30% acrylamide (0.26ml/gel), stacking buffer (0.5 ml/gel) (0.5M Tris-HCl, pH6.8) and 10% SDS (20µl/gel). There was also 10% ammonium per sulphate (APS; 10µl/gel) and TEMED (2µl/gel). A well-forming comb was inserted and the gel allowed to set, forming wells for loading samples. Once the stacking gel had polymerised the comb was removed and the gels transferred into the electrophoresis apparatus filled with 1x

tank buffer consisting of 1X ultra-pure 0.025 M Tris/ 0.192 M Glycine/ 0.1% SDS. Samples were loaded into the wells ensuring 20 µg of protein was loaded into each lane.

The apparatus was run at 220v and 20 mA per gel until the samples migrated through the stacking gel. At this point, the current was changed to 25 mA per gel and the samples allowed to resolve through the resolving gel. The latter was then cut to size, eliminating the stacking gel. Filter papers and PVDF membrane were cut to the size of the gel which was normally 6 cm in length and 9 cm in width. The PVDF membrane was soaked in methanol for 15 - 20 sec and then washed in DDW to remove excess methanol. The filter papers and gel were soaked in 1X transfer buffer prepared from a 10X stock consisting of 48mM Tris base (pH 7.5), 39mM glycine and 0.0375% SDS. The filter papers, membrane and resolving gel were set up in a sandwich as shown in Figure 2.13. Transfer buffer was poured onto the sandwich and a rolling pin used to remove any bubbles between the sandwich. The transfer cell was then connected to the mains and run for 15-20 minutes at 25 mA/gel.

←	Cathode
←	Blotting or filter paper
←	Gel
←	PVDF or nitrocellulose
←	Blotting or filter paper
←	Anode
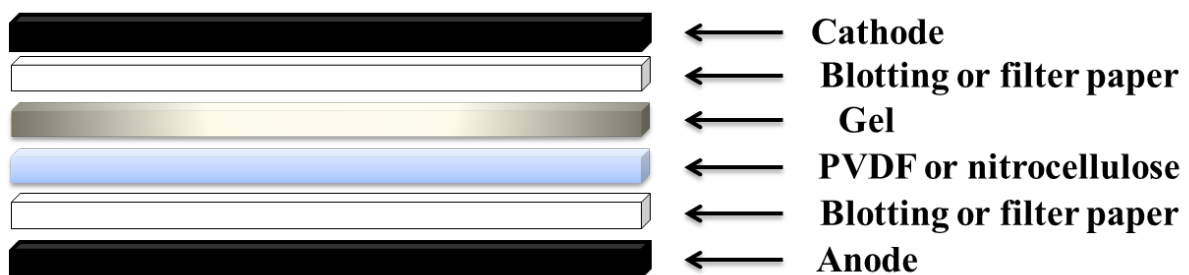
Figure 2.13: Sandwich of filter paper, membrane and gel for western blotting.

After 15 minutes, the membrane was removed from the transfer cell into blocking buffer consisting of 10 ml washing buffer (10 mM Tris-Base pH 7.5 and 100 mM NaCl) , 90 ml DDW, 100µl tween and 5g fat free milk or 3 g of BSA (for transcription factor or signalling molecule). The membrane was blocked for 1 hour before placing in a hybridization bag and sealed with the primary antibody of choice which was either iNOS antibody diluted 1:2500 in blocking buffer, Runx2 antibody diluted 1:200 in blocking buffer, phosphor-p38 MAPKs

antibody diluted 1:1000 in blocking buffer, phospho-Akt antibody diluted 1:1000, or a phosphop44/42 MAPK antibody diluted 1:2000 in blocking buffer. The membrane was then incubated on a shaker overnight at 4 ^{0}C in the cold room. At the end of this period, the membrane was removed from the hybridization bag, washed for 30 minutes, changing the washing buffer every 10 minutes before incubating with HRP conjugated β-actin antibody at a dilution of 1:10,000 in blocking buffer. Simultaneously, anti-biotin diluted at 1:1000 in blocking buffer dilutions and appropriated HRP conjugated secondary antibody at manufacturers recommended dilution were also added to the PVDF membrane for 1 hour at room temperature. The membrane was washed again for 30 minutes with the washing buffer changing every 10 minutes. After the last wash, the membrane was incubated with electrochemiluminescence (ECL) detection reagent. The reagents were prepared as reagent A (100 mM Tris pH 8.5- 5ml /gel + 25 µl 90 mM p- coumaric acid+ 50 µl 250 mM luminol) and reagent B (100 mM Tris PH 8.5- 5ml /gel + 3µl 30% H_2O_2). Both ECL reagents A and reagent B were mixed prior to addition to the PVDF membrane for 1-5 minutes before exposing the membrane to an auto-radiographic film in a cassette for 5-30 seconds (detecting iNOS) or 1-1.5 minutes (detecting β-actin). The film was subsequently developed using a developer solution for 30 sec, washed with water and placed into the fixer for 1 min before washing again in water and allowed to dry in air at room temperature. The bands visualized were quantified using scanning densitometry.

2.11- Data analysis:

All the experiments were performed at least three times except stated otherwise.All the experiments were performed at least three times except when stated otherwise. The letter (n) in each legend represents the number of aorta isolated from the male Sprague Dawley rat. An experiment denotes an independent culture (P3-P6) from a different rat. The data is expressed as means ± S.E.M. Statistical significance of two means was performed by independent or paired t test as appropriate. Statistical differences of three or more means was tested using one way analysis of variance (ANOVA) followed by post hoc Dunnett's test. Significance was tested at 95% confidence interval. Significance were denoted as *, **, *** or #, ##, ### if p values are less than 0.05, 0.01 and 0.001 respectively. All statistical analysis was carried out using GraphPad Prism version 5.0.

CHAPTER III

RESULTS

Regulation of vascular calcification and induced nitric oxide synthesis by calcification inducers and/or inflammatory mediators

3.1- Introduction:

As already discussed in the introduction, the role of NO in the development of VC is controversial with mixed reports claiming that NO promotes as well as inhibits the process. Moreover, where levels of NO have been shown to change, it has not been clearly demonstrated whether this is a consequence of or a prerequisite for calcification. To address these issues a series of experiments were designed and conducted in this thesis aimed specifically at establishing unequivocally whether VC is either promoted or blocked by NO. To start with, models of *in vitro* calcification, and of iNOS expression and NO production had to be personally established for this project using protocols that have been routinely used in our laboratory. The establishment of these models is described in this chapter. Further studies were also conducted to determine whether inflammatory mediators such as LPS and/or IFN-γ regulate calcification induced by $CaCl_2$ (7mM), β-GP (7mM) or in combination (CB). Additionally, other experiments were conducted to investigate how iNOS expression and NO production may be regulated under calcifying condition.

To induce calcification, subconfluent cells in culture were incubated with $CaCl_2$ (7mM), β-GP (7mM) alone or in combination. Calcification was monitored and detected by measuring the accumulation of calcium, staining HA crystal formed with ARS and by conducting FT-IR analysis of apatite crystals. The induction of iNOS was initiated using LPS and IFN-γ which our group had demonstrated causes sustained induction of iNOS in cultured RASMCs (Wilemen *et al*., 1995).

3.2: Experimental protocol:

Cells were cultured and quantification of NO production, total protein and calcium measurements as well as western blotting were performed as described in chapter 2, section 2.3, 2.5, 2.6 , and 2.10, respectively. In parallel experiments, ARS and FT-IR analysis was also performed as previously described in the method (sections 2.8 and 2.9, respectively).

3.2.1- Induction of calcification and nitric oxide synthesis:

Rat aortic smooth muscle cells were cultured as described previously (Methods, Section 2.1.2 and 2.1.3) and seeded in 24 well plates to reach a confluency of ~90 % in 72 hours. Calcification was induced by incubating cells with either $CaCl_2$, β-GP or a combination of both at 7mM each (CB) for 24 hours followed by the addition of same agents again at 48 hours. To establish the induction of iNOS, cells were incubated with LPS (100µg ml^{-1}) and/or IFN-γ (100 U ml^{-1}) for 24 hours followed by the addition of same agents again at 48 hours. Changes in calcification, NO production and iNOS expression were evaluated over a time course of 1, 3, 5 and 7 days.

3.3-Results:

3.3.1- Induction of calcification of RASMCs using CaCl$_2$, β-GP or in combination:

Cells incubated with CaCl$_2$ induced significant calcification throughout the time course of 1, 3, 5 and 7 days. On the other hand, β-GP did not induced significant calcification compared to control at any of the time courses. Furthermore, the degree of calcification induced by β-GP at all time points was lower when compared to CaCl$_2$ alone or CB (Figure 3.1). This suggests that CaCl$_2$ alone is able to induce calcification and the effect was significantly elevated to a maximum on day 5 (1.4 $\pm$ 0.2 nmole. μg^{-1} protein), decreasing on day 7 (1$\pm$ 0.23 nmole. μg^{-1} protein) but remaining higher than control (0.19$\pm$ 0.06 nmole. μg^{-1}protein), β-GP (0.26$\pm$ 0.04 nmole. μg^{-1} protein) or CB (1 $\pm$ 0.02 nmole. μg^{-1} protein) (Figure 3.1).

In addition, the degree of calcification or at least the levels of calcium detected was not significant different between cells incubated with CaCl$_2$ alone or in combination with β-GP.
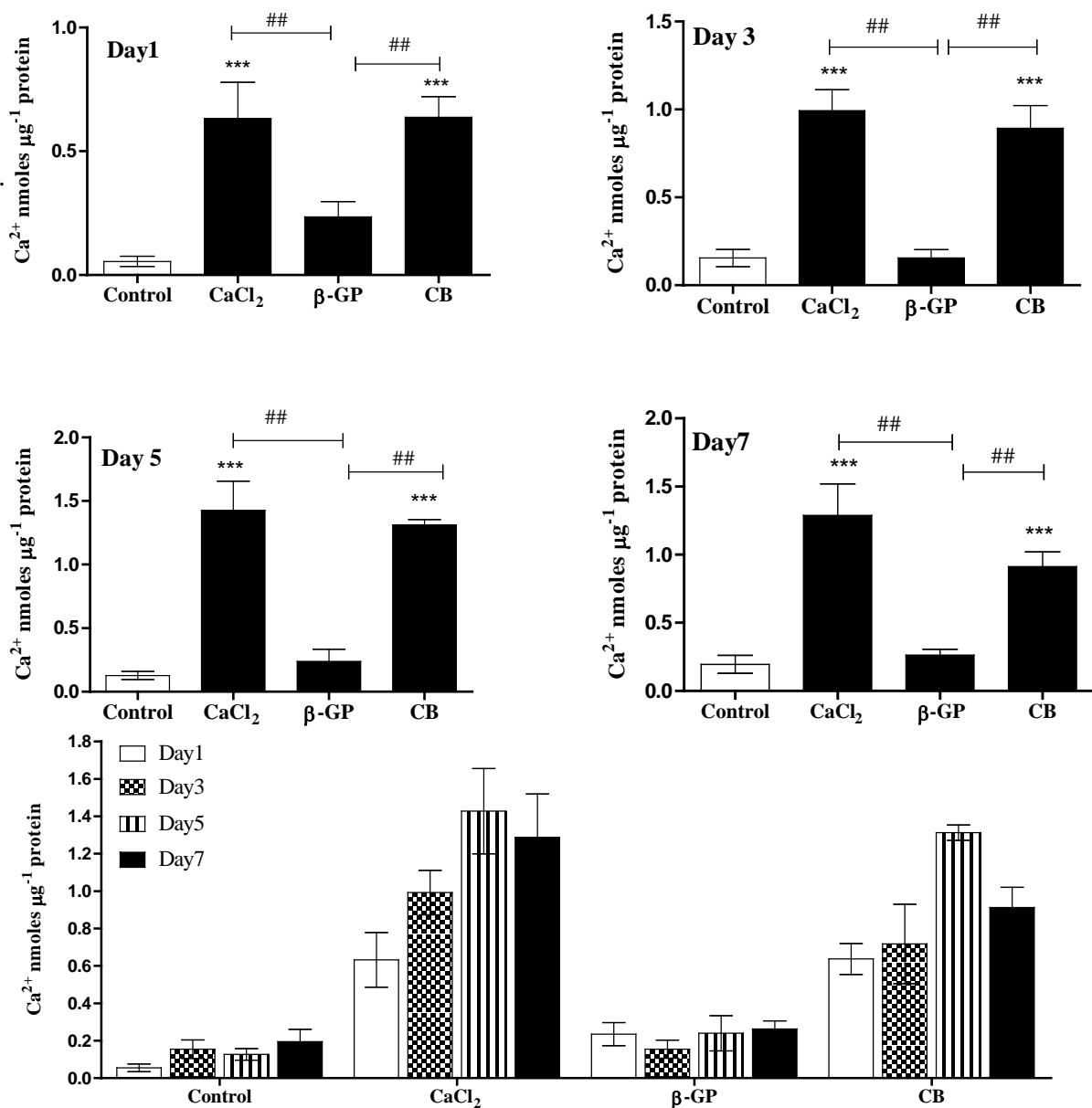
Figure 3.1: Induction of calcification of RASMCs using CaCl₂, β-GP or in combination

Cells were cultured to ~90% confluency and incubated either with culture medium alone (control), CaCl$_2$ (7mM), β-GP (7mM), or in combination (CB) for 1 to 7 days. Total calcium was quantified as described in the methods (Section 2.6). The data represents means ± S.E.M. from 4 experiments. *** denotes $p < 0.001$ when compared to control and #, ## denote $p < 0.05$ and $p < 0.001$ as shown in the figures.

3.3.2- Staining of calcific plaques with ARS:

Rat aortic smooth muscle cells were incubated with complete cell culture medium, $CaCl_2$, β-GP or CB for 5 days followed by staining with ARS described earlier (Chapter 2 section 2.8). Control cells and those incubated with β-GP did not reflected calcified plaques upon ARS staining. Interestingly, although $CaCl_2$ induced a similar degree of calcification compared to CB, ARS confirmed that calcified plaques were evident only in cells incubated with the CB and not with $CaCl_2$ alone (Figure 3.2).
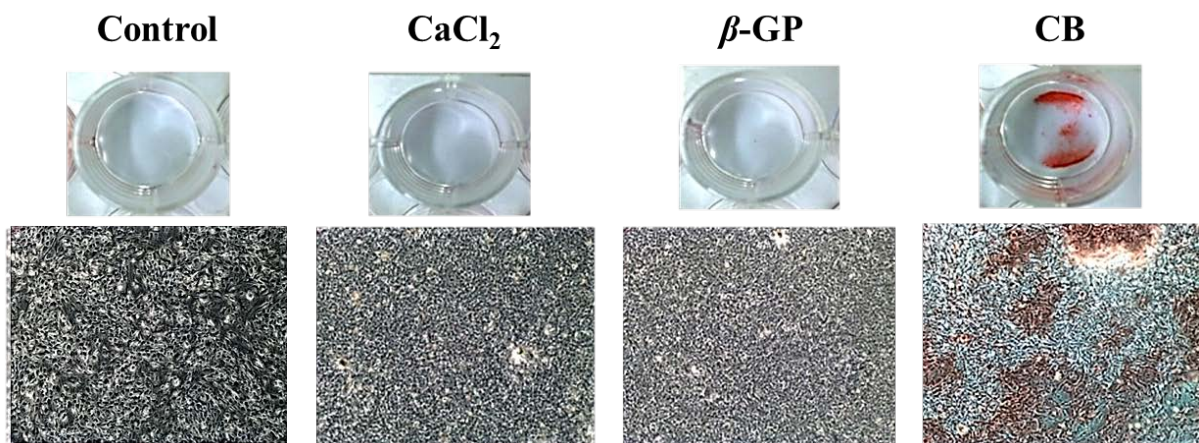
Figure 3.2: Alizarin red staining of calcified RASMCs.

Cells were cultured to ~90% confluency and incubated either with culture medium alone (control), $CaCl_2$ (7mM), β-GP (7mM), or in combination (CB) for 5 days. Cells were treated with 1x ARS at the end of the incubation period as described in the methods (Section 2.8). The images are representative of 3 individual experiments which were taken with an inverted Olympus microscope at 10X magnification using the GX capture programme.

3.3.3- Detecting HA crystals by FT-IR analysis:

The chemical nature of the calcified plaques was investigated by FT-IR spectroscopy. The spectra generated identified the presence of Amide-I, Amide-II, Amide-III and carbonate peaks at 1630-1637 cm^{-1}, 1514.53-1522.37 cm^{-1}, 1234-1243.99 cm^{-1}, and 1430-1450 cm^{-1} respectively in cell lysates analysed irrespective of the incubation conditions (Figure 3.3). Cells incubated with CaCl$_2$ reflected calcite (CO$_3^{2-}$) with a peak at 1430-1480 cm^{-1} and in samples treated with β-GP phosphate or mineral phosphate spectrum was detected at 1026, 1075,1072, 1055, 1154, and 1158 cm^{-1}. Hydroxyapatite crystals usually detected within the range 1089 – 1080 cm^{-1} was not found in the conditions above. In contrast, HA was present in cells treated with CB and this was detectable at 1085 cm^{-1} (Figure 3.3). Defining peaks of various components detected following FT-IR analysis are summarised in Table 3.1.

β-GP

CB

Hydroxyapatite crystal
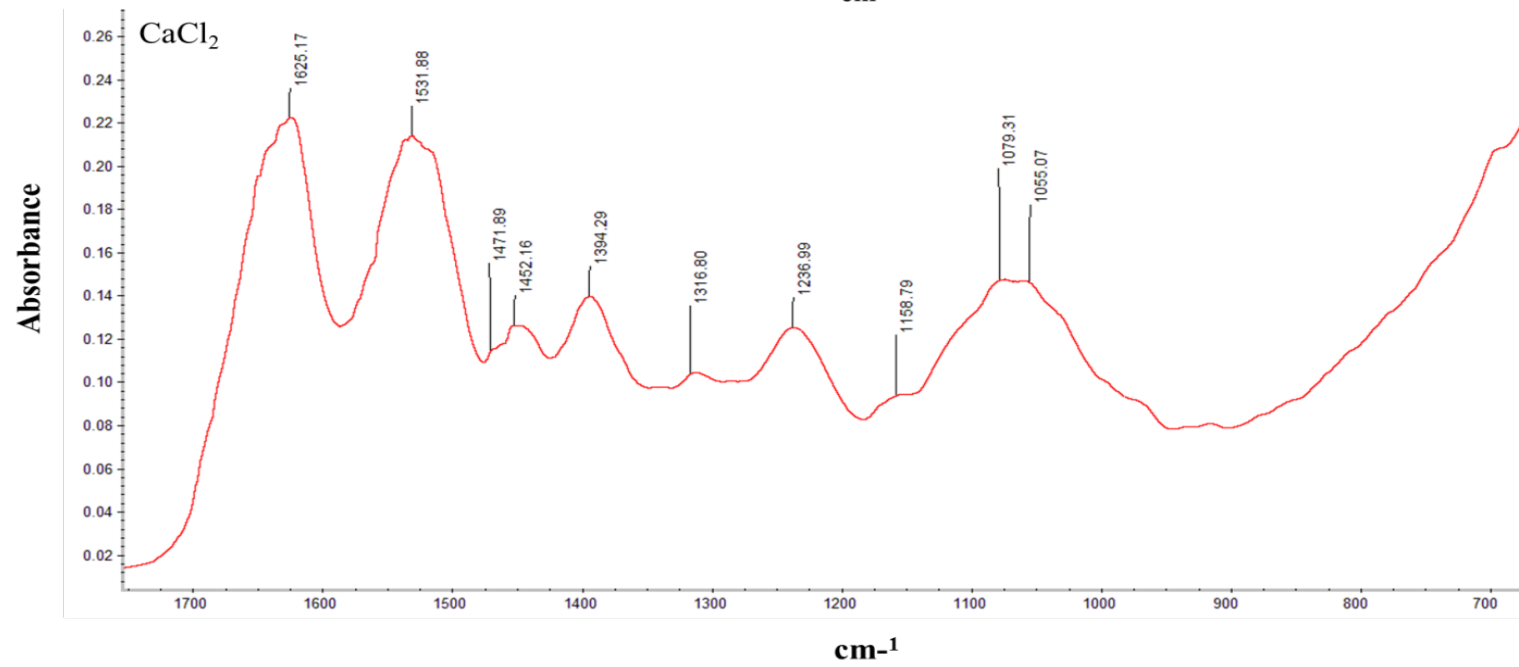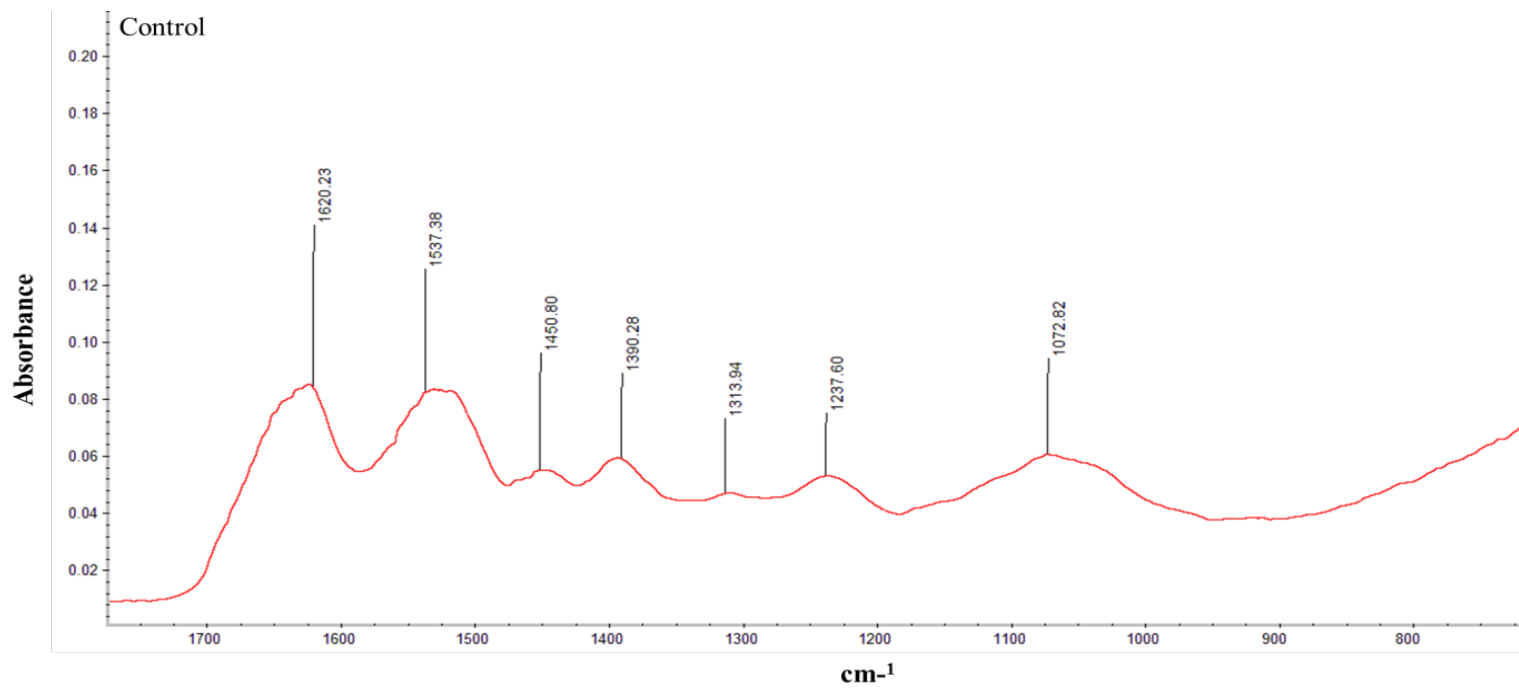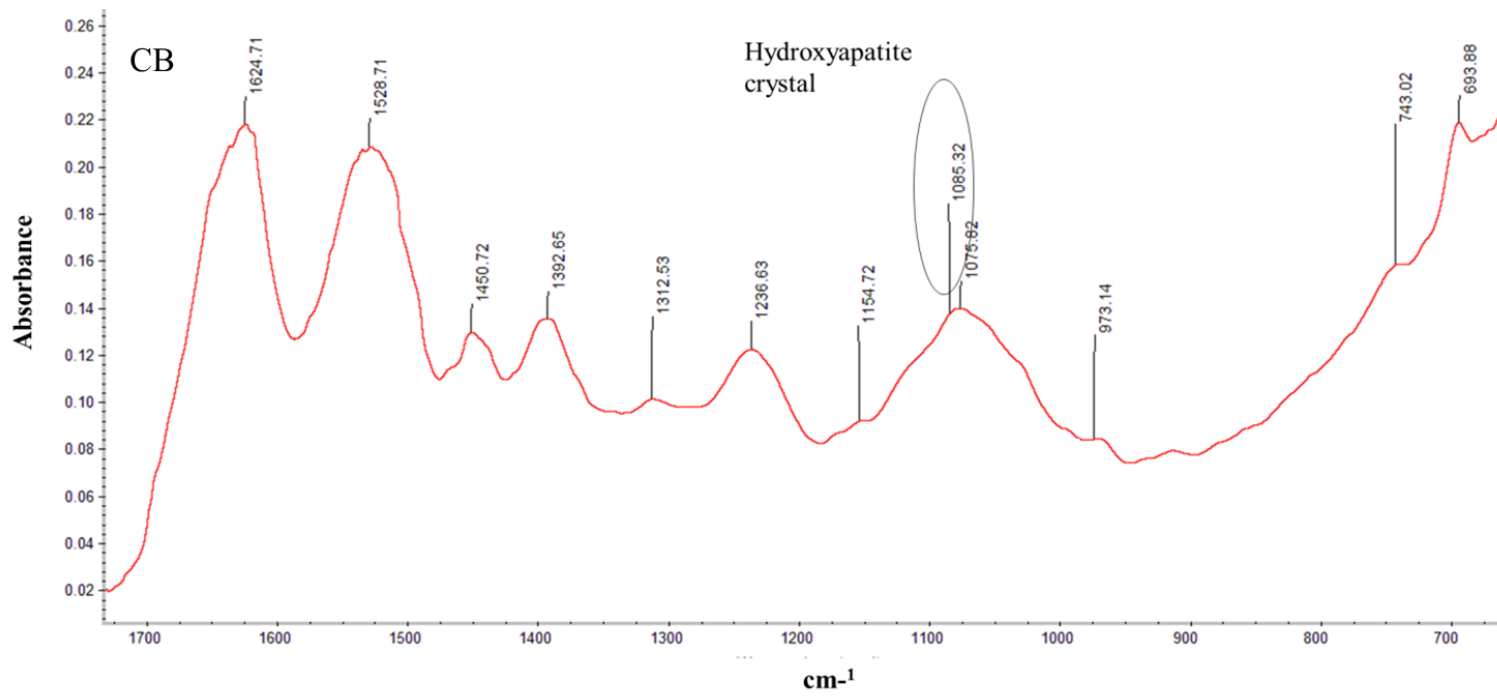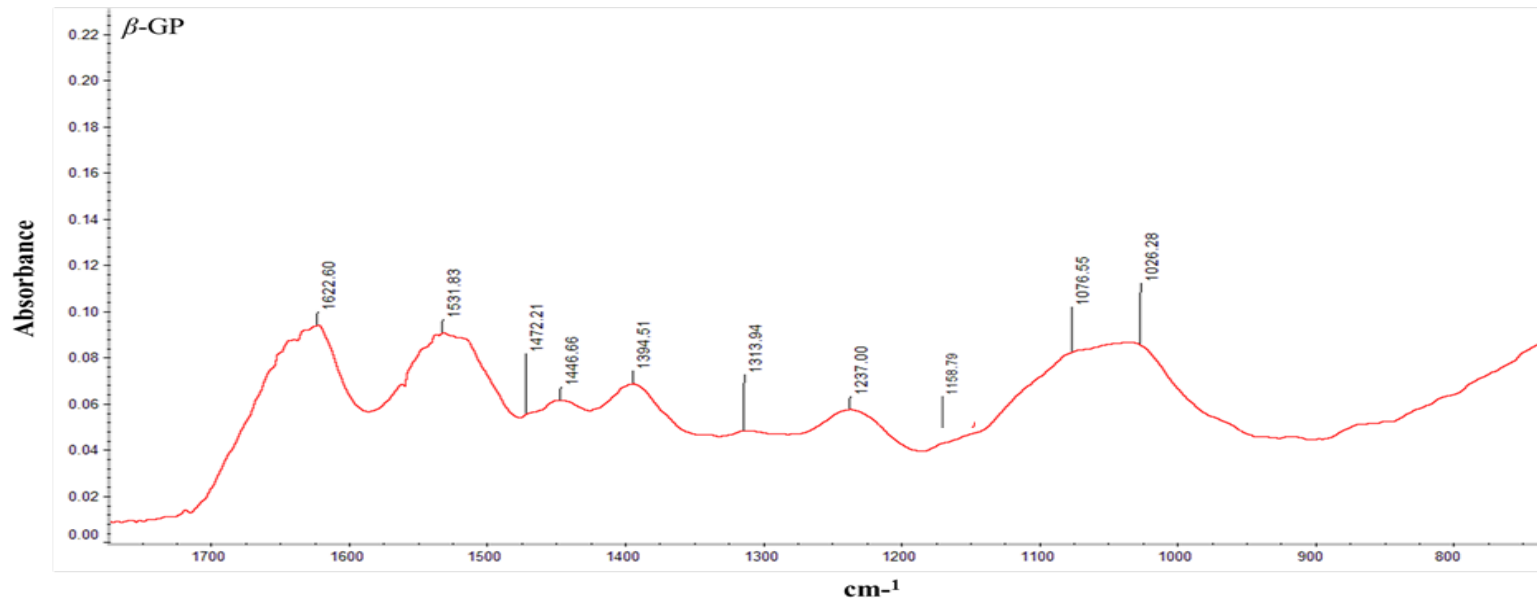
Figure 3.3: FT-IR spectrum analysis of activated RASMCs.

Cells were treated with medium alone or with calcification inducers (7mM $CaCl_2$, 7mM β-GP or in combination- CB) for 5 days. Cells were washed and scraped with 100% ethanol at the end of the incubation period and subjected to FT-IR spectra analysis as described in the methods (Section 2.9). The FT-IR spectra are representative of 3 individual experiments.

Table 3.1: Spectrum of molecules detected by FT-IR treated RASMCs with CaCl$_2$, β-GP, or in combination:

Data from Literature review			Data from current studies				
Stretch or bend of chemical compound	**wave number (cm^{-1})**	**Citation**	**Expected Wave number (cm^{-1})**	**Control**	**CaCl$_2$**	**β-GP**	**CB**
Amide I-(CON stretch), Amide II (NOH bend), Amide III (COH stretch, NOH bend)	1620-1632, 1515-1540, 1216-1290	(Alò *et al.*, 2009; Dritsa, 2012; Lin *et al.*, 2007)	1620, 1625,1622, and 1624 (Amide-I), 1528,1531, and1537 (Amide-II),1236 and 1237(Amide-III)	Present	Present	Present	Present
Calcium Carbonate (Calcite -CO$_3^{2-}$)	1430-1480	(Raynaud, *et al*., 2002)	1450,1452, and 1472 -CO$_3^{2}$	Present	Present	Present	Present
Tricalcium phosphate (TCP), β-Tricalcium phosphate (β- TCP)	700-750, 690	(Destainville, *et al*., 2003)	743 TCP 693 β- TCP	Not present	Not present	Not Present	Present
Phosphate	1154, 1075,1046, 1010 & 1020 or 975	(Destainville, *et al*., 2003; Han J-K., *et al*., 2006; Mobasherpour and Heshajin,2007; Raynaud, *et al*., 2002)	975, 1026, 1075,1072, 1055, 1154, and 1158 PO$_4^{3-}$	Present	Present	Present	Present
HA crystal C$_{10}$(PO$_4$)$_6$(OH)$_2$	1080 - 1089	(Kwon, *et al*.,2003: Alò *et al.*, 2009)	1085 Ca$_{10}$(PO$_4$)$_6$(OH)$_2$	Not present	Not present	Not Present	Present

3.3.4- Effect of LPS, IFN-γ alone or in combination (LPS+ IFN-γ) on NO production and iNOS expression:

As expected, control cells did not produced NO or expressed iNOS throughout time course ranging from day 1-7. In addition, IFN-γ induced only marginal NO production that was more than in controls but lower than the levels induced by LPS (0.06 ± 0.01 nmole μg^{-1} protein; $p < 0.001$) and did not altered significantly over the time course (Figure 3.4).

In time course studies LPS induced NO elevated significantly on day 7 ($0.19 \pm 0.03M$ nmole μg^{-1} protein; $p < 0.01$) with not much difference in the levels detected between days 1, 3 and 5 (Figure 3.4). When given in combination, LPS and IFN-γ significantly enhanced NO production in a time dependent manner well above that seen with either agent alone. Maximal NO production occurred on day 3 (0.20 nmole μg^{-1} protein; $p < 0.05$) and these levels were maintained up to day 7(Figure 3.4).

Figure 3.4: Induction of NO production of RASMCs using LPS, IFN-γ, either alone or in combination.

Cells cultured to ~90% confluency were incubated either with culture medium alone (control), LPS (100 μg ml^{-1}), IFN-γ (100 U ml^{-1}), in combination (LPS+IFN-γ) during a time course ranging from day 1 to day 7. Total NO was quantified as described in the methods (Section 2.3). The data represents means ± S.E.M. from 4 experiments. #, ## and ### denotes $p< 0.05$, $p< 0.01$, and $p<0.001$ respectively when compared to LPS alone.

Rat aortic smooth muscle cells were incubated under similar conditions as stated above and cell lysates were collected and subjected to western blotting to investigate the expression of iNOS. Similar to NO production control cells did not express iNOS at any of the time points. Interferon gamma alone did not induced iNOS expression or at least not sufficiently to be detectable by western blotting while LPS induced detectable amounts of iNOS which was further enhanced when given in combination with IFN-γ (Figure 3.5 A &B).

Expression of iNOS on day 1 in cells incubated with LPS and IFN-γ together was used as 100% to calculate relative expression of iNOS in other experimental conditions Figure 3.5 B. Standardising to this condition showed that LPS induced cells expressed approximately 40% iNOS on day 1 and increased to 81% ± 15 on day 3, dropping to ~50% on day 5 and day 7. The levels induced by LPS and IFN-γ also declined over time, reducing marginally on day 3 (80% ±9) and 5 (70% ± 10) followed by further reduction to ~40%± 5 on day 7 (Figure 3.5 B).

A

Figure 3.5 A: Induction of iNOS expression of RASMCs using LPS, IFN-γ, either alone or in combination.

Cells cultured to ~90% confluency were incubated with culture medium alone (control) and either with LPS (100 μg ml^{-1}), IFN-γ (100 U ml^{-1}) or in combination (LPS+IFN-γ) during a time course ranging from day 1 to day 7. Expression of iNOS was determined by western blotting as described in the methods (section 2.10). The sample from each day was run on the same gel to ensure that a reliable comparison of expression could be made, however the order of bands has been rearranged from the original gel, to the above order in the figure, to make it the same order as that provided in the graph figures, e.g. figure 3.5B.

B
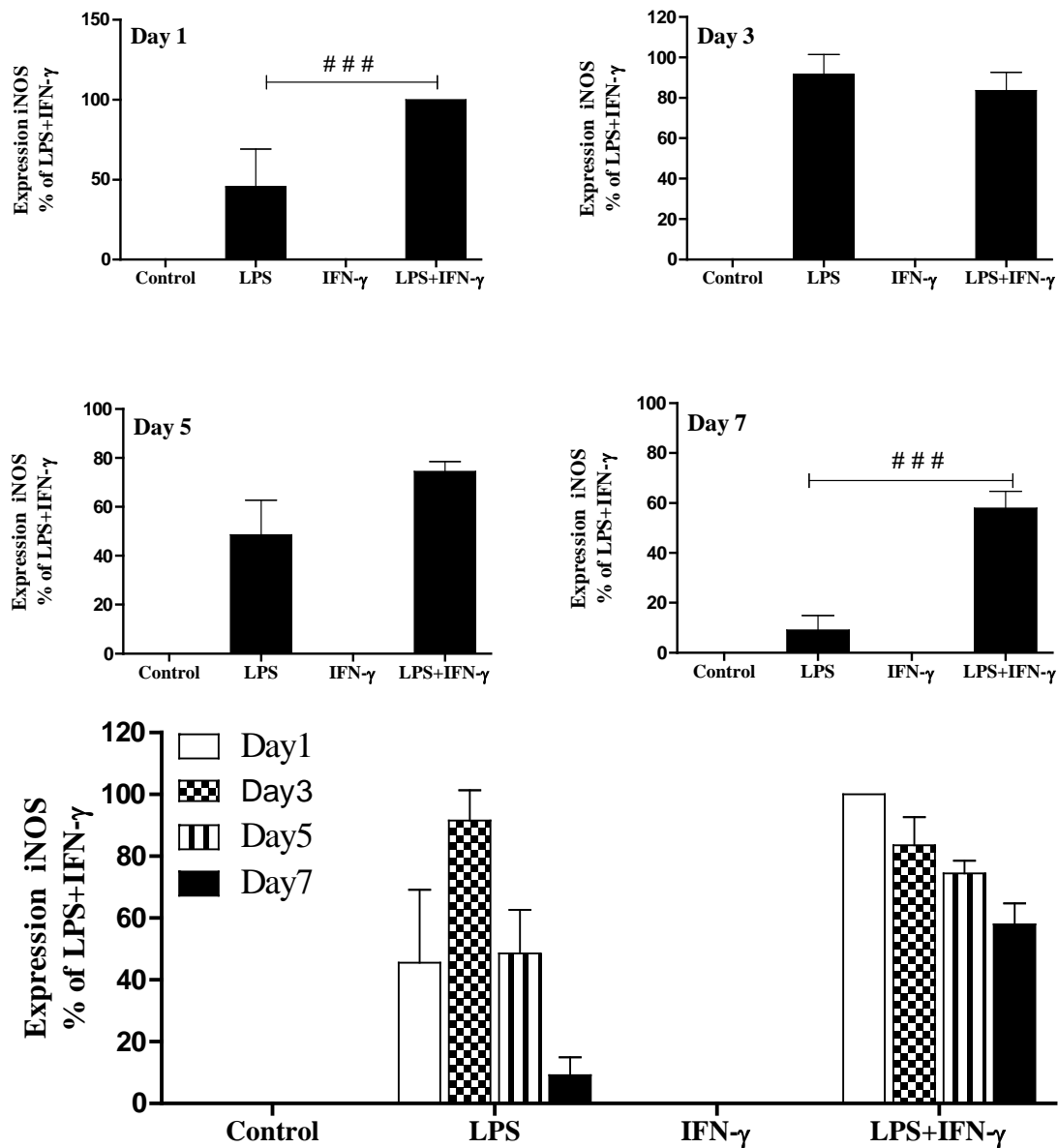
Figure 3.5 B: Induction of iNOS expression of RASMCs using LPS, IFN-γ, either alone or in combination.

Cells cultured to ~90% confluency were incubated with culture medium alone (control) and either with LPS (100 μg ml⁻¹), IFN-γ (100 U ml⁻¹) or in combination (LPS+IFN-γ) during a time course ranging from day 1 to day 7. Expression of iNOS was determined by western blotting as described in the methods (section 2.10). The data represents means ± S.E.M. from 4 experiments. ### denotes $p<0.001$ compared to LPS alone.

3.3.5- Effect of LPS and/or IFN-γ on calcification of RASMCs:

Treatment of cells with either LPS or IFN-γ appears to elevate calcium levels and this was marginally higher with LPS (Figure 3.6). Moreover, LPS induced maximum calcification on day 3 (0.5 ± 0.05 nmole. μg^{-1} protein) compared to day 1 (0.32 ± 0.04 nmole. μg^{-1} protein) but this subsequently declined on day 5 (0.32 ± 0.04 nmole. μg^{-1} protein) and day 7 (0.32 ± 0.04 nmole. μg^{-1} protein). The responses to IFN-γ appear to be more stable over the time course investigated.

The combination of LPS and IFN-γ induced significantly more calcification with maximal effects observed on day 5 (0.7 ± 0.08 nmole. μg^{-1} protein) declining marginally on day 7 (0.6 ± 0.09 nmole. μg^{-1} protein). Incubation of cells with CB caused even more calcification which, consistent with previous observations, was maximal on day 5 (1 ± 0.02 nmole. μg^{-1} protein) but declining by day 7 (0.6 ± 0.09 nmole. μg^{-1} protein), presumably due to cell death as indicated by data from the MTT assays (Figure 3.9). The levels of calcium measured in controls did not alter throughout the time course used.
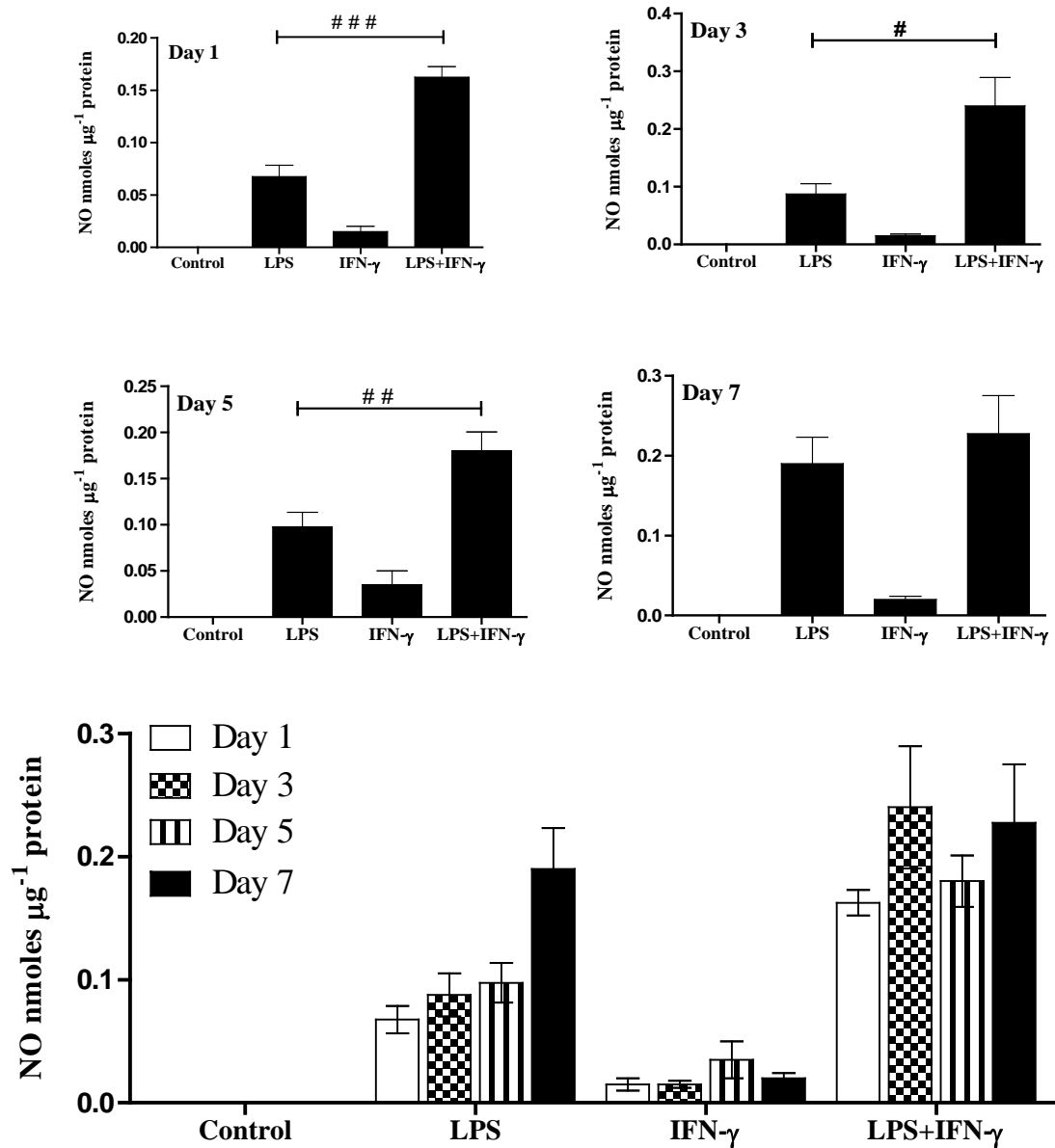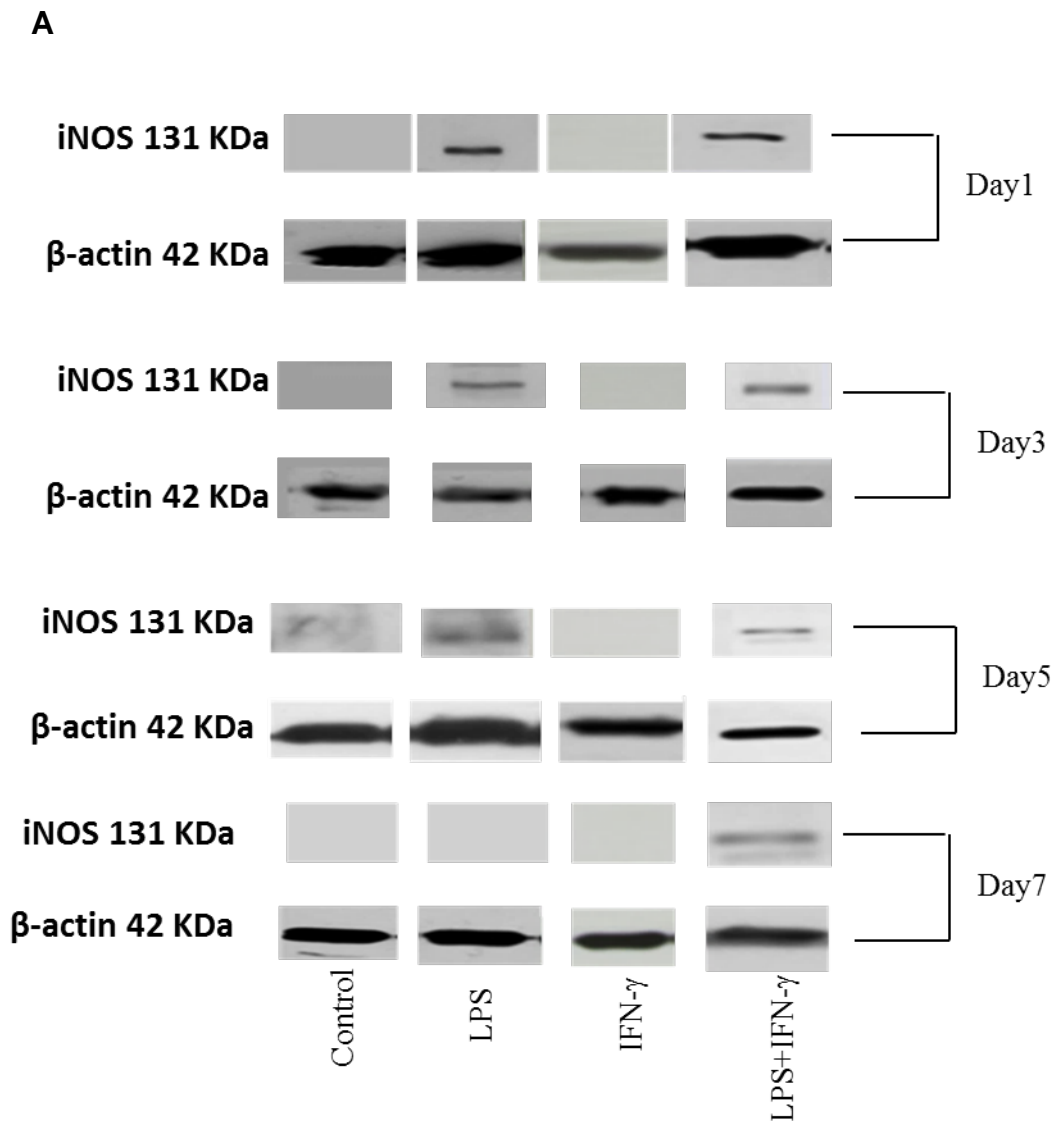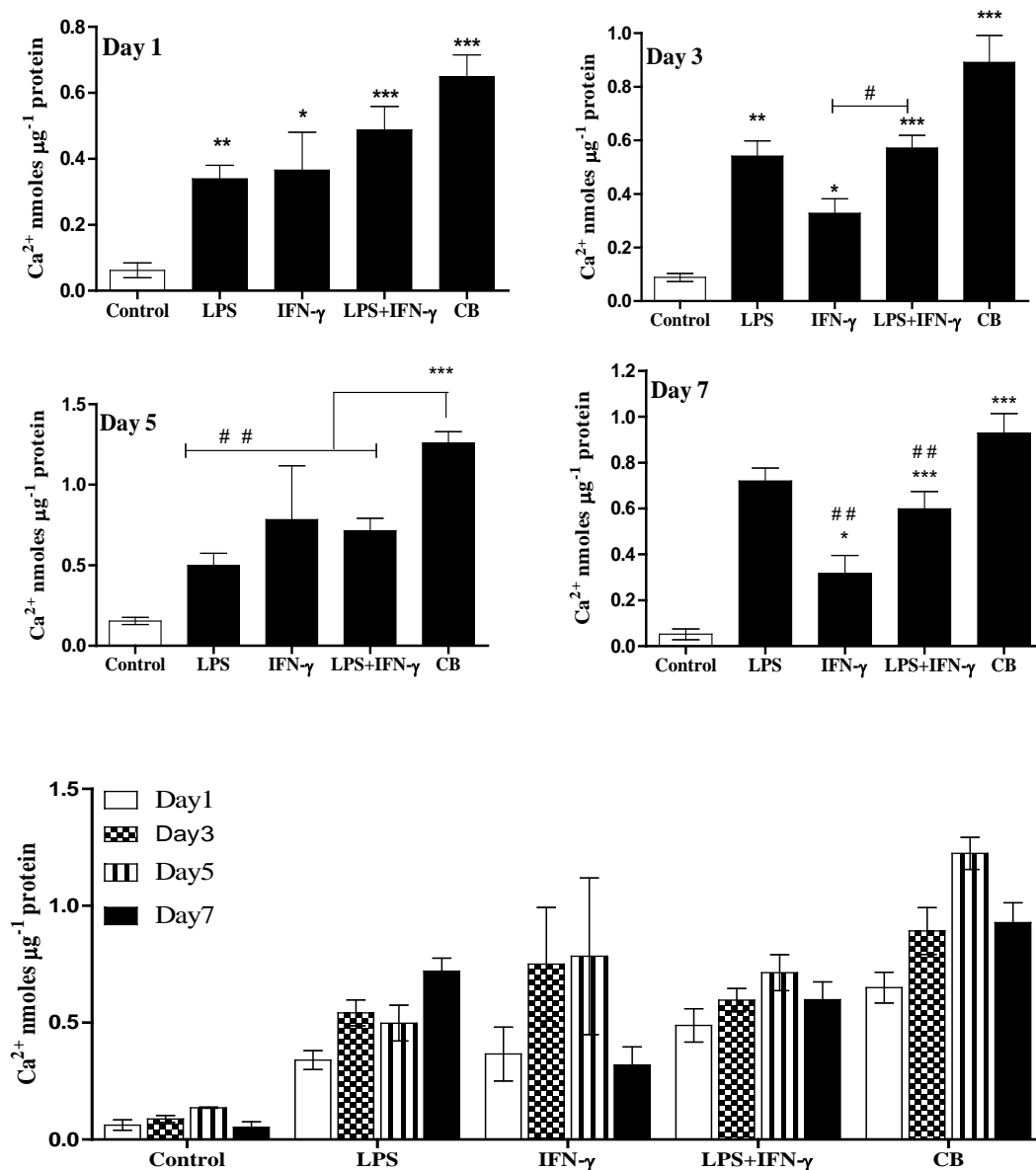
Figure 3.6: Induction of calcification of RASMCs using LPS, IFN-γ, either alone or in combination.

Cells cultured to ~90% confluency were incubated with culture medium alone (control) and either with LPS (100 μg ml^{-1}), IFN-γ (100 U ml^{-1}), or in combination (LPS+IFN-γ) for 1 to 7 days. For comparison, parallel cells were incubated with CB [CaCl$_2$ (7mM) + β-GP (7mM)] over the same time period. Total calcium content was quantified as described in the methods (Section 2.6). The data represents means ± S.E.M. from 4 experiments. * denotes $p<0.05$ ** denotes $p<0.01$ *** denotes $p<0.001$ when compared to control. # denotes $p<0.05$, ## and denotes $p<0.01$ as shown in the figures.

3.3.6- Staining of calcific plaques with ARS:

Rat aortic smooth muscle cells were incubated with complete cell culture medium, LPS, IFN-γ either alone or in combination for 5 days followed by staining with ARS as described earlier. Control cells and cells incubated with LPS, IFN-γ either alone or in combination did not reflect any presence of calcified plaques upon staining (Figure 3.7) but confirmed calcified plaques in cells incubated with CB (Figure 3.7).
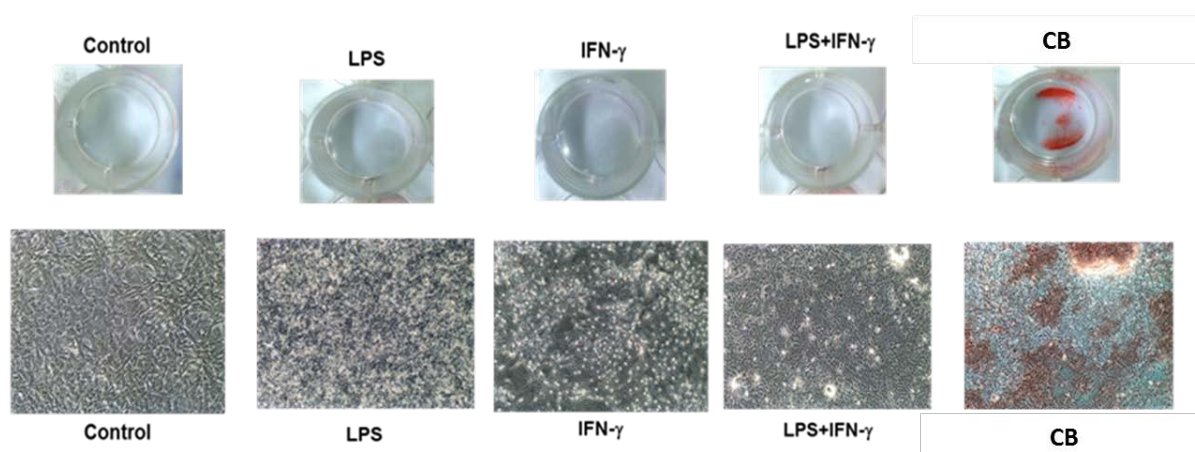
Figure 3.7: Alizarin red staining of calcified RASMCs

Cells were cultured to ~90% confluency and incubated either with culture medium alone (control), LPS (100µg ml^{-1}), IFN-γ (100 U ml^{-1}), in combination (LPS + IFN-γ) or CB for 5 days. Cells were treated with 1x ARS at the end of the incubation period as described in the methods (Section 2.8). The images are representative of 3 individual experiments which were taken with an inverted Olympus microscope at 10X magnification using the GX capture programme.

3.3.7- Detecting HA crystals by FT-IR analysis:

As mentioned before, HA crystal did not form when cells were coincubated with LPS and IFN-γ separately or in combination. In contrast, HA crystal was detected from cells treated with CB as shown in Figure 3.8. The full spectrum detected by FT-IR analysis in the lysates is summarised in Table 3.2.

Control

LPS

Phosphate compound PO_4^{-3}

IFN-γ

1621.16
1534.58
1471.28
1396.80
1308.36
1072.82
1028.14

Phosphate compound PO$_4$$^{-3}$

cm^{-1}

LPS+IFN-γ

Phosphate compound PO$_4$$^{-3}$

1629.90
1512.61
1441.84
1389.50
1315.83
1237.31
1079.31
1064.77
971.71
804.98
692.53

cm^{-1}

89
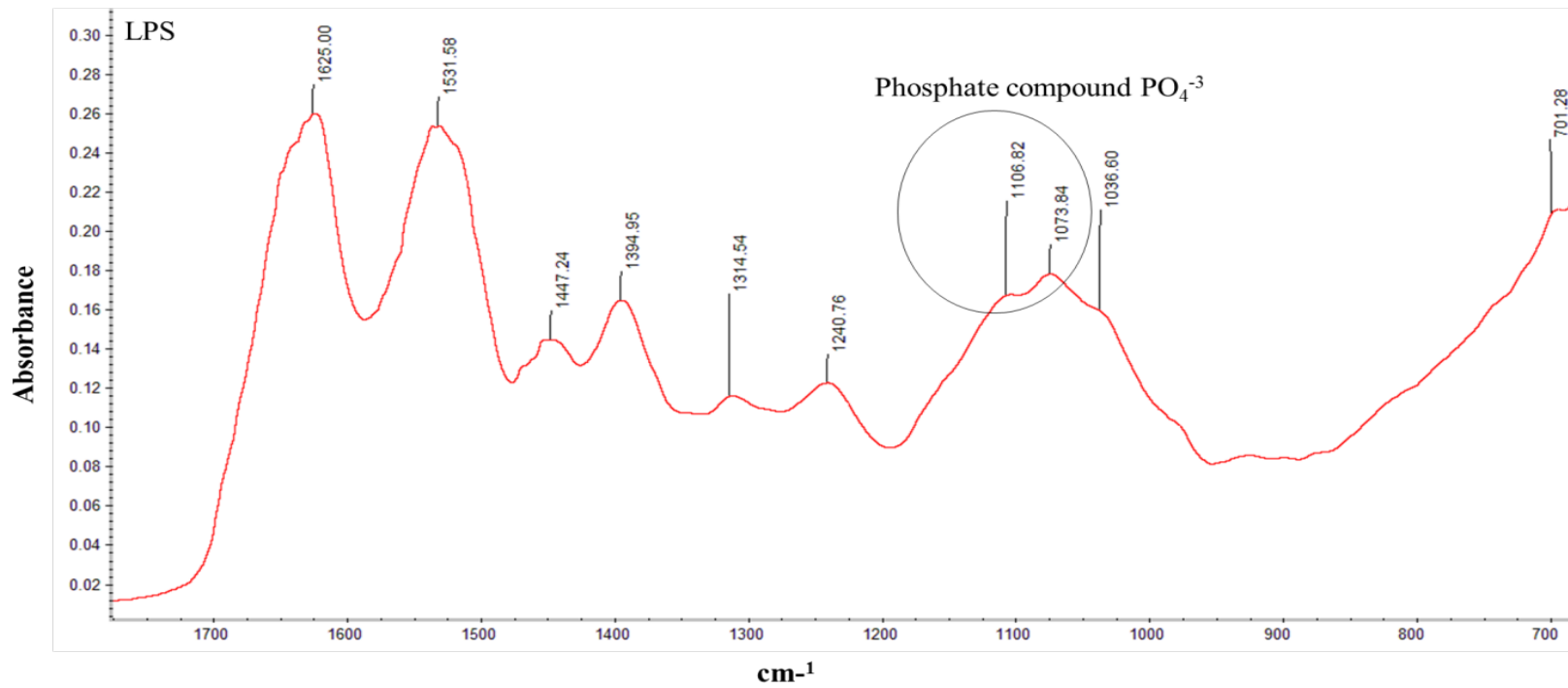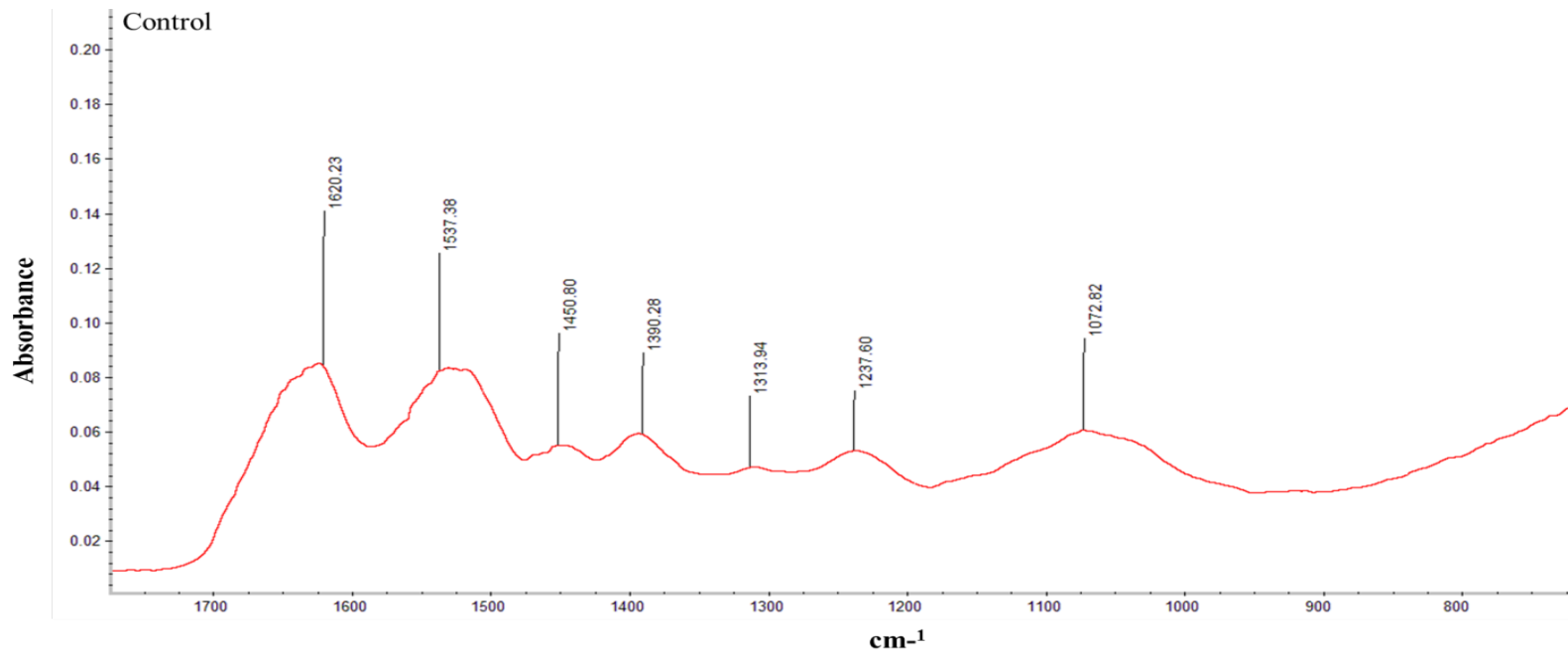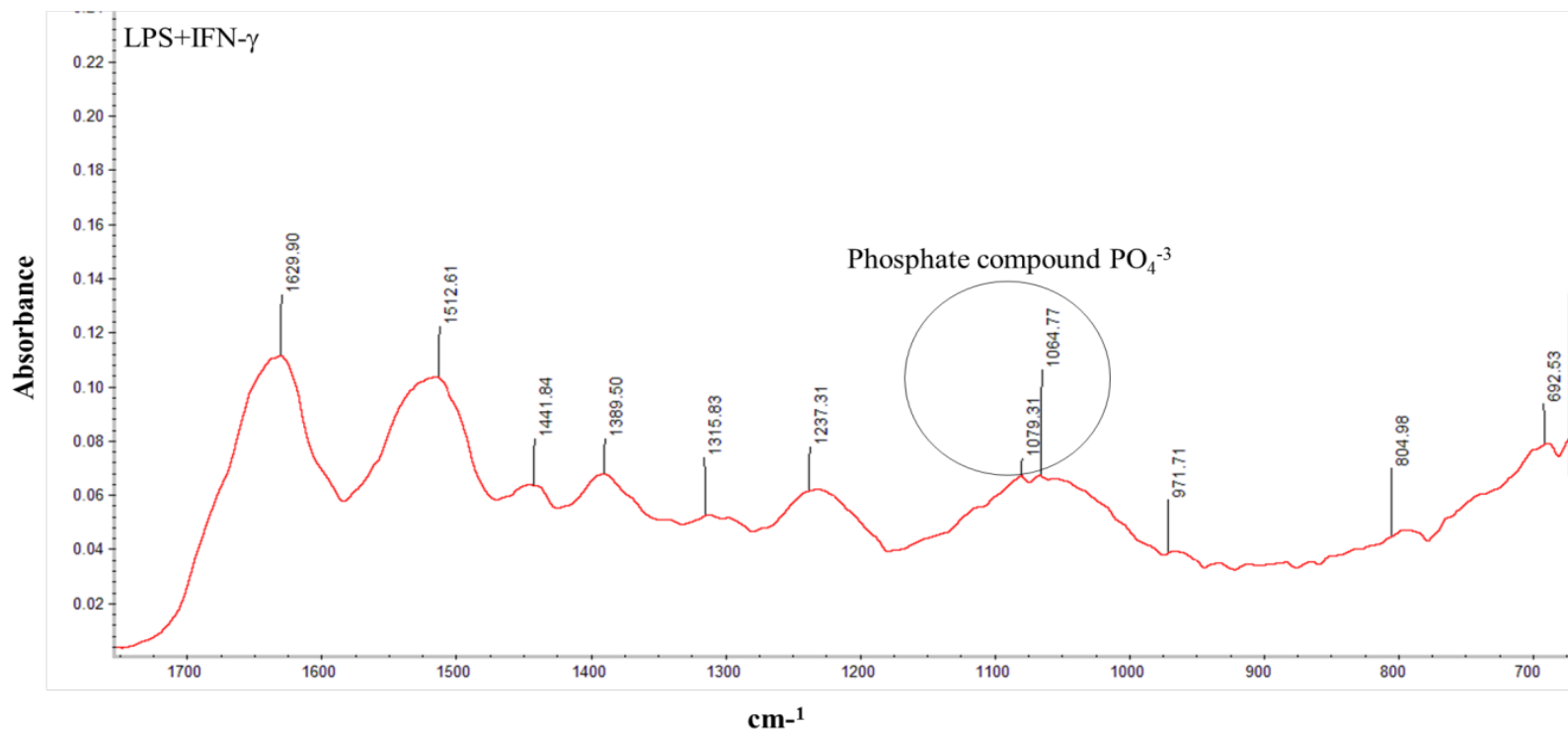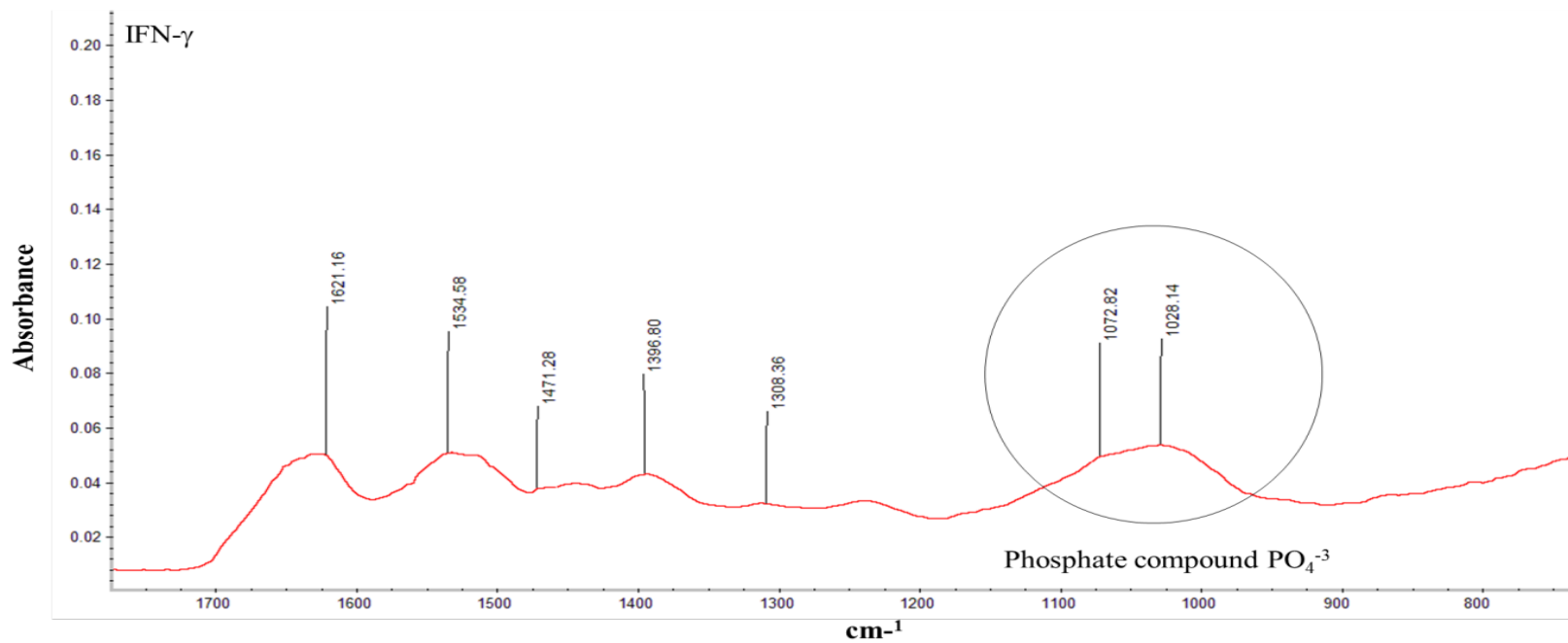
Figure 3.8: FT-IR spectrum analysis of activated RASMCs.

Cells cultured to ~90% confluency were incubated with culture medium alone (control) and either with LPS (100 μg ml^{-1}), IFN-γ (100 U ml^{-1}) or in combination (LPS+IFN-γ) for 5 days. Cells were washed and scraped with 100% ethanol at the end of the incubation period and subjected to FT-IR spectra analysis as described in the method (Section 2.9). The FT-IR spectra are representative of 3 individual experiments.

Table 3.2: Spectrum of molecules detected by FT-IR treated RASMCs with LPS, IFN-γ, or in combination:

Data from Literature review			Data from current studies				
Stretch or bend of chemical compound	wave number (cm^{-1})	Citation	Expected Wave number (cm^{-1})	Control	LPS	IFN-γ	LPS+IFN-γ
Amide I, Amide II, Amide III,	1620-1632, 1515-1540, 1216-1290	(Alò *et al.*, 2009; Dritsa, 2012; Lin *et al.*, 2007)	1620, 1621, 1623, and 1629 (Amide-I), 1512, 1531, 1534, 1537 (Amide-II),1237 and 1240 (Amide-III)	Present	Present	Present	Present
Calcite -CO_3^{2-}	1430-1480	(Raynaud, *et al.*, 2002)	1441, 1447, 1450, and 1450 -CO_3^{2}	Present	Present	Present	Present
TCP, *β*- TCP	700-750, 690	(Destainville, *et al.*, 2003)	----------------	----------	------------	------------	---------------
Phosphate	1154, 1075,1046, 1010 & 1020 or 975	(Destainville, *et al.*, 2003; Han J-K., *et al.*, 2006; Mobasherpour and Heshajin,2007; Raynaud, *et al.*, 2002)	971, 1028, 1064, 1073, 1072, and 1106 -PO_4^{3-}	Not Present	Present	Present	Present
HA crystal Ca $_{10}(PO_4)_6(OH)_2$	1080 - 1089	(Kwon, *et al.*,2003: Alò *et al.*, 2009)	Ca $_{10}(PO_4)_6(OH)_2$	Not present	Not present	Not present	Not present
Polysaccharides	Below 690	(Gómez-Ordóñez *et al.*, 2011; Parikh *et al.*, 2006).	Below 690- Polysaccharide	Not present	Present	Not present	Present

3.3.8- Cellular viability of RASMCs when incubated with calcification inducers:

To determine whether any of the effects reported are associated with changes in cell viability, the MTT assay was carried out in parallel with the experiments above. Lipopolysaccharide did not induce any significant toxicity when incubated with cells for 24 hours at up to 100µg ml^{-1} (Figure 3.9 inset A). Similarly, IFN-γ did not induced any significant toxicity up to 100U ml^{-1} (Figure 3.9 inset B). However, in time course studies, LPS (100µg ml^{-1}) and IFN-γ (100U ml^{-1}) combined resulted in 50% reduction in cellular viability at day 3 ($p<0.05$) and viability remained at a similar level on days 5 and 7 (Figure 3.9 inset C). Interestingly control cells also reflected ~50% or greater reduction in cell viability at day 7 (Figure 3.9 inset C, D, E and F).

Additionally, when cells were incubated with either 7mM of CaCl$_2$ or β-GP there were marginal reductions in cellular viability which although lower than controls did not change significantly over time (Figures 3.9 C and D). Similarly, CB also only caused marginal reduction in cell viability on days 1, 3 and 5. Viability of cells was however significantly reduced (17.29 %, $p<0.01$) on day 7. Note however that viability was also significantly reduced in controls on day 7. This suggests that the decreases seen in MTT metabolism at this time point may not necessarily be due to the treatment conditions but perhaps more likely to be related to the culture conditions which will be discussed.

93
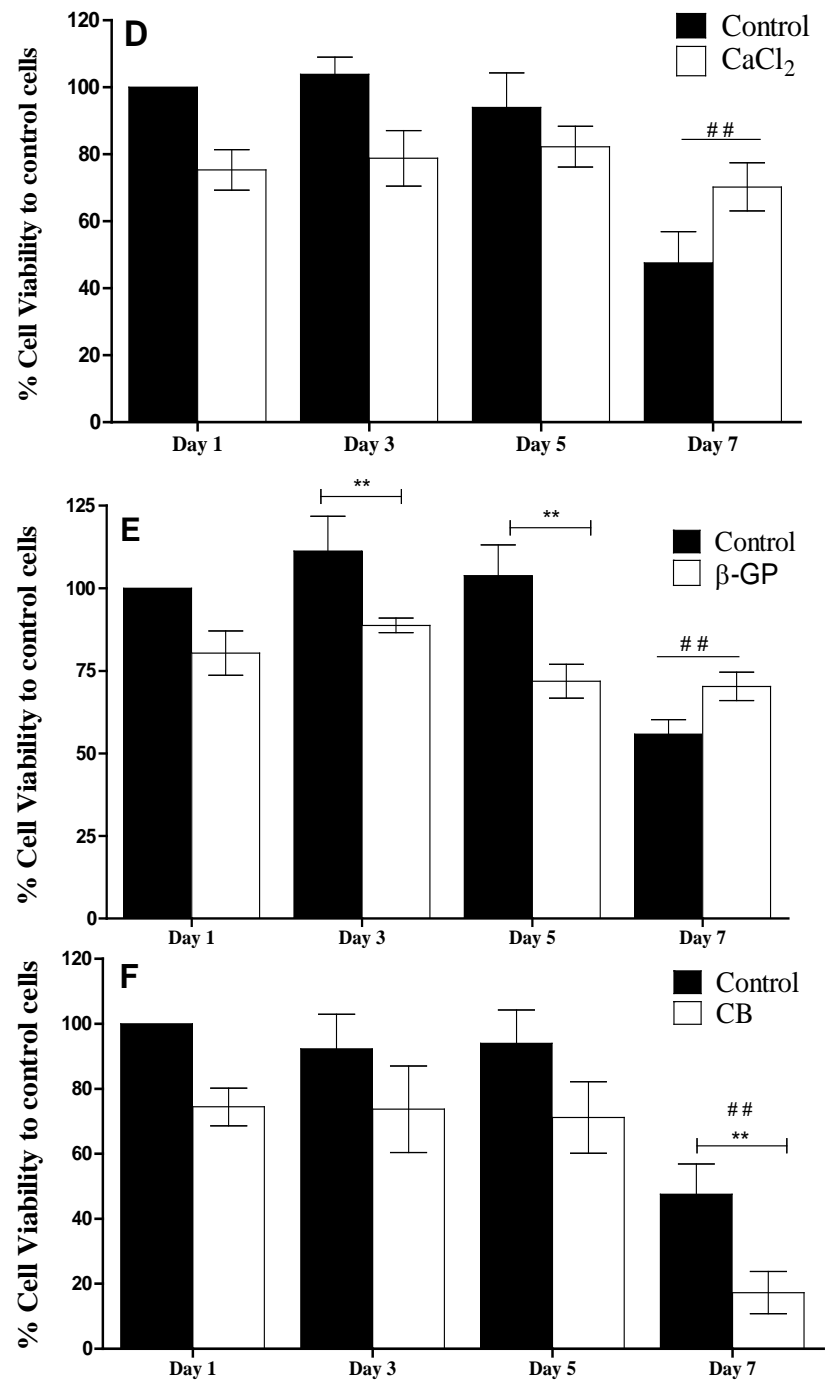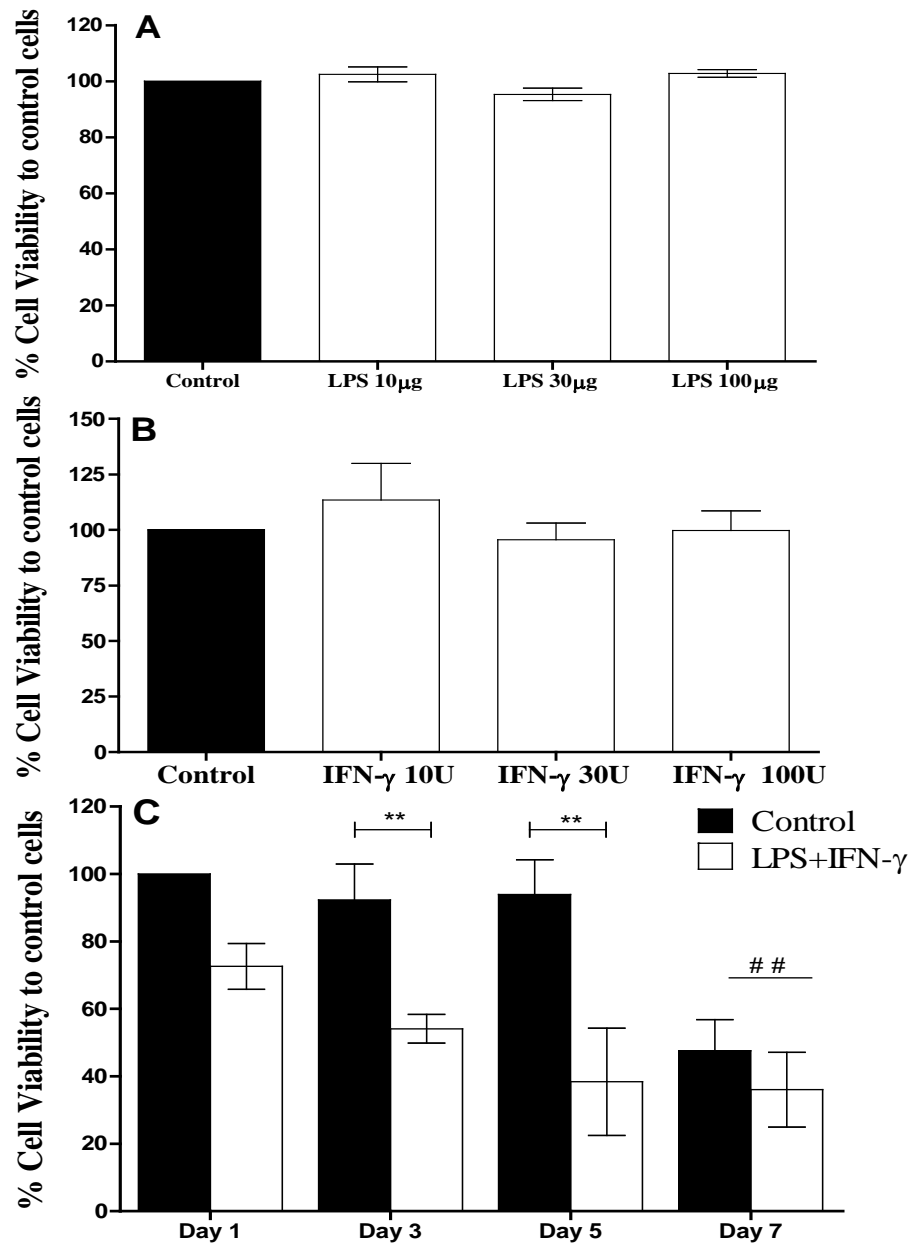
Figure 3.9: Cellular viability of RASMCs when incubated with calcification inducers

Cells were incubated with LPS (A; 10-100μg ml^{-1}), IFN-γ (B; 10-100 U ml^{-1}) for 24 hours and in combination (C) over a time course of 1 to 7 days. Similarly, cells were also incubated with $CaCl_2$ (D; 7mM), β-GP (E; 7mM) or with CB (F; 7mM $CaCl_2$ + 7mM β-GP) during a time course from day 1 to day 7. The data is represented as % change of cell viability taking controls as 100%. The data represent the means ± S.E.M from 4 individual experiments. ** denotes $p<0.01$, # # represents $p<0.01$ when compared to day 1 control or treated cells.

3.4-Discussion:

The studies described in this chapter have validated the *in vitro* model of calcification and confirmed the sustained induction of iNOS using LPS and IFN-γ which is consistent with our earlier observations (Wileman *et al.*, 1995). The data generated in the calcification studies show that incubation of cells with $CaCl_2$ caused a significant time dependent increase in calcium levels which was not observed with *β*-GP. Interestingly, $CaCl_2$ induced a similar degree of calcification which was comparable to that seen with the CB. This was initially thought to indicate calcification with the calcium levels detected representing calcium present in HA crystals. However, incubation of cells with ARS failed to stain cells treated with $CaCl_2$ but revealed significant staining of cells treated with the CB suggesting the presence of HA crystals, which is normally characteristic of calcification. These observations suggest that while $CaCl_2$ may increase cellular calcium, but calcified plaques could only be deposited when a combined with *β*-GP. This was further confirmed by FT-IR analysis which detected TCP and *β*- TCP but only in cells incubated with CB.

In our experiments, the fact that *β*-GP did not induced calcification does not mean that phosphate is not calcifying. Indeed high phosphate has been shown to contribute to the development of VC *in vivo* (Crouthamel *et al.*, 2013) and several other researches have highlighted that a marginally sustained increase in serum phosphate levels increases the risk of cardiovascular disease by 2-3 fold even in healthy individuals which extend to 30 fold high risk in patients with kidney failure (Ketteler *et al.*, 2012). A study by Shioi and coworker showed that incubation of (BVSMCs) with *β*-GP alone elevated calcification and this was confirmed by von Kossa staining which stained mineralised plaques. Further investigation was conducted through detecting ALP expression which could be responsible to form HA crystals in BVSMC (Shioi *et al.*, 1995).

One possible explanation why *β*-GP was without much effect in our studies may relate to the duration of the studies which were restricted to 5 days. This time point was chosen as it gave optimal plaque formation when *β*-GP was added together with $CaCl_2$ and did not result in any significant loss in cell viability. The reduction in cell viability on day 7 could be due to the fact that the cell culture medium was not changed during the incubation period.

In experiments where phosphate had been used alone the incubations had been for periods of two to three weeks to induce calcification (Byon *et al.*, 2008). These time points are much longer than the 5 day period used in this project. Another possible explanation why *β*-GP may not be effective in our studies may be because of the relatively low concentrations of *β*-GP used. In other studies, researchers have used high phosphate at concentrations of 10-14mM (Byon *et al.*, 2008) or used high phosphate medium supplemented with ascorbic acid which is claimed to enhance calcification (Cao *et al.*, 2013).

One aspect of the research conducted in this thesis was aimed at establishing whether NO production regulated calcification. Thus, to start with, studies were carried out to establish that iNOS can be induced in RASMCs using LPS and IFN-γ. Indeed, consistent with our earlier studies and with several other studies LPS and IFN-γ caused significant induction of iNOS accompanied by elevated NO production. The inductions were less pronounced with either LPS or IFN-γ alone. LPS caused marginal induction of iNOS and NO production while IFN-γ was without much effect presumably because this cytokine does not induce but rather act to stabilise the iNOS mRNA (Wileman *et al*., 1995). The induction of iNOS peaked at day 3 and then declined as confirmed by western blotting. These findings are consistent with several reports in the literature including several from our laboratory (Balligand *et al.*, 1994; Chan *et al.*, 2001; Wileman *et al.*, 2003).

In relation to calcification, the data generated demonstrate clearly that both agents increased detected calcium levels but with LPS causing the more profound effect which was significantly enhanced when administered together with IFN-γ. The responses even with LPS and IFN-γ combined were however less than those induced by CB.

The ability of LPS to induce calcification is consistent with reports that it stimulate the synthesis of proteins such BMP2 (Zeng *et al.*, 2014) through activating TLR2 and 4 (Heo *et al.*, 2008). Both proteins are well-known pro-calcific markers and play a critical role in calcification by inducing a phenotypic transition of aortic smooth muscle cells in to bone like cells (Tintut *et al.*, 2002; Zehnder *et al.*, 2002). At present, it is not known whether LPS acts through these mechanisms to induce calcification in our model nor is it clear whether it activates other osteoblast or osteoclast like cells marker such as Runx2/Cbfa1 and this may require further investigation. Similarly, further studies are required to determine the mechanism(s) through which IFN-γ acts. One possible action may relate to the upregulation of the expression of 1alpha-OHase (Stoffels *et al.,* 2006) which is extensively expressed in arterial smooth muscle cells of rats and humans and converts $25\text{-}(OH)_2D_2$ (Calcidiol*)* to $1,25 (OH)_2 D_3$(Calcitriol), resulting in elevated calcium level leading to hypercalcemia (Somjen *et al*., 2005*)*. Further studies are however again required to confirm that these mechanisms are indeed activated in our model.

In current study, the MTT assay used indicated cytotoxicity when the cells were incubated continuously for longer time periods in inflammatory mediators/calcifying agents. In these conditions the levels of NO were measured. While it is likely that cytotoxicity may interfere with NO levels, in chronic conditions such as cardiovascular disease involving vascular mineralisation, it is also likely that cytotoxicity is a phenomenon due to continuous inflammation (Willerson and Ridker, 2004). Furthermore, varying the replenishment of

media allowed comparison of the effect continuous incubation periods, and this may serve as a better model for the continuous blood flow *in vivo.*

When cells were incubated with the LPS and IFN-γ, there was significant generation of calcium levels compared to control. Published literature suggests that both LPS and IFN-γ can activate signalling mechanism(s) such as TLR 4 or 1alpha-OHase (Heo *et al.*, 2008) that could accumulate calcium and phosphate (Stoffels *et al.,* 2006). However more research is needed whether NO or iNOS can regulate calcification and understanding the mechanism(s) behind   that.

CHAPTER IV

RESULTS

Effects of LPS and/or IFN-γ on iNOS expression, NO synthesis and VC in the absence and presence of calcification inducers.

4.1- Introduction:

Data presented in the previous chapter suggest that incubation of cells with $CaCl_2$ and CB caused a significant time dependent increase in calcium levels which was not observed with β-GP. In term of NO production through iNOS, cells were pre activated with LPS and IFN-γ which caused significant induction of iNOS accompanied by elevated NO production. The inductions of NO was however less with either LPS or IFN-γ alone. In addition, previous research have shown that proinflammatory cytokines and other inflammatory mediators can induce dysrgulated calcium and phosphate metabolism, causing renal insufficiency, potentially contributing to the development of VC (Bellasi *et al.*, 2009). Furthermore, proinflammatory cytokines have been reported to stimulate osteoblast cells resulting not only in significant NO production by iNOS but also induce critical transcription factors of calcification such as Runx2 (Zaragoza *et al*., 2006). The latter causes high calcium deposition on osteoblast cells promoting HA crystals, contributing to calcification (Kreutz *et al.*, 1993;Somjen *et al.*, 2005).

These observations suggest that, in parallel with inducing iNOS, inflammatory mediators also activate processes associated with calcification. This raises the possibility that the iNOS pathway may be associated with VC; with the NO produced potentially regulating the calcification of blood vessels. The precise relationship between induced NO synthesis and VC however still remains to be defined and, as alluded to in the introduction chapter, it is not clear whether NO promotes or inhibits VC. Thus, in this chapter, further studies have been carried out to extend those conducted in chapter 3 and were aimed at establishing how calcification of cultured VSMCs may be altered in cells expressing iNOS. Additionally, other experiments were also carried out to determine whether the expression of iNOS and NO induced by inflammatory mediators is altered in the presence of conditions that induce calcification. For these studies, LPS and IFN-γ were used partly because the combination of

these two molecules has been shown to cause sustained induction of iNOS in VSMCs (Wileman *et al*., 2003;Guo *et al.*, 1997). More importantly, activation of TLR4 by LPS has been implicated in the induction of pro-calcific marker such as ALP and Cbfa1 (Heo *et al.*, 2008) while IFN-γ is reported to stimulate high expression of 1-α hydroxylase playing a crucial role in accelerating conversion of 25(OH) D_2 to 1,25 (OH)$_2$$D_3$ (Shioi *et al.*, 2002) and hence VC. These effects of LPS and IFN-γ show that in parallel with inducing iNOS they also activate processes associated with VC and thus raise the possibility that the inducible NO pathway may be associated with VC.

4.2- Experimental protocols:

Cell culture and quantification of NO production, total protein and calcium measurements as well as western blotting were performed as described in chapter 2, section 2.3, 2.5, 2.6, and 2.10, respectively. In parallel experiments, ARS and FT-IR analysis was also performed as previously described in the method (sections 2.8 and 2.9 respectively).

4.2.1-Induction of calcification, iNOS expression and NO production in RASMCs:

Rat aortic smooth muscle cells cultured to ~90 % confluency were incubated with LPS (100µg ml^{-1}), IFN-γ (100 U ml^{-1}) or in combination for 24 hours followed by induction of calcification using CaCl$_2$, β-GP or a combination of both (CB) in the continued presence of LPS, IFN-γ or in combination (LPS + IFN-γ). Cell lysates were generated at 1, 3, 5 and 7 days and used for the assessment of calcification and for determining changes in iNOS expression. In these experiments the medium was not changed and the NO measured was therefore the pooled amount produced over the incubation period. These studies were aimed at establishing whether the calcification process was regulated in any significant way if expression of the iNOS pathway precedes the initiation of calcification. The medium was not changed to ensure that plaque formation was not disrupted by regular washing of the cell monolayer. This however has the disadvantage of not removing metabolic waste from the cultures and replenishing required nutrients.

 In parallel studies, cells were activated with LPS (100 µg ml^{-1}) and IFN-γ (100 U ml^{-1}) either alone or in combination for 24 hours followed by the addition of calcification inducers (CaCl$_2$, β-GP or CB) at 7mM. In this experimental set up, the medium was changed every 24 hours and replaced with fresh medium containing LPS and/or IFN-γ as well as CaCl$_2$, β-GP or CB. iNOS expression, nitric oxide production and calcification were analysed at 1, 2, 3, 4, 5, 6 and 7 days. These experiments were carried out to establish whether regular

replenishment of nutrients and other factors required for cell growth affected iNOS induction, NO production or the calcification process. Moreover, this protocol allowed for NO production to be determined more accurately on a 24 hours basis rather than determining the accumulated levels over prolonged periods.

In further studies, cells were activated with LPS and IFN-γ for 24 hours followed by the addition of CB only without LPS and IFN-γ. Quantification of NO, iNOS and calcification were performed on day 3 after addition of CB as this was the time point found previously from the first experiment to induce maximal calcification. This was to determine whether sustained induction of iNOS and NO was essential for calcification to occur or whether the presence of NO at the onset of calcification rather than its continued and sustained production was the important factor. In another experimental set up, cells were activated with CB for 3 days followed by addition of LPS and IFN-γ only without adding of CB for 24 hours in order to determine whether calcification regulated iNOS and NO production.

In parallel studies, incubations with LPS + IFN-γ and/or CB were carried out at the onset and changes in iNOS expression, NO production and in intracellular calcium levels monitored over shorter time points ranging from 1, 3, 6, 9, 18, 24, 48 hours. This was to establish whether simultaneously inducing calcification and iNOS protein (and thus NO production) resulted in any significant alteration in either pathway or both.

At the end of each study, supernatants were assessed for NO and lysates generated analysed for calcification and for iNOS expression.

4.3- Results:

4.3.1- Effects of LPS on NO production, iNOS expression and calcification of RASMCs in the absence and presence of $CaCl_2$, β-GP or CB:

The data shown in Figures 4.1 to 4.3 represents the results from studies where cells were activated with LPS for 24 hours prior to coincubating with calcifying agents for further incubation periods which ranged from 1 to 7 days. Additionally, the medium was not changed throughout the incubation period in these series of experiments. In these experiments, RASMCs incubated with media alone (control) did not produce NO or express iNOS during the time course carried out. Incubation with LPS ($100 \mu g$ ml^{-1}) resulted in a gradual increase in NO which appeared to be significantly increased on day 7 (0.19 ± 0.006 $nmole.\mu g^{-1}$ protein) with not much difference in the levels detected between days 1, 3 and 5 (0.067 ± 0.02, 0.087 ± 0.03, and 0.097 ± 0.03 $nmole.\mu g^{-1}$ protein, respectively) (Figure $4.1A_1$). LPS also induced expression of iNOS which increased to a peak at day 3 (% 159.5 ± 67.15) but declining thereafter (Figure 4.2 A_1). When RASMCs were coincubated with LPS and $CaCl_2$ (7mM), there was further elevation in NO compared to the response of the LPS alone. Under these conditions, NO accumulation peaked on day 5 (0.305 ± 017 $nmole.\mu g^{-1}$ protein) and remained elevated at day 7 (Figure $4.1A_1$). There was no significant statistical difference between any of the time points in the presence of $CaCl_2$ but the changes were significantly different when compared to LPS treated cells. Initially, the addition of $CaCl_2$ to LPS activated cells resulted in the partial suppression of iNOS expression, at days 1 and 3 but increased significantly on day 5 (% 151.5 ± 64.9) when compared to cells treated with LPS alone before declining back to basal levels at day 7 (Figure 4.2 A_1).

β-GP like $CaCl_2$ enhanced LPS induced NO production and this was in a time dependent manner peaking at day 5 (0.305 ± 0.15 $nmole.\mu g^{-1}$ protein) and maintained up to day 7 (Figure

4.1 A$_2$). These increases were significantly different when compared to the increases at days 1 and 3 and to the LPS induced responses. In parallel experiments, iNOS expression was enhanced when cells were coincubated with LPS and β-GP at day 1 and maintained at days 3 (% 160 ±21) followed by a declined at day 5 and 7. The levels of iNOS in the presence of LPS and β-GP at day 5 did not decline as dramatically as the levels seen with LPS alone (Figure 4.2 A$_2$).

The use of CB caused a similar trend in NO production and iNOS expression (day1 to day3) to that seen with CaCl$_2$ or β-GP in that when used, CB potentiated the effects of LPS. Furthermore, iNOS expression did not decline as rapidly as seen when LPS was used alone (Figure 4.1A$_3$ and 4.2 A$_3$). In all these studies, CaCl$_2$, β-GP or CB did not cause any significant changes above control values when applied alone. Summary graphs showing the changes in NO production and iNOS expression are shown in Figures 4.1B and 4.2B.

In the calcification studies, incubation of cells with LPS alone resulted in significant elevation of calcium in the cells on day 1 to 7 (within range 0.34 - 0.7 ±0.10 - 0.14 nmole.μg^{-1} protein) when compared to controls (0.05 nmole.μg^{-1} protein) (Figure 4.3 A$_{1, 2, 3}$). Similarly, CaCl$_2$ and CB but not β-GP elevated calcium levels which was distinctly higher than in controls. Activation of cells with LPS in the presence of CaCl$_2$ or CB did not potentiate the effects of either CaCl$_2$ or CB as the responses seen under these conditions were not statistically different to those seen with each agent alone (Figure 4.3 A$_1$ and A$_3$). The addition of LPS with β-GP (7mM) did not cause any further elevation in calcium beyond that seen with LPS alone. Figure 4.3 A$_2$ and Figure 4.3 B represents the summary data of all the conditions above.
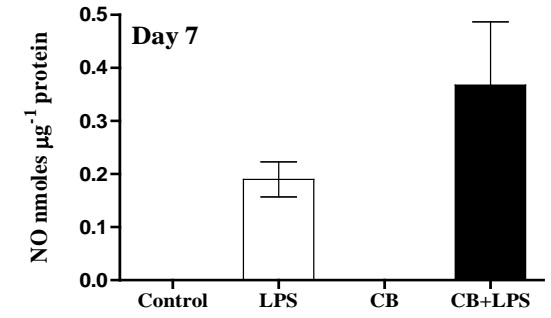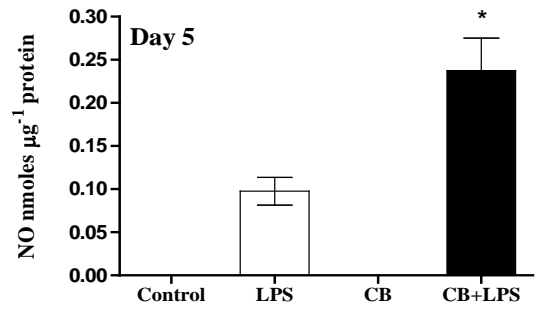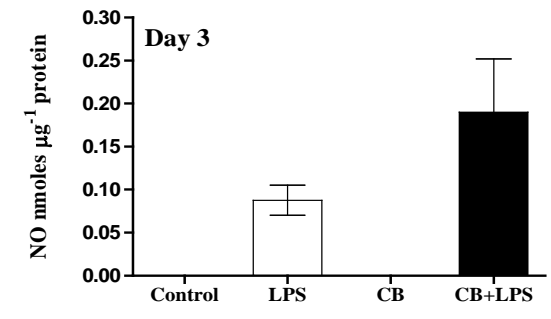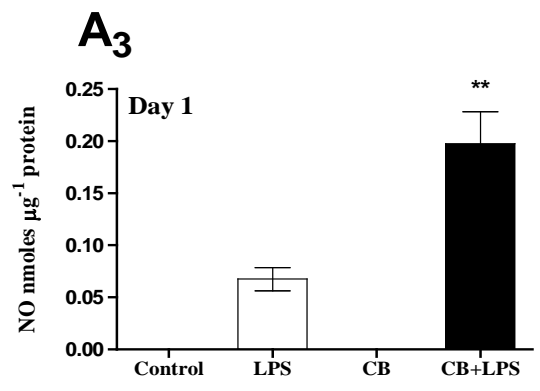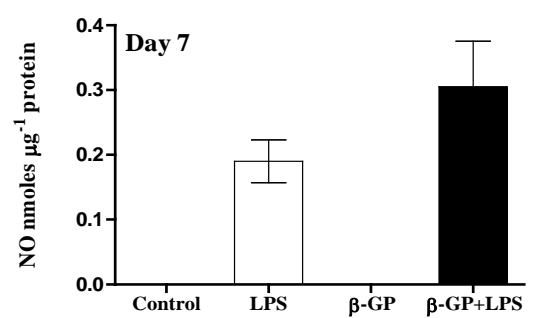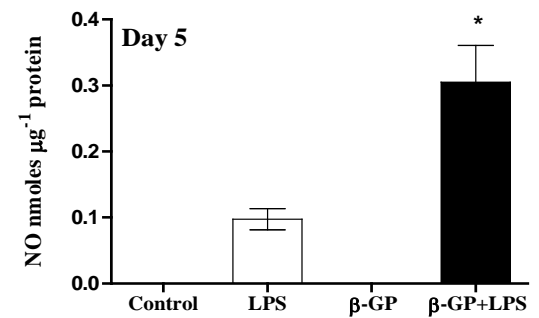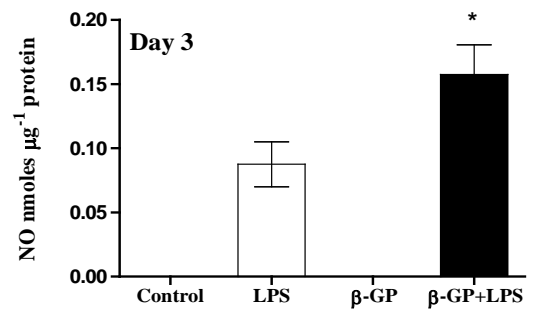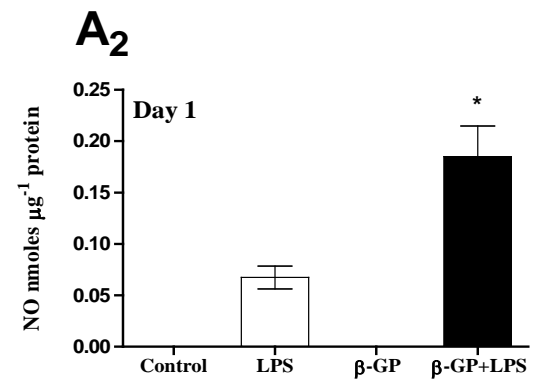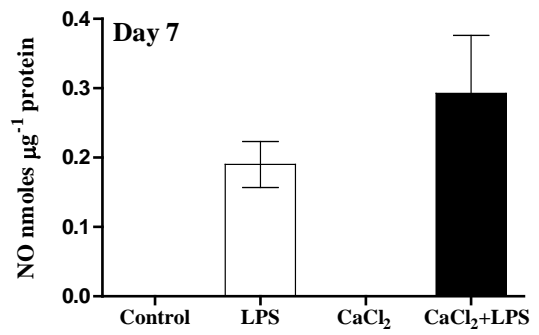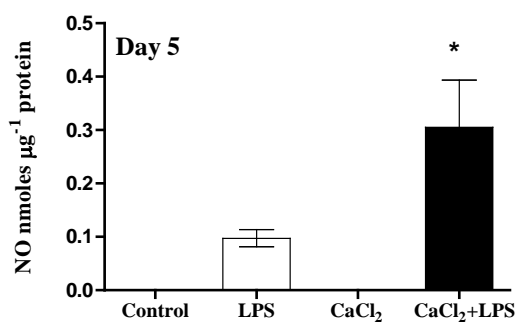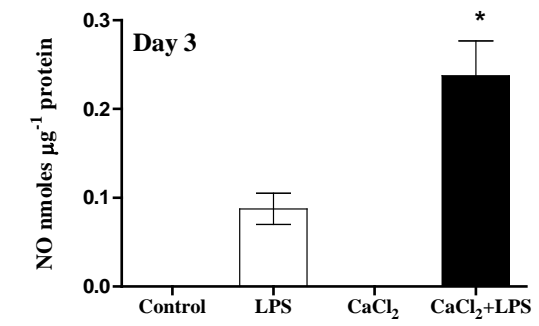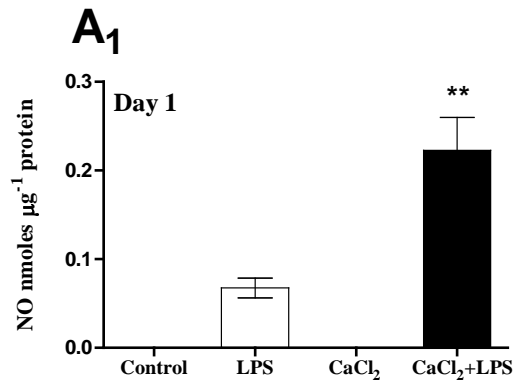
Figure 4.1 A: **Effect of CaCl$_2$, β-GP and CB on LPS induced NO production.**

Cells were cultured to ~90% confluency and activated with LPS (100 μg ml^{-1}) for 24 hours followed the addition of CaCl$_2$ (7mM; Panel A$_1$), β-GP (7mM; Panel A$_2$) or CB (Panel A$_3$) in the continued presence of LPS and incubated for a further period of 1, 3, 5 and 7 days. Total NO was quantified by the Griess assay as described in methods (section 2.3). The data represents means ± S.E.M. from 4 individual experiments. * denotes $p< 0.05$ and ** denotes $p<0.01$ compared to LPS alone for each time point.
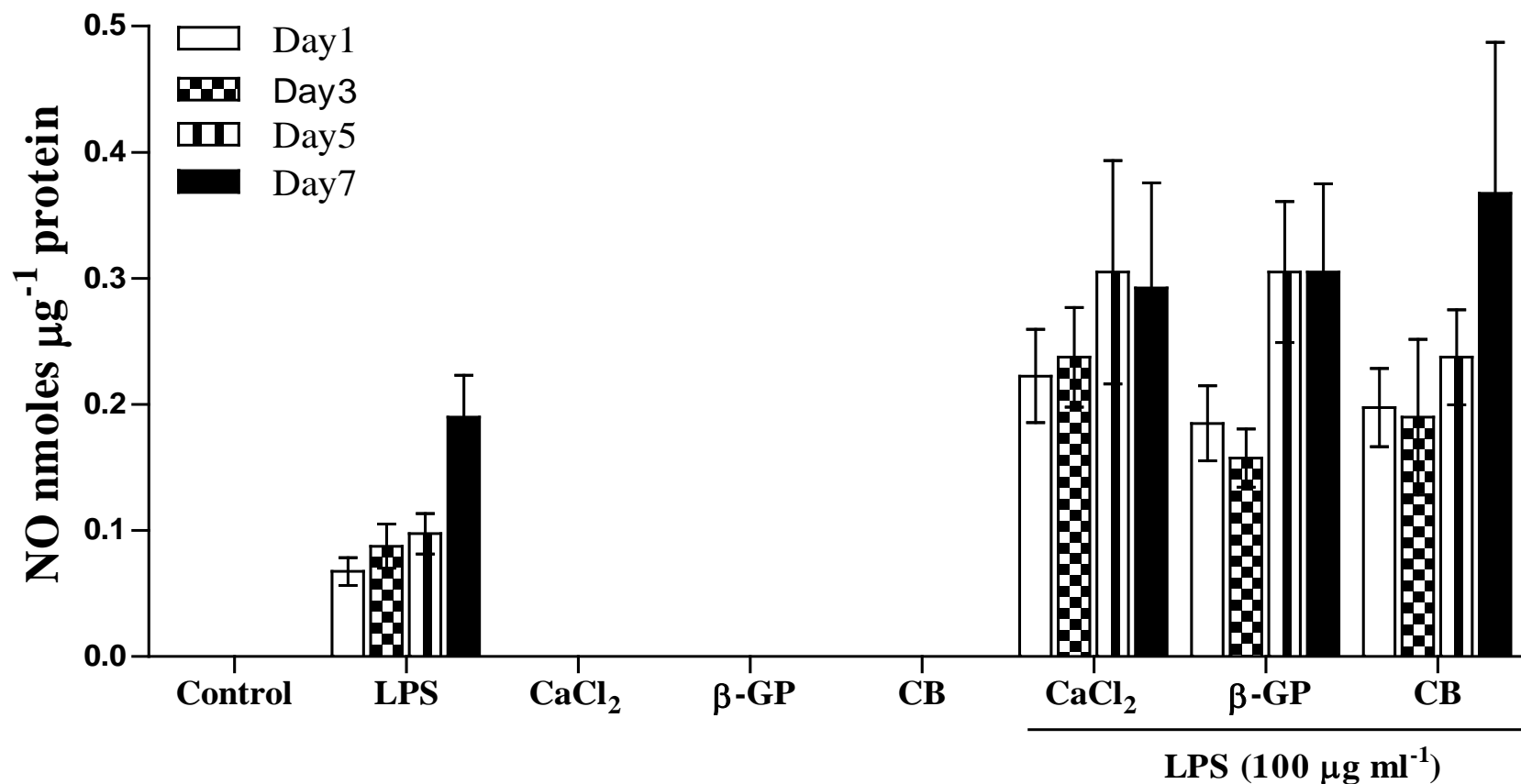
Figure 4.1 B: **Summary data of the effect of CaCl$_2$, β-GP and CB on LPS induced NO production.**

Cells were cultured to ~90% confluency and activated with LPS (100 μg ml^{-1}) for 24 hours followed the addition of CaCl$_2$ (7mM), β-GP (7mM) or CB in the continued presence of LPS and incubated for a further period of 1, 3, 5 and 7 days. Total NO was quantified by the Griess assay a as described in methods (section 2.3). The data represents means ± S.E.M. from 4 individual experiments.
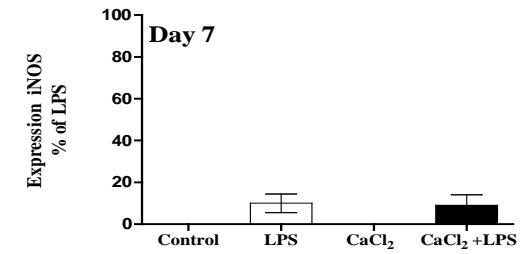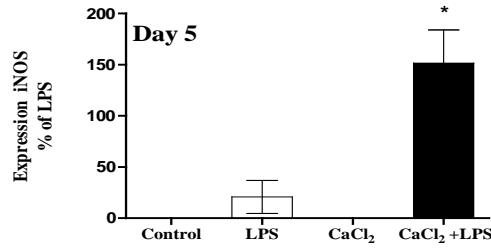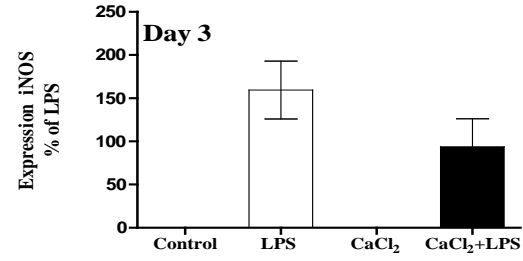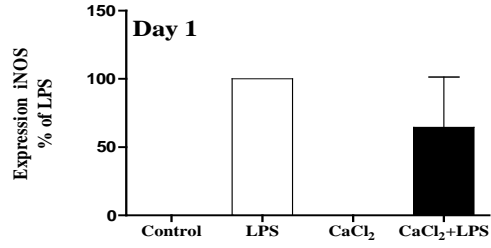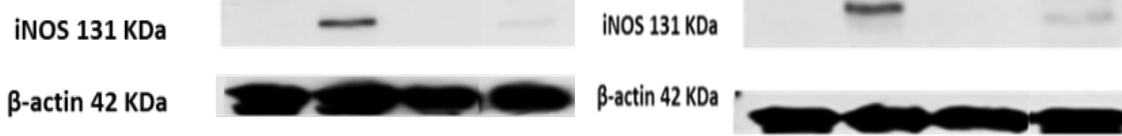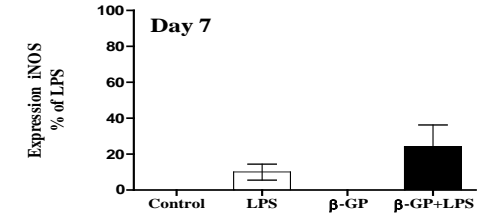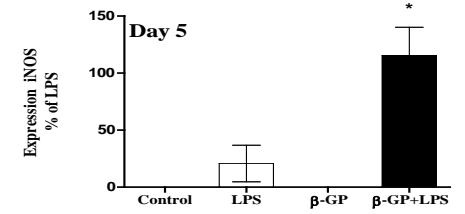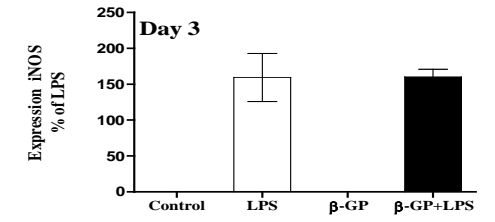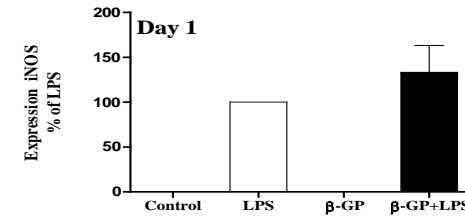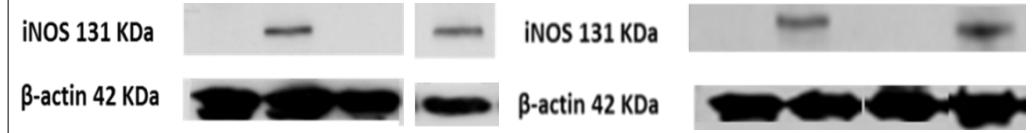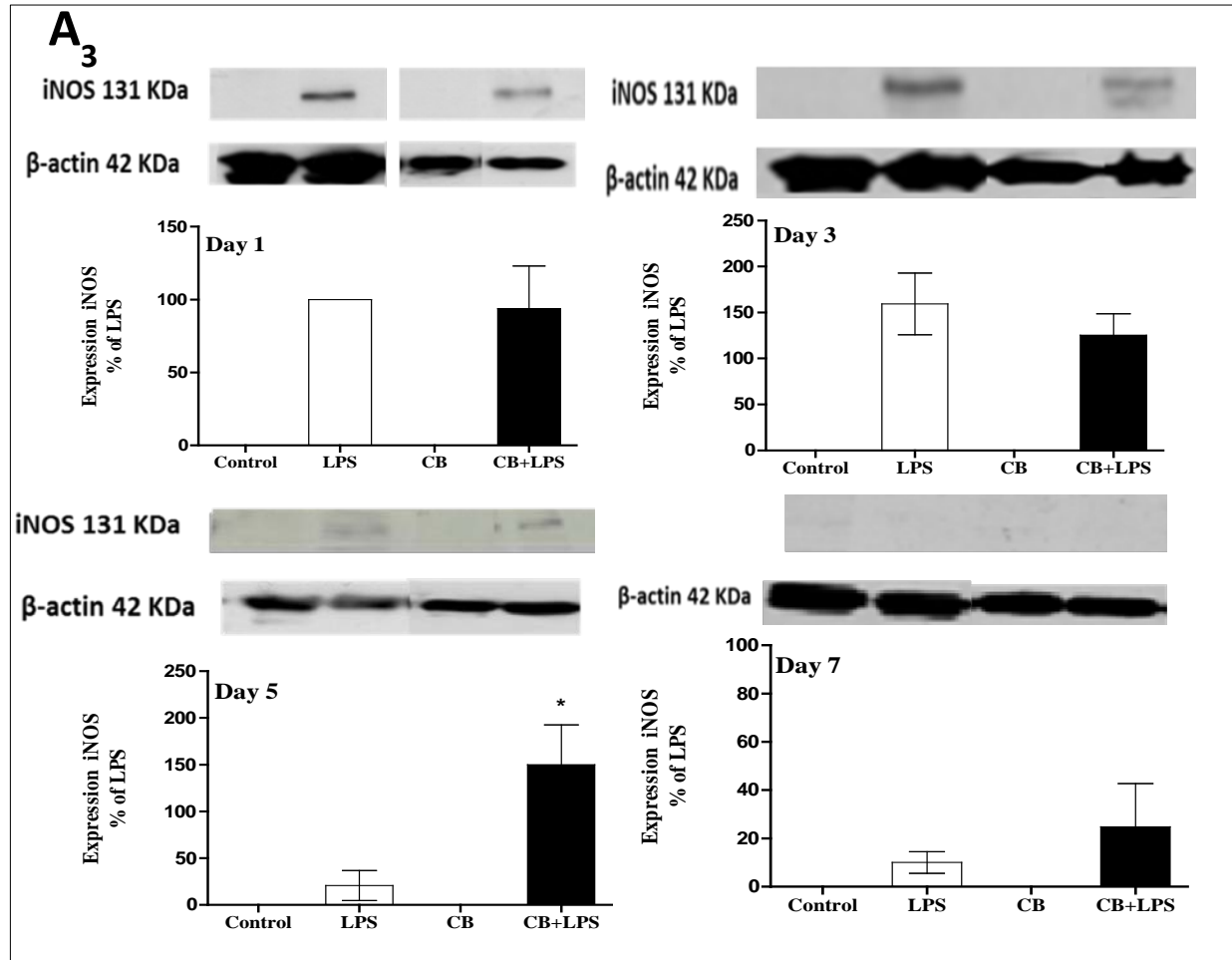
Figure 4.2 A: **Effect of CaCl₂, β-GP and CB on LPS induced iNOS expression.**

Cells were cultured to ~90% confluency and activated with LPS (100 μg ml^{-1}) for 24 hours followed the addition of CaCl₂ (7mM; Panel A₁), β-GP (7mM; Panel A₂) or CB (Panel A₃) in the continued presence of LPS and incubated for a further period of 1, 3, 5 and 7 days. Expression of iNOS was determined by western blotting as described in the methods (section 2.10). The data represents means ± S.E.M. from 4 individual experiments.* denotes $p < 0.05$ compared to LPS alone for each time point.
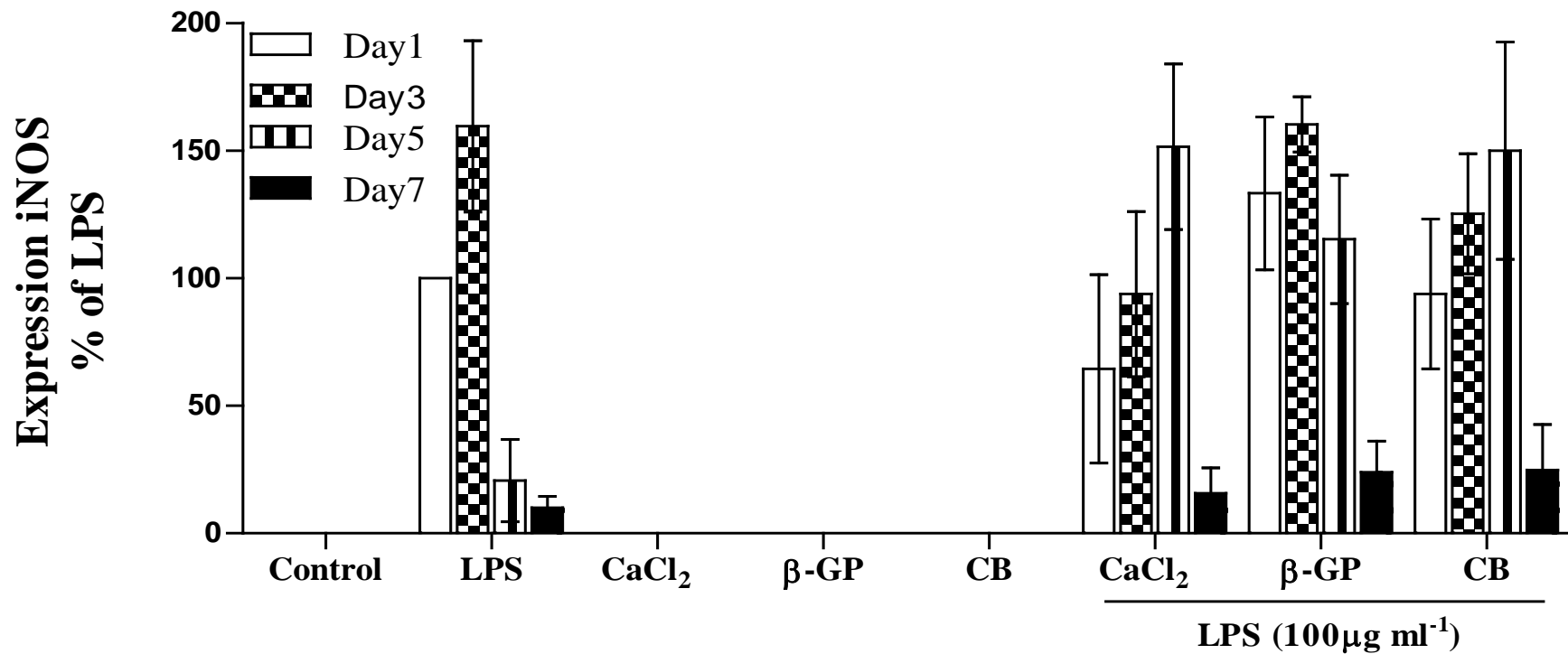
Figure 4.2 B: **Summary data of the effect of CaCl₂, *β*-GP and CB on LPS induced iNOS expression.**

Cells were cultured to ~90% confluency and activated with LPS (100 μg ml^{-1}) for 24 hours followed the addition of CaCl₂ (7mM), *β*-GP (7mM) or CB in the continued presence of LPS and incubated for a further period of 1, 3, 5 and 7 days. Expression of iNOS was determined by western blotting as described in the methods (section 2.10). The data represents means ± S.E.M. from 4 individual experiments.
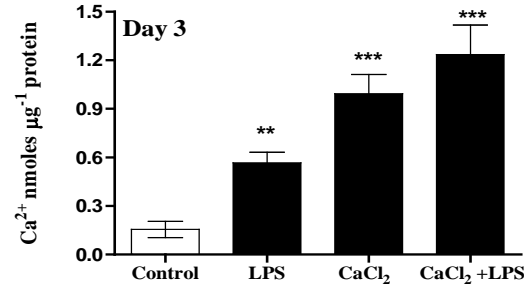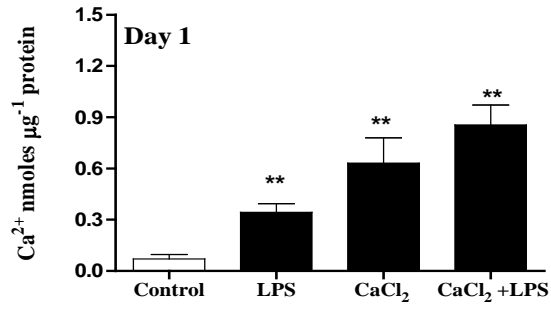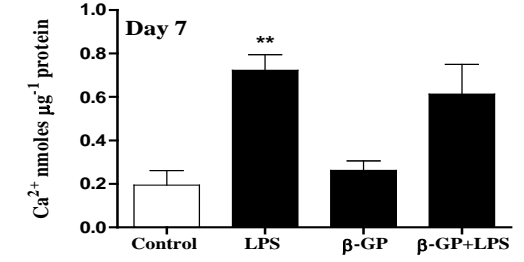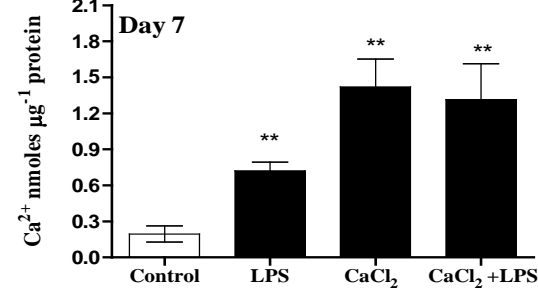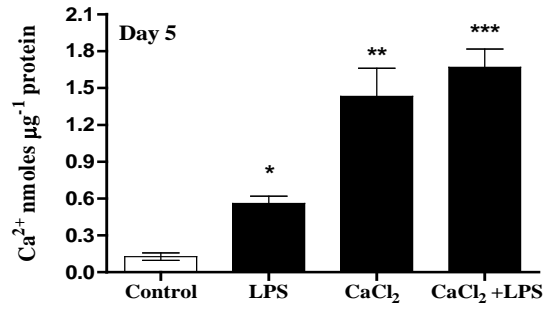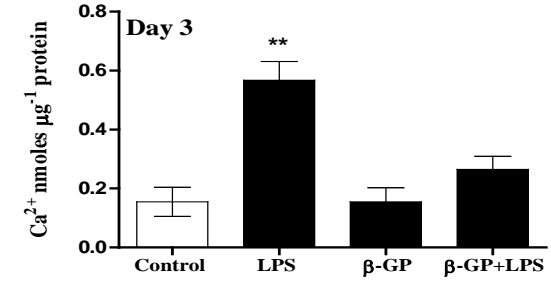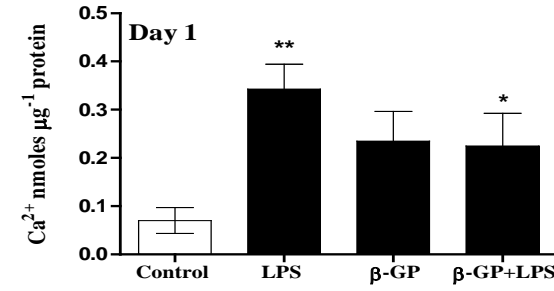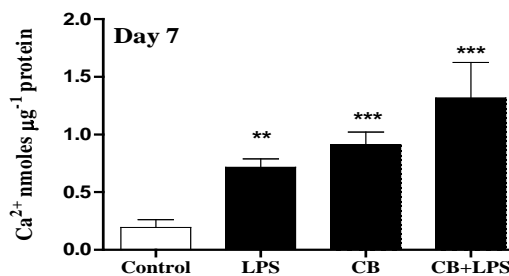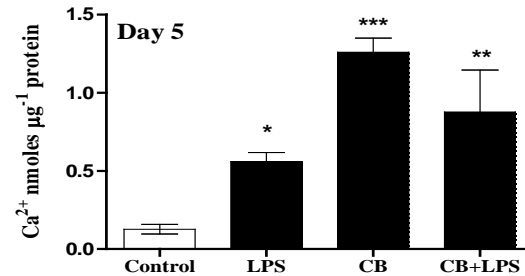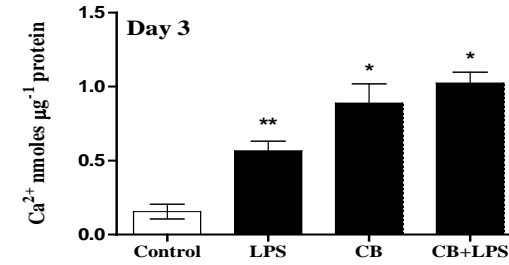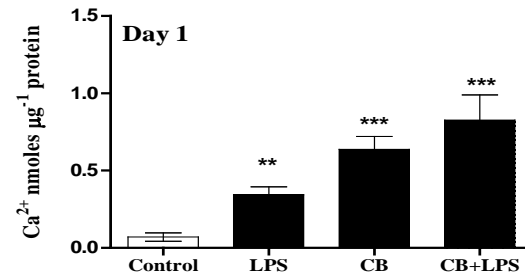
Figure 4.3 A: **Effect of CaCl$_2$, β-GP and CB on LPS induced calcification.**

Cells were cultured to ~90% confluency and activated with LPS (100 µg ml^{-1}) for 24 hours followed the addition of CaCl$_2$ (7mM; Panel A$_1$), β-GP (7mM; Panel A$_2$) or CB (Panel A$_3$) in the continued presence of LPS and incubated for a further period of 1, 3, 5 and 7 days. Total calcium was quantified as described in methods (section 2.6). The data represents means ± S.E.M. from 4 individual experiments.* denotes $p < 0.05$, ** denotes $p<0.01$ and *** denotes $p<0.001$ compared to control for each time point

Figure 4.3 B: **Summary data of the effect of CaCl$_2$, β-GP and CB on LPS induced calcification.**

Cells were cultured to ~90% confluency and activated with LPS (100 μg ml^{-1}) for 24 hours followed the addition of CaCl$_2$ (7mM), β-GP (7mM) or CB in the continued presence of LPS and incubated for a further period of 1, 3, 5 and 7 days. Total calcium was quantified as described in methods (section 2.6). The data represents means ± S.E.M. from 4 individual experiments.

4.3.2- Effects of IFN-γ on NO production, iNOS expression and calcification of RASMCs in the absence and presence of CaCl$_2$, β-GP or CB:

Similar to the studies with LPS, cells were activated with IFN-γ (100U ml^{-1}) for 24 hours before coincubating with CaCl$_2$, β-GP or with CB for the specified time periods without changing the medium Figure 4.4 to 4.6. Incubation of RASMCs with medium alone did not produced NO during 1, 3, 5, and 7 days (Figure 4.4A$_1$). Activation with IFN-γ produced much reduced amounts of NO when compared to LPS treated cells (0.028 ±0.005 nmole. µg^{-1} protein vs 0.097 ±0.02 nmole. µg^{-1} protein at day 5) and there was no statistically significant difference in the amounts produced over the time course. This observation was similar to that seen in cells treated with IFN-γ in the presence of CaCl$_2$, β-GP or with CB in that the changes were much lower than those seen when LPS was used. Thus, induction of NO production by IFN-γ was only marginal when compared to the effects induced with LPS (Figure 4.4 A$_1$). Consistent with the marginal effect on NO production, treatment of cells with IFN-γ alone or in the presence of calcification inducers did not induce iNOS as shown Figure 4.5. This is surprising because there was some detectable NO in the culture medium following exposure of cells to these agents (Figure 4.4A$_{1, 2, 3}$). At present the source of the NO detected is not known but we can rule out contamination in the medium as all the controls incubated with culture medium alone were blank. This therefore leaves the possibility that the NO may potentially come from very low levels of iNOS expressed which may be below the level of detection by western blotting. Quantitative polymerase chain reaction (PCR) analysis of iNOS mRNA expression was planned but unfortunately could not be completed because of time constraints. Figures 4.4B represent summaries of the data from all the conditions above.

Cells activated with IFN-γ appear to be more stable over the time course investigated (0.97± 0.3 nmole µg^{-1} protein) (Figure 4.6 A$_1$).

Coincubation of RASMCs with $CaCl_2$ and IFN-γ resulted in peak calcium levels significantly on day 3 (2.15 ± 1 nmole.µg^{-1} protein) and was sustained up to day 7 (Figure 4.6 A$_1$). The use of *β*-GP together with IFN-γ did not cause elevated calcium above that seen with IFN-γ alone (Figure 4.6 A$_2$). In contrast, cells coincubated with CB and IFN-γ induced significant calcium accumulation similar to effects seen with $CaCl_2$ but peaked at day 5 (3.40 ± 1.2 nmole.µg^{-1} protein) followed by a declined on day 7 (2.12 ± 0.7 nmole.µg^{-1} protein) (Figure 4.6 A$_3$). Thus, IFN-γ activated RASMCs coincubated with $CaCl_2$ or CB led to induced increases in calcium which was significantly higher compared to IFN-γ alone (Figure4.6B).

117
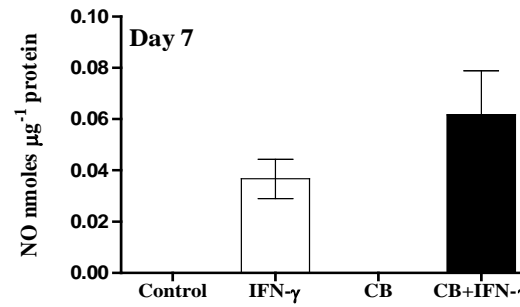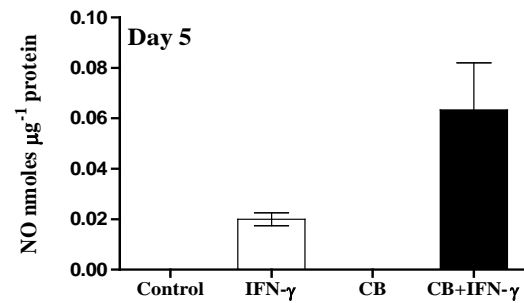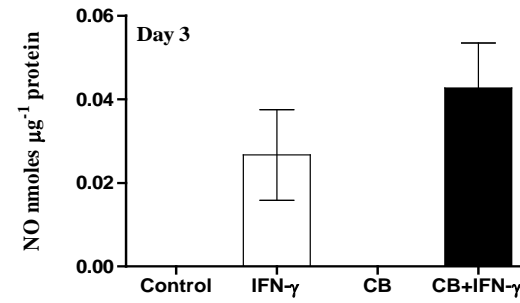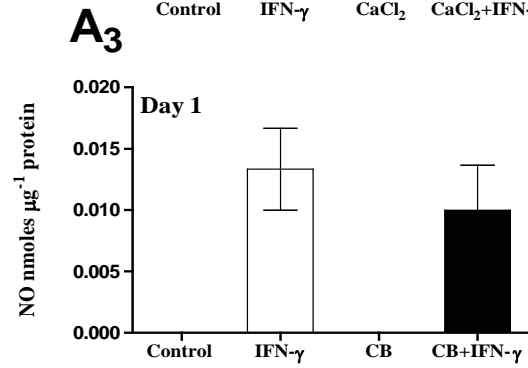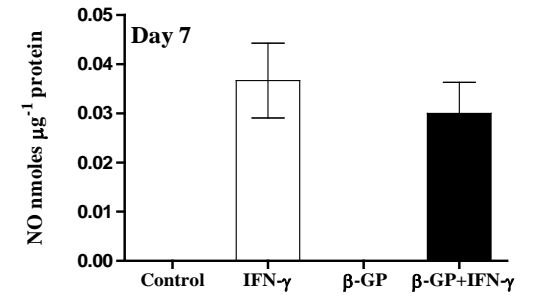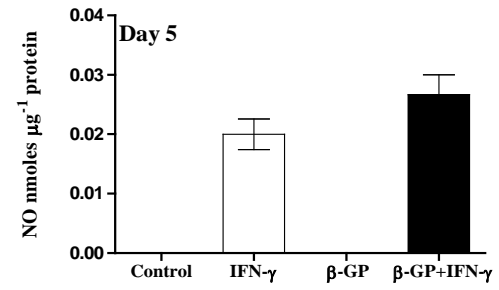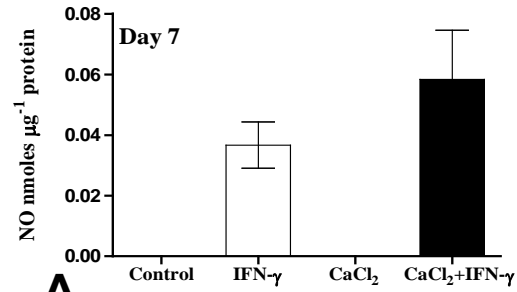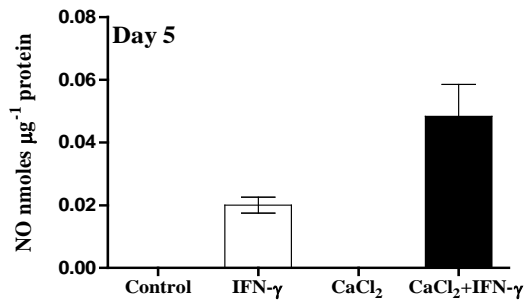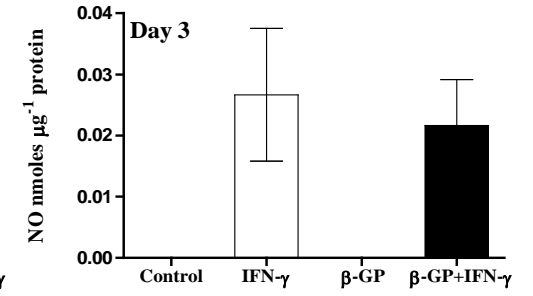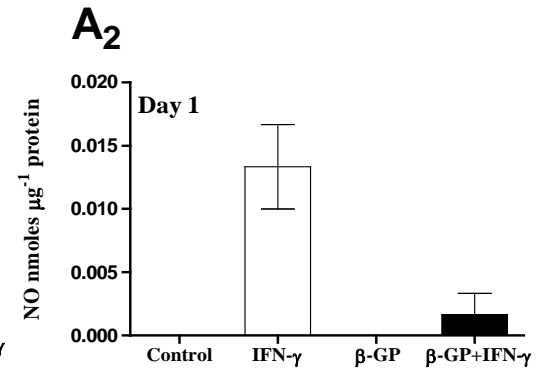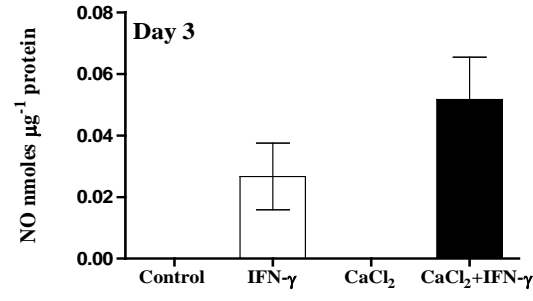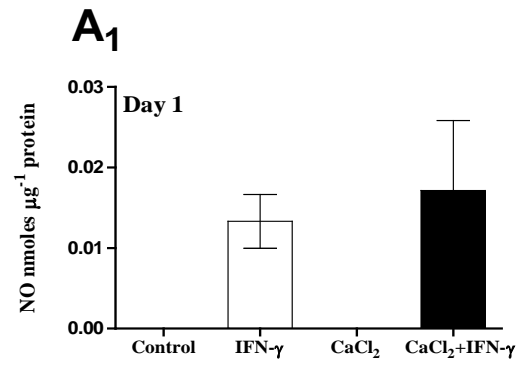
Figure 4.4 A: **Effect of $CaCl_2$, β-GP and CB on IFN-γ induced NO production.**

Cells were cultured to ~90% confluency and activated with IFN-γ (100 U ml^{-1}) for 24 hours followed the addition of $CaCl_2$ (7mM; Panel A_1), β-GP (7mM; Panel A_2) or CB (Panel A_3) in the continued presence of IFN-γ and incubated for a further period of 1, 3, 5, and 7 days. Total NO was quantified by the Griess assay as described in methods (section 2.3). The data represents means $\pm$ S.E.M. from 6 individual experiments.

Figure 4.4 B: **Summary data of the effect of CaCl$_2$, β-GP and CB on IFN-γ induced NO production.**

Cells were cultured to ~90% confluency and activated with IFN-γ (100 U ml^{-1}) for 24 hours followed the addition of CaCl$_2$ (7mM), β-GP (7mM) or CB in the continued presence of IFN-γ and incubated for a further period of 1, 3, 5, and 7 days. Total NO was quantified by the Griess assay as described in methods (section 2.3). The data represents means ± S.E.M. from 6 individual experiments.
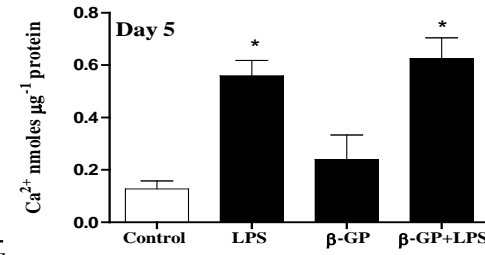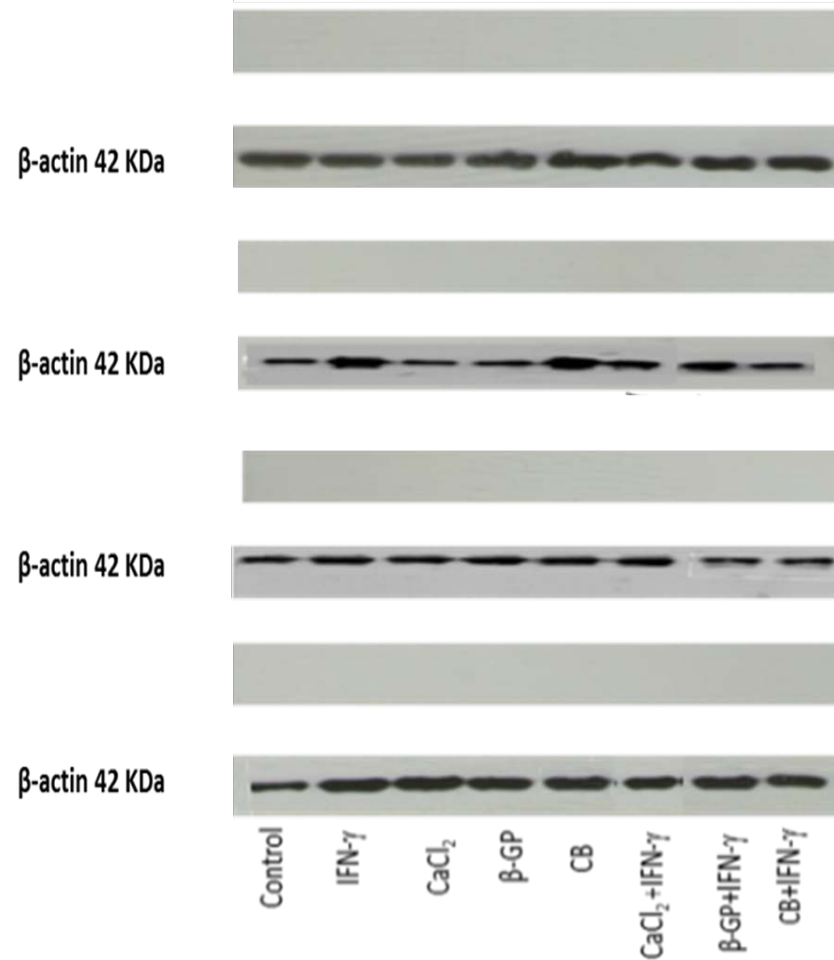
Figure 4.5: **Effect of CaCl₂, β-GP and CB on IFN-γ induced iNOS expression.**

Cells were cultured to ~90% confluency and activated with IFN-γ (100 U ml^{-1}) for 24 hours followed the addition of CaCl$_2$ (7mM), β-GP (7mM) or CB in the continued presence of IFN-γ and incubated for a further period of 1, 3, 5, and 7 days. Expression of iNOS was determined by western blotting as described in the methods (section 2.10). The data represents means ± S.E.M. from 4 individual experiments.

121
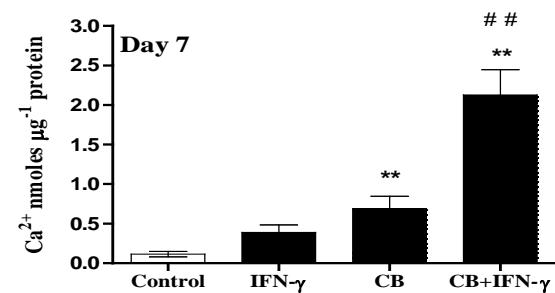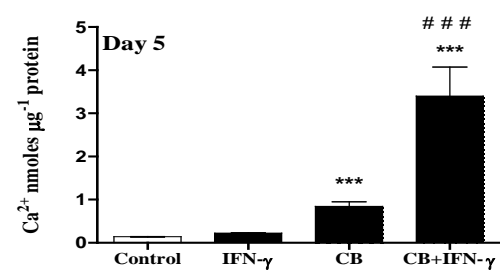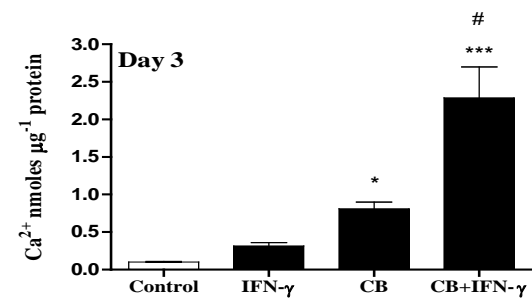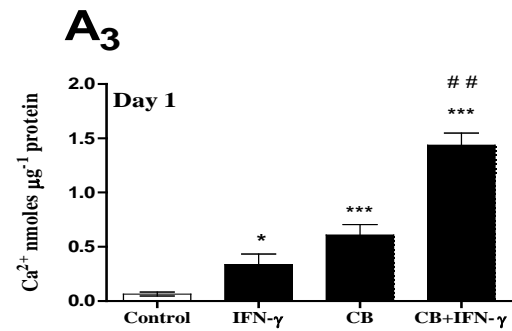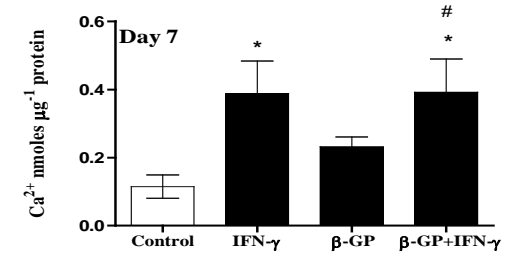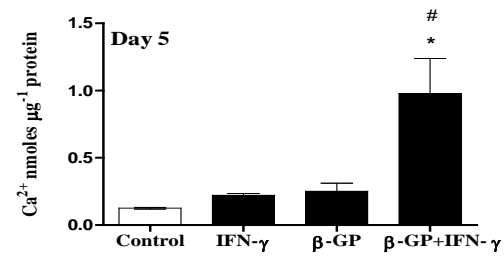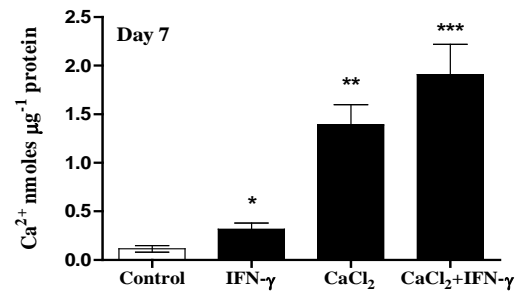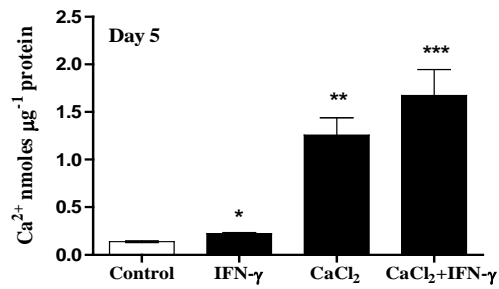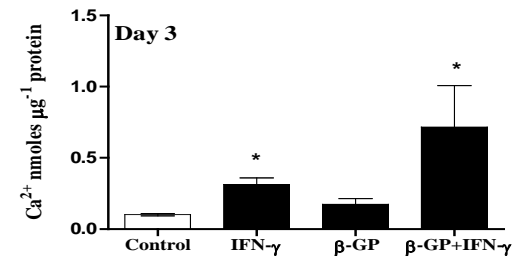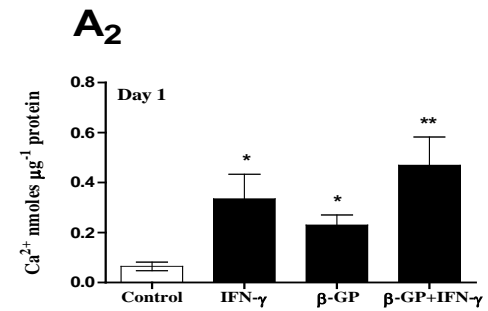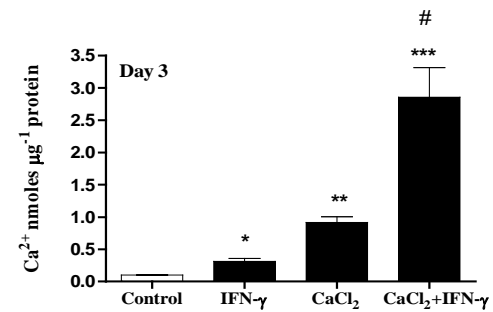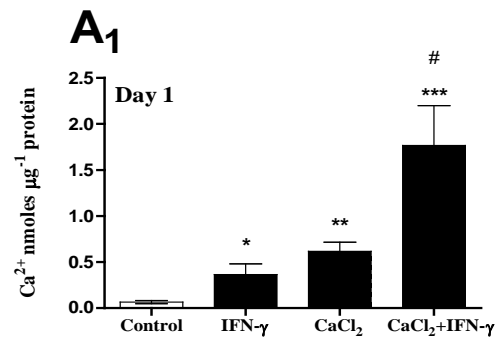
Figure 4.6 A: **Effect of CaCl$_2$, β-GP and CB on IFN-γ induced calcification.**

Cells were cultured to ~90% confluency and activated with IFN-γ (100 U ml^{-1}) for 24 hours followed the addition of CaCl$_2$ (7mM; Panel A$_1$), β-GP (7mM; Panel A$_2$) or CB (Panel A$_3$) in the continued presence of IFN-γ and incubated for a further period of 1, 3, 5, and 7 days. Total calcium was quantified as described in methods (section 2.6).The data represents means $\pm$ S.E.M. from 6 individual experiments.* denotes $p< 0.05$, ** denotes $p<0.01$, and $p<0.001$ compared to control. # denotes $p < 0.05$, ## denotes $p < 0.01$, and ### denotes $p <0.001$ compared to calcification inducers alone for each time point.
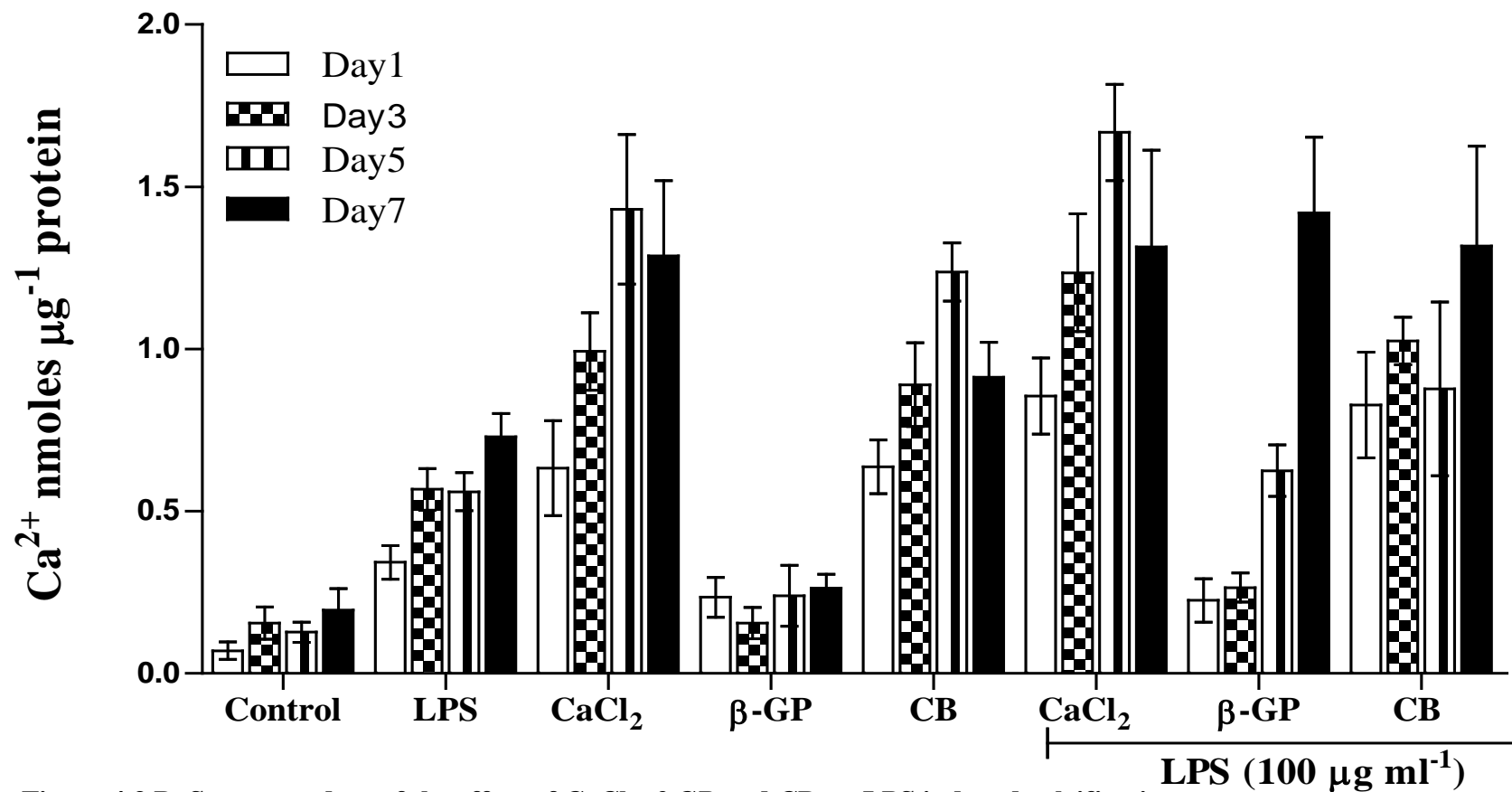
Figure 4.6 B: **Summary data of the effect of CaCl$_2$, β-GP and CB on IFN-γ induced calcification.**

Cells were cultured to ~90% confluency and activated with IFN-γ (100 U ml^{-1}) for 24 hours followed the addition of CaCl$_2$ (7mM), β-GP (7mM) or CB in the continued presence of IFN-γ and incubated for a further period of 1, 3, 5, and 7 days s. Total calcium was quantified as described in methods (section 2.6). The data represents means ± S.E.M. from 6 individual experiments.

4.3.3- Effects of LPS and IFN-γ on NO production, iNOS expression and calcification of RASMCs in the absence and presence of CaCl₂, β-GP or CB:

Following the observations above, further experiments were carried out looking at the combined effects of LPS and IFN-γ under similar conditions to those already described Figure 4.7 to 4.9. Consistent with the studies above, NO production was not detected when cells were incubated with medium alone (control) during 1, 3, 5, and 7 days. Activation of RASMCs with LPS and IFN-γ induced significantly more NO when compared to levels detected with either LPS or IFN-γ alone. The induction was pronounced at day 1 (0.18 ± 0.05 nmole μg^{-1} protein) and did not show much time dependent differences except at day 7 where total NO appeared to be marginally higher, increasing to 0.203 ± 0.09 nmole μg^{-1} protein. These responses to LPS and IFN-γ were significantly enhanced in the presence of CaCl₂, β-GP or CB but with no obvious significant differences between the responses induced. Moreover, CaCl₂, β-GP and CB did not individually induce NO production (Figure 4.7A$_{1, 2, 3}$). A summary figure of these trends is shown in Figure 4.7 B

Consistent with the stimulation of NO production, iNOS was induced in parallel and detectable on day 1, remaining sustained up to day 7 (Figure 4.8 A$_{1, 2, 3}$). The coincubation of RASMCs with LPS+IFN-γ and either CaCl₂, β-GP or CB induced significantly more iNOS expression but this was only evident on day 3. The levels seen at the other time points were not significantly different to the levels induced by LPS and IFN-γ alone. Moreover, CB did not cause any further increase to that caused by either CaCl₂ or β-GP (Figure 4.8 A$_{1, 2, 3}$; see Figure 4.8 B for summary data).

In the calcification experiments, there was no evidence of this process in control cells during the time course examined (Figure 4.9 A$_{1, 2, 3}$; see Figure 4.9 B). However, activation of RASMCs with LPS and IFN -γ resulted in elevation of calcium in a time dependent manner reaching

maximal induction at day 5 (0.87 ±0.2 nmole μg^{-1} protein) although calcification inducers were absent, Figure 4.9 $A_{1, 2, 3}$.

In addition, when activated cells were incubated with $CaCl_2$ and CB there was a more potent induction of calcification peaking at day 5 (2.77 ±0.7 and 3.10 ±0.7 nmole μg^{-1} protein, respectively) and declining marginally on day 7 (2 ±0.3 nmole μg^{-1} protein and 2.6 ±0.3 nmole μg^{-1} protein) (Figure 4.9 $A_{1 \& 3}$). Cells coincubated with β-GP+ LPS and IFN-γ (0.74 ±0.1 nmole μg^{-1} protein) did not cause more calcification than that seen with LPS/IFN-γ alone but levels were significant when compared the response to β-GP alone (Figure 4.9 A_2).

In conclusion, RASMCs when activated by LPS+IFN-γ and coincubated with $CaCl_2$ alone or in combination with β-GP (CB) resulted in further elevation of calcification Figure 4.9 B. This assists confirmation that a stable and functional iNOS might be playing a role in the development of calcification.
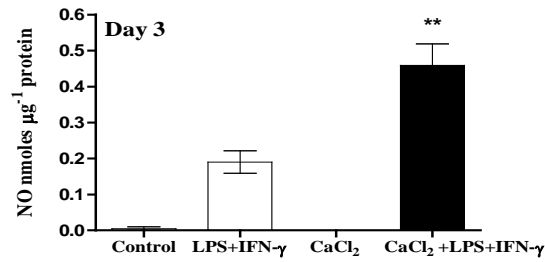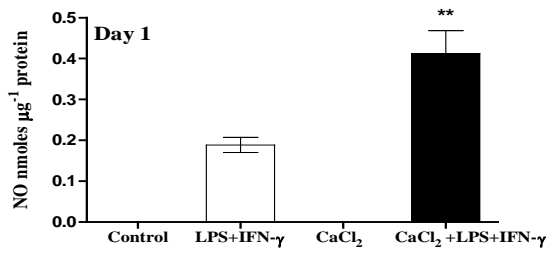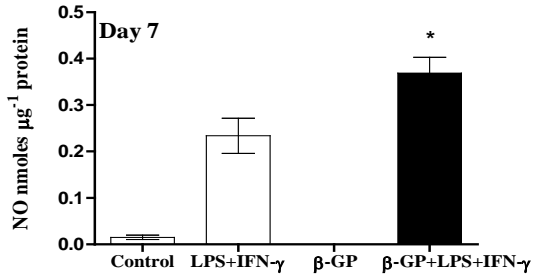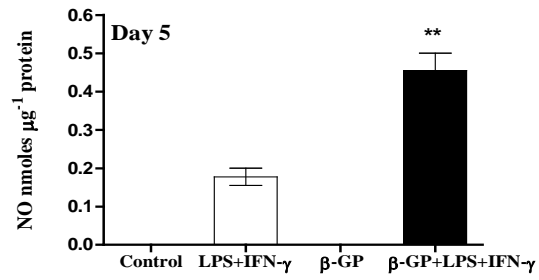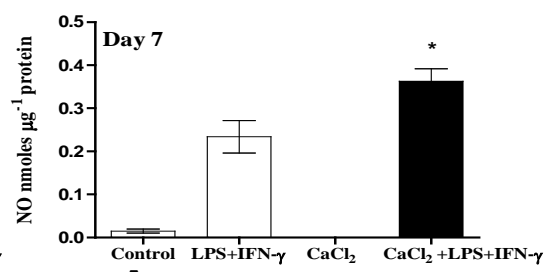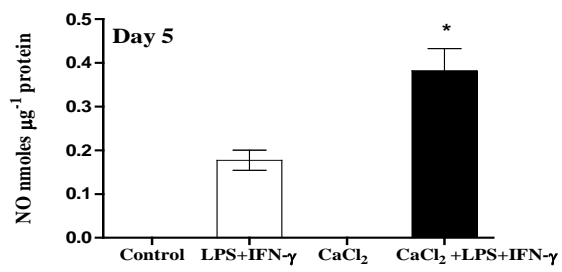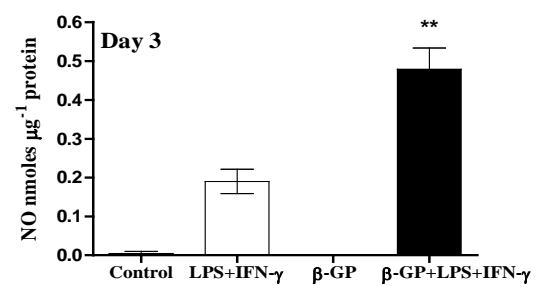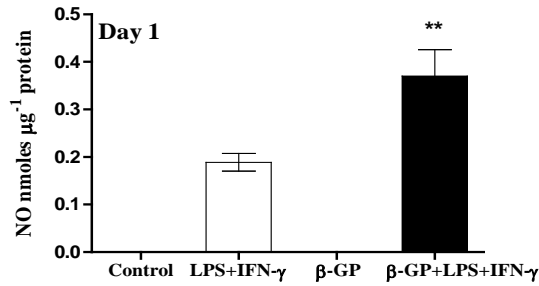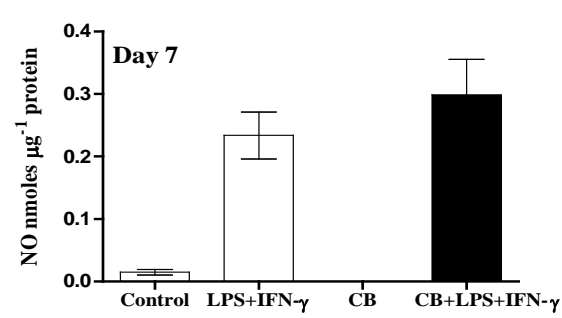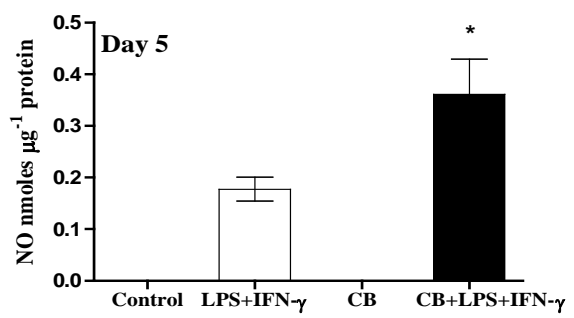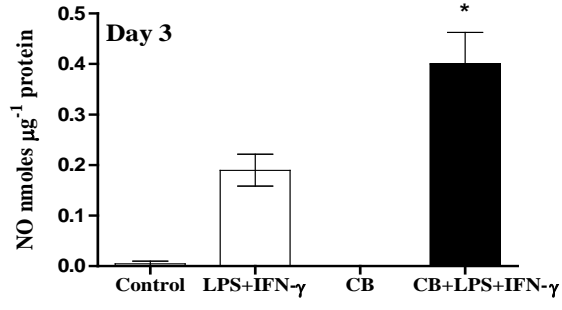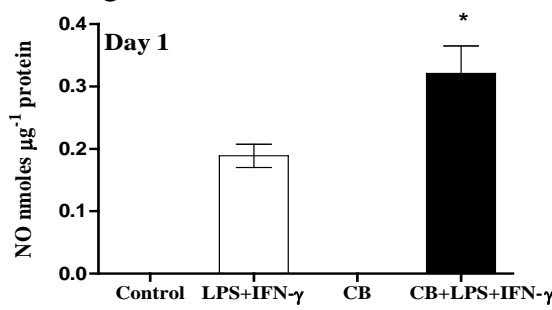
Figure 4.7 A: **Effect of CaCl$_2$, *β*-GP and CB on LPS +IFN-γ induced NO production.**

Cells were cultured to ~90% confluency and activated with LPS (100 µg ml^{-1}) + IFN-γ(100 U ml^{-1}) for 24 hours followed the addition of CaCl$_2$ (7mM; Panel A$_1$), *β*-GP (7mM; Panel A$_2$) or CB (Panel A$_3$) in the continued presence of LPS + IFN-γ and incubated for a further period of 1, 3, 5 and 7 days. Total NO was quantified by the Griess assay as described in methods (section 2.3). The data represents means ± S.E.M. from 8 individual experiments.* denotes *p* < 0.05 and ** denotes *p* <0.01 compared to LPS + IFN-γ alone for each time point.

Figure 4.7 B: **Summary data of the effect of CaCl$_2$, β-GP and CB on LPS +IFN-γ induced NO production.**

Cells were cultured to ~90% confluency and activated with LPS (100 μg ml^{-1}) + IFN-γ(100 U ml^{-1}) for 24 hours followed the addition of CaCl$_2$ (7mM), β-GP (7mM) or CB in the continued presence of LPS+IFN-γ and incubated for a further period of 1, 3, 5 and 7 days. Total NO was quantified by the Griess assay as described in methods (section 2.3). The data represents means ± S.E.M. from 8 individual experiments.
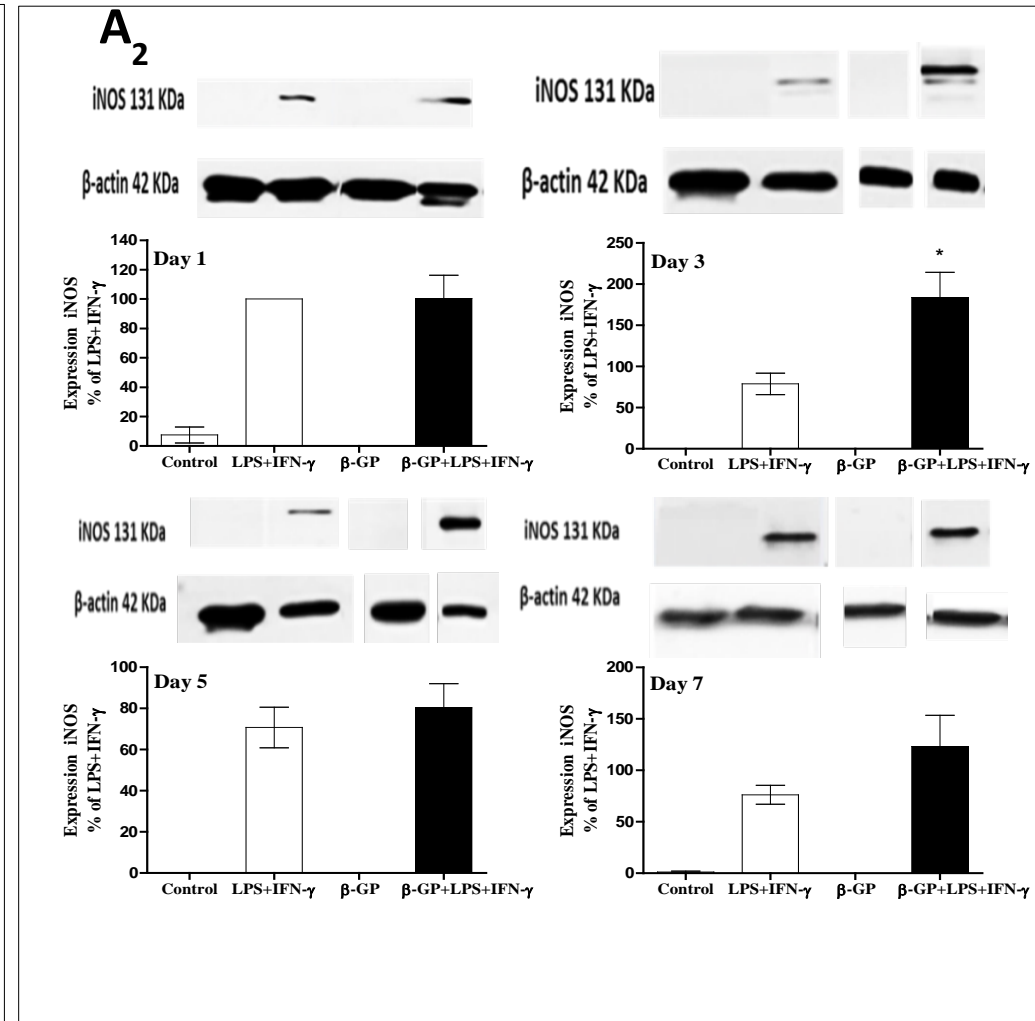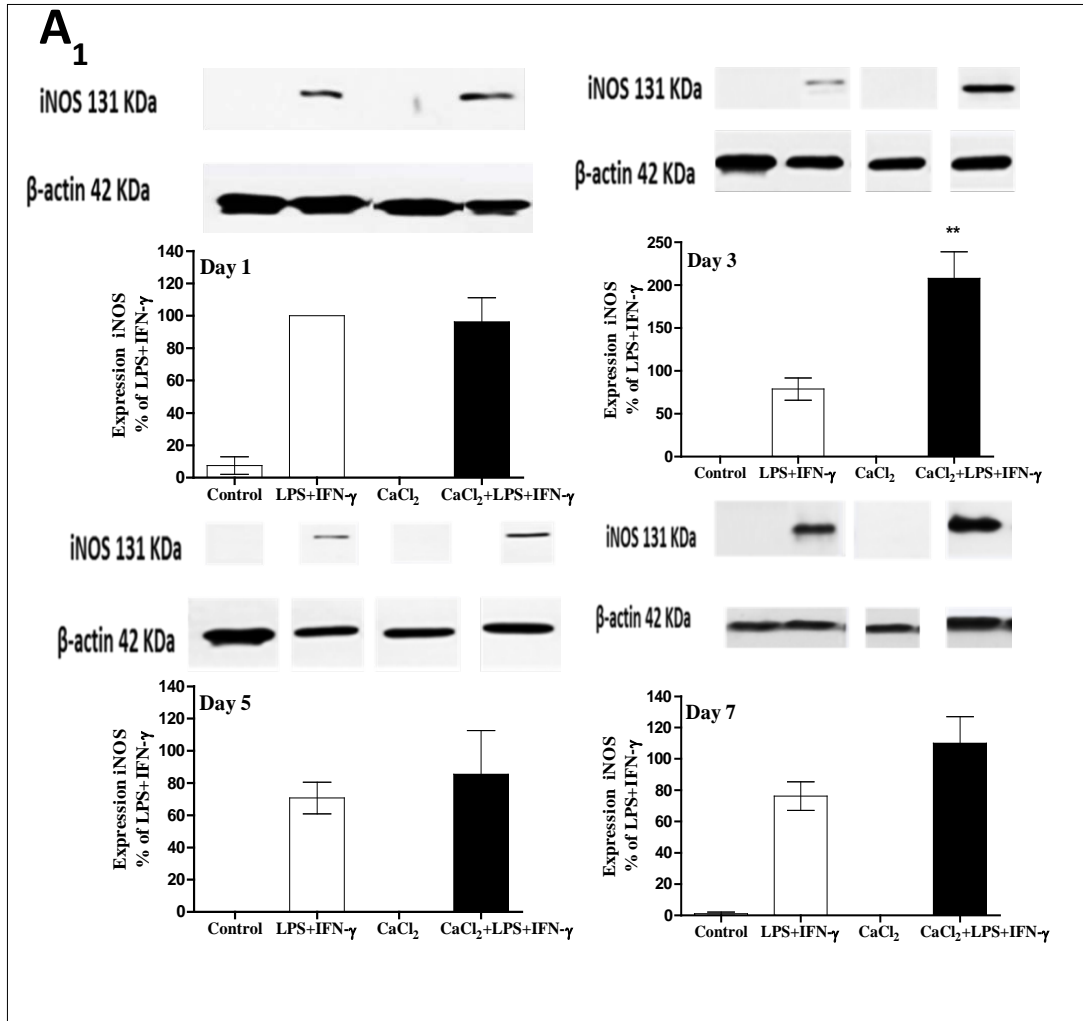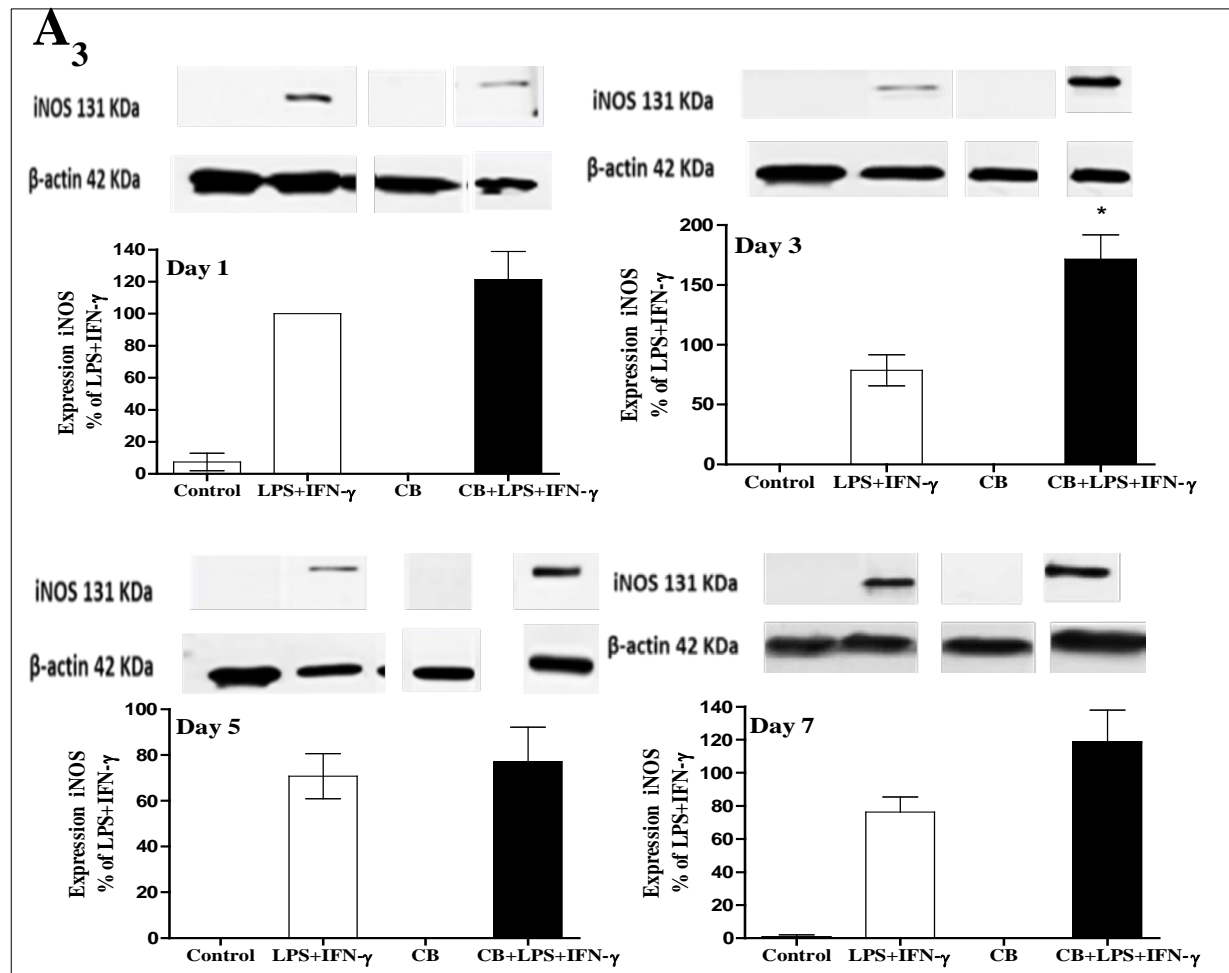
Figure 4.8 A: **Effect of CaCl$_2$, β-GP and CB on LPS+ IFN-γ induced iNOS expression.**

Cells were cultured to ~90% confluency and activated with LPS (100 μg ml^{-1})+ IFN-γ (100 U ml^{-1}) for 24 hours followed the addition of CaCl$_2$ (7mM; Panel A$_1$), β-GP (7mM; Panel A$_2$) or CB (Panel A$_3$) in the continued presence of LPS+ IFN-γ and incubated for a further period of 1, 3, 5 and 7 days. Expression of iNOS was determined by western blotting as described in the methods (section 2.10). The data represents means $\pm$ S.E.M. from 4 individual experiments.* denotes $p < 0.05$ and ** denotes $p < 0.01$ compared to LPS+ IFN-γ alone for each time point.

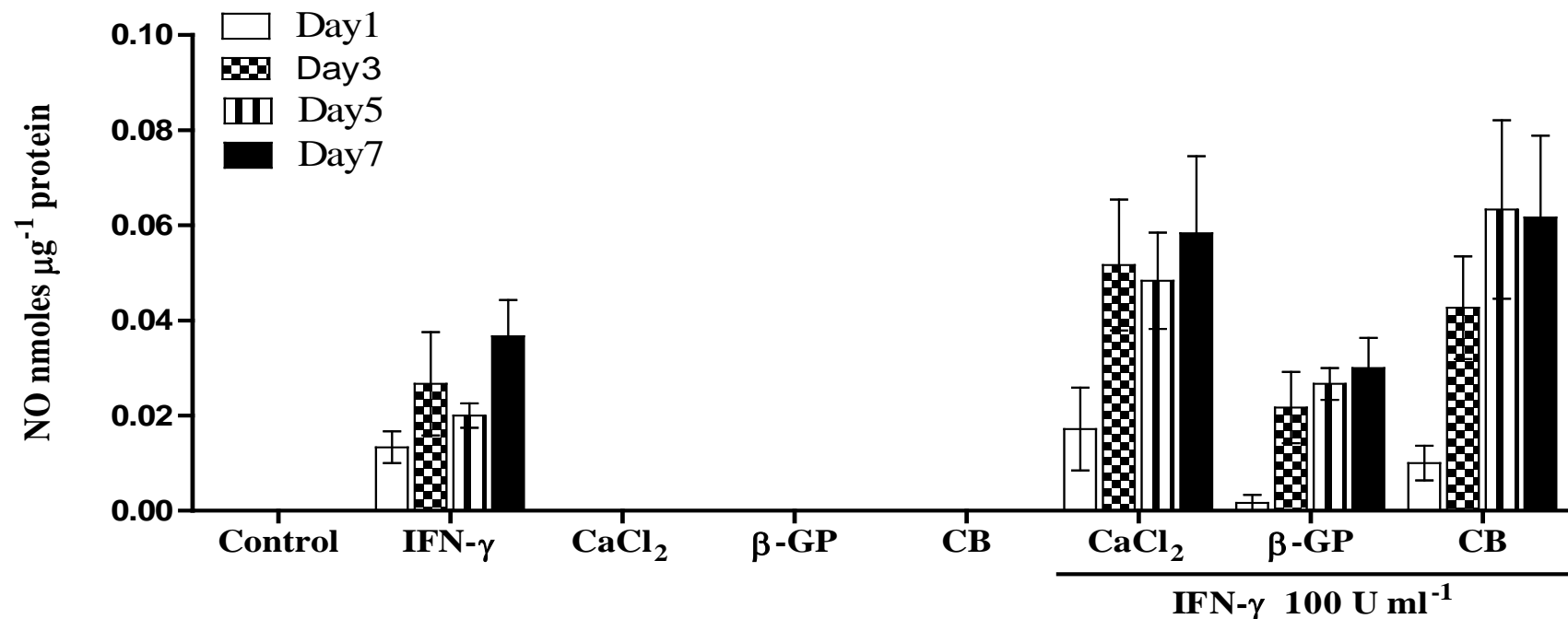**Figure 4.8 B**: **Summary data of the effect of CaCl₂, *β*-GP and CB on LPS+IFN-γ induced iNOS expression.**

Cells were cultured to ~90% confluency and activated with LPS (100 μg ml^{-1})+ IFN-γ (100 U ml^{-1}) for 24 hours followed the addition of CaCl₂ (7mM), *β*-GP (7mM) or CB in the continued presence of LPS+ IFN-γ and incubated for a further period of 1, 3, 5 and 7 days. Expression of iNOS was determined by western blotting as described in the methods (section 2.10). The data represents means ± S.E.M. from 4 individual experiments.
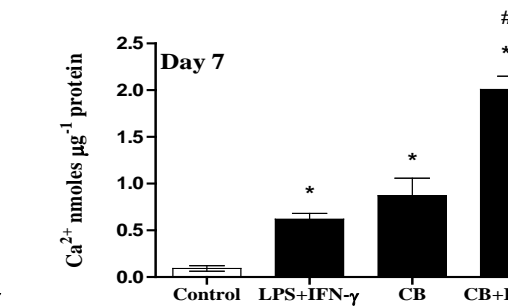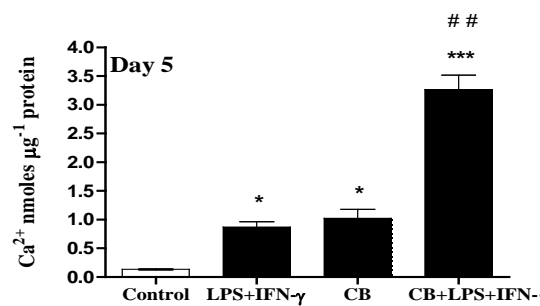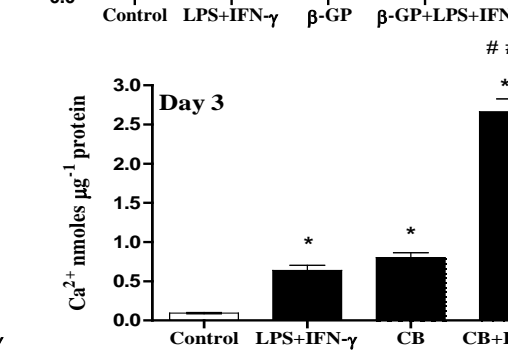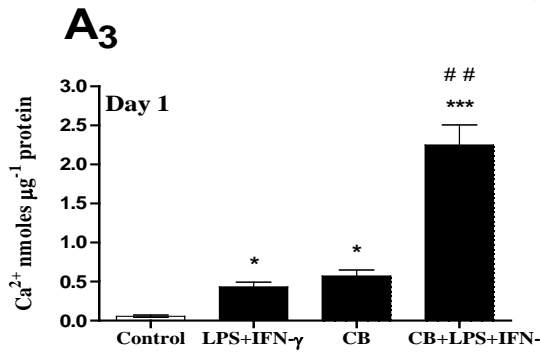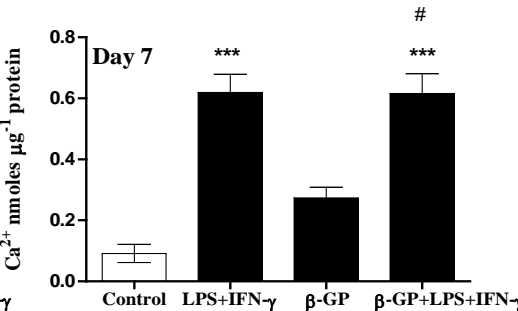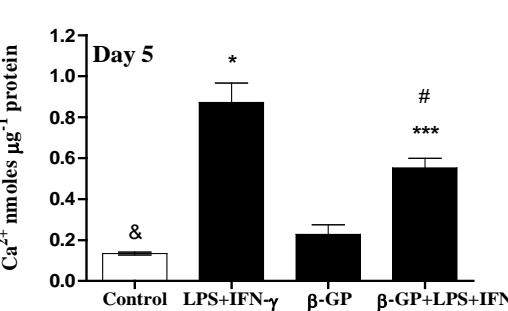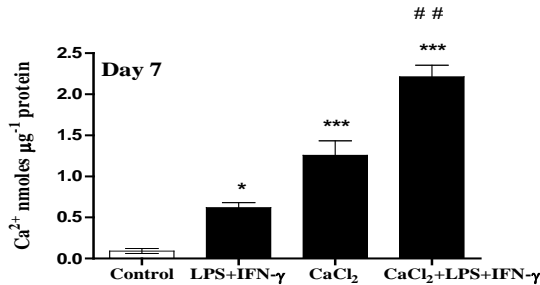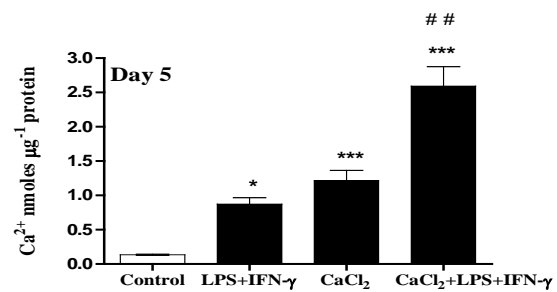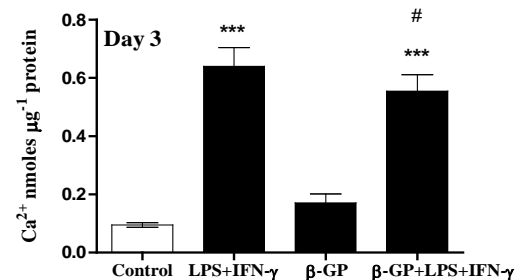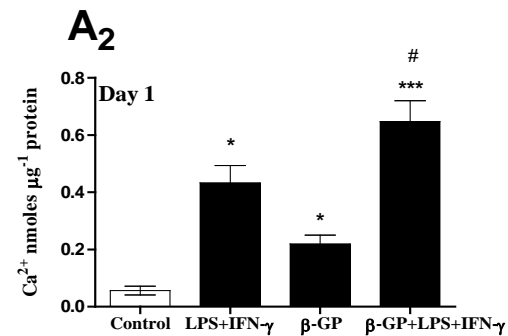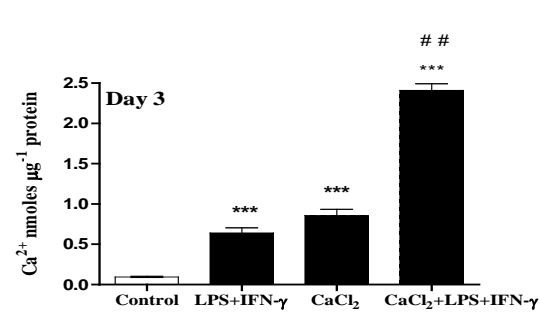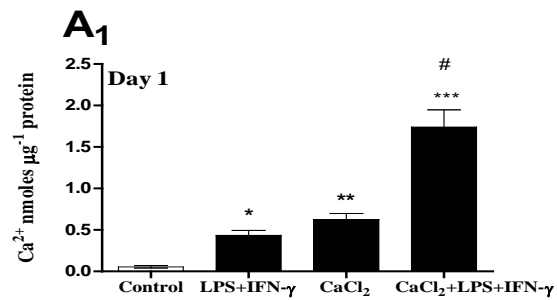
Figure 4.9 A: **Effect of CaCl$_2$, β-GP and CB on LPS +IFN-γ induced calcification.**

Cells were cultured to ~90% confluency and activated with LPS (100 µg ml^{-1})+ IFN-γ (100 U ml^{-1}) for 24 hours followed the addition of CaCl$_2$ (7mM; Panel A$_1$), β-GP (7mM; Panel A$_2$) or CB (Panel A$_3$) in the continued presence of LPS+ IFN-γ and incubated for a further period of 1, 3, 5 and 7 days. Total calcium was quantified as described in methods (section 2.6). The data represents means ± S.E.M. from 8 individual experiments. .* denotes $p< 0.05$, ** denotes $p<0.01$ and $p<0.001$ compared to control. # denotes $p < 0.05$, ## denotes $p < 0.01$, and ### $p<0.001$ compared to calcification inducers alone for each time point.

Figure 4.9 B: **Summary data of the effect of CaCl$_2$, *β*-GP and CB on LPS+IFN-γ induced calcification.**

Cells were cultured to ~90% confluency and activated with LPS (100 μg ml^{-1})+ IFN-γ (100 U ml^{-1}) for 24 hours followed the addition of CaCl$_2$ (7mM), *β*-GP (7mM) or CB in the continued presence of LPS+ IFN-γ and incubated for a further period of 1, 3, 5 and 7 days. Total calcium was quantified as described in methods (section 2.6). The data represents means ± S.E.M. from 8 individual experiments.

### 4.3.4- Detection of components of calcification plaque using ARS and FT-IR:

4.3.4.1- Staining of calcific plaques with ARS:

To establish whether the changes in calcium levels described above were indeed associated with the formation of calcific plaques, further experiments were conducted staining cells with ARS and also subjecting cell lysates generated from different conditions to FT-IR analysis for detection of HA crystals. These studies were conducted at the single time point of 5 days because this was the time point found to cause maximum or reproducible elevations in calcium under the various conditions described above. Cells coincubated with medium only did not stain with ARS at day 5 (Figure 4.10 A, B and C). Staining of calcific plaques did not occur when RASMCs were coincubated with LPS, IFN-γ or in combination, nor was there any staining detected with $CaCl_2$ or β-GP alone. However, when RASMCs were incubated with $CaCl_2$ and LPS, there was less detectable staining of cells with ARS but not when β-GP was used in place of $CaCl_2$ (Figure 4.10A). Staining was also prominent with CB (was little detected) and when CB or $CaCl_2$ was incubated with both inflammatory agents. LPS and IFN-γ together did not cause any detectable staining (Figure 4.10 C). The use of CB and IFN-γ also causes significant staining of RASMCs (Figure 4.10 B) suggesting a good degree of calcification Figure 4.10B. There was little or no staining in cells treated with LPS, IFN-γ or β-GP (Figure4.10 A and B).
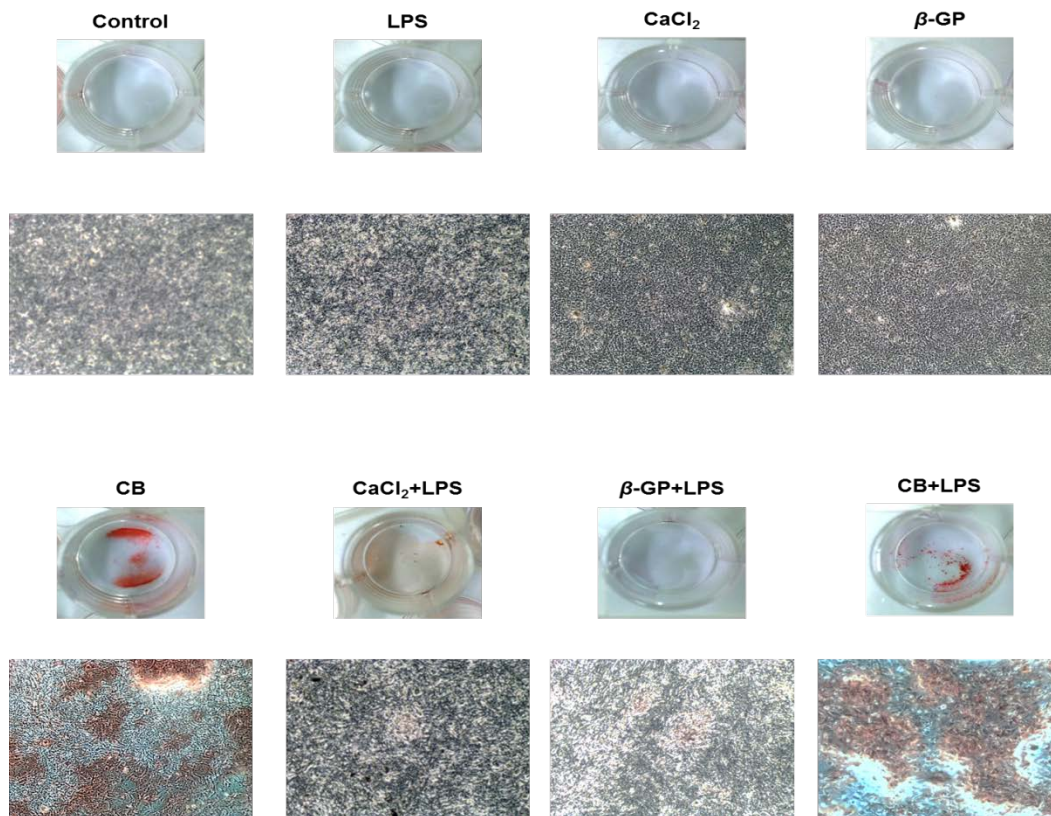
Figure 4.10 A: Alizarin red staining of calcified RASMCs.

Cells were cultured to ~90% confluency and incubated with culture medium alone (control), or activated with LPS (100 μg ml^{-1}) for 24 hours followed the addition of 7 mM CaCl$_2$, 7 mM β-GP or CB (CaCl$_2$ +β-GP) for 5 days. In parallel studies CaCl$_2$, β-GP or CB were added without LPS. Cells were treated with 1x of ARS (1: 10 stock solution) at the end of the treatment period as described in method (Section 2.8). The images are representative of 3 individual experiments which were taken with an inverted Olympus microscope at 10X magnification using GX capture programme.
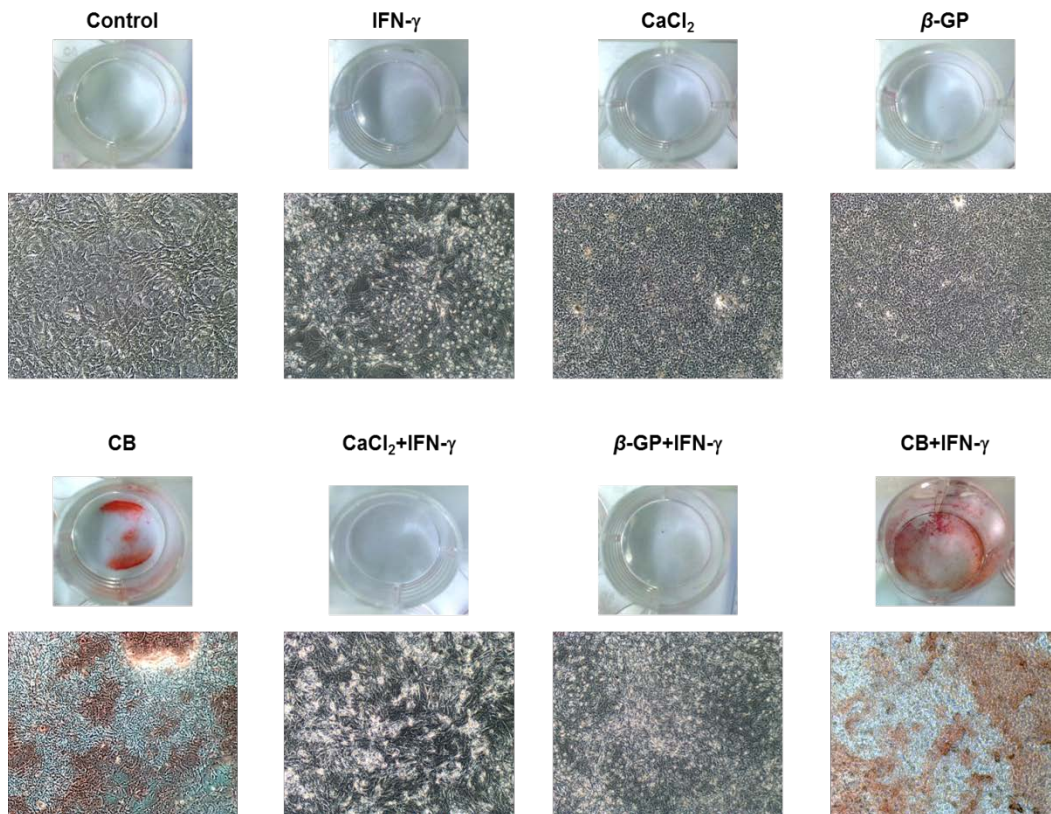
Figure 4.10 B: **Alizarin red staining of calcified RASMCs.**

Cells were cultured to ~90% confluency and incubated with culture medium alone (control), or activated with IFN-γ (100 U ml^{-1}) for 24 hours followed the addition of 7 mM CaCl$_2$, 7 mM β-GP or CB (CaCl$_2$ +β-GP) for 5 days. In parallel studies CaCl$_2$, β-GP or CB were added without IFN-γ. Cells were treated with 1x of ARS (1: 10 stock solution) at the end of the treatment period as described in method (Section 2.8). The images are representative of 3 individual experiments which were taken with an inverted Olympus microscope at 10X magnification using GX capture programme.

Figure 4.10 C: **Alizarin red staining of calcified RASMCs.**

Cells were cultured to ~90% confluency and incubated with culture medium alone (control), or activated with LPS (100 µg ml^{-1}) + IFN-γ (100 U ml^{-1}) for 24 hours followed the addition of 7 mM CaCl$_2$, 7 mM β-GP or CB (CaCl$_2$ +β-GP) for 5 days. In parallel studies CaCl$_2$, β-GP or CB were added without LPS+IFN-γ. Cells were treated with 1x of ARS (1: 10 stock solution) at the end of the treatment period as described in method (Section 2.8). The images are representative of 3 individual experiments which were taken with an inverted Olympus microscope at 10X magnification using GX capture programme.

4.3.4.2-Detecting HA crystals by FT-IR analysis:

In vitro calcification was investigated by FT-IR in order to determine the spectra that identified HA crystal under the different experimental conditions already examined. The control spectra shown in Figure 4.11 A identifies Amide I, Amide II and Amide III at 1630-1637 cm^{-1}, 1514.53-1522.37 cm^{-1}, and 1234-1243.99 cm^{-1} respectively. When RASMCs were incubated with β-GP in the presence of LPS, phosphate was detected at 1076 cm^{-1} but no HA crystal was identified. In contrast, HA crystal was present at 1088 and 1083 cm^{-1} when cells were exposed to CB with LPS or IFN-γ but not for CaCl$_2$ with LPS (Figure 4.11 A).

As with LPS, incubation of cells with IFN-γ in the presence of CB caused formation of HA crystal which was detected at 1085 cm^{-1} (Figure 4.11B). In contrast, when β-GP was used with IFN-γ, only phosphate was detected and at 1077 cm^{-1}. There was no HA crystal identified (Figure 4.11 B). The different molecules identified by the FT-IR analysis together with their vibrational frequencies are summarised in Tables 4.1, 4.2 and 4.3. Interestingly, CaCl$_2$ or CB in the presence of LPS and IFN-γ could support formation of HA crystal with a spectrum at 1080-1089 cm^{-1}. Incubation of cells with CaCl$_2$, β-GP alone or in combination with LPS or IFN-γ at day 5, did not result in HA crystal whereas CB alone or with inflammatory mediators did cause HA crystal formation as shown in Figure 4.11 A, B and C. Table 4.1, 4.2, and 4.3 showed summary of spectrum of molecules detected by FT-IR treated RASMCs either by LPS, IFN-γ, or LPS+IFN-γ in presence or absence of CaCl$_2$, β-GP/ CB.

141
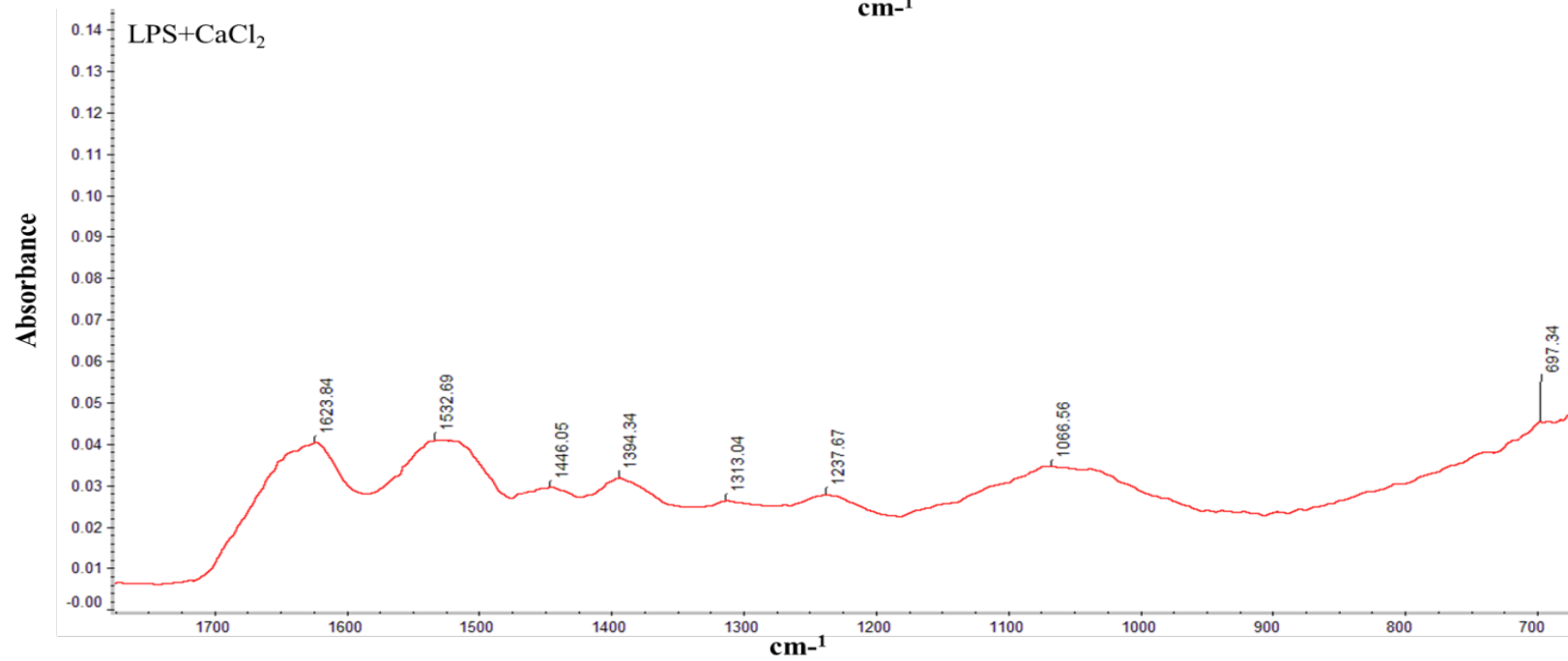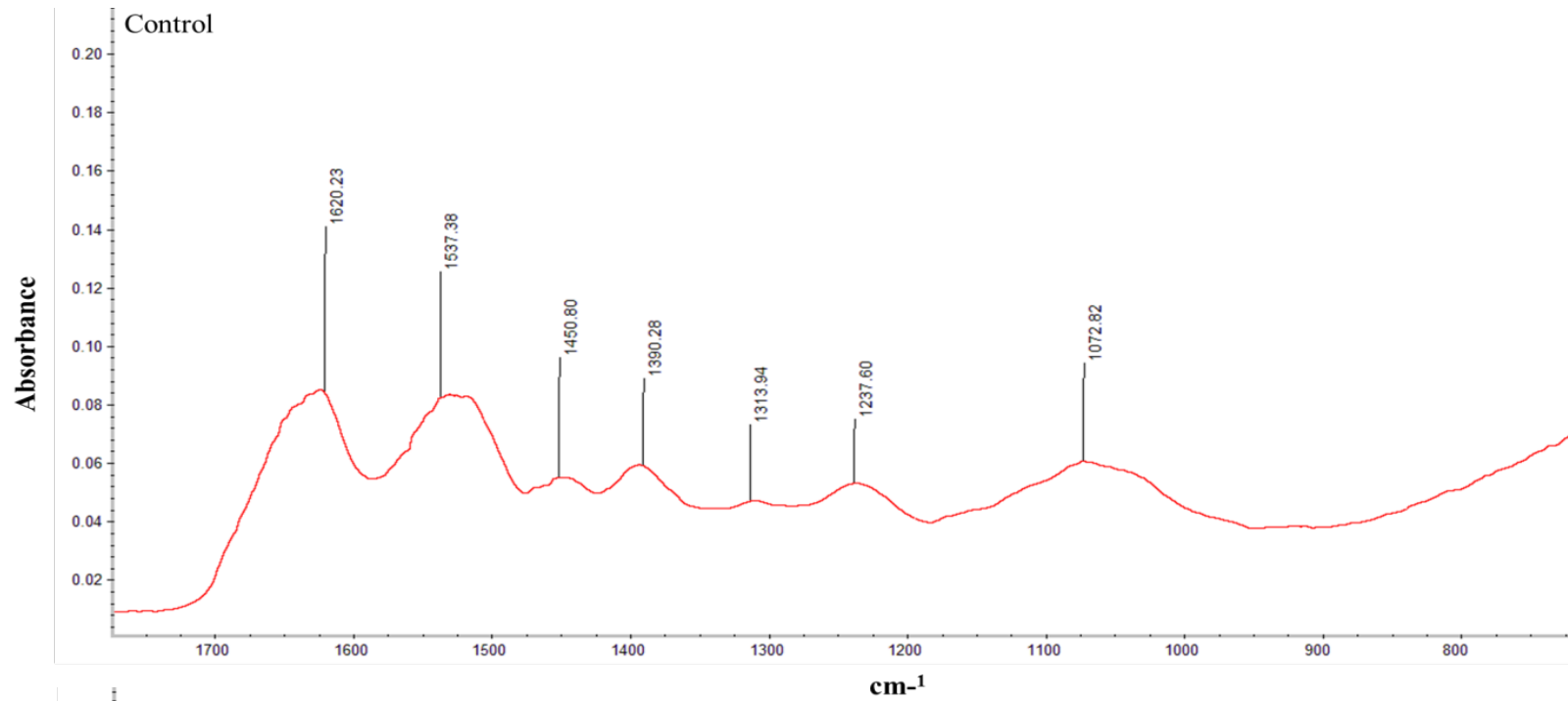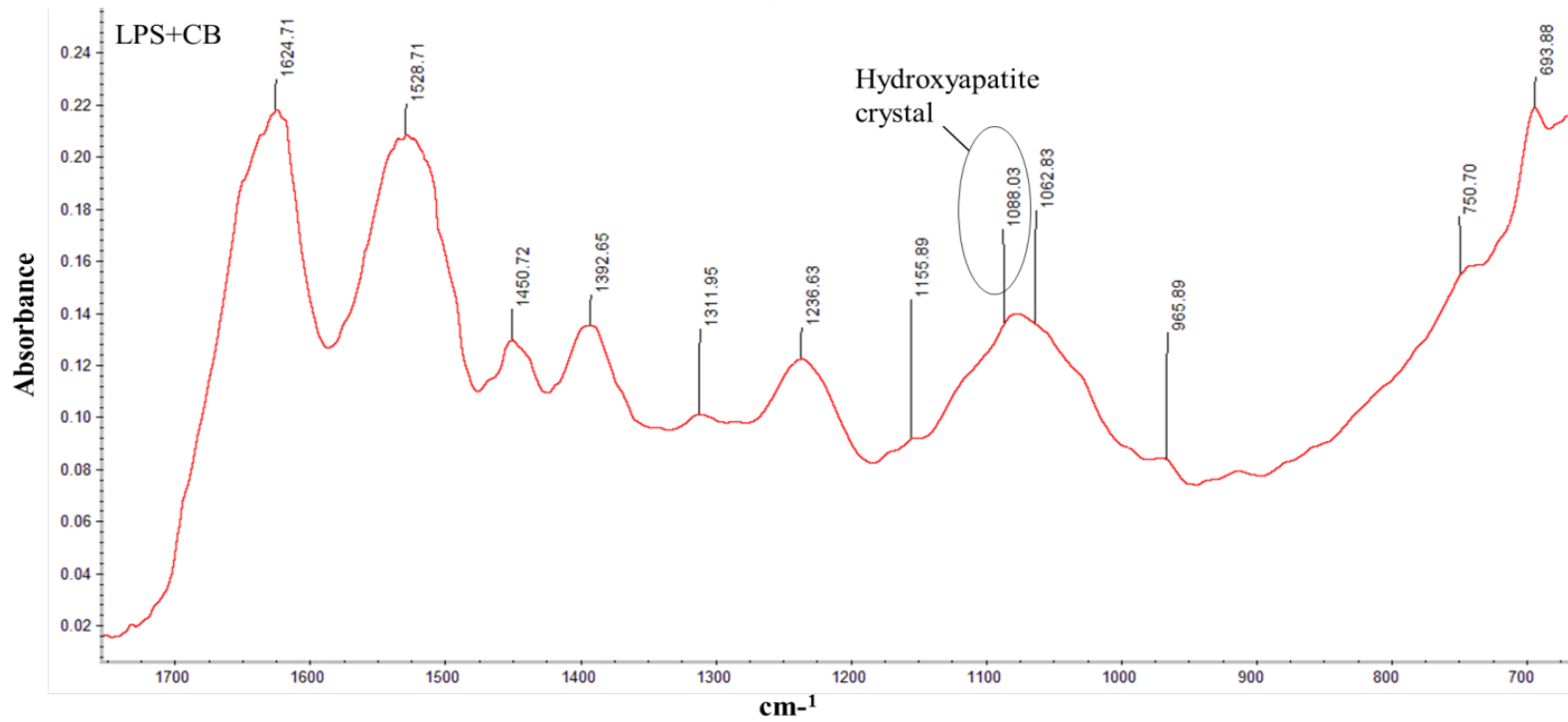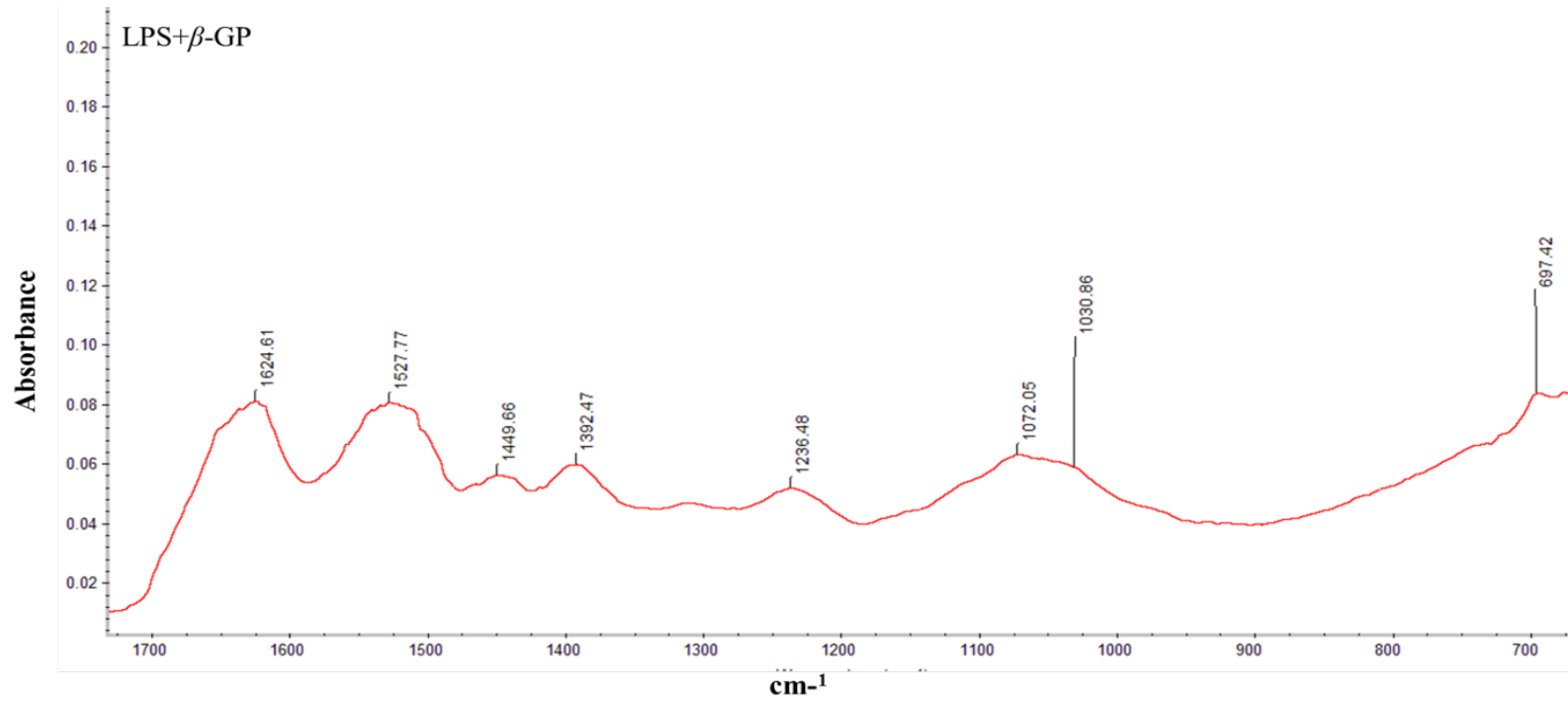
Figure 4.11 A: FT-IR spectrum analysis of activated RASMCs.

Cells were cultured to ~90% confluency and incubated with culture medium alone (control) and either with LPS (100 μg ml^{-1}) followed the addition of $CaCl_2$, β-GP or in combination at 7mM for 5 days. Cells were washed and scraped with 100% ethanol at the end of the incubation period and subjected to FT-IR as described in method (section 2.9). The FT-IR spectra are representative of 3 individual experiments.

143
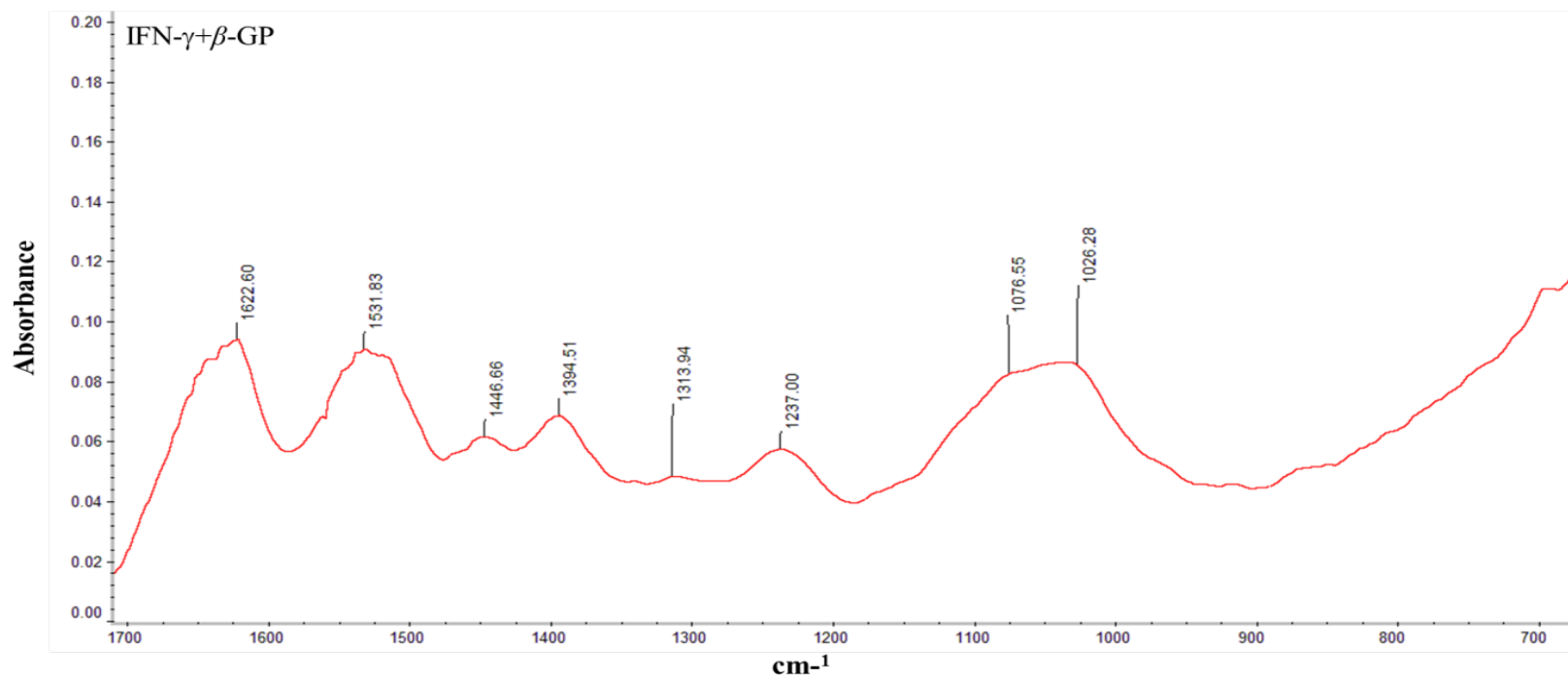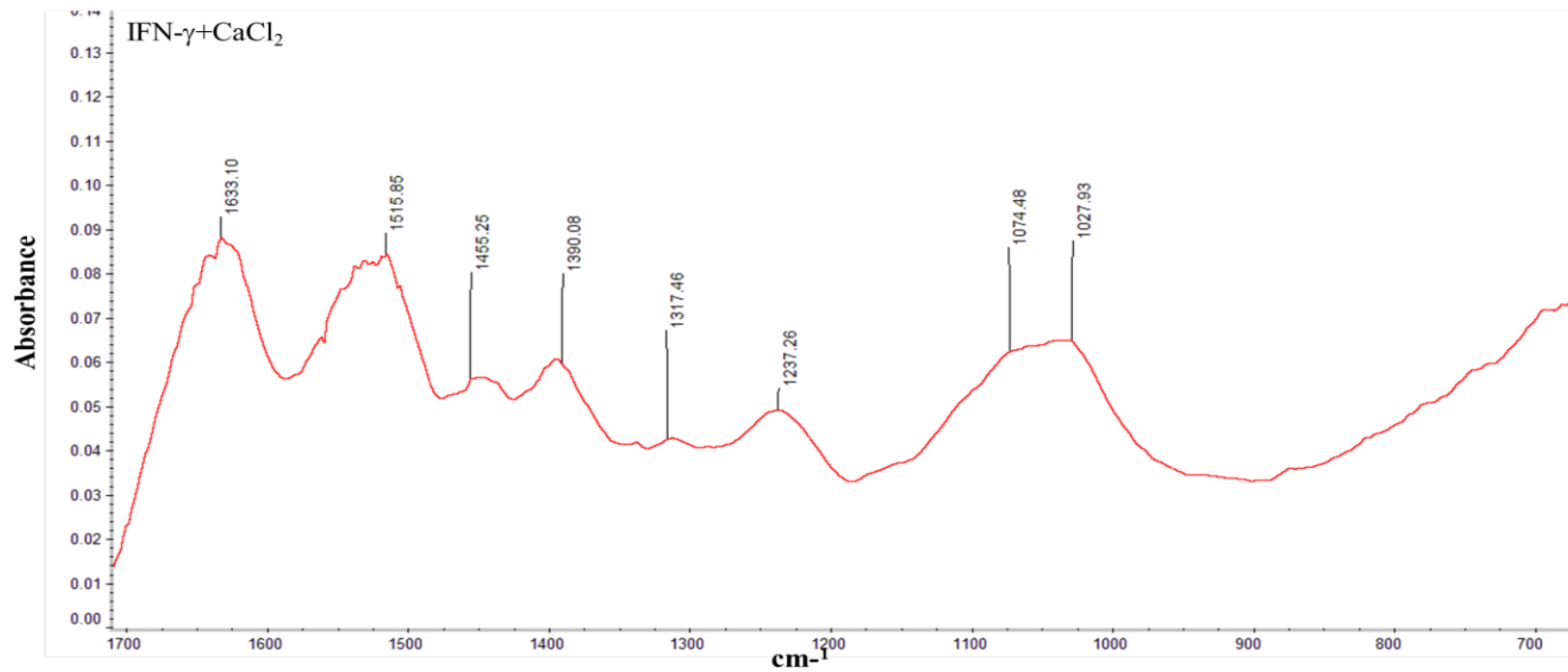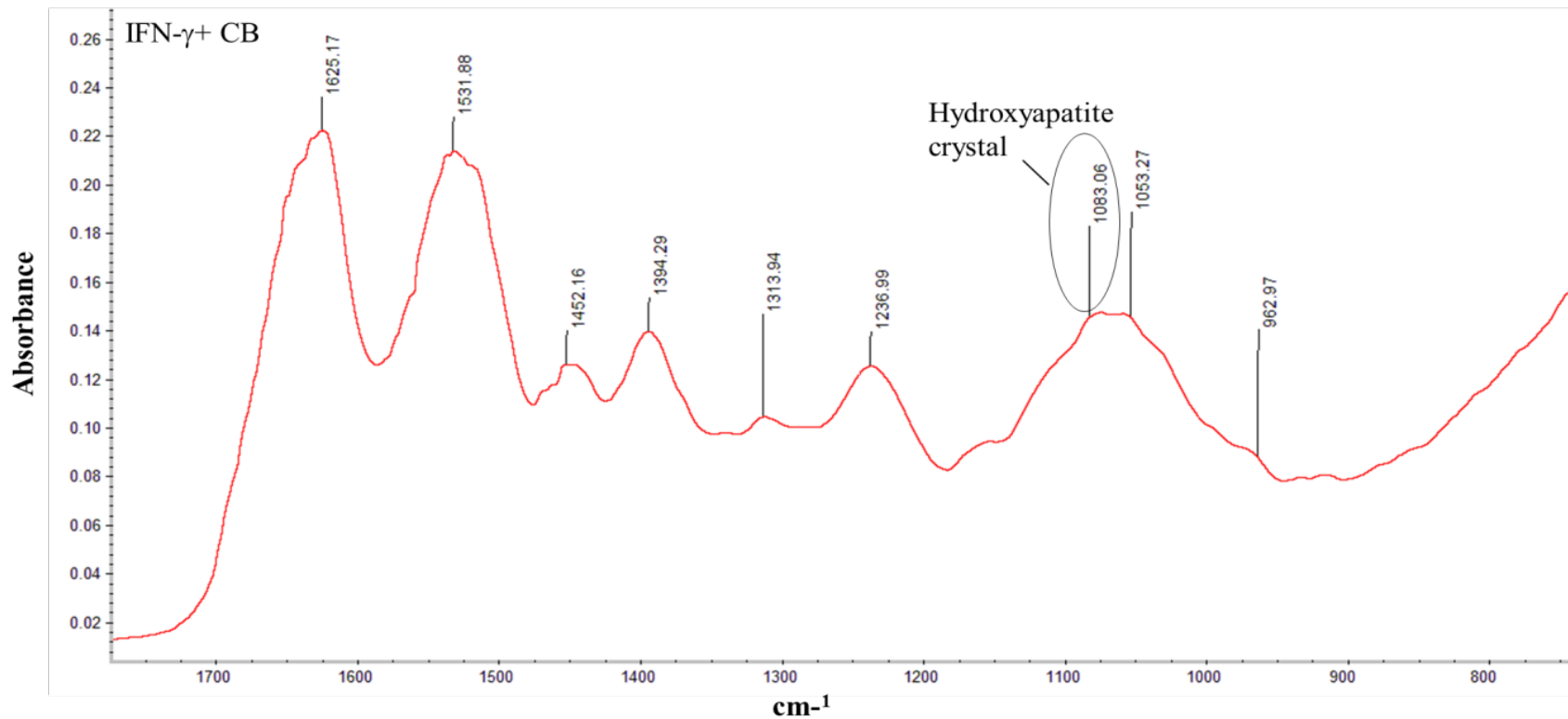
Figure 4.11 B: FT-IR spectrum analysis of activated RASMCs.

Cells were cultured to ~90% confluency and incubated with culture medium alone (control) and either with IFN-γ (100 U ml⁻¹) followed the addition of CaCl₂, β-GP or in combination at 7mM for 5 days. Cells were washed and scraped with 100% ethanol at the end of the incubation period and subjected to FT-IR as described in method (section 2.9). The FT-IR spectra are representative of 3 individual experiments.

145
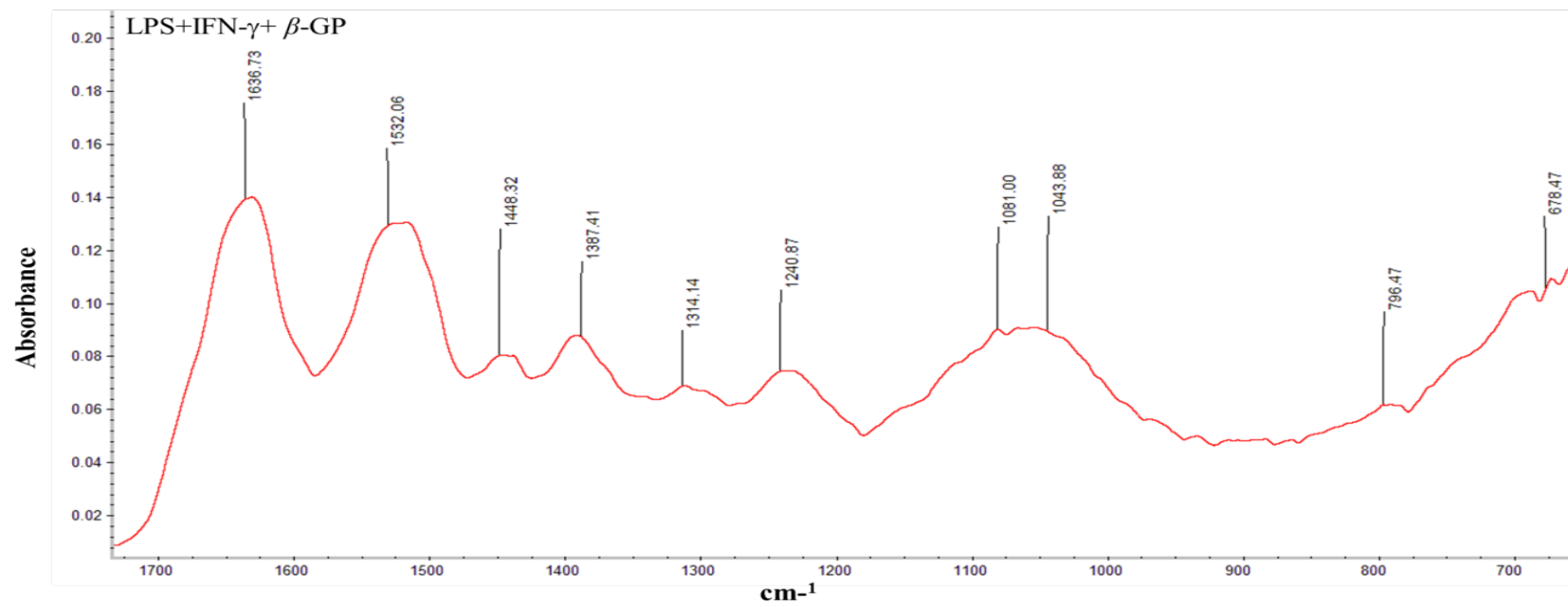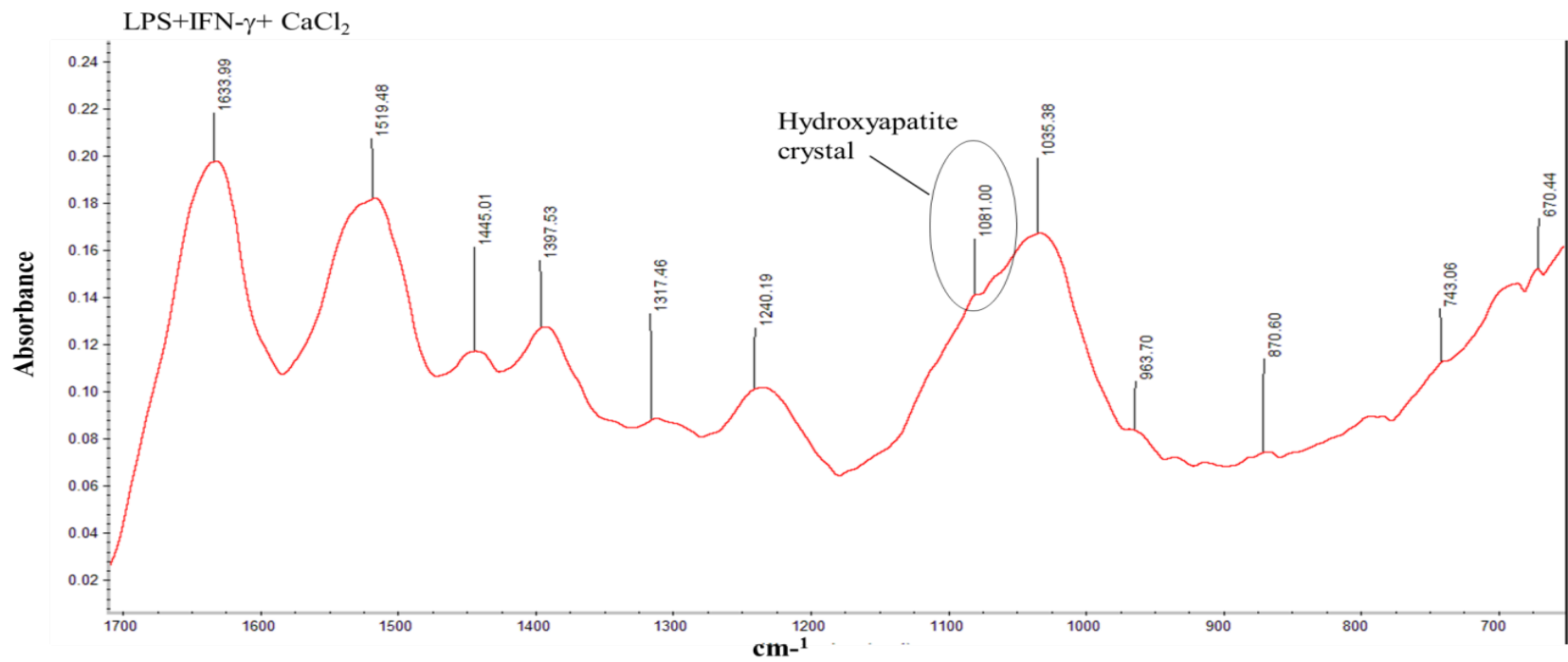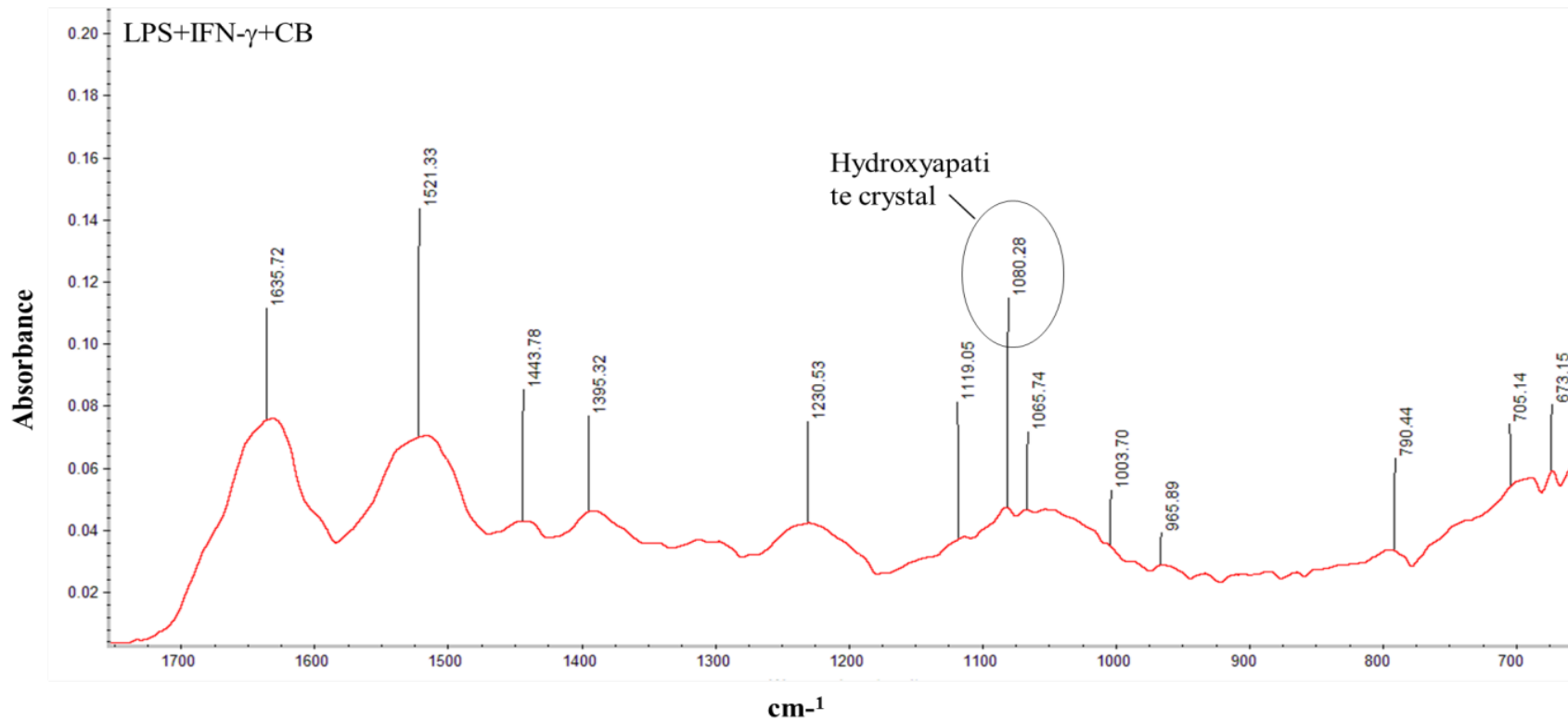
Figure 4.11 C: FT-IR spectrum analysis of activated RASMCs.

Cells were cultured to ~90% confluency and incubated with culture medium alone (control) and either with LPS (100µg ml^{-1})+ IFN-γ (100 U ml^{-1}) followed the addition of CaCl$_2$, β-GP or in combination at 7mM for 5 days. Cells were washed and scraped with 100% ethanol at the end of the incubation period and subjected to FT-IR as described in method (section 2.9). The FT-IR spectra are representative of 3 individual experiments.

Table 4.1: Spectrum of molecules detected by FT-IR treated RASMCs with LPS, IFN-γ or LPS+IFN-γ in presence CaCl₂:

Data from Literature review			Data from current studies				
Stretch or bend of chemical compound	**wave number (cm⁻¹)**	**Citation**	**Expected Wave number (cm⁻¹)**	**Control**	**LPS+CaCl₂**	**IFN-γ+ CaCl₂**	**LPS+IFN-γ+ CaCl₂**
Amide I-(CON stretch), Amide II (NOH bend), Amide III (COH stretch, NOH bend)	1620-1632, 1515-1540, 1216-1290	(Olsztyńska-Janus et $al.$, 2012)	1620, 1623, and 1633 (Amide-I),1515, 1519, 1532, and 1537 (Amide-II),1237 and 1240 (Amide-III)-	Present	Present	Present	Present
Calcite ($-CO_3^{2-}$)	1430-1480	(Meejoo, et al., 2006)	1445,1455, and 1450 - CO_3^2	Present	Present	Present	Present
Tricalcium phosphate (TCP), β Tricalcium phosphate (β-TCP)	700-750, 690	(Destainville, et al., 2003)	743 (TCP), 690 (β- TCP)	Not present	Not Present	Not present	Present
Phosphate (stretch PO_4^{3-})	1154, 1075,1046, 1010 & 1020 or 975	(Destainville, et al., 2003;Han J-K., et al., 2006; Mobasherpour; Heshajin,2007; Raynaud, et al., 2002)	1027, 1035, 1066, 1072, and 1106 (PO_4^{3-})	Present	Present	Present	Present
HA crystal ($Ca_{10}(PO_4)_6(OH)_2$)	1080 - 1089	(Kwon, et al.,2003: Alò et $al.$, 2009)	1081 $Ca_{10}(PO_4)_6(OH)_2$	Not Present	Not present	Not present	Present
Polysaccharide	Below 690	(Gómez-Ordóñez et $al.$, 2011; Parikh et $al.$, 2006).	Polysaccharide 670	Not present	Present	Not present	Present

Table 4.2: Spectrum of molecules detected by FT-IR treated RASMCs with LPS, IFN-γ or LPS+IFN-γ in presence *β*-GP:

Data from Literature review			Data from current studies				
Stretch or bend of chemical compound	**wave number (cm^{-1})**	**Citation**	**Expected Wave number (cm^{-1})**	**Control**	**LPS+*β*-GP**	**IFN-γ+ *β*-GP**	**LPS+IFN-γ+ *β*-GP**
Amide I-(CON stretch), Amide II (NOH bend), Amide III (COH stretch, NOH bend)	1620-1632, 1515-1540, 1216-1290	(Olsztyńska-Janus *et al.*, 2012)	1624, 1633, and 1636 (Amide-I), 1515, 1527, and 1532 (Amide-II),1236, 1237, and 1240 (Amide-III)-	Present	Present	Present	Present
Calcite (-CO_3^{2-})	1430-1480	(Meejoo, *et al.*, 2006)	1445,1446,and 1448 - CO_3^2	Present	Present	Present	Present
Tricalcium phosphate (TCP), β Tricalcium phosphate (β-TCP)	700-750, 690	(Destainville, *et al.*, 2003)	797 -TCP	Not present	Not Present	Not present	Present
Phosphate (stretch PO_4^{3-})	1154, 1075,1046, 1010 & 1020 or 975	(Destainville, *et al.*, 2003;Han J-K., *et al.*, 2006; Mobasherpour; Heshajin,2007; Raynaud, et al., 2002)	1027, 1030, 1070, and 1070 PO_4^{3-}	Not present	Not present	Not present	Present
HA crystal (Ca $_{10}(PO_4)_6(OH)_2$)	1080 - 1089	(Kwon, *et al.*,2003: Alò *et al.*, 2009)	Ca $_{10}(PO_4)_6(OH)_2$	Not Present	Not Present	Not present	Not present
Polysaccharide	Below 690	(Gómez-Ordóñez *et al.*, 2011; Parikh *et al.*, 2006).	Polysaccharide 679	Not present	Present	Not present	Present

Table 4.3: Spectrum of molecules detected by FT-IR treated RASMCs with LPS, IFN-γ or LPS+IFN-γ in presence CB:

Data from Literature review			Data from current studies				
Stretch or bend of chemical compound	wave number (cm^{-1})	Citation	Expected Wave number (cm^{-1})	Control	LPS+CB	IFN-γ+ CB	LPS+IFN-γ+CB
Amide I-(CON stretch), Amide II (NOH bend), Amide III (COH stretch, NOH bend)	1620-1632, 1515-1540, 1216-1290	(Olsztyńska-Janus *et al.*, 2012)	1620, 1623, and 1633 (Amide-I),1515, 1519, 1532, and 1537 (Amide-II),1237 and 1240 (Amide-III)-	Present	Present	Present	Present
Calcite (-CO$_3^{2-}$)	1430-1480	(Meejoo, *et al.*, 2006)	1445,1455, and 1450 - CO$_3^2$	Present	Present	Present	Present
Tricalcium phosphate (TCP), β Tricalcium phosphate (β-TCP)	700-750, 690	(Destainville, *et al.*, 2003)	743 (TCP), 690 (β- TCP)	Not present	Present	Not present	Present
Phosphate (stretch PO$_4^{3-}$)	1154, 1075,1046, 1010 & 1020 or 975	(Destainville, *et al.*, 2003;Han J-K., *et al.*, 2006; Mobasherpour; Heshajin,2007; Raynaud, *et al.*, 2002)	1027, 1035, 1066, 1072, and 1106 (PO$_4^{3-}$)	present	present	present	Present
HA crystal (Ca $_{10}$(PO$_4$)$_6$(OH)$_2$)	1080 - 1089	(Kwon, et al.,2003: Alò *et al.*, 2009)	1080,1083, and 1088 Ca $_{10}$(PO$_4$)$_6$(OH)$_2$	Not present	Present	Present	Present
Polysaccharide	Below 690	(Gómez-Ordóñez *et al.*, 2011; Parikh *et al.*, 2006).	Polysaccharide 670	Not present	Present	Present	Present

4.3.5- Effects of CaCl$_2$, *β*-GP, CB, LPS and/or IFN-γ on cell viability:

To determine whether any of the effects reported are associated with changes in cell viability, the MTT assay was carried in parallel with the experiments above. LPS (30 and 100 μg.ml^{-1}; Figure 4.12 A) or IFN-γ (30 and 100 U.ml^{-1}); Figure 4.12 B) did not cause any statistically significant change in MTT metabolism when used alone or in combination with CB at 1mM, 5 mM and 7 mM. Studies with LPS plus IFN-γ alone and also in combination with calcification inducers did show marked reductions in MTT metabolism, indicating toxicity to cells. This was more evident when LPS and IFN-γ were used with CaCl$_2$ or with CB and less so with *β*-GP. In each case the reductions in MTT metabolism were significant at days 3, 5 and 7. LPS plus IFN-γ or CB also caused significantly more decreases in MTT metabolism at day7 (Figures4.12C, D and E).

A

B
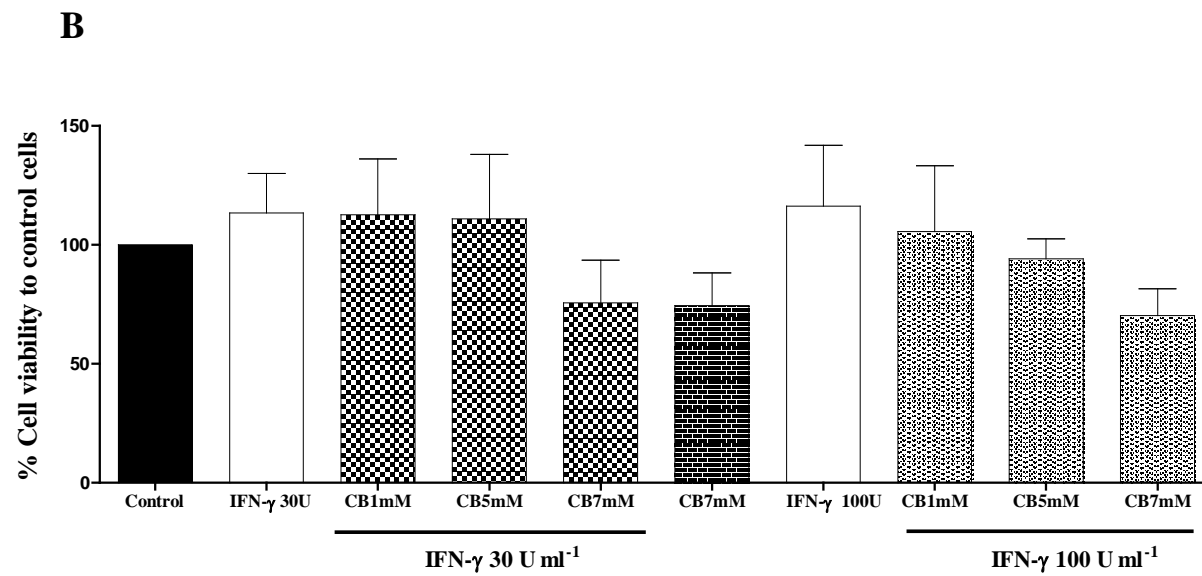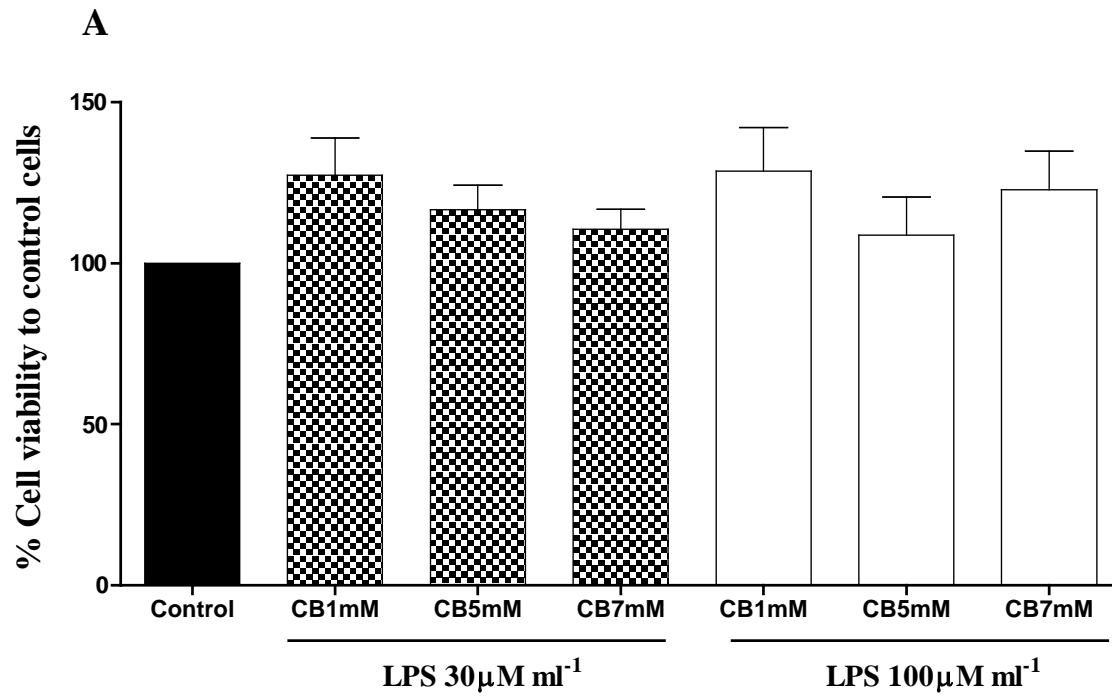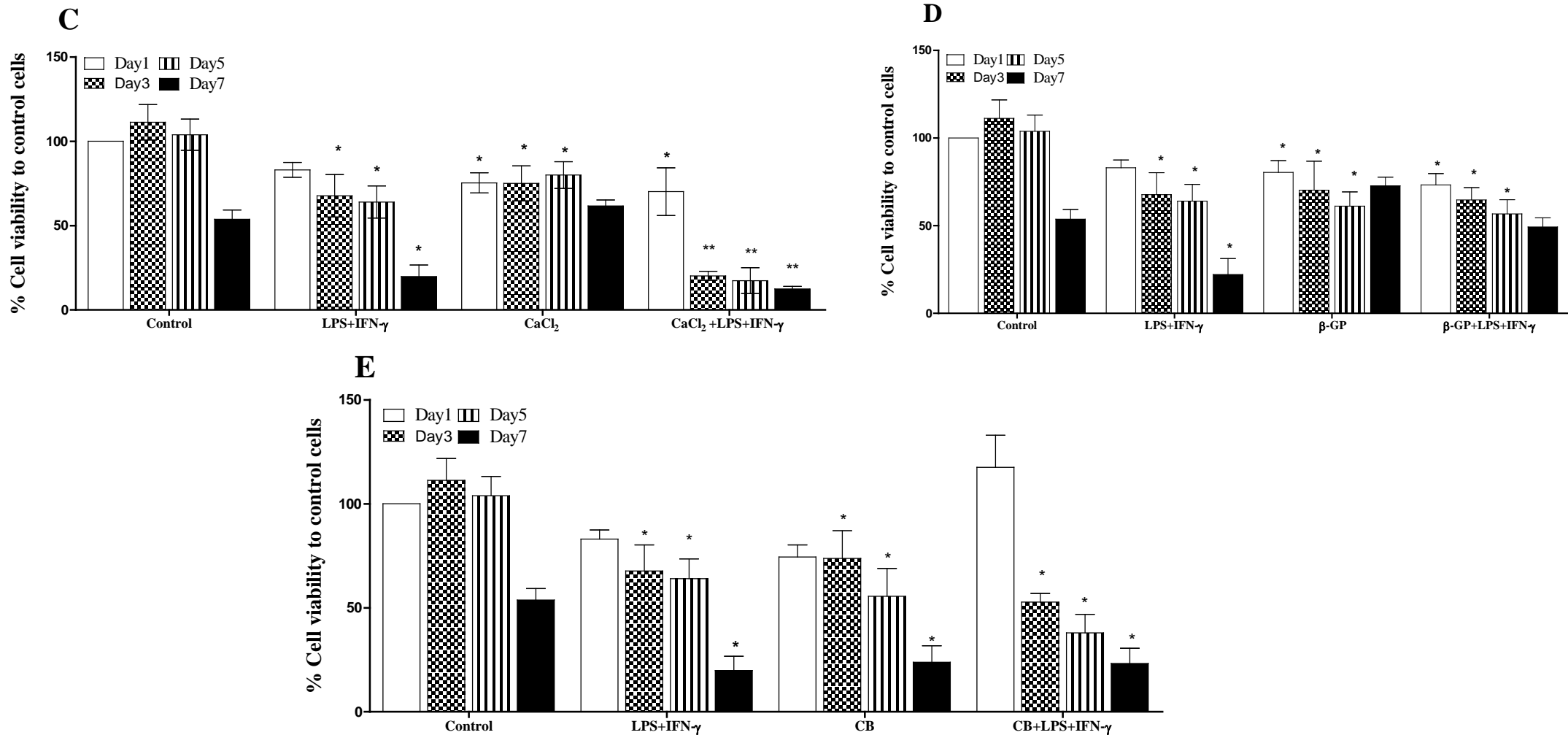
Figure 4.12: Effects of CaCl$_2$, β-GP, CB, LPS and/or IFN-γ on cell viability.

Cells were cultured to ~90% confluency and incubated with either medium alone or with LPS, IFN-γ, or a combination in the absence and presence of CaCl$_2$, β-GP or CB. Incubations were either for 24 hours (Figures 4.12 A and B) or for 1, 3, 5 and 7 days (Figures 4.12C, D and E). The data is represented as % change of cell viability taking controls as 100%. The values represent the mean ± SEM from 4 experiments * denotes $p < 0.05$ and ** $p < 0.01$ compared to control on the same day.

4.3.6-Effects of daily medium change on the production of NO, iNOS expression and calcification of RASMCs induced by LPS and IFN-γ in the absence and presence of CaCl₂, *β*-GP or CB.

In the studies described previously, the experiments were designed such that the culture medium was not changed throughout the incubation period. This was so as not to disrupt the calcification process and have an uninterrupted continuous period when the process can take place. However, prolonged incubations of cells in the same culture medium may lead to decreased cell viability which could be exacerbated when cells are treated with other agents including LPS and IFN-γ. More importantly, this may also influence calcification of cells. Further studies were therefore carried out where cells were activated for 24 hours with LPS and IFN-γ and then coincubated with calcification inducers but changing the culture medium daily and replacing all the reagents.

Cells cultured to ~ 90 % confluency incubated with media alone or medium containing CB did not produce NO or express iNOS over the period of incubation. In contrast, RASMCs treated with LPS and IFN-γ resulted in the expected induction of NO production which increased and reached a maximum at day 3, declining at 4, 5, 6, and 7 days but to levels still higher than controls. Similarly, the use of CB and LPS + IFN-γ resulted the same trend in the daily production of NO to that seen with LPS and IFN-γ but the decline in NO levels after day 3 (0.30 ±0.14 nmole μg^{-1} protein) was more noticeable than when LPS and IFN-γ were used alone (Figure 4.13 A). The cumulative data (ie pooled data) did not show statistical differences between the effects with LPS and IFN-γ (0.71 ±0.22 nmole μg^{-1} protein;Day3) when compared to these seen when CB as also present (0.64 ±0.17 nmole μg^{-1} protein;Day3) (Figure 4.13 B; see Figure 4.13 B_1 and B_2 for summary data).

While the cumulative data of LPS and IFN-γ caused significant elevation of NO production to that seen with no change medium. CB alone was without significant effect when compared to controls (Figure 4.13 B_1 and B_2).

Similar to trends with NO, iNOS expression was not detectable in controls or in cells treated with CB alone. LPS and IFN-γ however induced iNOS expression which increased over time up to day 3 declining thereafter but maintained above basal levels. The levels of iNOS did not changes significantly when CB was added with LPS and IFN-γ. The levels of expression reached a maximum at day 3 (193 %) followed by a partial decline thereafter (Figure 4.14 A). Changing the medium daily and replacing LPS and IFN-γ led to induce NO/iNOS which was higher compared to that seen in studies where the medium was not change (0.30 ±0.14 nmole μg^{-1} protein vs 0.18 ±0.05 nmole μg^{-1} protein; Day 3). Using CB with LPS and IFN-γ without changing the medium caused marginal induction of NO which was 0.35 ±0.17 nmole μg^{-1} protein on day 3 compared to the seen when the medium was changed daily (0.28 ± 0.05 nmole μg^{-1} protein ; Day 3).

In relation to calcification, cells incubated with media alone (control) did not induce increases in calcium levels. Calcification buffer however caused time dependent induction of calcium levels which peaked at day 3 (0.87 ±0.2 nmole μg^{-1} protein) and then sustained thereafter. These results suggest that changing the medium daily has similar the elevations in calcium levels when compared to studies were the medium was not changed (0.6 ±0.09 nmole μg^{-1} protein).However, The calcium level peaked at day 3 with changing medium compared to that seen when the medium was not changed where the peak response was seen on day 5.

Cells activated with LPS + IFN-γ resulted in significant increases in calcium levels compared to the control but the levels, although sustained at the various time points, were lower than those seen with CB (Figure 4.15 A; see Figure 4.15 B_1 for summary data).

The levels of calcium were not significant higher when compared to studies were the medium was not changed or to pooled data.

When combined, LPS + IFN-γ and CB together caused significantly more elevation in calcium than the individual responses combined. Moreover, the changes in calcium were reduced 1.8 ±0.7 nmole μg^{-1}protein when compared to studies were the medium was not changed 3.10 ±0.7 nmole μg^{-1}protein. However, pooled data (Figure 4.15 B_2) did show statistical differences between the effects with LPS + IFN-γ+CB (5.2 ±0.7 nmole μg^{-1}protein) when compared to these seen when CB as also present alone.

In cytotoxicity studies (Figure 4.16), there was significant reduction in cell viability at day 2 and over in cells treated with LPS+IFN-γ. The degree of cytotoxicity did not show a time dependent effect in that there were no significant differences in MTT metabolism between the different time points from day 2 upwards. CB did not show any marked cytotoxicity and in combination with LPS+IFN-γ did not cause any further changes in MTT metabolism beyond that seen with LPS+IFN-γ alone (Figure 4.16). Interestingly, in these series of experiments, LPS+IFN-γ (Figure 4.16) did cause marked reduction in MTT metabolism as seen in previous studies above shown in Figure 4.12 E.

In conclusion, it seems from the data above that changing the medium every 24 hours does not accelerate NO production and calcification any more significantly than in studies where the medium was not replenished daily. The mechanisms through which these changes occur now remain to be addressed.
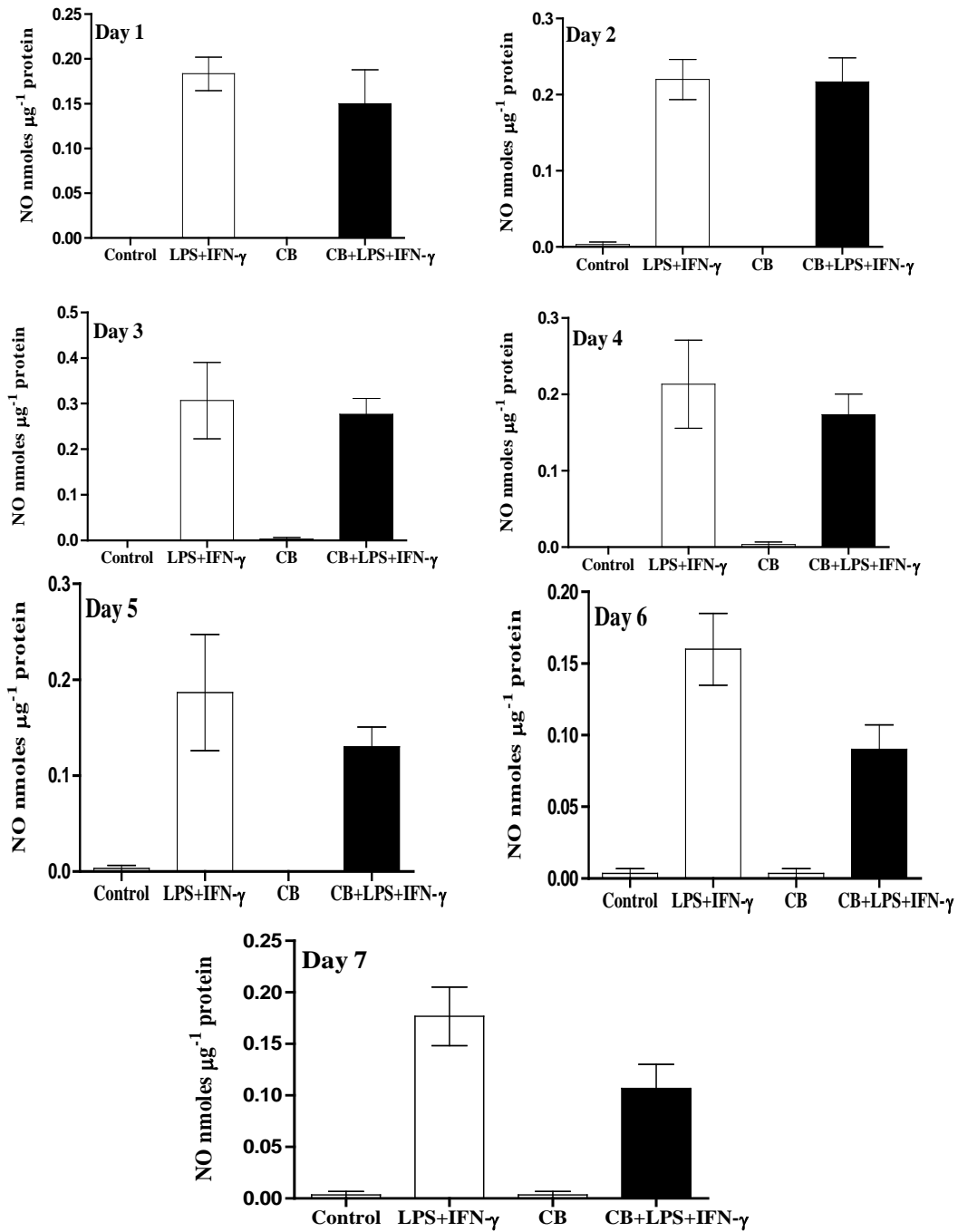
Figure 4.13 A: **Effect of CB on LPS +IFN-γ induced NO production.**

Cells were cultured to ~90% confluency and activated with LPS (100 μg ml^{-1}) + IFN-γ (100 U ml^{-1}) for 24 hours after which the medium was replaced every 24 hours for up to 7 days with fresh medium containing LPS + IFN-γ with and without CB. Controls were incubated with medium alone and parallel batches of cells were incubated with CB alone. Total NO produced was quantified by the Griess assay as described in methods (section 2.3). The data represents means ± S.E.M. from 3 individual experiments.

B₁

B₂
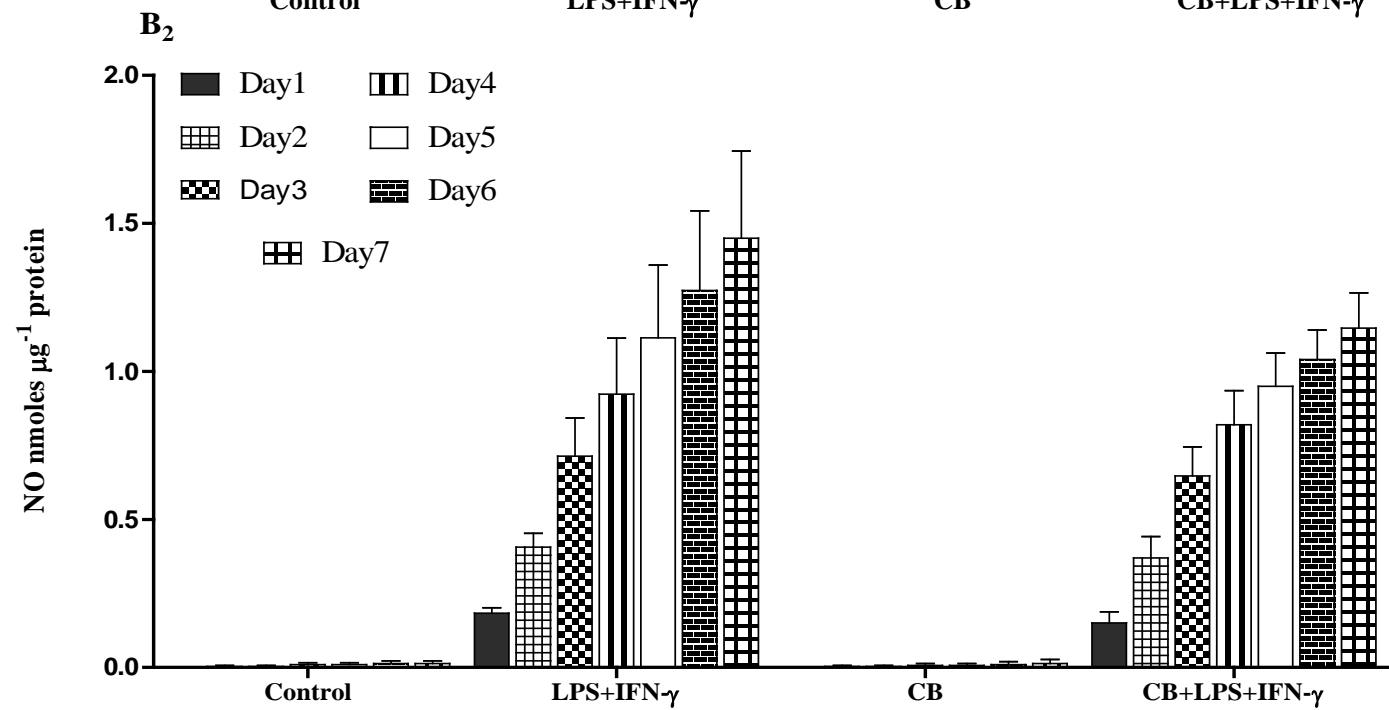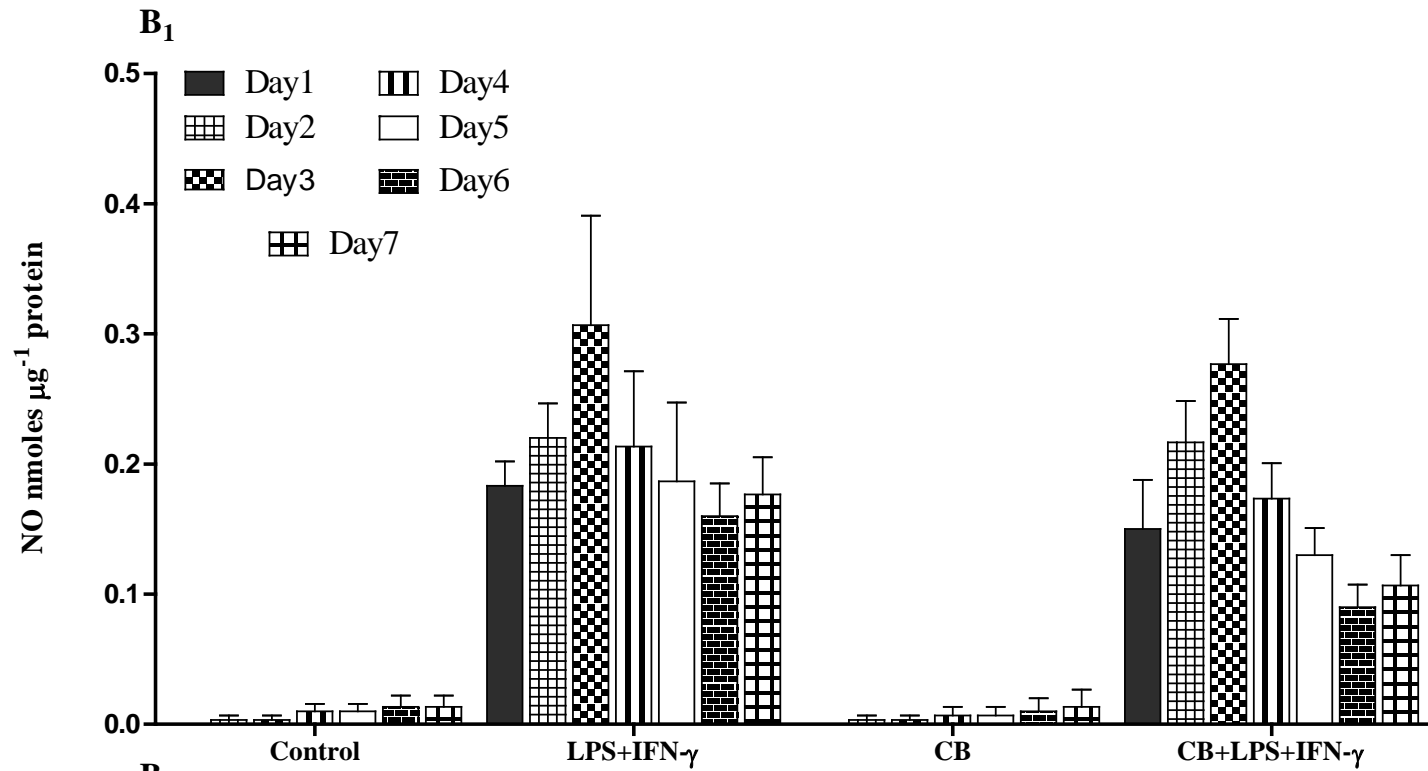
Figure 4.13 B: **Summary data of the effect of CB on LPS + IFN-γ induced NO production.**

Cells were cultured to ~90% confluency and activated with LPS (100 μg ml^{-1}) + IFN-γ (100 U ml^{-1}) for 24 hours after which the medium was replaced every 24 hours for up to 7 days with fresh medium containing LPS + IFN-γ with and without CB. Controls were incubated with medium alone and parallel batches of cells were incubated with CB alone. Total NO produced was quantified by the Griess assay as described in methods (section 2.3). Analysis of NO production was carried out by determining amounts produced every 24 hours (B$_1$) or by analysing the cumulative production (B$_2$). The data represents means ± S.E.M. from 3 individual experiments.
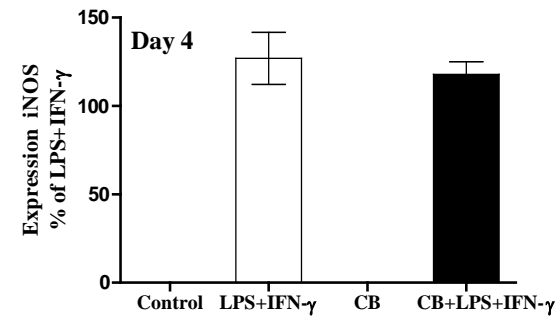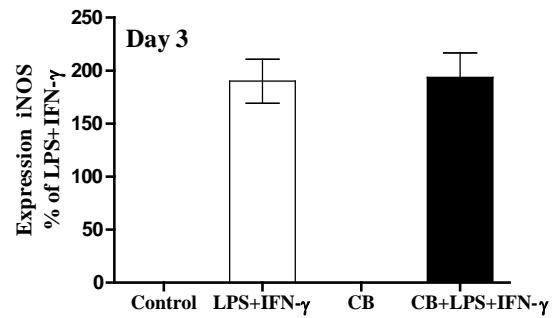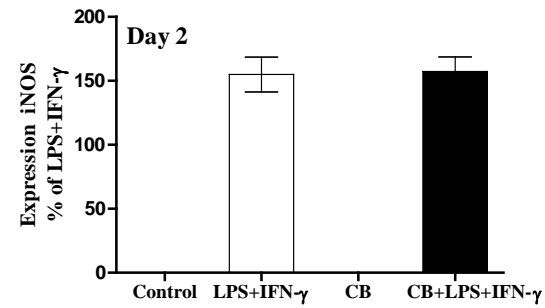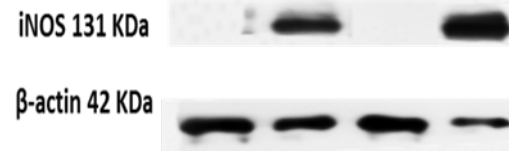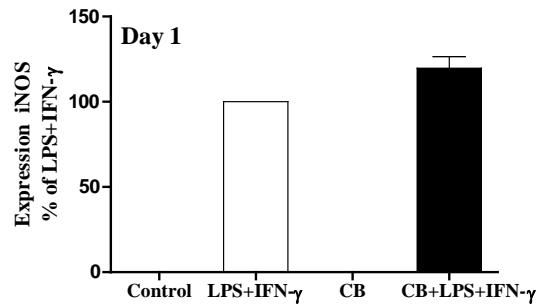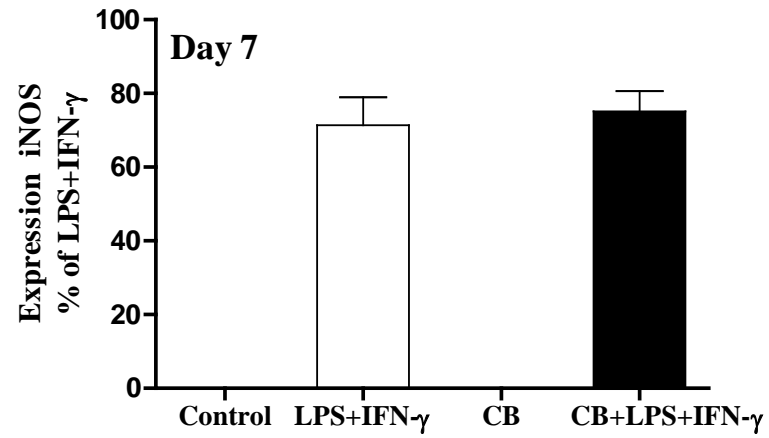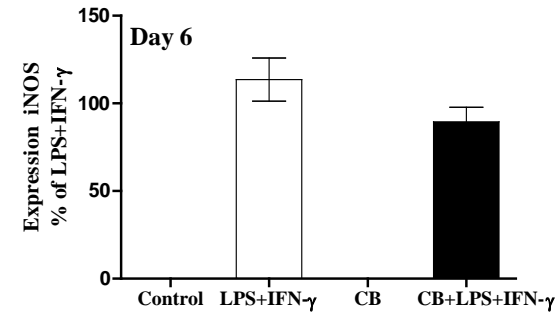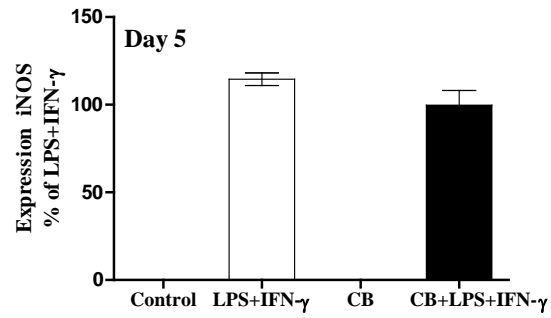
Figure 4.14 A: **Effect of CB on LPS+ IFN-γ induced iNOS expression.**

Cells were cultured to ~90% confluency and activated with LPS (100 μg ml^{-1}) + IFN-γ (100 U ml^{-1}) for 24 hours after which the medium was replaced every 24 hours for up to 7 days with fresh medium containing LPS + IFN-γ with and without CB. Controls were incubated with medium alone and parallel batches of cells were incubated with CB alone. Expression of iNOS was evaluated by western blotting as described in methods (section 2.10). The data represents means ± S.E.M. from 3 individual experiments.
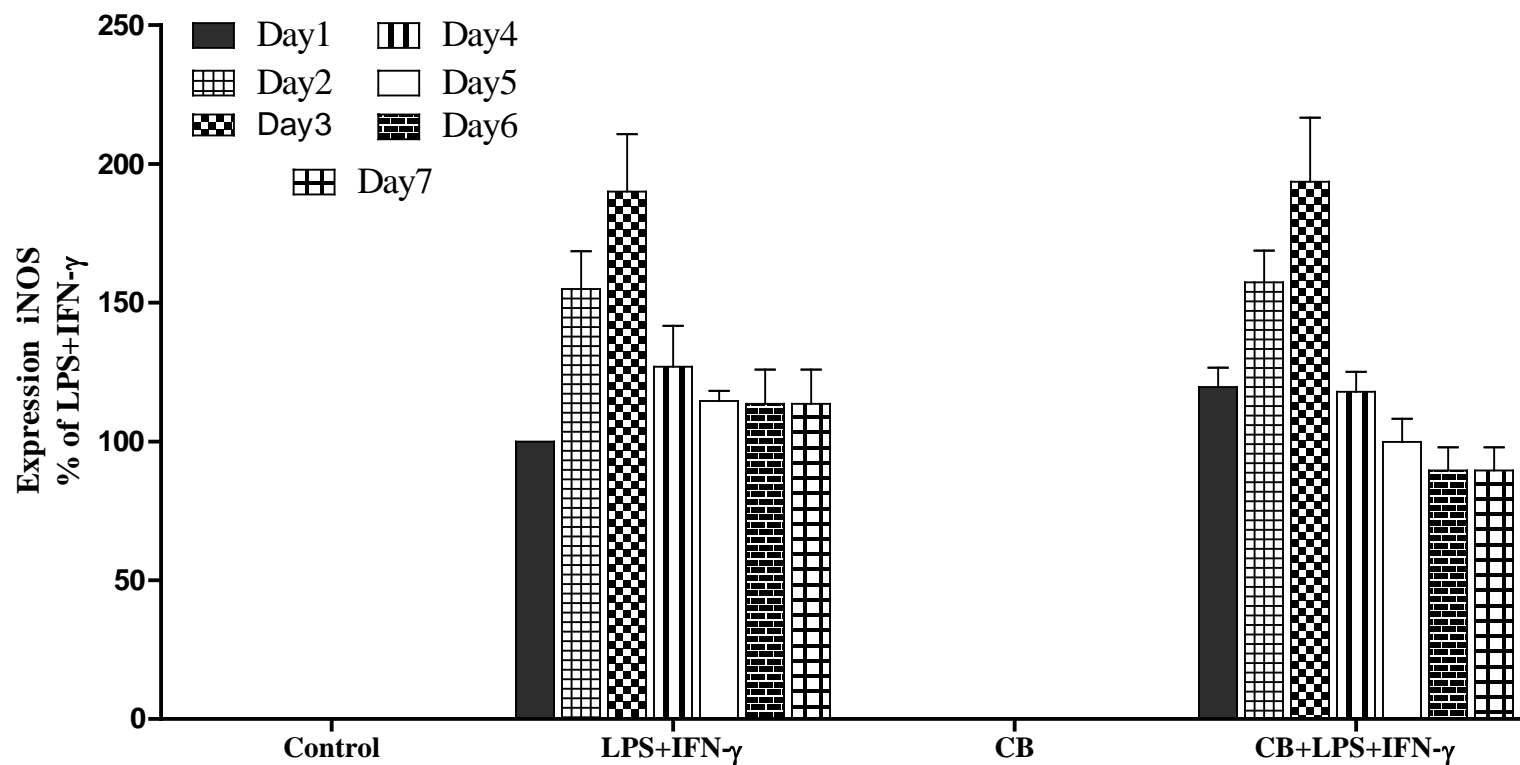
Figure 4.14 B: **Summary data of the effect of CB on LPS+ IFN-γ induced iNOS expression.**

Cells were cultured to ~90% confluency and activated with LPS (100 μg ml^{-1}) + IFN-γ (100 U ml^{-1}) for 24 hours after which the medium was replaced every 24 hours for up to 7 days with fresh medium containing LPS + IFN-γ with and without CB. Controls were incubated with medium alone and parallel batches of cells were incubated with CB alone. Expression of iNOS was evaluated by western blotting as described in methods (section 2.10). The data represents means ± S.E.M. from 3 individual experiments.

163
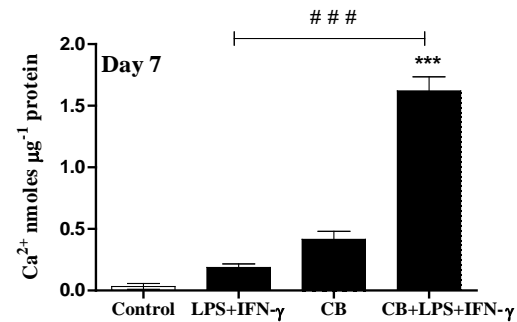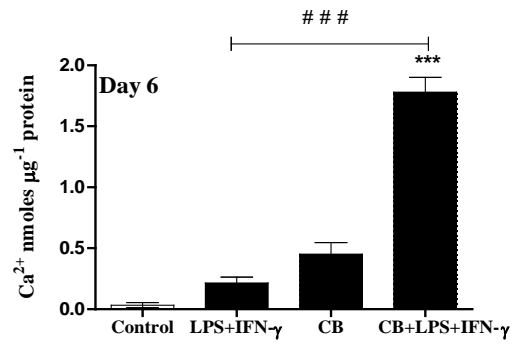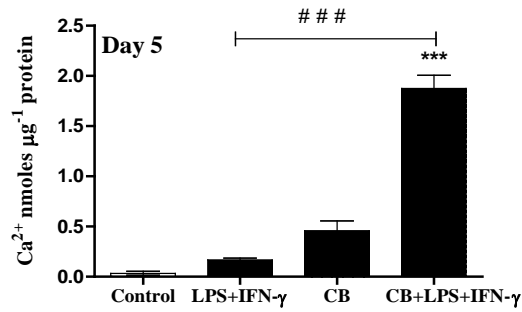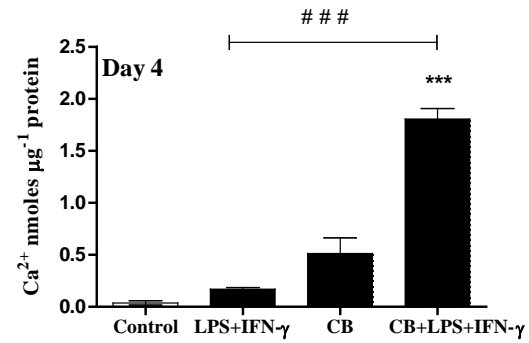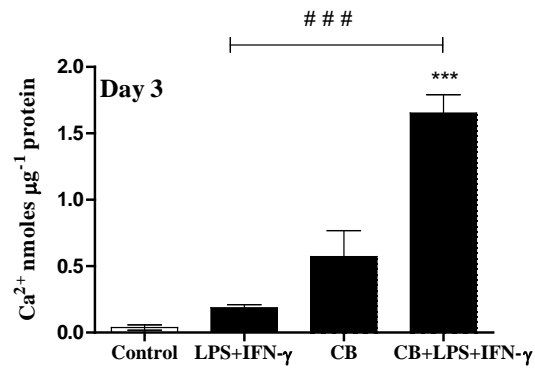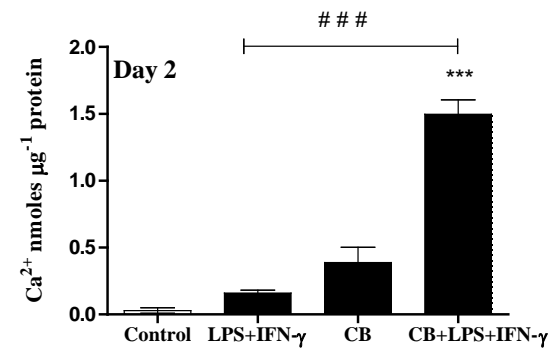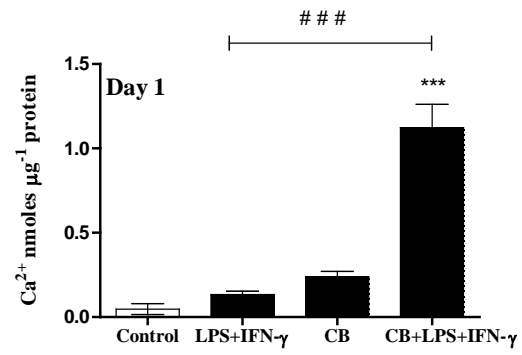
Figure 4.15 A: **Effect of CB on LPS +IFN-γ induced calcification.**

Cells were cultured to ~90% confluency and activated with LPS (100 μg ml^{-1}) + IFN-γ (100 U ml^{-1}) for 24 hours after which the medium was replaced every 24 hours for up to 7 days with fresh medium containing LPS + IFN-γ with and without CB. Controls were incubated with medium alone and parallel batches of cells were incubated with CB alone. Total calcium was quantified as described in methods (section 2.6). The data represents means ± S.E.M. from 3 individual experiments. *** denotes $p<0.001$ compared to control or ### denotes $p<0.001$ compared to CB alone for each time point.

B₁

B₂
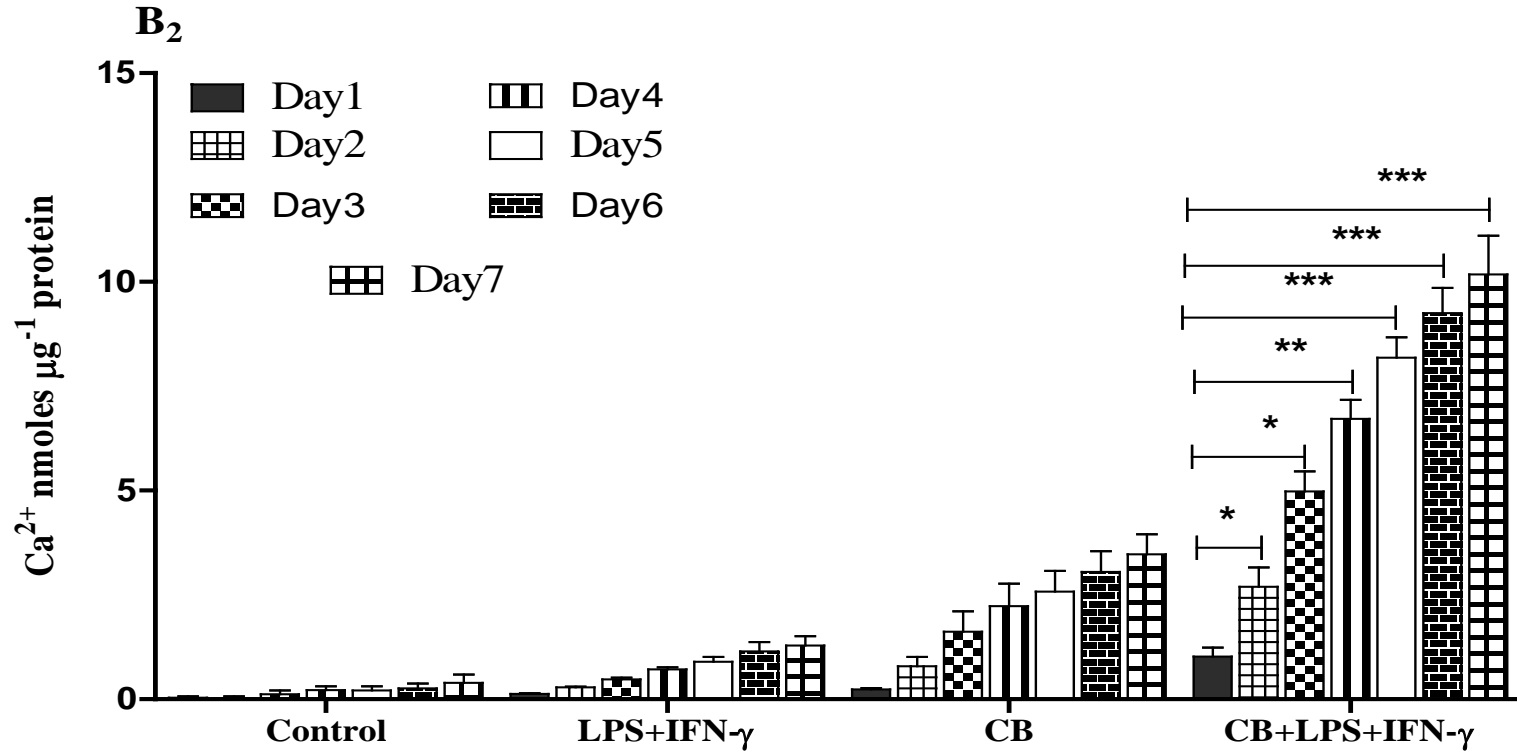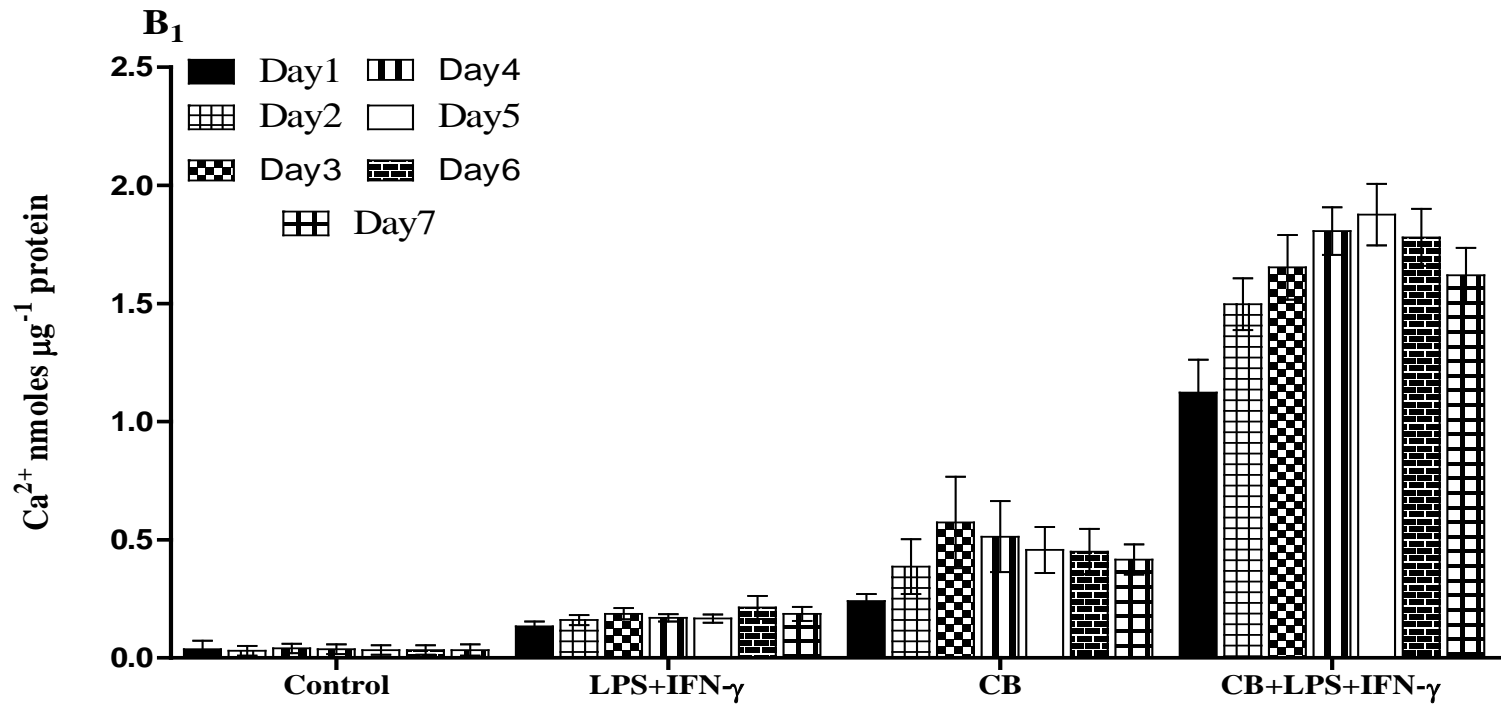
Figure 4.15 B: Summary data of the effect of CB on LPS+IFN-γ induced calcification.

Cells were cultured to ~90% confluency and activated with LPS (100 µg ml^{-1})+ IFN-γ (100 U ml^{-1}) for 24 hours followed by adding of LPS+ IFN-γ and CB during a time course of 1,2,3,4,5,6 and 7 days. Total calcium was quantified as described in methods (section 2.6). The measurement of calcium levels was done by two different ways, as normal calculation (B$_1$) while cumulative calculation is represented on (B$_2$) The data represents means ± S.E.M. from 4 individual experiments.* denotes $p< 0.05$, denotes $p< 0.01$ **, and *** denotes $p< 0.001$ and compared to the time points indicated for each experimental condition.
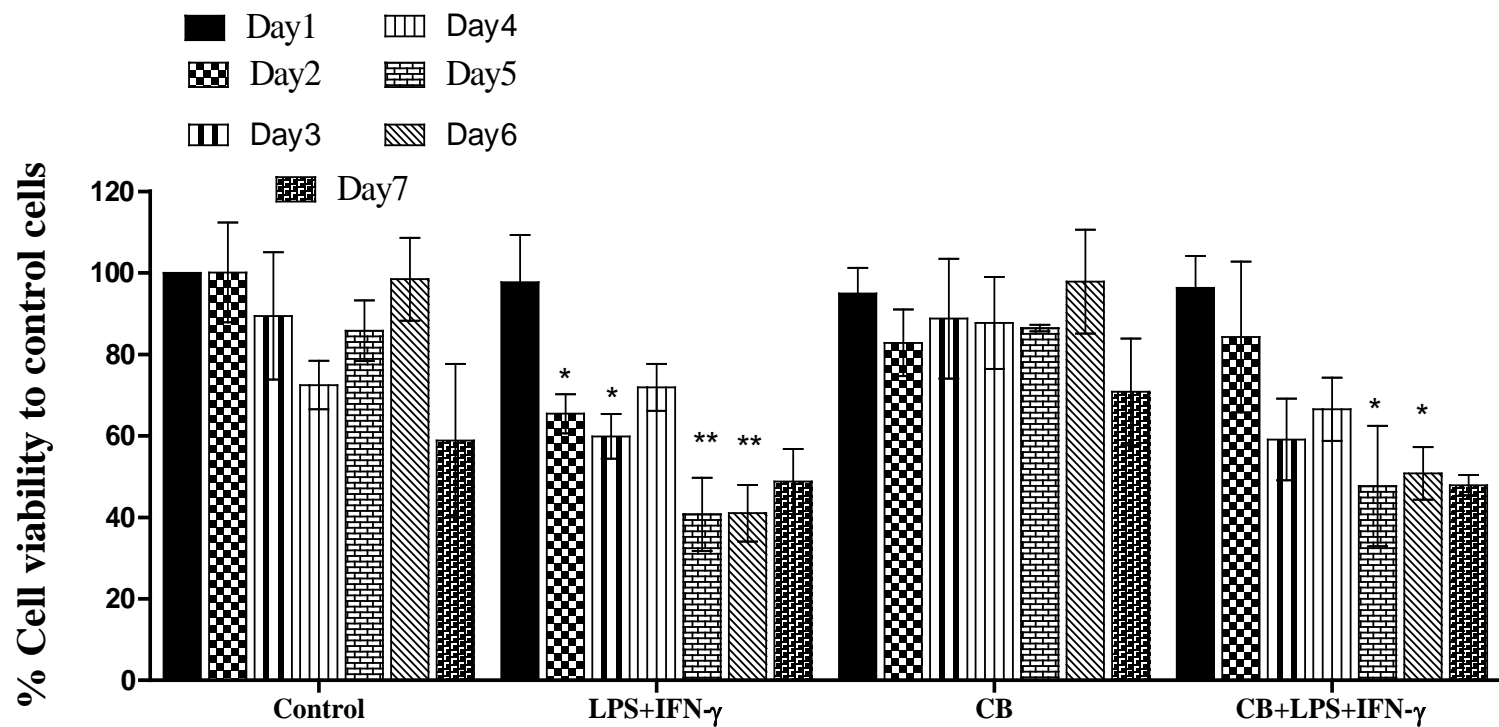
Figure 4.16: Effects of CB, LPS + IFN-γ or in combination on cell viability.

Cells were cultured to ~90% confluency and activated with LPS (100 μg ml^{-1})+ IFN-γ (100 U ml^{-1}) for 24 hours followed by adding of LPS+ IFN-γ and CB during a time course of 1,2,3,4,5,6 and 7 days. The data is represented as % change of cell viability taking controls as 100%. The values represent the mean ± SEM from 3 experiments * denotes $p < 0.05$ and ** $p < 0.01$ compared to control on the same day.

4.3.7- Effects of coincubation of cells with CB together with LPS and IFN-γ on NO production, iNOS expression and on calcification.

In these studies, RASMCs cultured to ~ 90 % confluency were incubated for 1 to 48 hours with either media alone or medium containing CB (combination of $CaCl_2$ and β-GP at 7 mM) with / without LPS and IFN-γ. Consistent with earlier findings, medium with and without CB alone did not produce NO or induce expression of iNOS during a period of 48 hours incubation (Figure 4.17 A). In contrast, RASMCs coincubated with both inflammatory mediators and CB resulted in significant NO production detectable at 18 hours (0.06 ±0.01 nmole μg^{-1}protein) after incubation and its induction gradually increased reaching maximal production at 48 hours with the levels of NO produced being significantly higher (0.22 ±0.03 nmole μg^{-1}protein) when compared to LPS and IFN-γ alone (0.11 ±0.02 nmole μg^{-1}protein) (Figure 4.17 A; see Figure 4.17 B for summary data). Similarly, iNOS expression was significantly enhanced at 18 hours (%107± 12.5), with level of expression reaching maximal at 48 hours (% 174.02 ±33.4) (Figure 4.18 A; see Figure 4.18 B for summary data).

Cells incubated with media alone (control) did not induce calcification. This was marginally enhanced by incubating cells with LPS + IFN-γ during a 48 hour period (0.4 ±0.01 nmole μg^{-1}protein vs 0.1 nmole μg^{-1}protein in controls). CB alone caused the expected time-dependent elevation in calcium levels (0.9 ±0.2 nmole μg^{-1}protein; Figure 4.19). More importantly, calcium levels were highly elevated by CB in the presence of LPS + IFN-γ (1.4 ±0.05 – 2.6 ±0.1 nmole μg^{-1}protein) and this was also time dependent (18 – 48 hours), being more prominent at 48 hours (Figure 4.19 A). Figure 4.19 B shows the summary data from the calcification studies.
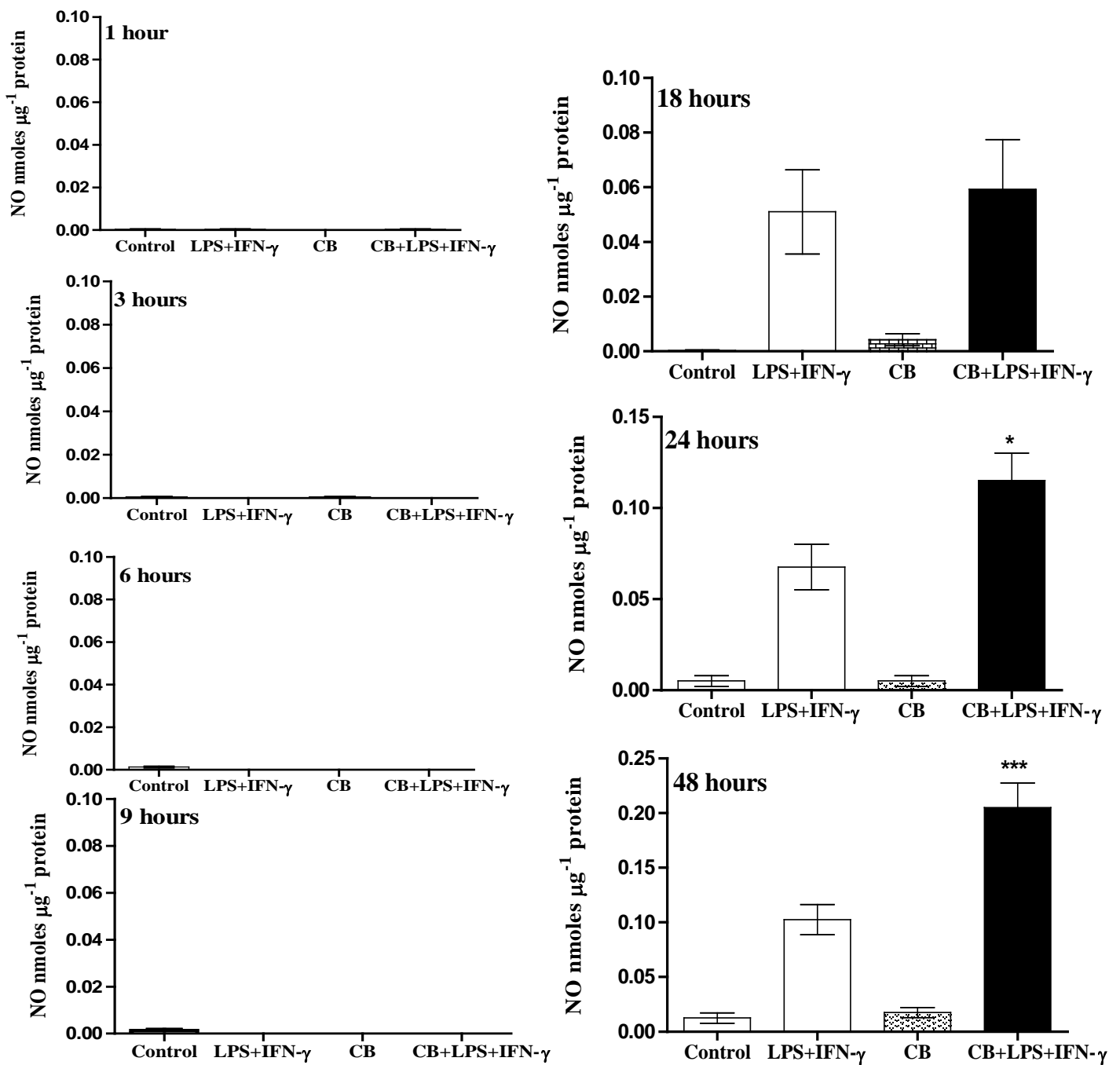
Figure 4.17 A: **Effect of coincubation of CB with LPS +IFN-γ on induced NO production.**

Cells cultured to ~90% confluency were activated by LPS (100 µg ml^{-1}) + IFN-γ(100 U ml^{-1}) with adding CB during a time course of 1, 3, 6, 9, 18, 24, and 48 hours. Total NO was quantified by Griess assay as described in methods (section 2.3). The data represents means ± S.E.M. from 4 individual experiments.* denotes $p < 0.05$ and *** denotes $p < 0.001$ compared to LPS + IFN-γ alone on each time point.
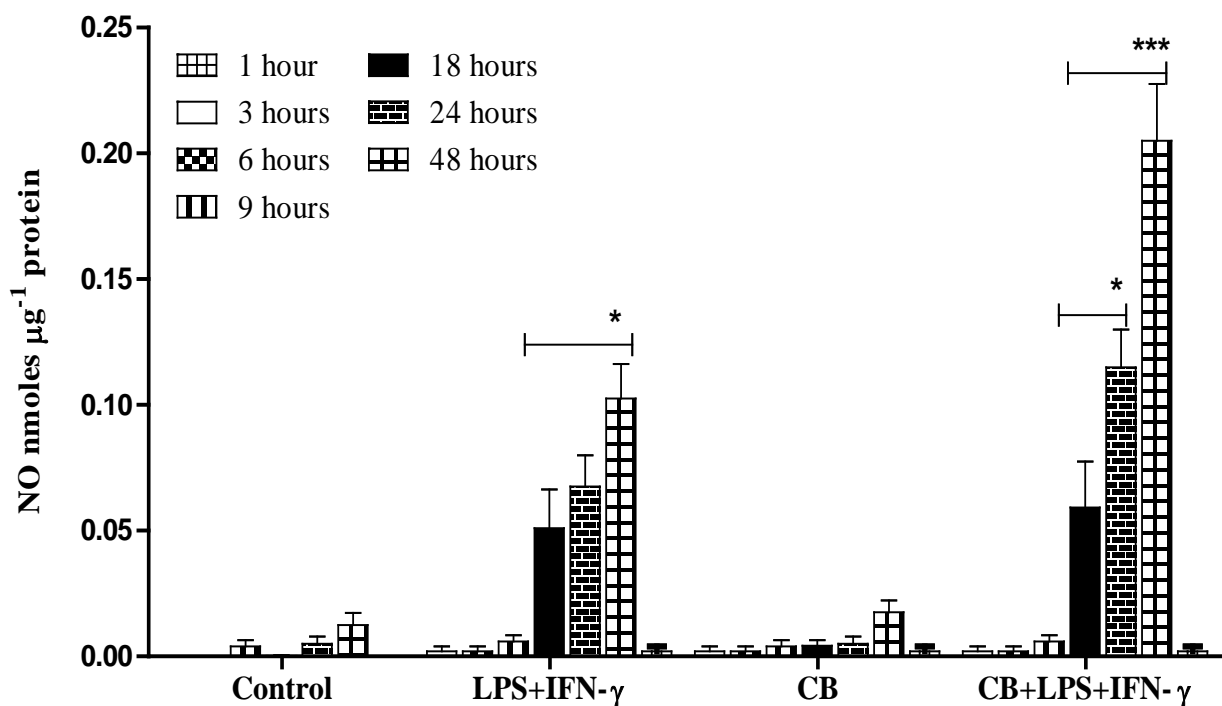
Figure 4.17 B: **Summary data of the effect of coincubation of CB and LPS +IFN-γ on induced NO production.**

Cells cultured to ~90% confluency were activated by LPS (100 μg ml^{-1}) + IFN-γ(100 U ml^{-1}) with adding CB during a time course of 1, 3, 6, 9, 18, 24, and 48 hours. Total NO was quantified by Griess assay as described in methods (section 2.3). The data represents means ± S.E.M. from 4 individual experiments.* denotes $p< 0.05$ and *** denotes $p<0.001$ compared to each experimental conditions.
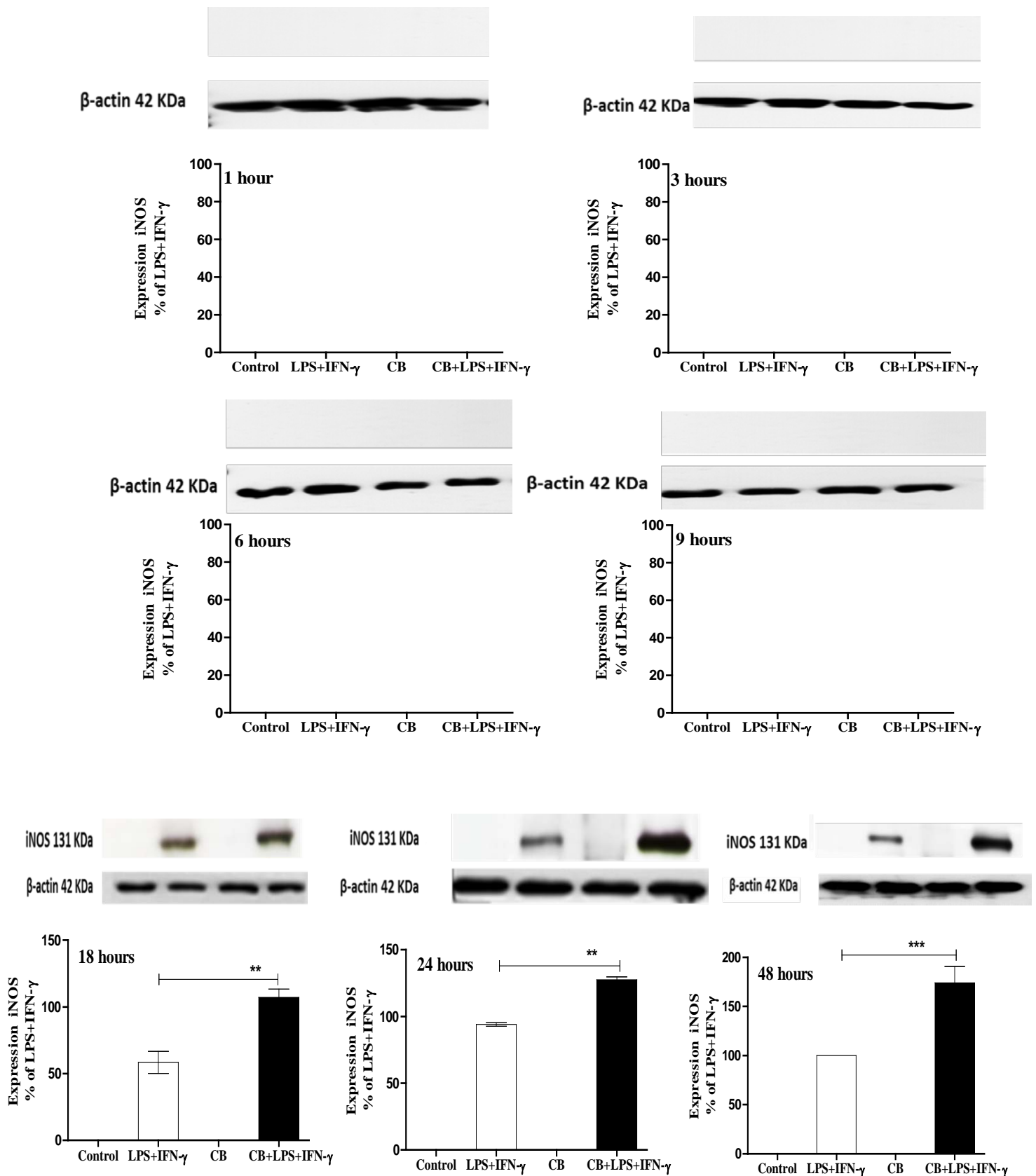
Figure 4.18 A: **Effect of coincubation of CB and LPS + IFN-γ on induced iNOS expression.**

Cells cultured to ~90% confluency were activated by LPS (100 μg ml⁻¹)+ IFN-γ (100 U ml⁻¹) with adding of CB during a time course of 1, 3, 6, 9, 18, 24, and 48 hours. Expression of iNOS was evaluated by western blotting as described in methods (section 2.10). The data represents means ± S.E.M. from 4 individual experiments.** denotes $p < 0.01$ and *** denotes $p < 0.001$ compared to LPS+ IFN-γ alone on each time point.
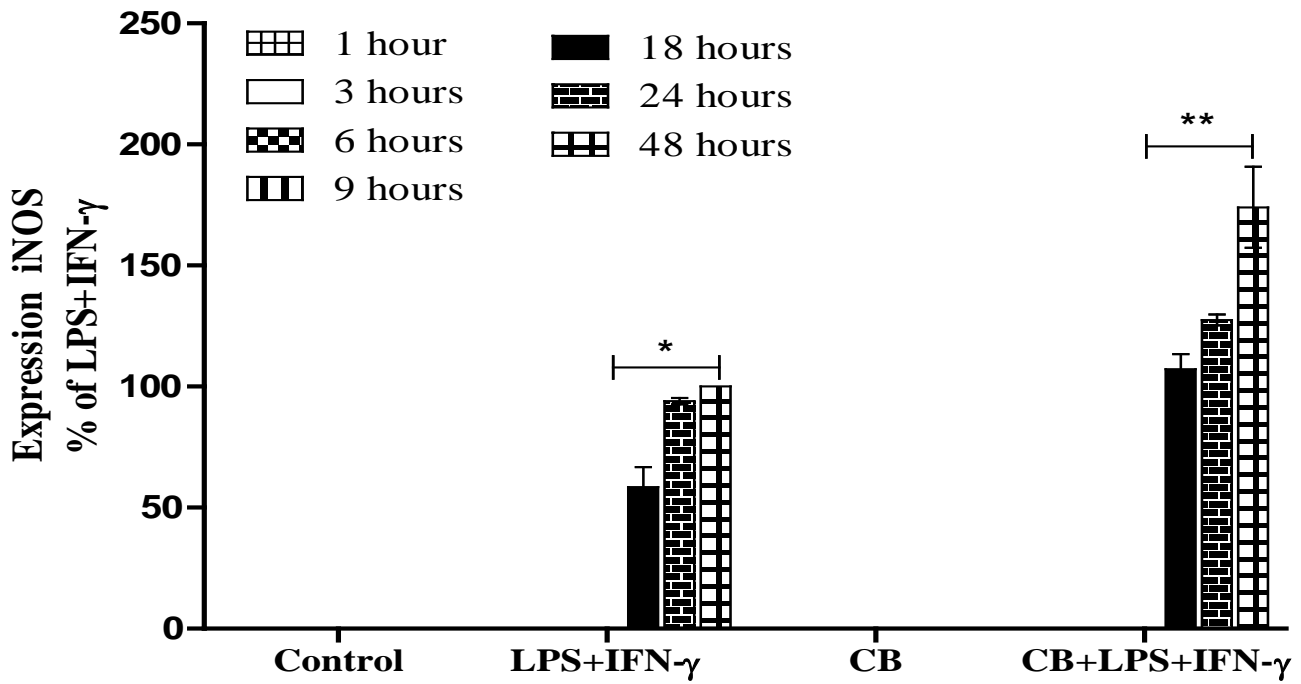
Figure 4.18 B: **Summary data of the effect of coincubation of CB and LPS + IFN-γ on induced iNOS expression.**

Cells cultured to ~90% confluency were activated by LPS (100 µg ml^{-1}) + IFN-γ (100 U ml^{-1}) with adding of CB during a time course of 1, 3, 6, 9, 18, 24, and 48 hours. Expression of iNOS was evaluated by western blotting as described in methods (section 2.10). The data represents means ± S.E.M. from 4 individual experiments.* denotes $p < 0.05$ and ** denotes $p<0.01$ compared to LPS+ IFN-γ alone on each time point.
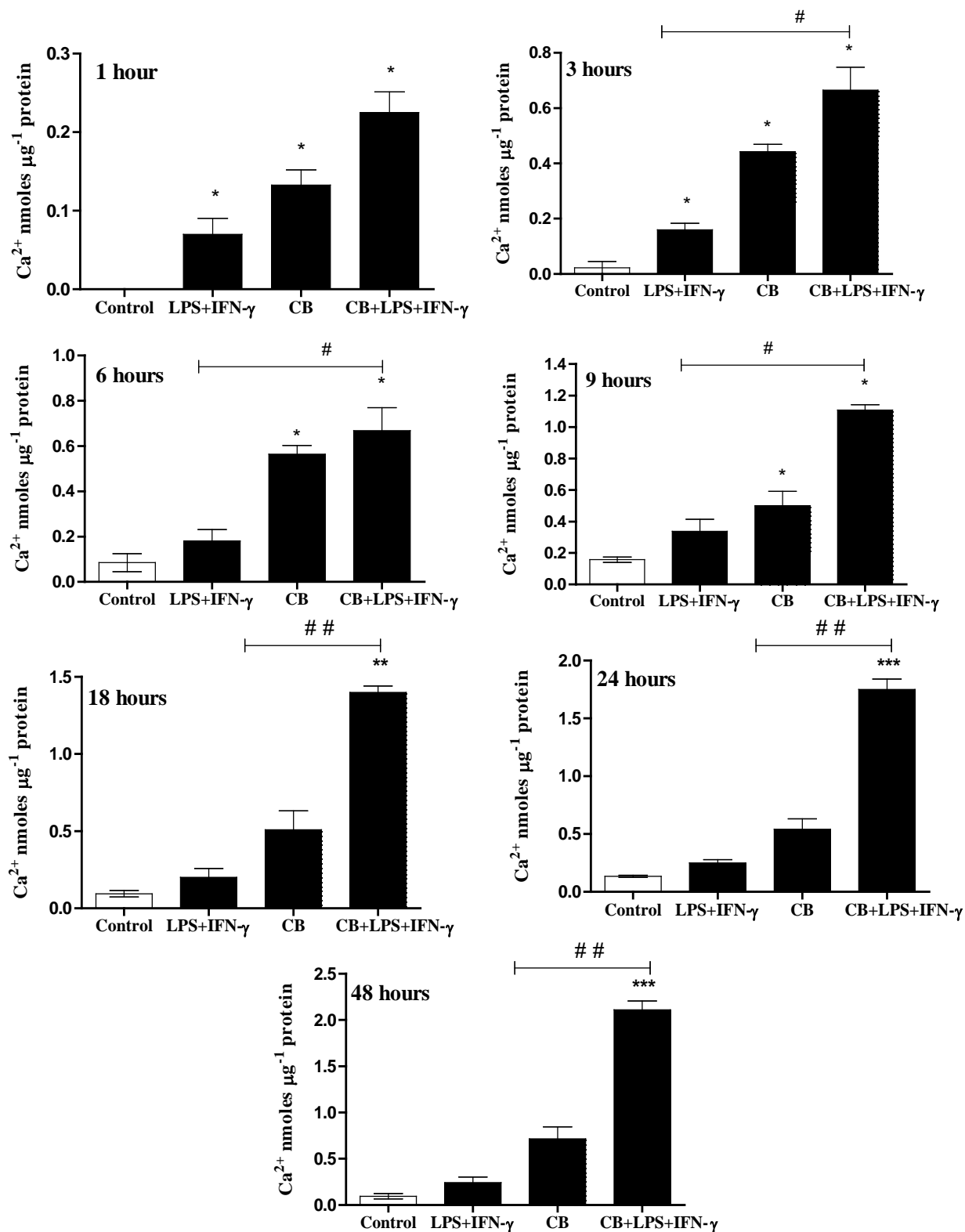
Figure 4.19 A: **Effect of coincubation of CB and LPS +IFN-γ on induced calcification.**

Cells cultured to ~90% confluency were activated by LPS (100 μg ml^{-1}) + IFN-γ (100 U ml^{-1}) together with CB during a time course of 1, 3, 6, 9, 18, 24, and 48 hours. Total calcium was quantified as described in methods (section 2.6). The data represents means ± S.E.M. from 4 individual experiments.* denotes $p < 0.05$,** denotes $p < 0.01$ and *** denotes $p < 0.001$ respectively compared to control while # and ## denotes $p < 0.05$ and $p < 0.01$ respectively when compared to CB on each time point.

174
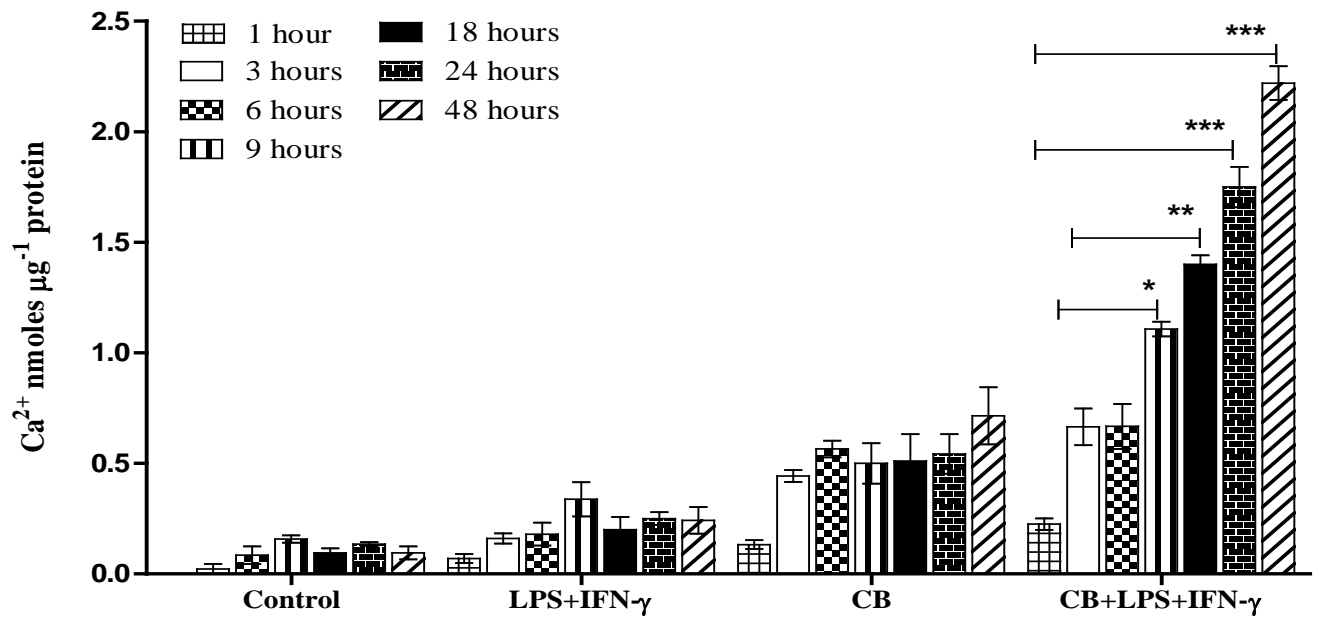
Figure 4.19 B: **Summary data of the effect of coincubation of CB and LPS +IFN-γ on induced calcification.**

Cells cultured to ~90% confluency were activated by LPS (100 μg ml⁻¹) + IFN-γ (100 U ml⁻¹) with adding of CB during a time course of 1, 3, 6, 9, 18, 24, and 48 hours. Total calcium was quantified as described in methods (section 2.6). The data represents means ± S.E.M. from 4 individual experiments. The data represents means ± S.E.M. from 4 individual experiments.* denotes *p*< 0.05, ** denotes *p*< 0.01 and *** denotes *p*< 0.001 compared to CB at each experimental   conditions.

4.3.8- Effects of preinduced NO production and iNOS expression on CB induced calcification of RASMCs.

In these studies, cells were initially induced for 24 hours with LPS and IFN-γ to initiate NO production before inducing calcification. This was to determine whether regulation of the latter required the sustained presence of NO or whether the availability of NO at the initiation of calcification was sufficient to regulate the calcification process.

Incubation of cells with medium or CB alone did not caused NO production or iNOS expression throughout the time course of the studies. RASMCs activated with inflammatory mediators for 24 hours followed CB resulted in significant elevation in NO production (0.103 ±0.02 nmoles µg^{-1} protein) above that seen with LPS+IFN-γ alone (0.07 ±0.01 nmoles µg^{-1} protein) (Figure 4.20 A). Similarly, iNOS expression was also enhanced by CB (46% increase) when applied after activation of cells with LPS and IFN-γ even though the latter were removed from the incubation after 24 hours and were not present for the remaining 3 days of incubation with CB.(Figure 4.20 B).

Consistent with the above trends, calcification was also enhanced when CB was added after LPS and IFN-γ. The increase was well above that seen with LPS and IFN-γ and indeed CB (Figure 4.20 C), suggesting that the presence of NO at the initiation of calcification may be critical for the latter and further suggests that NO may promote calcification. This requires further clarification and is addressed in the next chapter of this thesis.
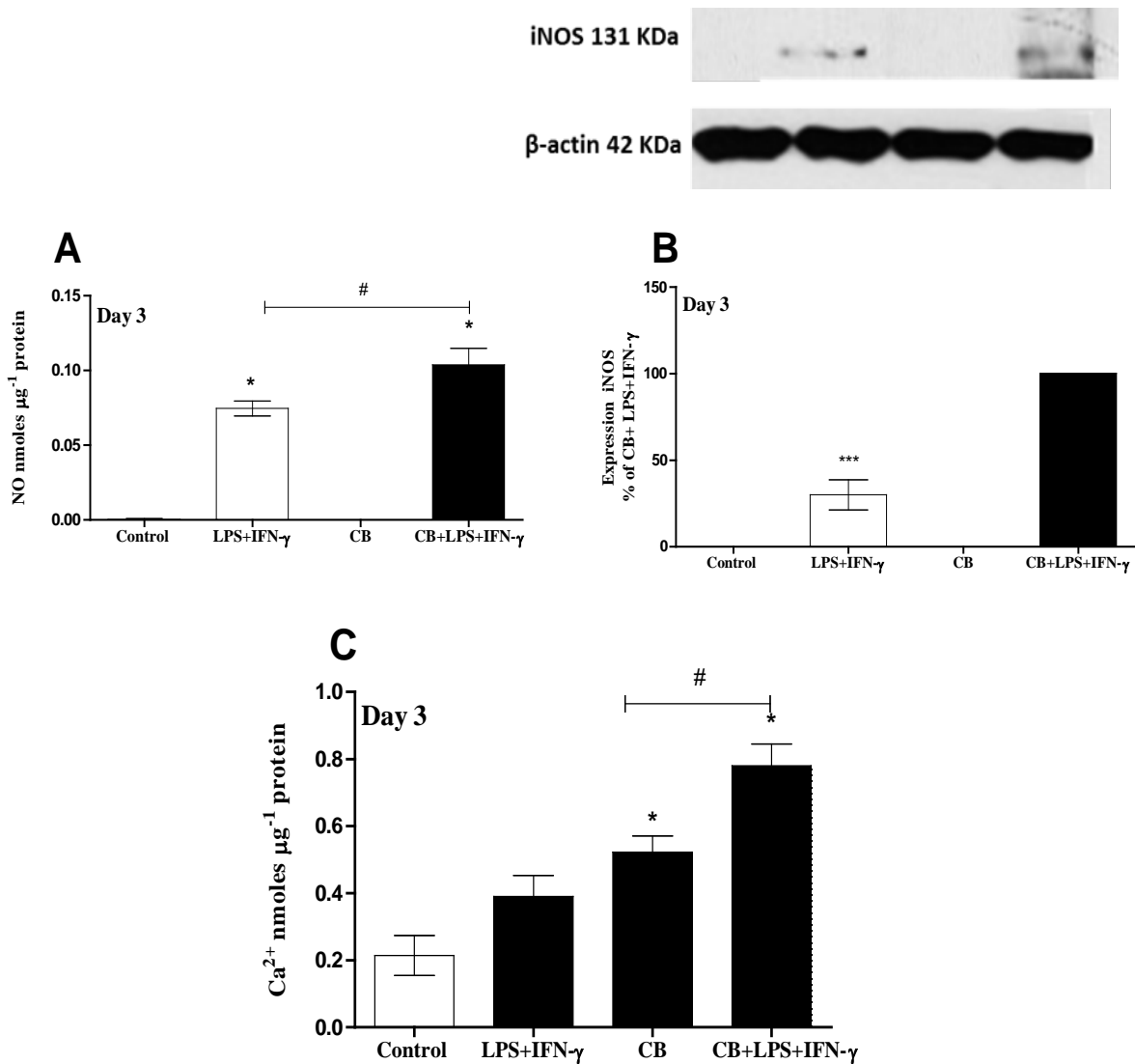
Figure 4.20: Effect of preinduced NO production and iNOS expression on CB induced calcification.

Cells cultured to ~90% confluency were incubated with culture medium alone (control). Cells were co incubated with LPS (100 μg ml^{-1}) + IFN-γ (100 U ml^{-1}) for 24 hours, then replaced by CB only. A: Total NO production was quantified by Griess assay as described in methods (section 2.3). B: iNOS expression was quantified by western blotting as described in methods (section 2.10). C: Total calcium was quantified as described in methods (section 2.6). The data represents means ± S.E.M. from 5 experiments. * denotes $p<0.05$ or #$p<0.05$ as stated.

4.3.9- Effects of calcification on induced production of NO and iNOS expression in RASMCs.

These experiments were the reverse of those described in section 4.3.8 above and looked at how the induction of calcification prior to that of iNOS and NO regulated the latter two processes. In these experiments, cells were initially incubated with CB for 3 days and then activated with LPS+IFN-γ for 24 hours. Medium or CB alone had no effect on basal NO release or iNOS expression (Figure 4.21 A). However, incubation with CB first followed by LPS+IFN-γ did not enhance the effects seen with the latter two alone. Both NO production and iNOS expression remained comparable to the levels seen under all conditions (Figure 4.21 A and B).

With regards to calcification, there was an increase in calcium levels in cells incubated with LPS+IFN-γ (0.35 ± 0.1 nmole. μg^{-1} protein) compared to control cells (0.1 ± 0.03 nmole. μg^{-1} protein) Figure 4.21 C. Incubation with CB alone enhanced calcium levels further as has been demonstrated (0.7 ± 0.20 nmole. μg^{-1} protein) but the addition of LPS + IFN-γ after CB reduced the levels of calcium back to those seen before the addition of CB.
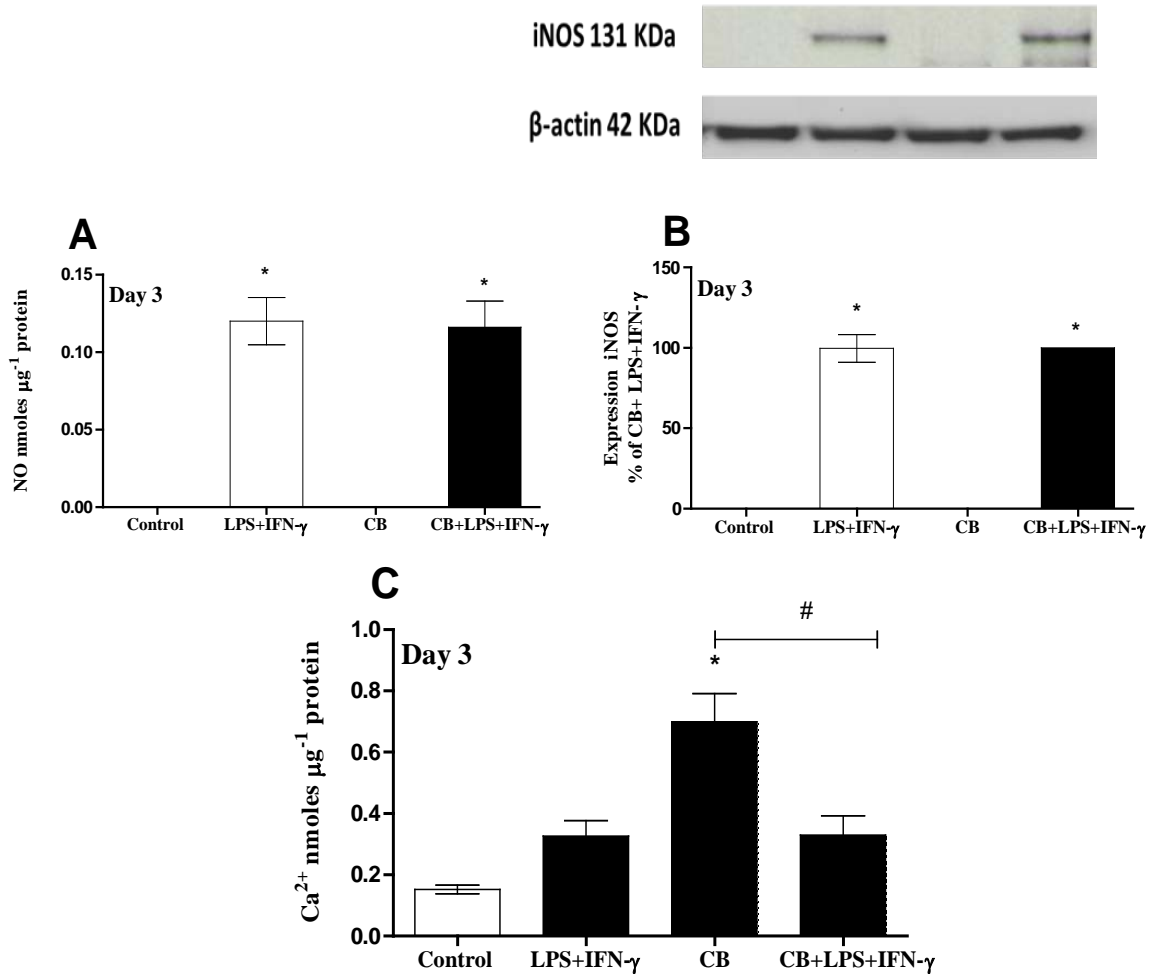
Figure 4.21: Effects of calcification on induced production of NO and iNOS expression in RASMCs.

Cells cultured to ~90% confluency were incubated with culture medium alone (control). Cells were co incubated with CB for 72 hours followed by adding LPS (100 µg ml^{-1}) + IFN-γ (100 U ml^{-1}). A: Total NO production was quantified by Griess assay as described in methods (section 2.3). B: iNOS expression was quantified by western blotting as described in methods (section 2.10). C: Total calcium was quantified as described in methods (section 2.6). The data represents means ± S.E.M. from 5 experiments. * denotes $p<0.05$ or #$p<0.05$ as stated.

179

4.4-Discussion:

As mentioned in previous chapter, one of the objectives of this project is to establish the role of NO in the calcification process and to determine whether it regulates the severity of the process, especially when the source of the NO is from the iNOS enzyme. The latter, induced by inflammatory mediators such as LPS and IFN-γ, may be critical in calcification since it has been shown to be enhanced in VC. Despite these observations, it is poorly understood whether NO (added or induced) contributes to the development of calcification or in fact protects against this process.

The first set of experiments incubated cells in medium which was not replenished for 7 days. Our data has demonstrated that cells incubated with medium alone did not produced NO or induce iNOS expression and this is in agreement with the fact that RASMCs in culture do not express iNOS under basal conditions. Literature review revealed that LPS mediated activation of TLR4 elevates NO production and iNOS expression over 24 hours which was induced in a time dependent manner (Heo *et al.*, 2008). This could explain part of the underlying mechanism of action of LPS in inducing iNOS. Furthermore, the induction iNOS by LPS is not only on RASMCs but also reported in rat liver where the effect is also time dependent over 48 hours (Billiar *et al.*, 1990). LPS *in vivo* can induce proliferation and inflammation of VSMCs contributing to diseases such as atherosclerosis and arterial restenosis (Jiang *et al.*, 2014). These consequences can accelerate the formation of vulnerable plaques.

At the signalling level, LPS activates certain pathway to stimulate the induction of iNOS and thus NO production. For instance, LPS activates TLR4 as already stated above, and this triggers TRIP factor which in turn stimulate MAPK causing phosphorylation of p 38 MAPK (Meng *et al.*, 2013) and then activator protein-1 (AP-1). AP-1 is an important transcription

factor which is capable of stimulating gene transcription resulting in protein expression including iNOS (Chyu *et al.*, 2004).

In the current project, studies have been carried out using LPS alone in the presence of calcification inducers (CaCl$_2$ or β-GP or in combination; CB). The effect of each condition on NO levels and calcification was assessed during long time points (1, 3, 5, and 7 days). Activation of cells with LPS for 24 hours did caused the induction of iNOS expression which reached a maximum at day 3 (72 hours) followed by a decline thereafter. Other studies have demonstrated that LPS could express iNOS at 12- 18 hours reaching maximal expression at 24 hours following by a declined thereafter in rat smooth muscle cells (Hung, 1995;Tsutsumi *et al.*, 2008). Our results demonstrated that NO production continued to increase even through iNOS expression had declined and this is because NO production is measured cumulatively and therefore increases with time.

Interestingly, the use of CaCl$_2$ after activation of RASMCs by LPS caused marginal but not significant suppression of iNOS expression at day1 because of the large error bars suggesting noise in the data. Significant induction was however evident from day 3 to day 5, declining to basal levels at day 7. It seems from the western blots that CaCl$_2$ may prolong the half-life of iNOS protein expressed significantly at day 5 which is against the findings of LPS alone.

The mechanism by which CaCl$_2$ may induce NO production by iNOS possibly includes CaCl$_2$ entering cells through voltage – dependent calcium channel (Lin *et al.*, 2009)or receptor operated calcium channel (McFadzean *et al.*, 2002) which causes the induction of NO production indirectly. This may however be independent of the classical physiological mechanism where calcium activates calmodulin which subsequently binds to NOS (eNOS or nNOS) causing activation of the enzyme. With regards to iNOS, calmodulin is apparently already tightly bound to the enzyme protein when produced and iNOS is therefore referred to as calcium independent (Jones *et al.*, 2007)

Changes in intracellular calcium may however be important for the actual induction of iNOS. In support of this it has been reported that its gene may be induced by 17β-estradiol through enhancing calcium and it has been demonstrated that inhibition of extracellular and intracellular calcium suppressed while enhanced calcium influx enhanced iNOS expression and NO production (Azenabor *et al.*, 2009). Similarly, the use of *β*-GP or CB in the presence of LPS followed quit similar trends as has been seen with $CaCl_2$. The use of CB did not however show any additive effect on induction of NO and iNOS which was the same trend as seen with either $CaCl_2$ or *β*-GP alone. Therefore, this study confirm that iNOS expression and NO production are enhanced under conditions that favour calcification which could be a mechanism through which iNOS and NO contribute to regulate calcification in blood vessels. In the calcification state, incubation of cells with LPS for 24 hours followed by the continued presence of LPS caused significant elevation of calcium level compared to the control. LPS activate TLR2/4 leading to the elevation of the expression of the proinflammatory and pro-calcific agent BMP2, which in turn causes aortic valve calcification in humans. BMP 2 antagonism abolishes the activity of TLR2/4, which results in inhibition of BMP2 and ALP. Furthermore, the silencing of the gene of TLR2/4 contributed to the reduction of BMP2 (Yang *et al.*, 2009). Further study explained that activation of the TLR2/4 receptor is known to promote BMP2 production which causes phosphate uptake by the cell and hence calcification in human VSMCs (Heo *et al.*, 2008).

In our model, the calcification which occurred in RASMCs might follow one of the mechanisms mentioned above, but this needs to confirm by further studies in future. However, when cells were activated by LPS, followed by the continued presence of LPS in the media with $CaCl_2$, *β*-GP or CB there were no significant changes in calcium levels compared to when LPS was not present. The reason for this difference is not understood, however previous studies have found that LPS inhibits BMP 2 in osteoblasts via crosstalk

between TLR4/MyD88/NF-κB and BMP/Smad signalling (Huang *et al.*, 2013). Therefore the same may be occurring here, resulting in an increase in calcium levels, albeit marginal.

Incubation of cells with IFN-γ resulted in marginal production of NO which was much less when compared to LPS alone. This suggests that IFN-γ is a weaker inducer of NO production. This result confirms other studies demonstrating that IFN-γ on its own had little effect on basal NO levels and this may be because this cytokine does not induce but rather act to stabilise the iNOS mRNA (Chan *et al.*, 2001). Consistent with the weak induction of NO production, was the lack of expression of detectable levels of iNOS when examined by western blotting. It is possible however that iNOS was induced but at a much lower level which perhaps was below the limit if detection by western blotting. To confirm this, it would have been helpful to detect whether iNOS mRNA was expressed following treatment with IFN-γ. Unfortunately, there were time constraints and it was not possible to extend the studies to qPCR analysis of iNOS mRNA expression. Additionally, experiments could also have been carried out using a selective iNOS inhibitor such as GW274150 to block iNOS activity and see if this had any significant on the low levels of NO produced by IFN-γ. Again time constraints meant these experiments could not be carried out but should be planned for future studies.

With regards to calcification, IFN-γ appears to be more stable over the time course investigated but was elevated calcium level to that seen with cells containing medium only. This result agrees with that obtained with LPS and suggests that IFN-γ, like LPS, is a good enhancer of calcium accumulation in RASMCs. Interestingly, although IFN-γ did not induce as much NO production as LPS it did increase the levels of calcium detected even higher than those seen with LPS alone. This is interesting because it suggest that IFN-γ may be enhancing calcium levels via a mechanism independent of NO.

Although the mechanism that caused this increase in calcium has not been investigated, other studies have shown that IFN-γ upregulates the expression of 1alpha-OHase (Stoffels *et al*., 2006). The possibility that this may occur in RASMCs is supported by the fact that 1alpha-OHase is extensively expressed in arterial smooth muscle cells of rat and human (Somjen *et al*., 2005) and converts 25-$(OH)_2D_2$ (calcidiol) to 1,25 $(OH)_2$ D_3(calcitriol), resulting in elevated calcium level leading to hypercalcemia. (Chakrabarty *et al*., 2011; Segersten *et al*., 2002). Activation of RASMCs with IFN-γ followed by the adding of calcification inducers resulted in significant elevation of calcium levels which increased dramatically over time course. Incubation of cells with $CaCl_2$/CB and IFN-γ caused significant induction of calcium levels when compared to $CaCl_2$ or CB alone. Unlike $CaCl_2$, *β*-GP in the presence of IFN-γ did not caused any significant changes in cellular calcium level or indeed in calcification. It is possible therefore that the lack of calcium may be the key limiting factor in calcification not taking place. Furthermore, it could be that the time of incubation was not long enough to enhance calcium levels as it has been seen with other studies showing incubation of VSMCs with *β*-GP for 10 days while it was 7 days in this study.

The combination of LPS and IFN-γ caused significant and sustained induction of NO. The induction of iNOS on the other hand peaked and then declined as confirmed by western blotting. The reason behind this elevation and sustainable NO production and iNOS expression may be due to the fact that LPS induces and IFN-γ stabilises the mRNA of iNOS (Raghavan *et al.*, 2001) and this could explain why there was more NO produced by iNOS in RASMCs. These findings are consistent with several reports demonstrated in the literature review (Chester *et al.*, 1998; Hattori *et al.*, 1994;Wileman *et al.*, 1995).

Further investigations were carried out in order to establish whether regular replenishment of nutrients and other factors required for cell growth affected iNOS induction, NO production or the calcification process. Interestingly, it was clearly seen that incubation of cells with LPS+IFN-γ using this protocol caused significant elevation in NO production and sustained iNOS expression which were higher compared to levels seen without replenishment of nutrients protocol. The sustained expression of iNOS also contrasts with the generally reported profile of expression of iNOS protein which has been shown to peak at 24 hours but declining over 48h (Browner *et al.*, 2004). Replenishing the medium provides nutrients and other factors essential to sustain optimal cell function and growth. This may enhance iNOS activity as well as sustaining its expression which could explain why levels are higher than when the medium was not changed where nutrients could be depleted resulting in poor viability and function of cells. These results are new, as they have not been demonstrated by previous studies. It may be that when LPS and IFN-γ were replenished the activation of iNOS expression was sustained, and thus NO is produced for a longer time course such as 5 or 7 days.

In terms of the role of CB in NO or iNOS expression, when LPS + IFN-γ was used to activate the cells, the presence of CB caused marginal changes to the level of NO and iNOS when the medium was replenished daily. Similarly, when the medium was not replenished daily the presence of both LPS and IFN-γ did not significant change when compared to studies where the medium was replenished daily.

Cell viability experiments were conducted to determine whether any of the effects mentioned above were specific or due to cytotoxic consequences of the experimental conditions. A significant decrease in cell viability was noted when LPS+IFN-γ alone or in combination with calcification inducers were used at day 2 to 7. This may have been due to the prolonged

incubation period of the cells. Thus, to separate the effect of cell viability on calcification from the effect of the agents themselves, the protocol was revised by introducing daily replenishment of the incubation medium. However, with the daily replenishment of the medium with CB+LPS and IFN-γ in combination did not cause significant changes to NO levels or iNOS expression levels in comparison to conditions where the cell culture medium was not replenished. Thus, the viability of the cells did not impact upon the level of NO/iNOS in this model.

Further experiments were conducted to determine whether there was a difference in effects when the cells were activated with either LPS and /or IFN-γ prior to CB being added to the medium versus coincubation with addition of CB at the same time as the others to the cell culture. In previous studies (Iadecola *et al.*, 1996; Kessler *et al.*, 1997) the presence of iNOS detected by western blotting was noted to occur earlier in VSMCs, between 12 – 18 hours. However, our data showed that there is no change of the levels of NO production by iNOS at 18 hours when both LPS and IFN-γ were present, but there was significant induction of iNOS and increase in NO after 18 hours as shown in the 24 hours results. This was also true of when the cells were coincubated with CB+LPS +IFN-γ. Interestingly, the addition of CB with both LPS and IFN-γ caused significant induction of NO/iNOS at 48 hours compared to when LPS and IFN-γ alone. These results may be explained if CB acts at the post transcriptional, thus stabilising iNOS mRNA. This however was not investigated and requires further studies.

The addition of CB with LPS and IFN-γ resulted in the increased expression of iNOS followed by the elevation of NO which was comparable to when both LPS and IFN-γ were used to stimulate the cells. In comparison with the study where the medium was not changed for 7 days, incubation of the cells with LPS+IFN-γ for 24 hours followed by the addition of CB at day 1 did not cause any significant changes to the induction of NO by iNOS. There

was however a lower level of induction. For instance, the activation cells by LPS+IFN-γ followed with addition of CB caused ~0.24 nmole.µg^{-1} protein versus ~0.2 nmole.µg^{-1} protein incubating cells with CB+LPS+IFN-γ at 48 hours.

Further studies carried out were aimed at establishing whether the induction of NO/iNOS regulated calcification when subsequently induced in the absence of the continued presence of the inflammatory mediators. Cells were therefore activated with LPS and IFN-γ for 24 hours followed by the addition of CB alone for 3 days. This was the time point found previously from the first experiment to induce maximal calcification and NO production. A significant increase in both NO and iNOS was noted. It thus appears that CB may be involved in the mechanism that elevates NO and iNOS production in RASMCs. The mechanism is still not known although the expression of iNOS is dependent of calcium because CB contains both $CaCl_2$ and *β*-GP. This should not cause elevation of the iNOS protein, as this has not been seen with previous research, and it has been demonstrated that iNOS does not bind to calcium (Ding *et al.*, 1998). In this thesis, CB has however been shown to have a significant effect in the induction of NO and iNOS in RASMCs even when LPS and IFN-γ were not continually present in the medium.

A further investigation was set up in which cells were activated with CB for 3 days followed by the addition of LPS and IFN-γ only for 24 hours without adding CB in order to determine whether calcification regulated iNOS and NO production. The data showed that there was a similar trend in NO and iNOS expression compared to incubating either with LPS and IFN-γ or CB only. The presence of CB first did not cause any changes to the levels of NO/iNOS when compared to the reverse of this method. Thus, incubating cells with CB first followed by LPS and IFN-γ did not enhance the effects seen with the latter two alone.

In relation to calcification, the activation of cells with both inflammatory agents caused significant elevation of calcium levels over a time course which reached a maximum on day 5 when compared to control. Moreover, there was significant induced of calcium levels with LPS+IFN-γ when compared to LPS or IFN-γ alone as already discussed in chapter 3. This explains that LPS induce calcium levels through activating TLR2 and 4.

An interesting observation form the studies carried out so far is that LPS + IFN-γ and the calcification inducers such as $CaCl_2$ / CB resulted in induction of mineralisation as it has been detected either by ARS or FT-IR. Further study found an acceleration of calcification (maximal elevation of calcium day 3) in comparison to CB alone (maximal elevation of calcium day 5). LPS stimulate the synthesis of proteins such BMP2 and ALP through activating TLR2 and 4. Both proteins are well-known pro-calcific markers and play a critical role in calcification, by inducing a phenotypic transition of aortic smooth muscle cells in to bone like cells (Tintut *et al.*, 2002; Zehnder *et al.*, 2002). Thus, it is likely that LPS + IFN-γ with calcification inducers might regulate the calcification under the inflammatory condition. At present, the full mechanism of action of inflammatory mediators is not known and it is not clear whether in our cell system, LPS does activate other osteoblast or osteoclast like cells marker, such as Runx2/Cbfa1 and this may require further investigation.

Several methods were used to see whether NO/iNOS regulates VC in this study. When the medium was changed every 24 hours and cells were coincubated with LPS and IFN-γ alone there was a significant induction of calcium levels compared to the control. These results were not significantly different to the calcium levels seen when the medium was not changed for 7 days. Similarly, when CB+LPS+IFN-γ were in the medium replenished daily there were no significant changes to the calcium levels when compared to cells incubated in the same medium for 7 days. For example with continued incubation in the same media iNOS

expression was 170%, while in daily changed media it was 200% at day 3 with an overlap in the margin of error of both these results. There was however a significant increase in calcium compared to the CB being present in the medium alone. Moreover, there was a slight reduction in calcium levels when the cell medium was changed every 24 hours (with CB+LPS+IFN-γ) compared to that seen when the medium was not changed. When the media was replenished daily no significant changes in the levels of NO/iNOS (as seen by western blot) were seen compared to not changing the media. However, the data for the unchanged media did show a marginally higher level of NO/iNOS compared to that seen when the medium was changed.

The cumulative increase in calcium levels could be explained by accumulation of calcium over the time course due to addition of calcium caused by buffer replenishment. When the cells were incubated with CB alone, the calcium level was significantly higher, but the levels when the media was changed daily were similar to those when the medium was not changed at every time point. This suggests that the daily replenishment of the medium could be saturating the cellular mechanism responsible for calcification, rather than the induction of calcium level itself. Another possibility is that the cells are retaining the calcium, and these cells are unable pump out the calcium from the plasma membrane due to the low levels of adenosine triphosphate (ATPase) and which in turn maintains high cytosolic calcium concentrations for longer durations rather than exchanging these with other ions such as the hydrogen ion. Thus, there would be no further induction of calcium deposition when the medium was changed daily, as demonstrated by a previous study (Clapham, 2007).

However, when the data over the 7 days is pooled, calcium levels were significantly elevated. Thus, it may be that when the buffer was replenished calcium accumulated from the first day, and this produced a significant level measured from the first day of incubation.

The calcium levels reached approximately 11 nmole.μg^{-1} protein. This is a significant increased when compared to incubation in CB media alone. Yet when the cells were incubated in CB alone the pooled data showed approximately 2 nmole.μg^{-1} protein being present. This data indicates the limitation of RASMCs cultured in the presence of calcium.

Coincubation experiments were performed whereby cells coincubated with CB and LPS+IFN-γ were compared to cells incubated in CB alone for a 48 hour period. The levels of NO/iNOS and intracellular calcium were measured throughout 1, 3, 6, 9, 18, 24 and 48 hours in order to determine the changes in NO, iNOS expression and elevated intracellular calcium. Calcium was detected earlier, beginning at 3 hours when CB alone was present. An explanation for this phenomenon could be that the activity of the calcium receptor is increased by the addition of CB.

When NO/iNOS production is stimulated by the presence of LPS and IFN-γ, with CB also present, the elevation in calcium levels was significantly higher than that compared to CB alone or just LPS and IFN-γ at 3, 6 and 9 hours. However beyond this (18 – 48 hours) a significant increase in found only when comparing CB coincubated with LPS+IFN-γ to LPS+IFN-γ alone. However, iNOS appears at 18 hours in media containing LPS+IFN-γ but was not seen in the control. There was a strong link between the presence of NO/iNOS and calcification. Thus, the significant differences beyond 18 hours may be due to the synergistic effect of iNOS and CB in inducing calcification. This may be because iNOS depends on the presence of calcium. CB contains calcium and phosphate which is raised in the cell.

Previous studies have shown that iNOS was involved in the binding to free intracellular calcium and calmodulin irreversibly (Panda *et al.*, 2001). However, our findings have supported that CB and LPS+IFN-γ induced calcium significantly compared to the control or CB alone and this result in elevation of iNOS expression in RASMCs.

In comparison with other studies, the calcium levels were elevated by incubating cells with LPS+IFN-γ first followed by the addition of CB at day 1. The levels were ~2.2 nmole.µg^{-1} protein compared to when the both the inflammatory agents were added at the same time to the media, approximately ~2 nmole.µg^{-1} protein.

A further investigation was conducted using two alternative methods in order to understand whether sustained induction of iNOS and NO was essential for calcification, and determine if CB is involved in regulation iNOS or NO production. In the first method cells were activated with LPS+IFN-γ for 24 hours, followed by the addition of CB alone; with quantification of iNOS and NO on the third day. This time period for quantification was selected as prior experiments had indicated maximal calcification at 3 days postactivation of iNOS expression. The results indicated a significant induction of calcium for the 3 days of incubation compared to the control. The levels of iNOS were however lower than previous experiments where LPS and IFN-γ continued to be present in the medium. For example after 3 days of continuous incubation with replenishing media the % expression of iNOS was 200% compared to 100% when only CB was present for 3 days postactivation. The NO levels were also lower, e.g. 0.125nmole. µg^{-1} protein with CB only compared to 0.38 nmole. µg^{-1} protein when LPS and IFN-γ continued to be present with CB.

The cells also showed a significant increase in calcium levels when cells activated by LPS and IFN-γ had their media replaced and included CB compared to those incubated in CB alone, i.e. 0.5 nmole. µg^{-1} protein compared to 0.78 nmole. µg^{-1} protein. This was in agreement with other studies where it was found that the expression of iNOS was involved in the induction of calcification in the MC3T3-E1 osteoblasts not VSMCs (Zaragoza *et al.*, 2006). Importantly, both the induction of NO/iNOS and increase of calcium levels significantly at day 3 supports the idea of the involvement of iNOS in the calcification

process, in turn causing the formation of HA crystals. On the other hand, when the method was reversed whereby cells were activated for 3 days with CB and thereafter the media replaced with one containing LPS and IFN-γ, there was a reduction of calcium levels. Therefore, using this novel result it is possible to demonstrate that the elevation of NO/iNOS by the inflammatory mediators enhances the effect of CB in the elevation of calcium in the cell. This indicates a strong link between the calcium and NO/iNOS levels in the vasculature. Thus an increased level of intracellular calcium generated less calcification than when inflammatory mediators activate iNOS/NO production prior to the calcium levels being increased.

It is also interesting to note that when the media was not replenished for 7 days, i.e. incubation for 24 hours with LPS and IFN-γ was followed by the addition of CB, calcium concentration were considerably higher, reaching levels of 2.4 nmole. μg^{-1} protein at day 3. This indicates activation of calcification when all 3 agents are present together which may be an additive effect due to the continued presence of NO promoting free radical formation and hence calcification (Guzik *et al.*, 2002). Thus, the increased iNOS levels noted at day 3 when coincubation was continuous and correlates with increased levels of calcium level leads to accelerate calcification process.

The biochemical assays indicated elevated calcium levels under the conditions described above. There was however little staining with ARS evident in the treated cells. This could however be due to the fact that while there was an elevation in calcium levels there was less HA crystal formation presumably because there was no parallel increase in phosphate levels. Similarly when *β*-GP was used alone there was no detectable HA stained possibly because of the lack of parallel increase in calcium. Thus for HA to be formed and ARS to show a positive result there has to be an increase in both calcium and phosphate.

The FT-IR analysis however did show evidence of HA crystal formation in the uses of CB/ CB+LPS /CB+ IFN-γ /CaCl$_2$ +LPS+IFN-γ / CB+LPS+IFN-γ. While cells containing medium only, LPS and/or IFN-γ, CaCl$_2$ or β-GP alone did not formed HA crystals as shown by the FT-IR analysis. Interestingly, these treatments, other that LPS/ β-GP, caused significant increases in cellular calcium levels as detected by the calcium assay kit. It could be that limitation of other factors such as calcium in the medium which is needed to form HA crystals was not present when cells were treated with β-GP. Moreover, the fact that calcium was elevated would suggest that the cells may be primed to calcify once exposed to phosphate and the lack of detectable plaques may be due to phosphate not being present. This therefore suggests that these treatments increased cellular calcium, they did not necessarily cause plaques to form or the cells to calcify.

However, ARS was obviously seen on RASMCs incubated with the treatments such as CB alone, CB+LPS, CB+ IFN-γ, CB+LPS+IFN-γ, CaCl$_2$+LPS+IFN-γ. All these treatments induced HA which was stained significantly by ARS compared to control cells as well as to CB. It could be explained that these agents support formation of HA crystal which was confirmed by FT-IR. FT-IR analysis of mineralised plaques revealed the presence of HA crystals peak at 1080 cm^{-1} - 1089 cm$^{-1.}$ These readings represent HA with poor and strong crystallisation structures respectively. These findings were in agreement with a study demonstrating that HA can form either strong or poor spectrum in calcific tendonitis (Alò *et al.*, 2009; Chiou *et al.*, 2009; Lin *et al.*, 2007). However, the confirmation of the presence of HA crystals by ARS and FT-IR was not conducted for the experiments involving daily change of media, or alternating between exposing cells to either CB or IFN-γ and LPS first. It is recommended that these experiments are carried out in future work.

The results of the experiments indicate that the calcifying agents are important in inducing crystallisation, and inflammatory mediators may accelerate this process noted by the presence of HA crystal 3 days after incubation, even though this results has not been published by other studies. The mechanisms that leads to HA formation has not been examined in the current studies, but there is at least one study that has demonstrated that peroxidation of lipid formed in human smooth muscle cells as a result of oxidative stress from hydroxyl radicals, can induce the characteristic crystallisation of HA. Hydroxyl radicals can attached the fatty acid bond and thus damage the membrane of foam cells leading to mineralisation of plaques (Alò et al., 2009; Dritsa, 2012; Sklepkiewicz et al., 2011). Whether oxidative stress plays any role in our system remains to be established.

In summary, the studies carried out to date clearly show that induction of NO by both inflammatory mediators may be enhanced in a calcifying environment. Moreover, the presence of NO appears to enhance calcification caused by inflammatory mediators, and calcification inducers. In terms of the disease state in man it may be that increased intracellular calcium in vivo enhances iNOS expression and thus NO production. Moreover, increased iNOS expression and NO production enhance calcification. This indicates that there may be a cascade effect whereby one condition i.e. inflammation promotes calcification, while calcification promotes inflammation. This is important to consider when seeking to address the disease condition.

Further studies were carried out detailed in the later chapters of this project, in order to fully understand the link between iNOS/NO and calcification, and the associated mechanisms. Figure 4.22 below shows the partial confirmation of the hypothesis in this project:
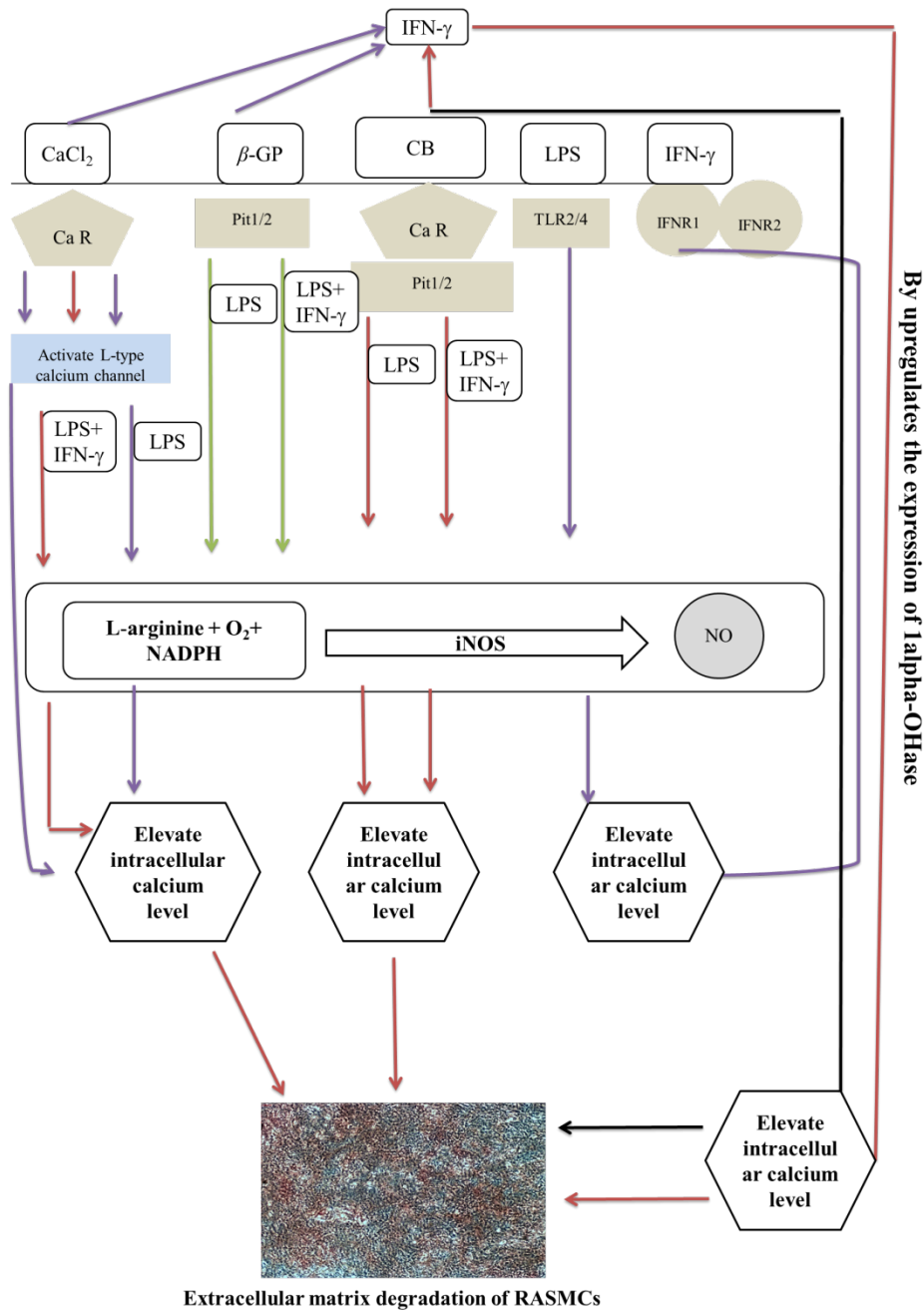
Figure 4.22: Expected formation of extracellular matrix degradation caused by NO production through iNOS.

CHAPTER V

RESULTS

Effects of NO donors and of the selective iNOS inhibitor, GW274150, on calcification of smooth muscle cells

5.1- Introduction:

The data presented in chapter 4 showed that exposure of RASMCs to LPS + IFN-γ resulted in calcification of the cells and this effect was further enhanced when coincubated with CB. Since these effects occurred in parallel with enhanced NO synthesis and iNOS expression, it is reasonable to speculate that induced NO synthesis may promote calcification of RASMCs which would be consistent with the notion that NO is a promoter of calcification (Zaragoza *et al.*, 2006;Ehnes *et al.*, 2015). This however contrasts with the other suggestion that NO may inhibit calcification (Richards *et al.*, 2013). Thus, to conclusively demonstrate whether NO promotes or inhibits calcification, further studies were carried out using GW274150, a selective inhibitor of iNOS activity (Chatterjee *et al.*, 2003; De Alba *et al.*, 2006; Høivik *et al.*, 2010), to confirm whether the induction of calcification by LPS and IFN-γ was associated with the expression of iNOS and thus NO production.

In addition, parallel studies were carried out supplementing the culture medium with NO donors and inducing calcification using CB in the absence of LPS and IFN-γ. The reason for taking this approach was to establish categorically that NO itself in the absence of any potential influences that may be induced by LPS and IFN-γ contributed to the calcification seen. The donors (Cai *et al.*, 2005) were diethylenetriamine/nitric oxide adduct (DETA NONOate/NOC18) and *s*odium nitroprusside (SNP). These compounds were chosen in order to establish whether the profile of NO release correlates with the induction and degree of calcification. Diethylenetriamine/nitric oxide adduct (Lam *et al.*, 2003) is a small molecule manufactured to release NO at a slow rate and has a half-life which is around 22 hours. Sodium nitroprusside (Giachelli, 2009) on the other hand is a fast releasing NO donor with a half-life of a few seconds. Interestingly, sodium nitroprusside could also protect against apoptotic bodies by B-cell lymphoma 2 (bcl2) gene which may in turn prevents accelerated

calcification (Ho *et al.*, 2009). This therefore makes SNP an interesting NO donor to investigate.

Diethylenetriamine/nitric oxide adduct has been shown to elevate calcium deposition and when coincubated with *β*-GP promotes mineralisation crystals (Yasuhara *et al.*, 2007). Contrasting these findings, other reports have suggested that incubation of cells with CB in the presence of NOC18 caused significant reduction in calcification (Kanno *et al.*, 2008 ;Pardali *et al.*, 2012). Similarly, SNP has been found to inhibit mineralisation in cultured chondrogenic cells (ATDC5). This inhibition occurred via c-GMP through independent pathway which in turn inhibits formation of mineralisation plaques (Huitema *et al*., 2006a). Further studies investigated whether this inhibition was mediated through releasing of NO by SNP or through other mechanisms. Interestingly, the data generated suggested that iron moiety released from SNP rather than the NO generated was responsible for inhibiting mineralisation detected by ARS (Huitema *et al.*, 2006b).

Taken together, these findings highlight the controversy associated with the role of NO in VC and this requires further studies which will be addressed in this chapter. The studies designed were aimed at establishing whether:

(i)   GW274150 inhibits iNOS activity in RASMCs.

(ii)   Blockade of iNOS activity by GW274150 regulate calcification of RASMCs.

(iii)   Calcification inducers cause significant changes in NO production.

(iv)   NO donors regulate calcification of RASMCs and whether this is determined by the profile of NO release.

5.2 - Experimental protocol:

Cells culture and quantification of NO production, total protein and calcium measurements as well as western blotting were performed as described in chapter 2, section 2.3, 2.5, 2.6, and 2.10, respectively. In parallel experiments, ARS and FT-IR analysis was also performed as previously described in the method (sections 2.8 and 2.9, respectively).

5.2.1- Effects of GW274150 on NO production and calcification of RASMCs.

RASMCs were cultured to ~ 90 % confluency and preincubated for 30 minutes with GW247150 at 10, 50 and 100µM before adding calcification inducers and / or LPS and IFN-γ together. Quantification of NO produced and calcification induced was determined at 3 days by the Griess and calcium assays, respectively. This was the time point found previously from the first experiment to induce maximal calcification.

5.2.2- Effects of nitric donors on calcification of RASMCs

RASMCs at ~ 90 % confluency were coincubated with the NO donor NOC 18 (10, 30, 50 µM) or SNP (10, 30 and 50 µM) in the presence or absence of CB (7 mM) for 3 days, and this was the time point found previously from the first experiment to induce maximal calcification. Calcification was determined using the calcium assays.

5.3- Results:

5.3.1 - Effects of GW274150 on NO production and on calcification of RASMCs:

Incubation of RASMCs with medium alone did not produce NO. Cells that were pretreated with LPS + IFN-γ (0.035 ±0.002 nmole µg^{-1} protein) and in combination with CB (0.06 ±0.003 nmole µg^{-1} protein) resulted in the production of NO which was significantly inhibited by GW274150 at 10, 50, and 100 µM (Figure 5.1) at day 3. The inhibitions did not show much concentration dependency as shown in Figure 5.1. iNOS expression was also significantly induced when cells were incubated with LPS+IFN-γ either alone or in the presence of CB where levels of iNOS protein were higher than those seen with LPS+IFN-γ alone Figure 5.2. The inductions were not affected by GW274150 at 10 and 50 µM. The uses of 100 µM however caused significant inhibition of iNOS expression. Cells that were incubated with CB alone did not alter basal NO production or iNOS expression.

Cells that were incubated with medium alone did not show any significant increase in accumulated calcium levels. Interestingly, in these studies, treatment of cells with LPS and IFN-γ (0.116 ±0.05 nmole µg^{-1} protein) failed to cause any significant increase in calcium levels above control (0.07 ± 0.01 nmole µg^{-1} protein) (Figure 5.3). This is to be expected as a different protocol was used which aimed to have minimal NO present at the start of the calcifying process.

The inclusion of GW274150 in the culture medium enhanced calcification in cells treated with either CB or with LPS+IFN-γ. This effect was more marked with LPS+IFN-γ [(0.28 ± 0.05 nmole µg^{-1} protein; 10 µM) or (0.4 ± 0.25 nmole µg^{-1} protein; 50 µM)] than with CB [(1.2 ± 0.5 nmole µg^{-1} protein; 10 µM) or (2.1 ± 0.5 nmole µg^{-1} protein; 50 µM)] and was seen only with 10 µM and 50 µM of the drug. At 100 µM, GW274150 significantly

inhibited elevations in calcium levels induced by LPS+IFN-γ alone and in combination with

CB but only partially suppressed that cause by CB alone (Figure 5.3).
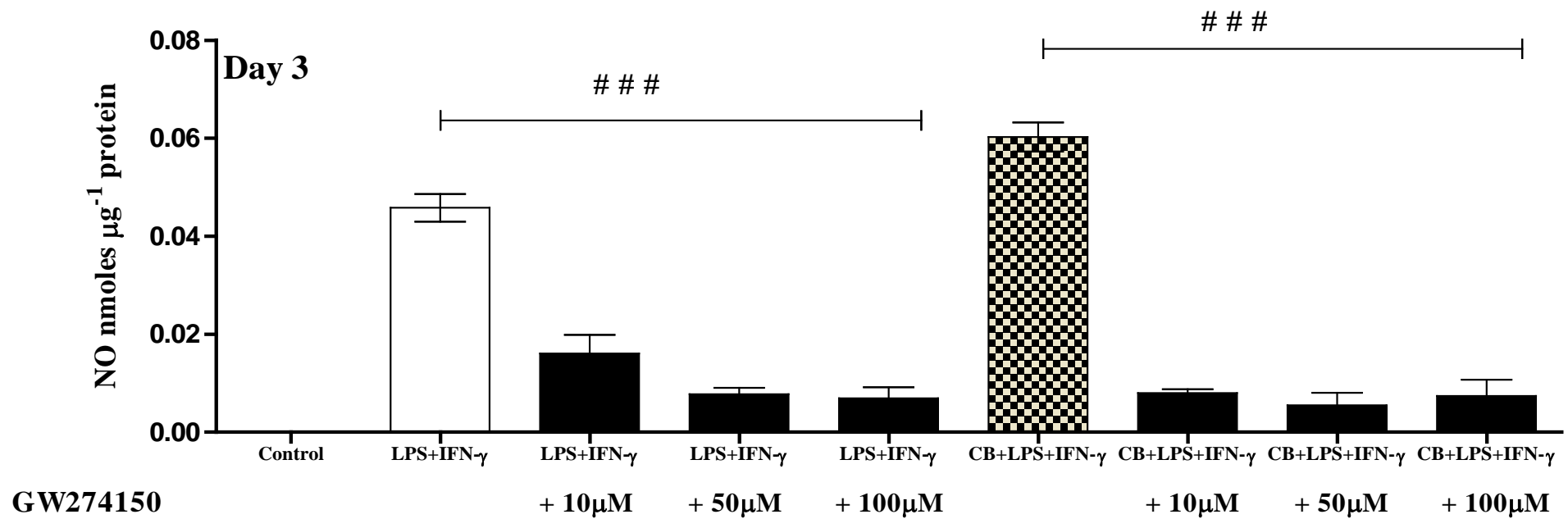
Figure 5.1: Effect of GW274150 on LPS+IFN-γ induced NO production in RASMCs.

Cells were cultured to ~90% confluency and incubated either with culture medium alone (control), LPS (100 μg ml^{-1}) + IFN-γ (100 U ml^{-1}) alone or in combination with CB in the presence or absence of GW274150. Total NO was quantified by the Griess assay as described in methods (section 2.3). The data represents means ± S.E.M. from 4 experiments. # # # denotes *p*<0.001 compared to condition not incubated with GW274150.
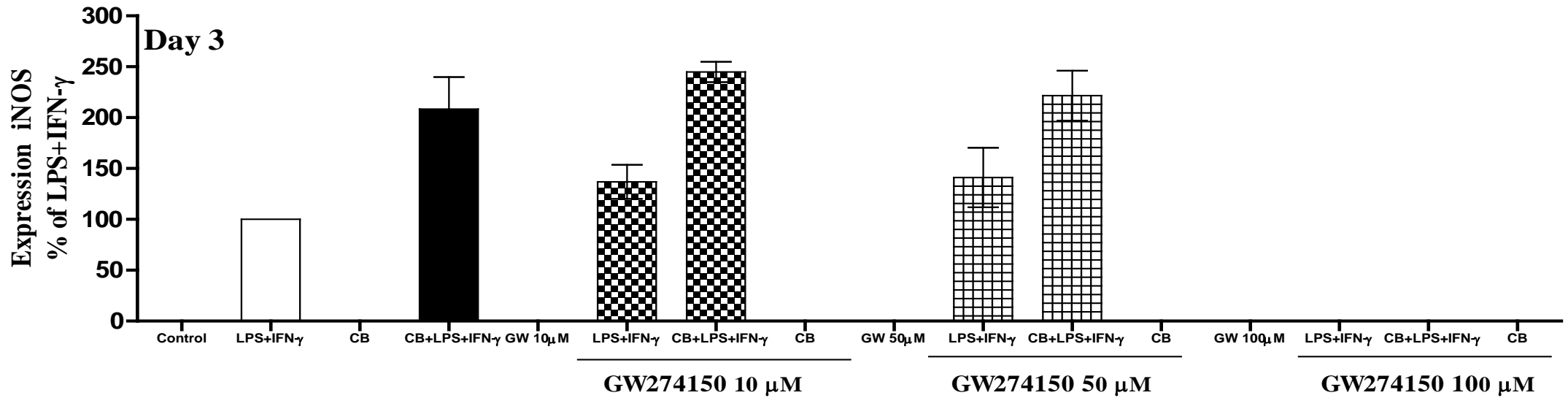
Figure 5.2: Effect of GW274150 on LPS+IFN-γ induced iNOS expression in RASMCs.

Cells were cultured to ~90% confluency and incubated either with culture medium alone (control), LPS (100 μg ml^{-1}) + IFN-γ (100U ml^{-1}) alone or in combination with CB in the presence or absence of GW274150. Expression of iNOS was determined by western blotting as described in methods (Section 2.10). The data represents means ± S.E.M. from 4 individual experiments.
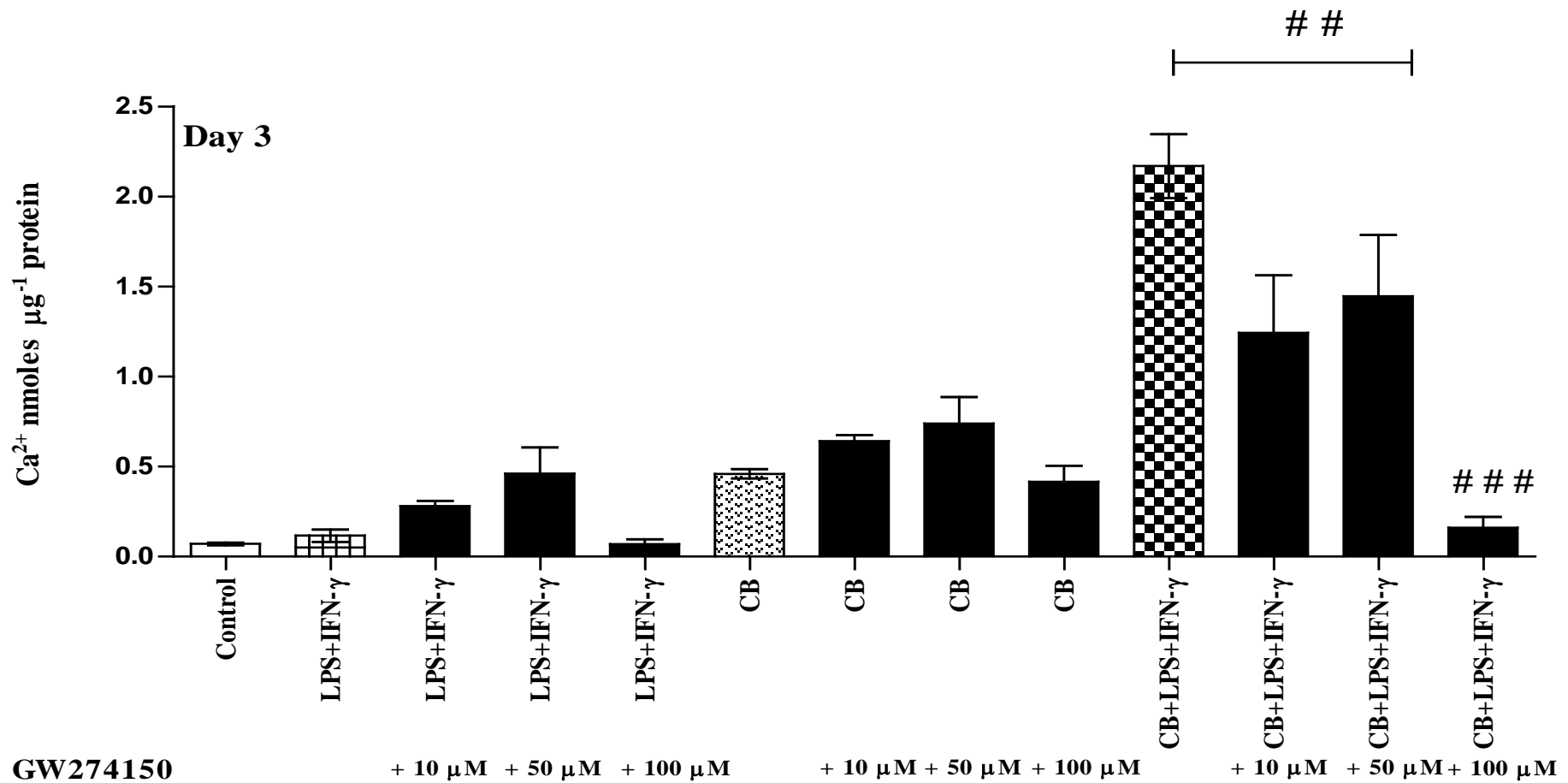
Figure 5.3: Effect of GW274150 on LPS+IFN-γ induced calcification in RASMCs.

Cells were cultured to ~90% confluency and incubated either with culture medium alone (control), LPS (100 μg ml^{-1}) and IFN-γ (100 U ml^{-1}) alone or with CB in the presence or absence of GW274150. Total calcium was quantified as described in methods (section 2.6). The data represents means ± S.E.M. from 4 experiments. ## denote $p<0.01$ compared to the CB+LPS+IFN-γ.

5.3.2- Detection of components of calcification plaque using ARS and FT-IR:

5.3.2.1- Staining of calcific plaques with ARS:

As has been observed previously, control cells and cells activated with LPS and IFN-γ did not show any staining when exposed to ARS. Similarly, cells that were coincubated with GW274150 (10, 50 or 100 µM) were not stained by ARS (Figure 5.4 A, B, and C). In contrast, RASMCs treated with CB alone or with LPS+IFN-γ caused distinct formation of HA crystals which were stained significantly by ARS. The staining was significantly higher in the presence of CB+LPS+IFN-γ (Figure 5.4). When included, GW274150 at 10, 50 or 100 µM Figure 5.4 A, B, and C, respectively completely abolished the staining observed under the conditions above.

A

| Control | LPS+IFN-γ | CB | CB+ LPS+IFN-γ |

GW274150 10 μM

| GW274150 10 μM | LPS+IFN-γ | CB | CB+LPS+IFN-γ |

B

| Control | LPS+IFN-γ | CB | CB+ LPS+IFN-γ |

GW274150 50 μM

| GW274150 50 μM | LPS+IFN-γ | CB | CB+LPS+IFN-γ |
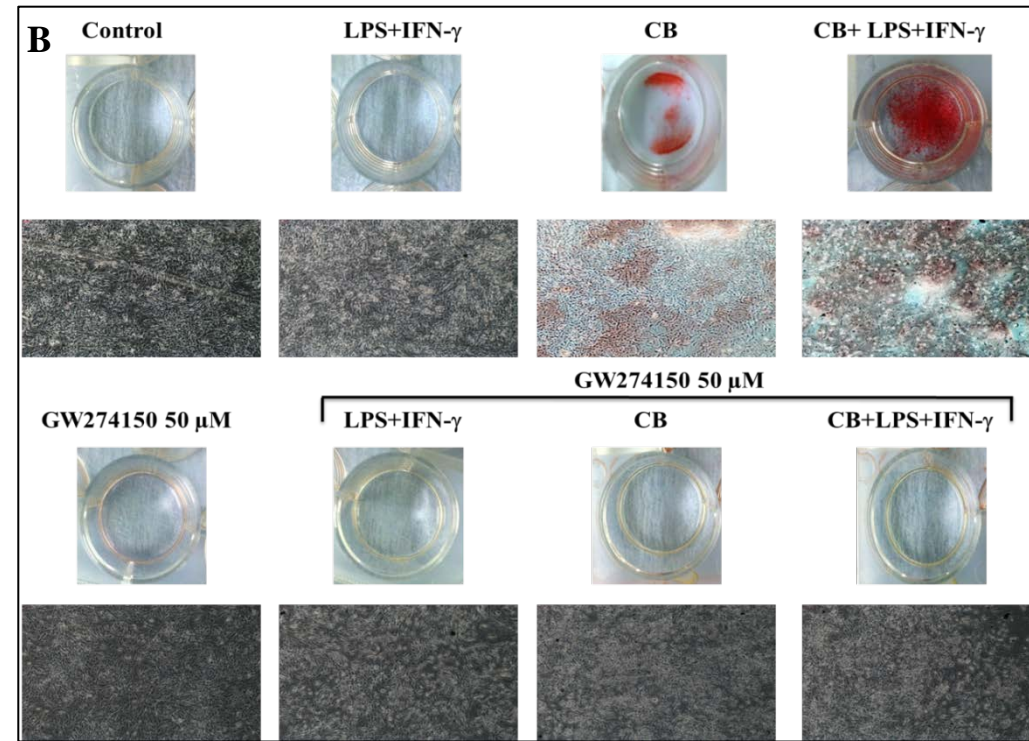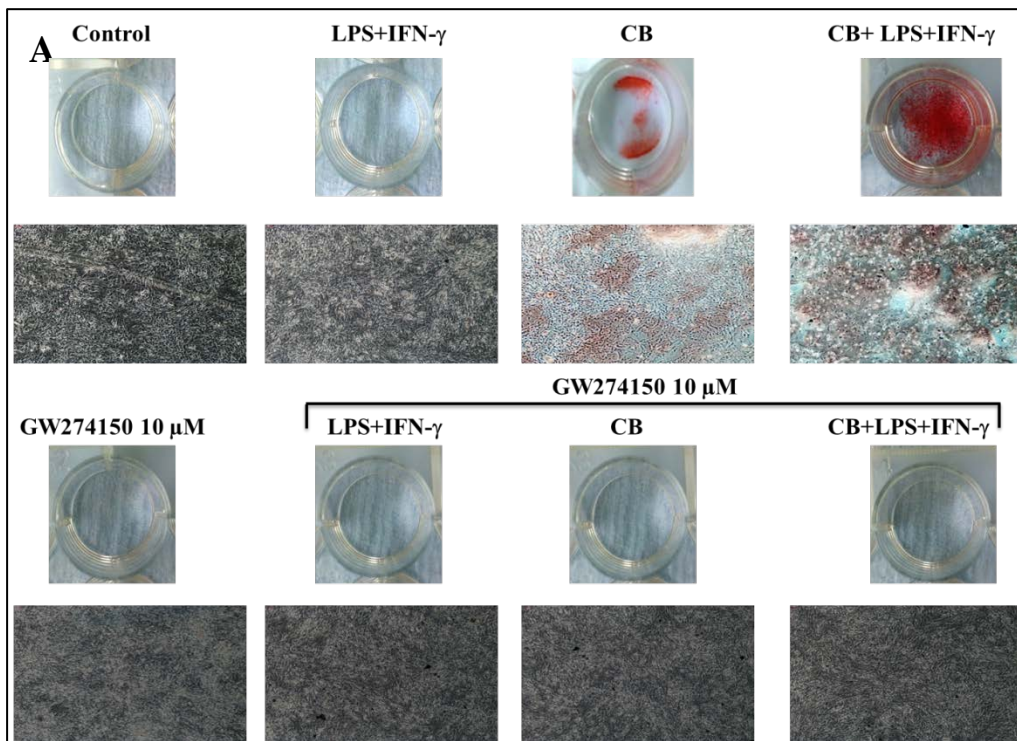
Figure 5.4: Alizarin red staining of calcified RASMCs.

Cells were cultured to ~90% confluency and incubated either with culture medium alone (control), CB, LPS (100µg ml⁻¹) + IFN-γ (100 U ml⁻¹), or in combination with CB in the presence or absences of GW274150 at 10 µM (Panel: A), 50 µM (Panel: B), or 100 µM (Panel: C) for 5 days. Cells were treated with 1x of ARS (1: 10 stock solution) at the end of the treatment period as described in method (Section 2.8). The images are representative of 3 individual experiments which were taken with an inverted Olympus microscope at 10X magnification using GX capture programme.

5.3.2.2 - Detecting HA crystals by FT-IR analysis:

As mentioned in previous chapters, amide spectra (I: 1633, II: 1515, III: 1234 CM^{-1}) were found in all samples analysed from different experimental conditions. Cells coincubated with GW274150 alone at 10 µM (Figure 5.5 A), 50 µM (Figure 5.5B) or 100 µM (Figure 5.5C) did not show any detectable peaks for HA crystals consistent with the lack of staining with ARS reported. In contrast, treatment of cells either with CB or CB+LPS+IFN-γ did result in HA formation. Summary spectra of the different molecules detected are summarised in Tables 5.1 and 5.2, and shown in Figures; Figure 5.5 A, B, C compared to the Figure 5.5 D.

209

CB+GW274150 10μM

Peaks: 1622.60, 1531.83, 1446.66, 1394.51, 1237.00, 1037.14

Absorbance vs cm⁻¹

CB+LPS+IFN-γ+GW274150 10μM

Peaks: 1624.61, 1527.77, 1449.66, 1392.47, 1236.48, 1072.05

Absorbance vs cm⁻¹

210
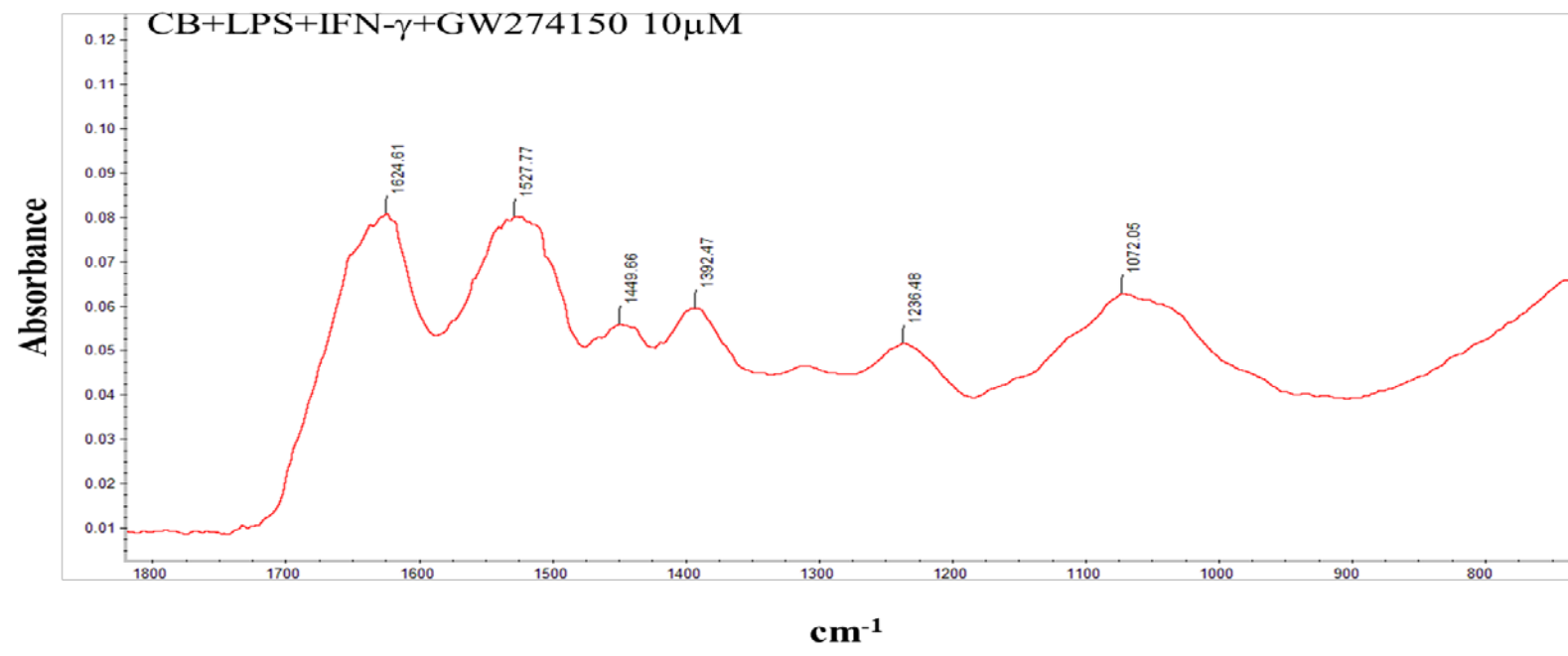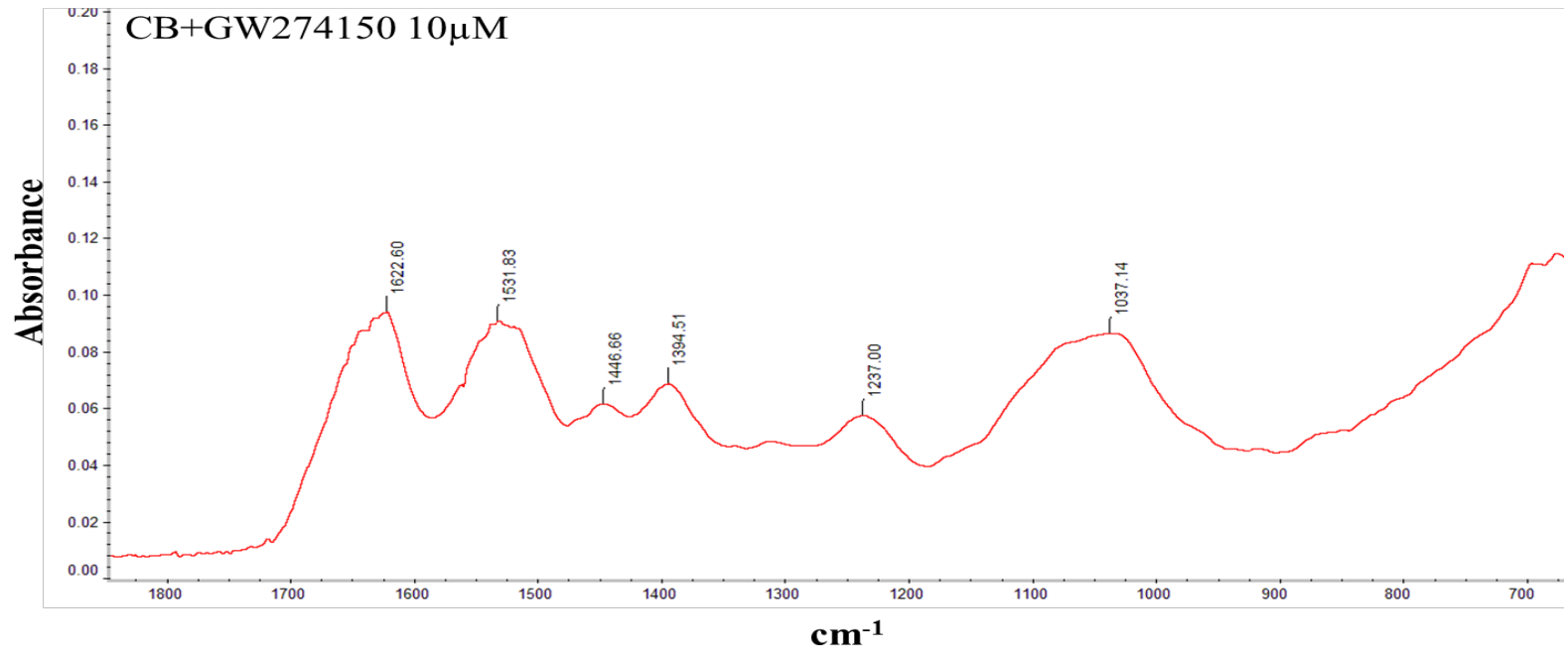
Figure 5.5 A: FT-IR spectrum analysis of activated RASMCs.

Cells were cultured to ~90% confluency and incubated with culture medium alone (control), CB, LPS (100 μg ml^{-1}) + IFN-γ (100 U ml^{-1}), or in combination with CB in the presence of GW274150 at 10 μM for 5 days. Cells were washed and scraped with 100% ethanol at the end of the incubation period and subjected to FT-IR as described in method (section 2.9). The FT-IR spectra are representative of 3 individual experiments.

212

CB+GW274150 50 µM

CB+LPS+IFN-γ+GW274150 50 µM
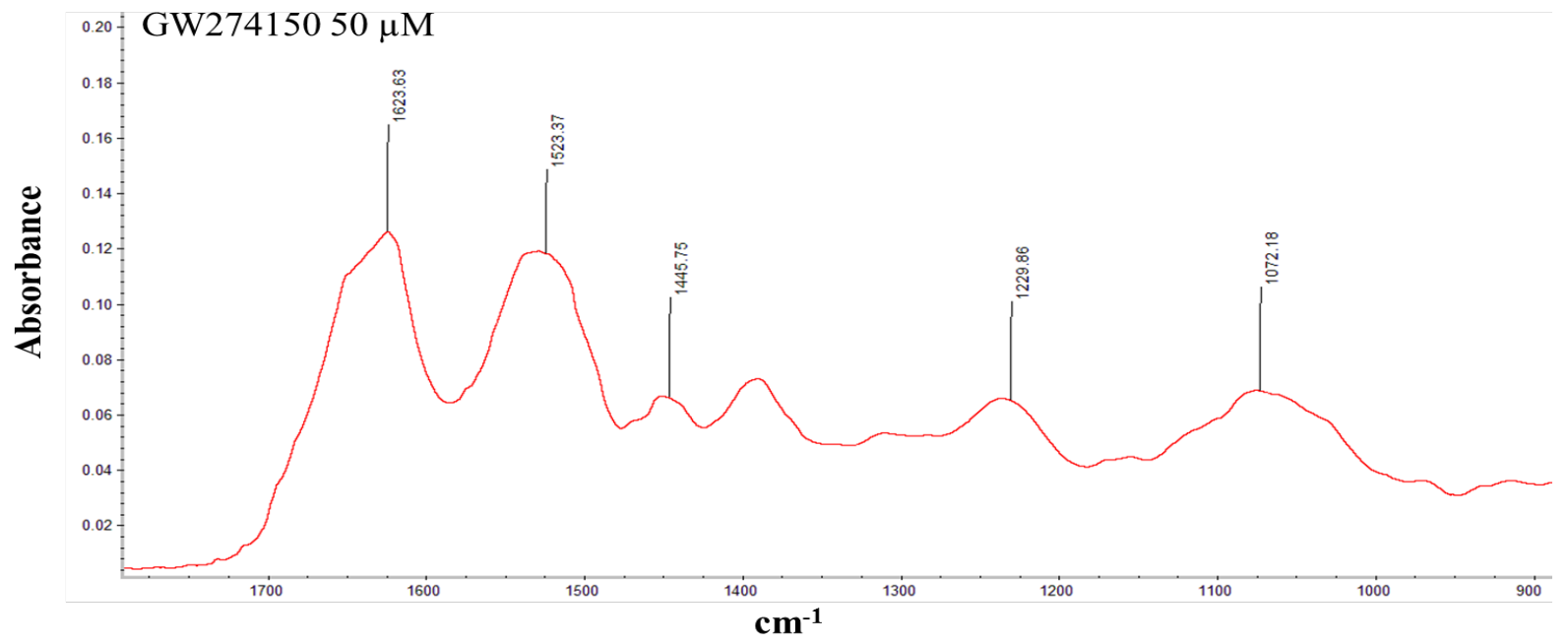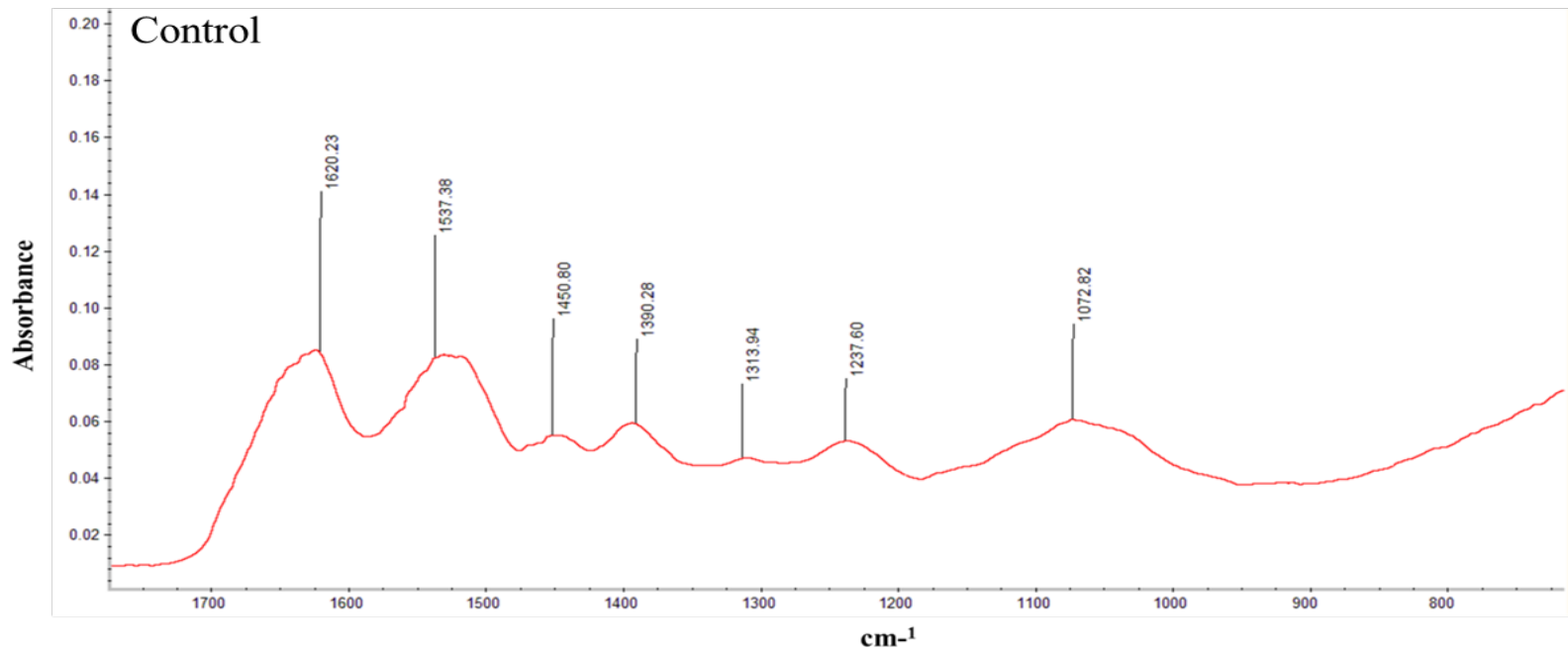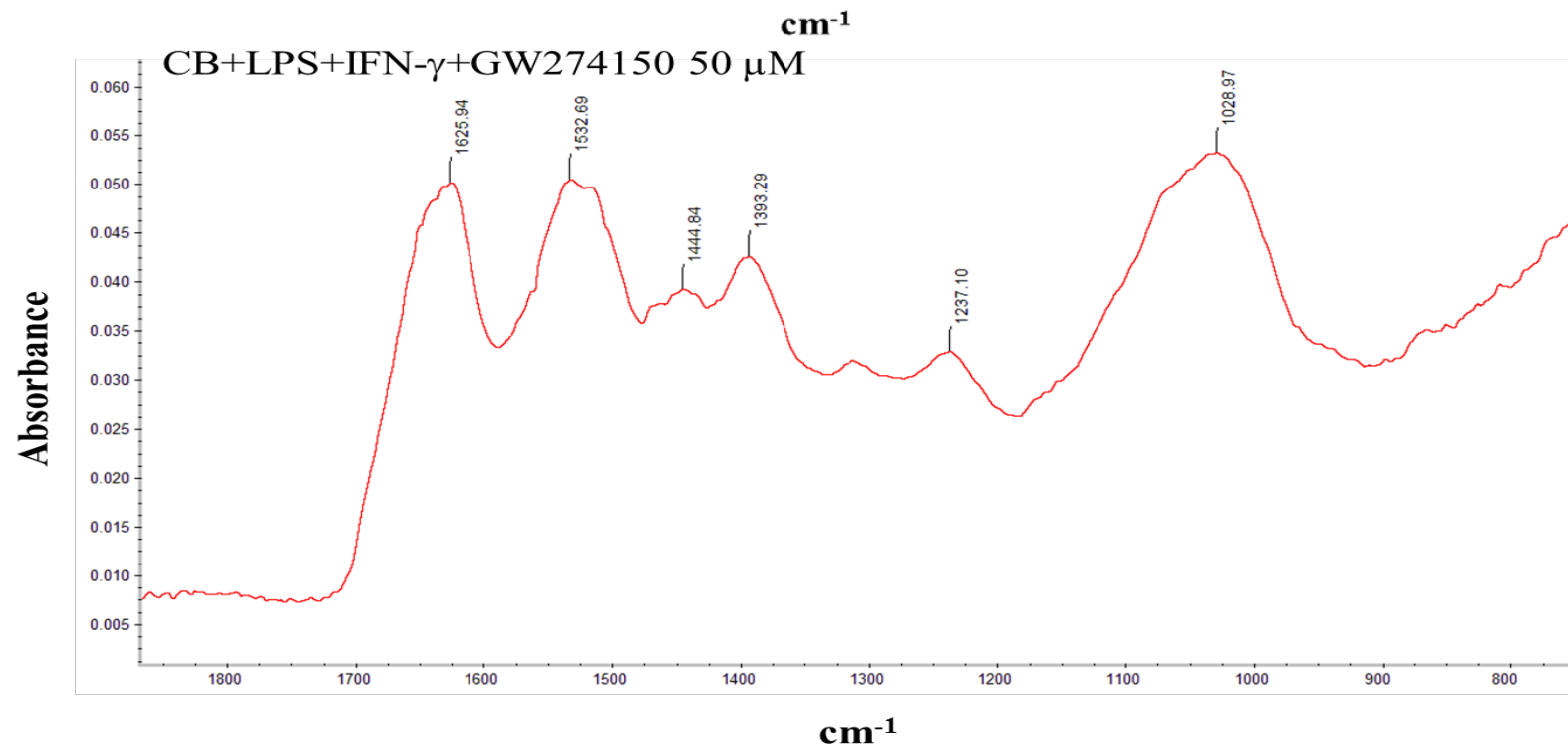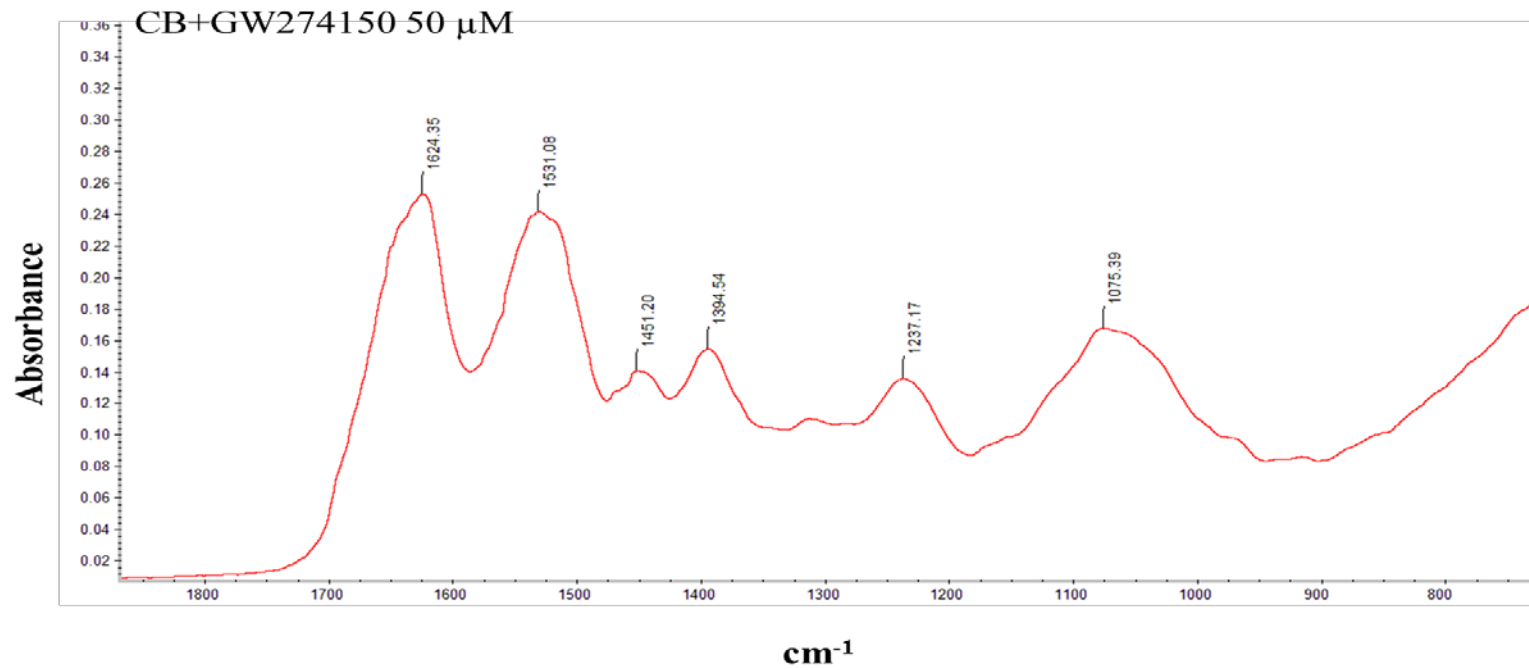
Figure 5.5 B: FT-IR spectrum analysis of activated RASMCs.

Cells were cultured to ~90% confluency and incubated with culture medium alone (control), LPS (100 μg ml^{-1}) + IFN-γ (100 U ml^{-1}), or in combination with CB in the presence of GW274150 at 50 μM for 5 days. Cells were washed and scraped with 100% ethanol at the end of the incubation period and subjected to FT-IR as described in method (section 2.9). The FT-IR spectra are representative of 3 individual experiments.

215
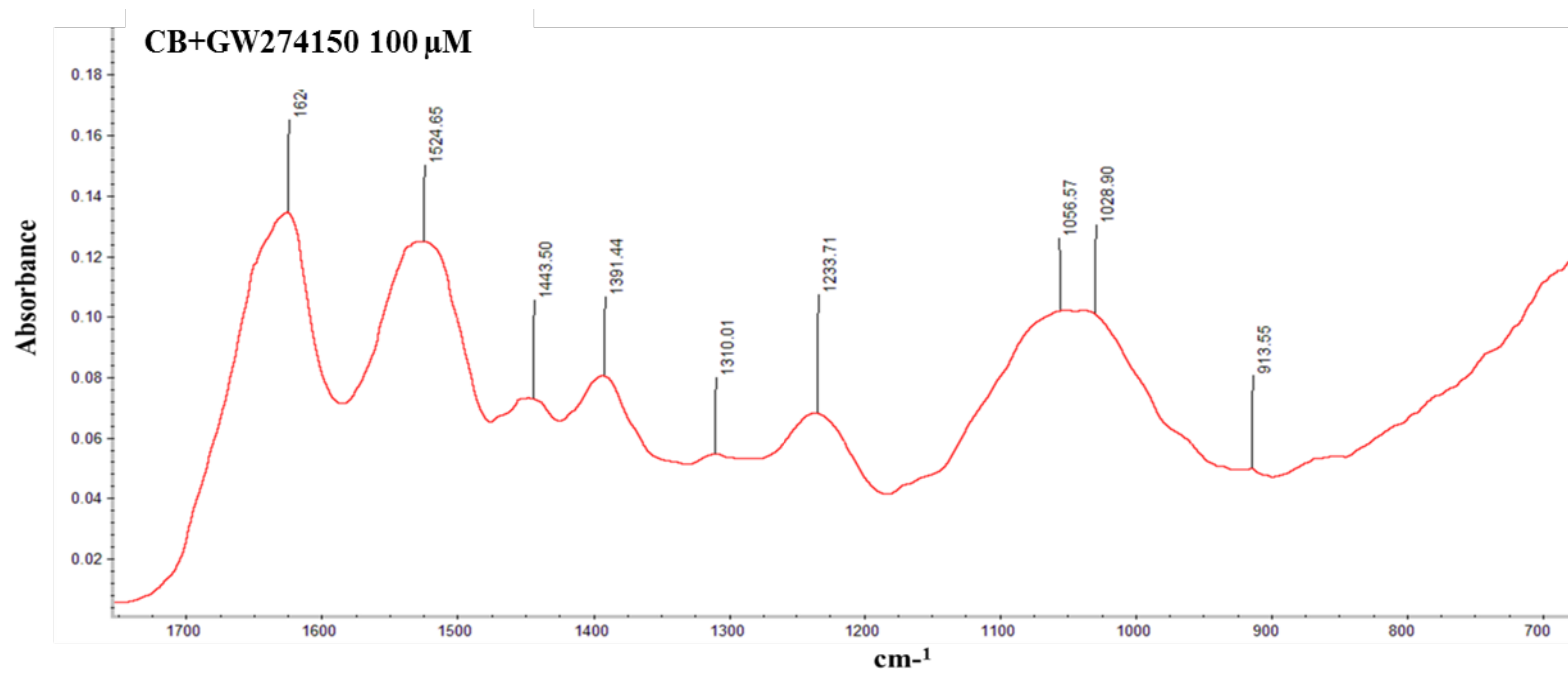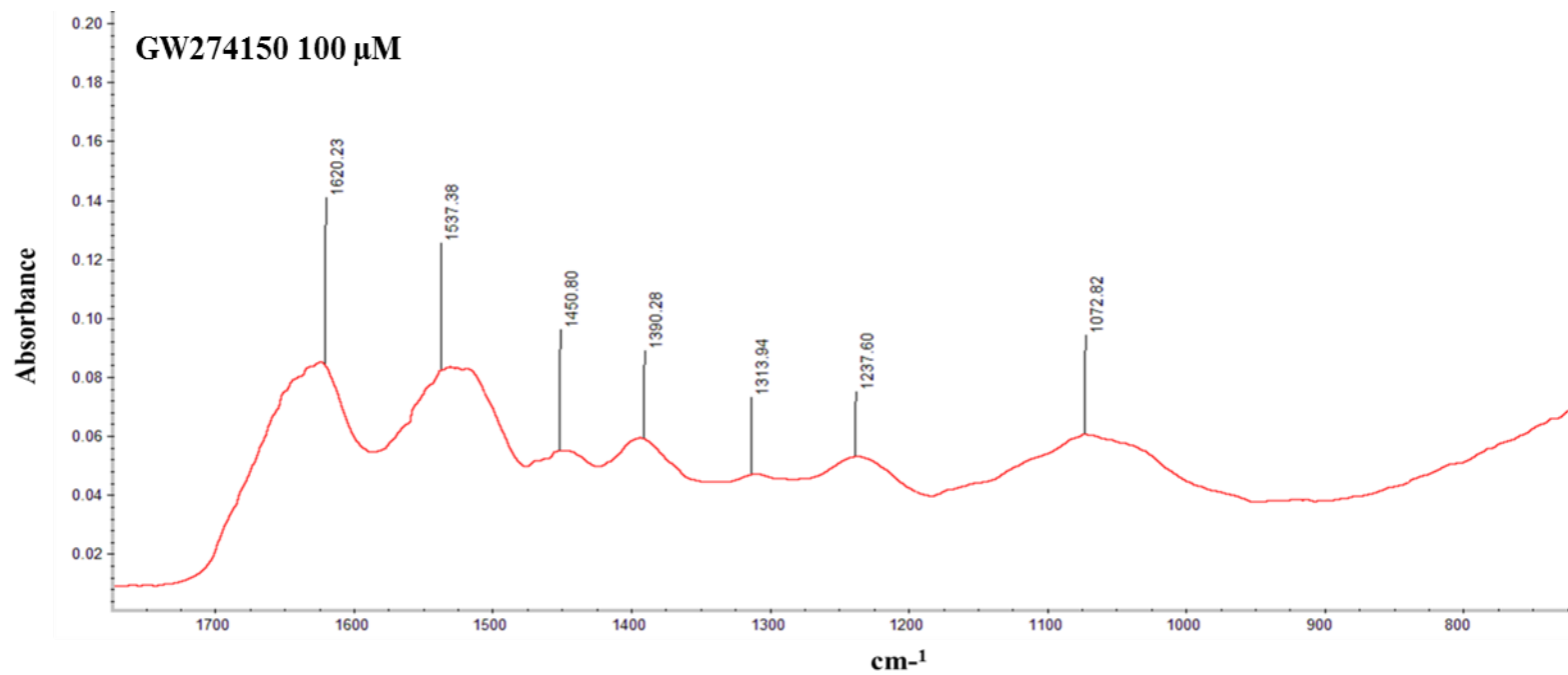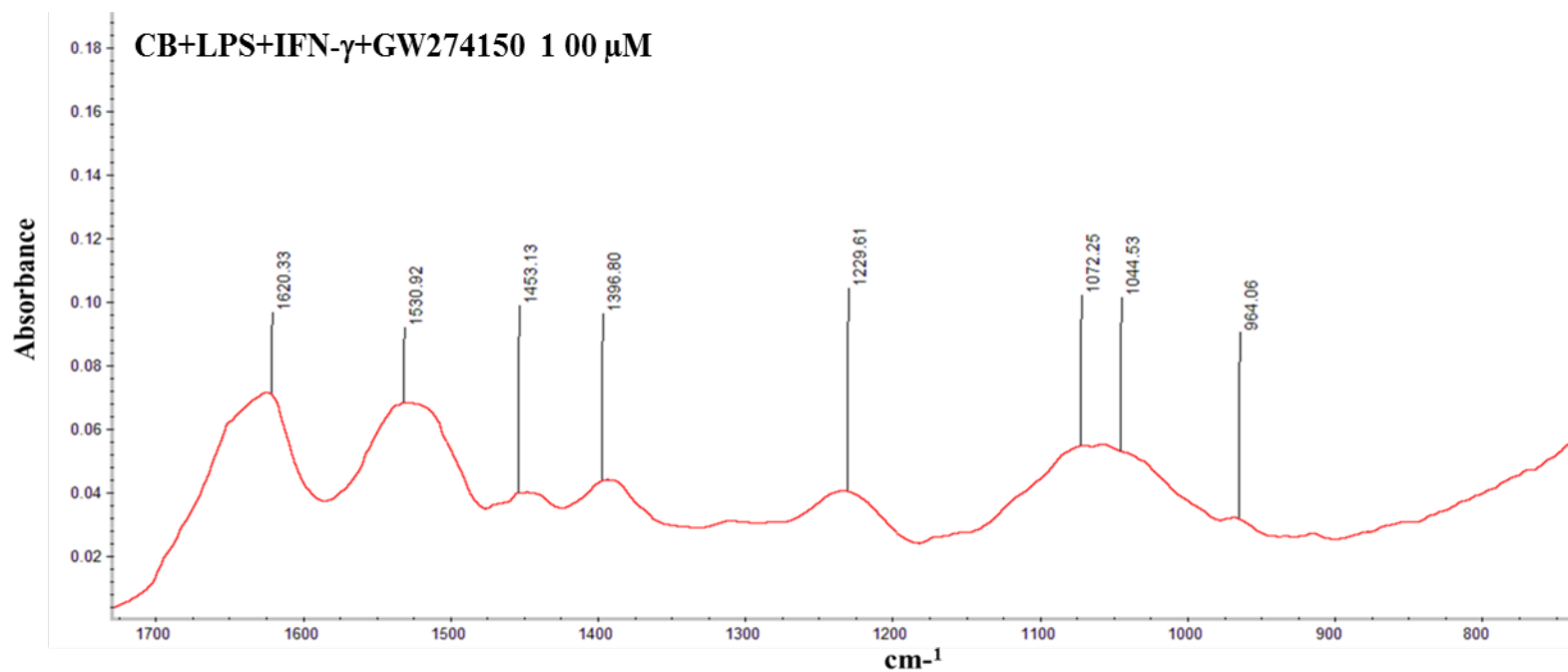
Figure 5.5 C: FT-IR spectrum analysis of activated RASMCs.

Cells were cultured to ~90% confluency and incubated with culture medium alone (control), LPS (100 μg ml^{-1}) + IFN-γ (100 U ml^{-1}), or in combination with CB in the presence of GW274150 at 100 μM for 5 days. Cells were washed and scraped with 100% ethanol at the end of the incubation period and subjected to FT-IR as described in method (section 2.9). The FT-IR spectra are representative of 3 individual experiments.

CB

Hydroxyapatite
crystal

1624.71
1528.71
1450.72
1392.65
1312.53
1236.63
1154.72
1085.32
1075.62
973.14
743.02
693.88

Absorbance

cm-1

LPS+IFN-γ

Phosphate compound PO_4^{-3}

1629.90
1512.61
1441.84
1389.50
1315.83
1237.31
1064.77
1079.31
971.71
804.98
692.53

Absorbance

cm-1

217
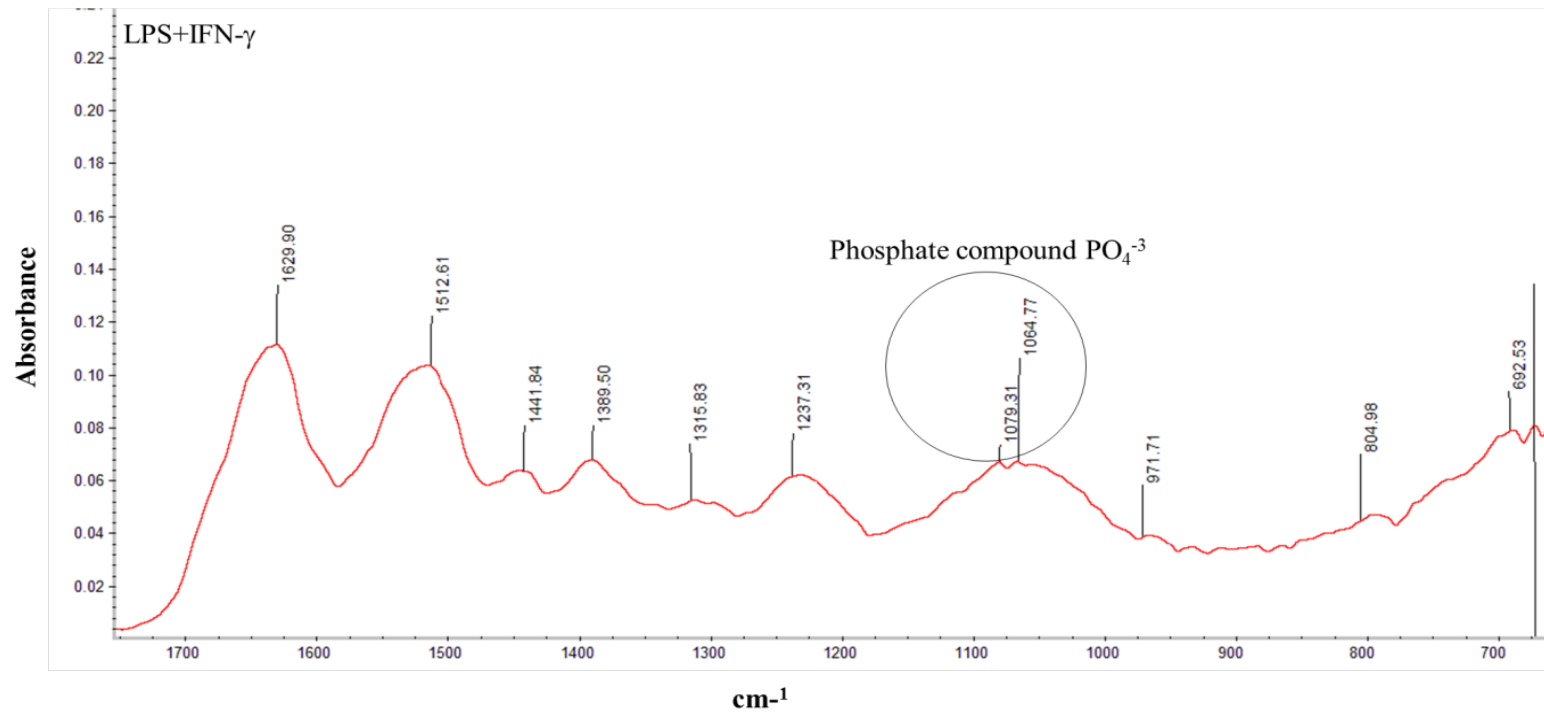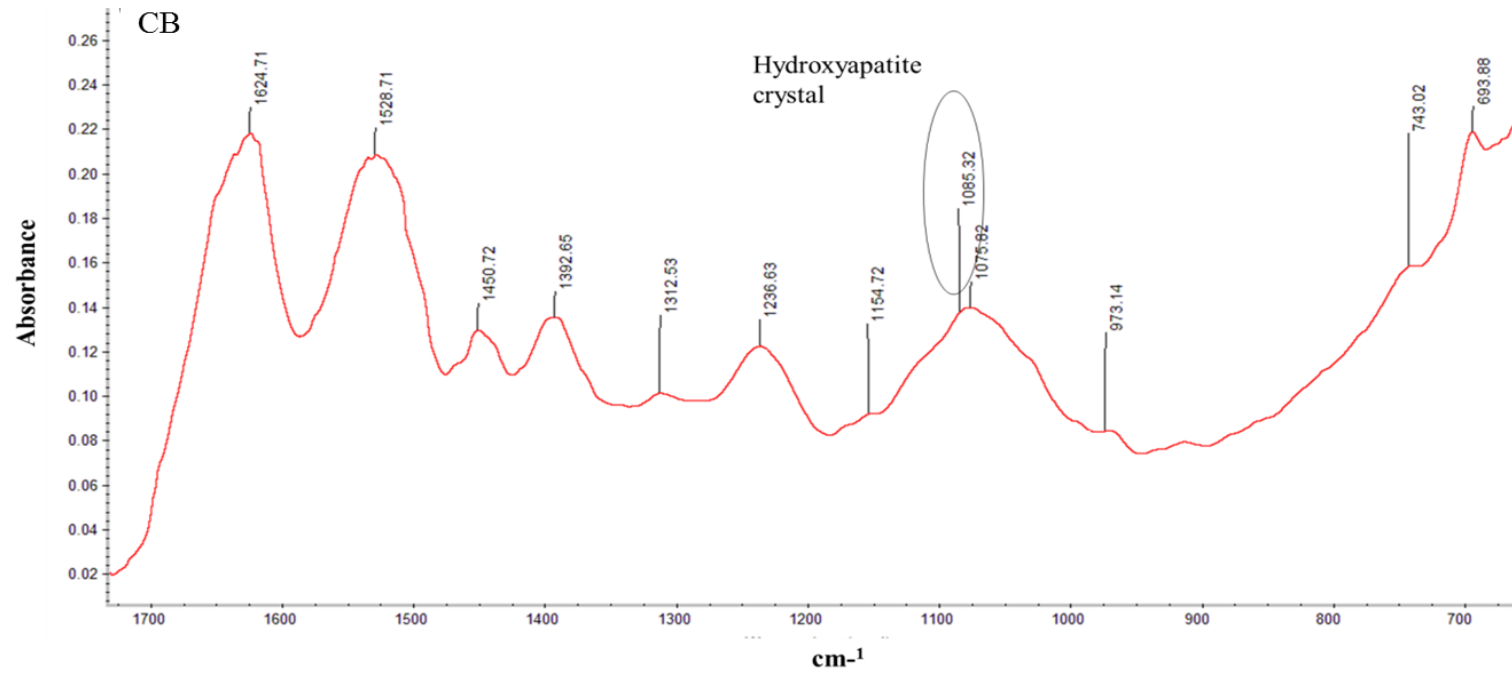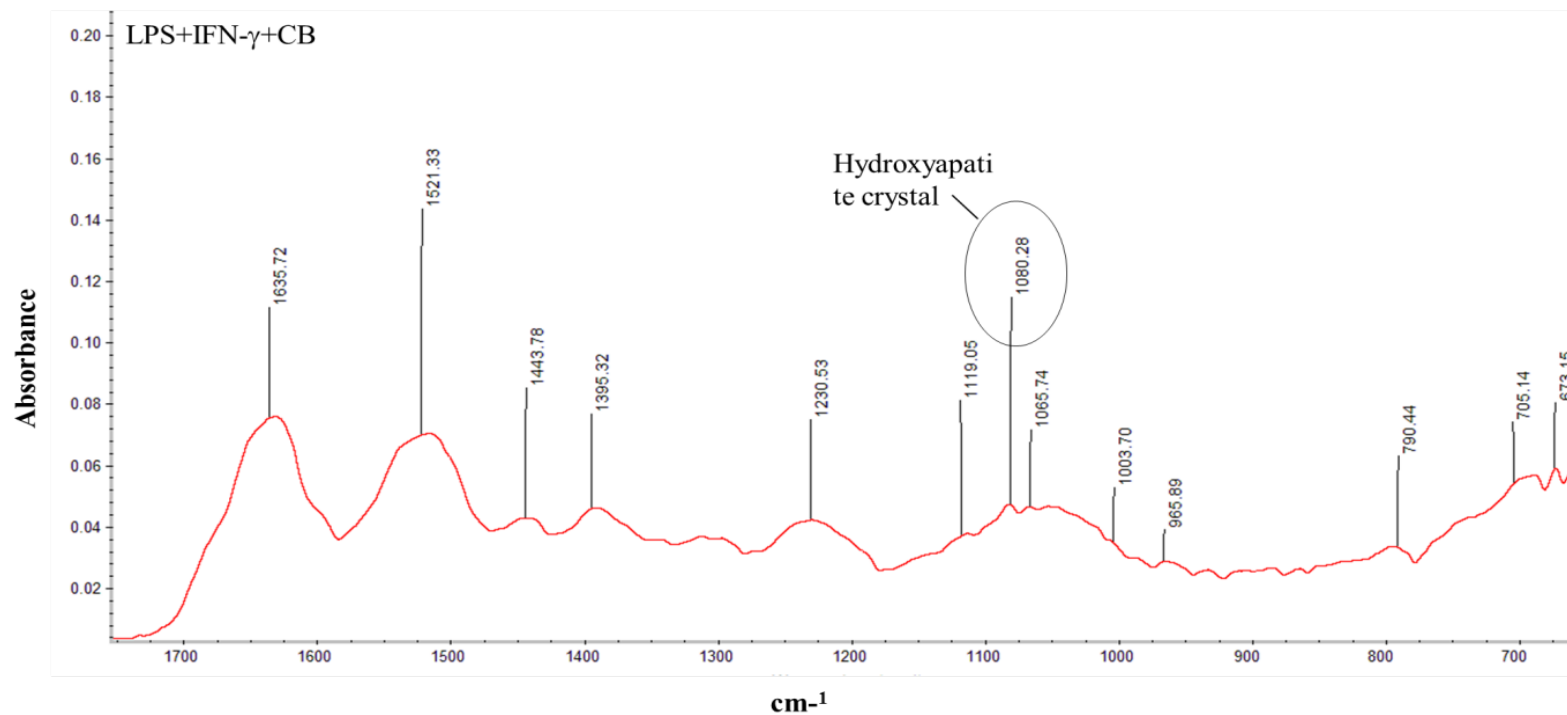
Figure 5.5 D: FT-IR spectrum analysis of activated RASMCs.

Cells were cultured to ~90% confluency and incubated with culture medium alone (control), LPS (100 μg ml^{-1}) + IFN-γ (100 U ml^{-1}), CB, or in combination for 5 days. Cells were washed and scraped with 100% ethanol at the end of the incubation period and subjected to FT-IR as described in method (section 2.9). The FT-IR spectra are representative of 3 individual experiments.

Table 5.1: Spectrum of molecules detected by FT-IR treated RASMCs with GW274150, GW+CB, or GW+LPS+IFN-γ+CB:

Data from Literature review			Data from current studies				
Stretch or bend of chemical compound	wave number (cm^{-1})	Citation	Expected Wave number (cm^{-1})	Control	GW2742150 10, 50 or 100 μM	GW10, 50 or 100 μM +CB	GW10, 50 or 100 μM +LPS+IFN-γ+CB
Amide I-(CON stretch), Amide II (NOH bend), Amide III (COH stretch, NOH bend)	1620-1632, 1515-1540, 1216-1290	(Alò *et al.*, 2009; Dritsa, 2012; Lin *et al.*, 2007)	1620, 1621, 1623, and 1629 (Amide-I), 1512, 1531, 1534, 1537 (Amide-II),1237 and 1240 (Amide-III)	Present	Present	Present	Present
Carbonate and Calcite (-CO$_3^{2-}$)	1430-1480	(Raynaud, *et al.*, 2002)	1441, 1447, 1450, and 1450 -CO$_3^2$-CO$_3^2$	Present	Present	Present	Present
Tricalcium phosphate (TCP), *β*-Tricalcium phosphate (*β*- TCP)	700-750, 690	(Destainville, *et al.*, 2003)	--------------	----------	--------------	----------	--------------
Phosphate (stretch PO$_4^{3-}$)	1154, 1075,1046, 1010 & 1020 or 975	(Destainville, *et al.*, 2003; Han J-K., *et al.*, 2006; Mobasherpour and Heshajin,2007; Raynaud, *et al.*, 2002)	1028, 1064, 1073, 1072, and 1106 -PO$_4^{3--}$	Not present	Not present	Not present	Not present
HA crystal Ca$_{10}$(PO$_4$)$_6$(OH)$_2$	1080 - 1089	(Kwon, *et al.*,2003: Alò *et al.*, 2009)	Ca$_{10}$(PO$_4$)$_6$(OH)$_2$	Not Present	Not Present	Not Present	Not Present
Polysaccharides	Below 690	(Gómez-Ordóñez *et al.*, 2011; Parikh *et al.*, 2006).	Below 690- Polysaccharide	Not Present	Not Present	Not Present	Present

Table 5.2: Spectrum of molecules detected by FT-IR treated RASMCs with LPS+IFN-γ, CB, or in combination:

Data from Literature review			Data from current studies			
Stretch or bend of chemical compound	wave number (cm^{-1})	Citation	Expected Wave number (cm^{-1})	CB	LPS+IFN-γ	LPS+IFN-γ+CB
Amide I-(CON stretch), Amide II (NOH bend), Amide III (COH stretch, NOH bend)	1620-1632, 1515-1540, 1216-1290	(Alò *et al.*, 2009; Dritsa, 2012; Lin *et al.*, 2007)	1620, 1621, 1623, and 1629 (Amide-I), 1512, 1531, 1534, 1537 (Amide-II),1237 and 1240 (Amide-III)	Present	Present	Present
Carbonate and Calcite (-CO_3^{2-})	1430-1480	(Raynaud, *et al.*, 2002)	1441, 1447, 1450, and 1450 -CO_3^2-CO_3^2	Present	Present	Present
Tricalcium phosphate (TCP), β-Tricalcium phosphate (β- TCP)	700-750, 690	(Destainville, *et al.*, 2003)	---------------	Present	----------------	Present
Phosphate (stretch PO_4^{3-})	1154, 1075,1046, 1010 & 1020 or 975	(Destainville, *et al.*, 2003; Han J-K., *et al.*, 2006; Mobasherpour and Heshajin,2007; Raynaud, *et al.*, 2002)	1028, 1064, 1073, 1072, and 1106 -$PO_4^{3- -}$	Present	Present	Present
HA crystal Ca $_{10}$(PO$_4$)$_6$(OH)$_2$	1080 - 1089	(Kwon, *et al.*,2003: Alò *et al.*, 2009)	1080 or Ca $_{10}$(PO$_4$)$_6$(OH)$_2$	Present	Not present	Present
Polysaccharides	Below 690	(Gómez-Ordóñez *et al.*, 2011; Parikh *et al.*, 2006).	Below 690- Polysaccharide	Not present	Present	Present

5.3.3-Effects of diethylenetriamine/nitric oxide adduct (NOC 18) on calcification of RASMCs.

To determine whether NOC 18 was able to regulate calcification of RASMCs, experiments were conducted where cells were pretreated with the compound either alone or for one hour prior to the addition of CB. In parallel studies, NOC 18 and CB were added together to see whether availability of calcifying agents in the presence of immediate NO release had any effects on calcification that were different to those seen when cells were pre-exposed to NO before inducing calcification.

In these studies, RASMCs coincubated with different concentrations of NOC 18 resulted in a dose and time dependent release of NO production with 10 µM, 30 µM and 50 µM resulting in approximately 0.06 ± 0.02 nmole µg $^{-1}$ protein, 0.16 ± 0.09 nmole µg $^{-1}$ protein and 0.26 ± 0.07 nmole µg $^{-1}$ protein of NO being detected respectively 24 hours after exposure to cells. These concentrations increased to 0.10 ± 0.05, 0.19 ± 0.06, and 0.31 ± 0.08 nmole µg $^{-1}$ protein at day 7, respectively (Figure 5.6 B). Levels of NO detected in controls in the absence of NOC 18 was 0.002 nmole µg $^{-1}$ protein on day 7 (Figure 5.6 B). These levels of NO were not significantly altered in the presence of CB either when added together with or 1 hour after NOC 18 (Figure 5.6 $A_{1, 2, 3}$). A summary of the trends described are shown in Figure 5.6 B.

Analysis of calcification of cells in the presence of NOC 18 alone (10, 30, and 50 µM) showed a degree of elevation of calcium levels which was more pronounced when compared to controls at days 1 and 3, but the changes at days 5 and 7 although above controls did not appear to be statistically different (Figure 5.7 B). Moreover, the responses to NOC 18 were not concentration dependent in that changes in calcium occurred to approximately the same levels irrespective of the concentration used (Figure 5.7 $A_{1,2,3}$). As already demonstrated previously, CB alone (0.7 ± 0.1 nmole µg $^{-1}$ protein) induced calcification of RASMCs but of

more importance is the observation that when added to cells 1 hour after NOC 18 pretreatment, induced significantly greater calcification of RASMCs [(0.9 ±0.08 nmole μg^{-1} protein; 10µM, 1.2 ± 0.22 nmole μg^{-1} protein;30 µM, 1.3 ± 0.17 nmole μg^{-1} protein;50 µM)]. The enhancements appear greater in cells pretreated with NOC 18 and particularly at the earlier time periods (1 and 3 days). Once again the changes were not dependent on the concentrations of NOC 18 used and these trends are more clearly demonstrated in the summary graph shown in Figure 5.7 B.
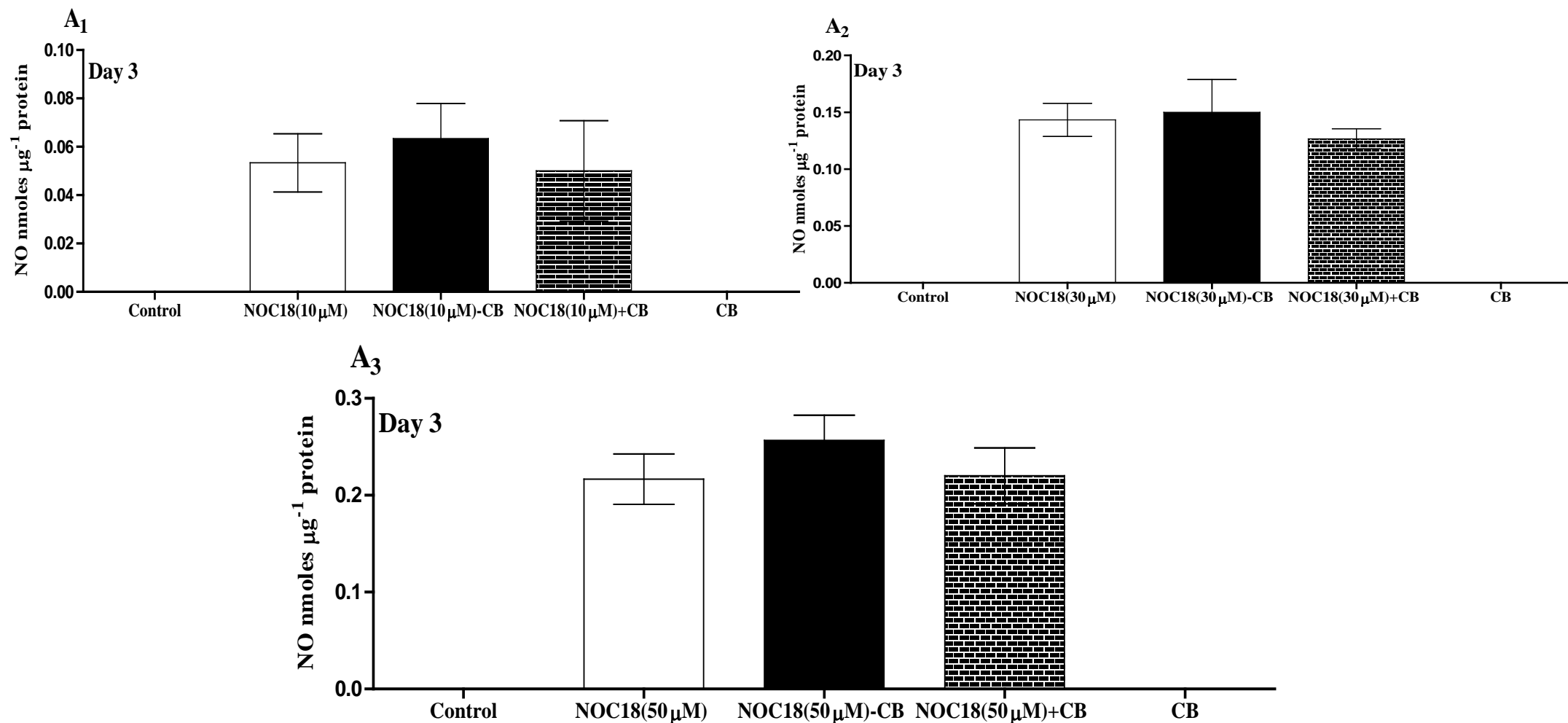
Figure 5.6 A: Effects generation of NO from NOC 18 in RASMCs.

Cells were cultured to ~90% confluency and incubated either with culture medium alone (control) or treated with NOC 18 at different concentrations in the presence or absence of CB (7mM $CaCl_2$, 7mM β-GP). NOC 18-CB represents data from cells pretreated with the NO donor for 1 hour before adding CB, and NOC 18+CB represents coincubation of both for 3 days. Total NO was quantified by the Griess assay as described in methods (section 2.3). The data represents means $\pm$ S.E.M. from 3 experiments.
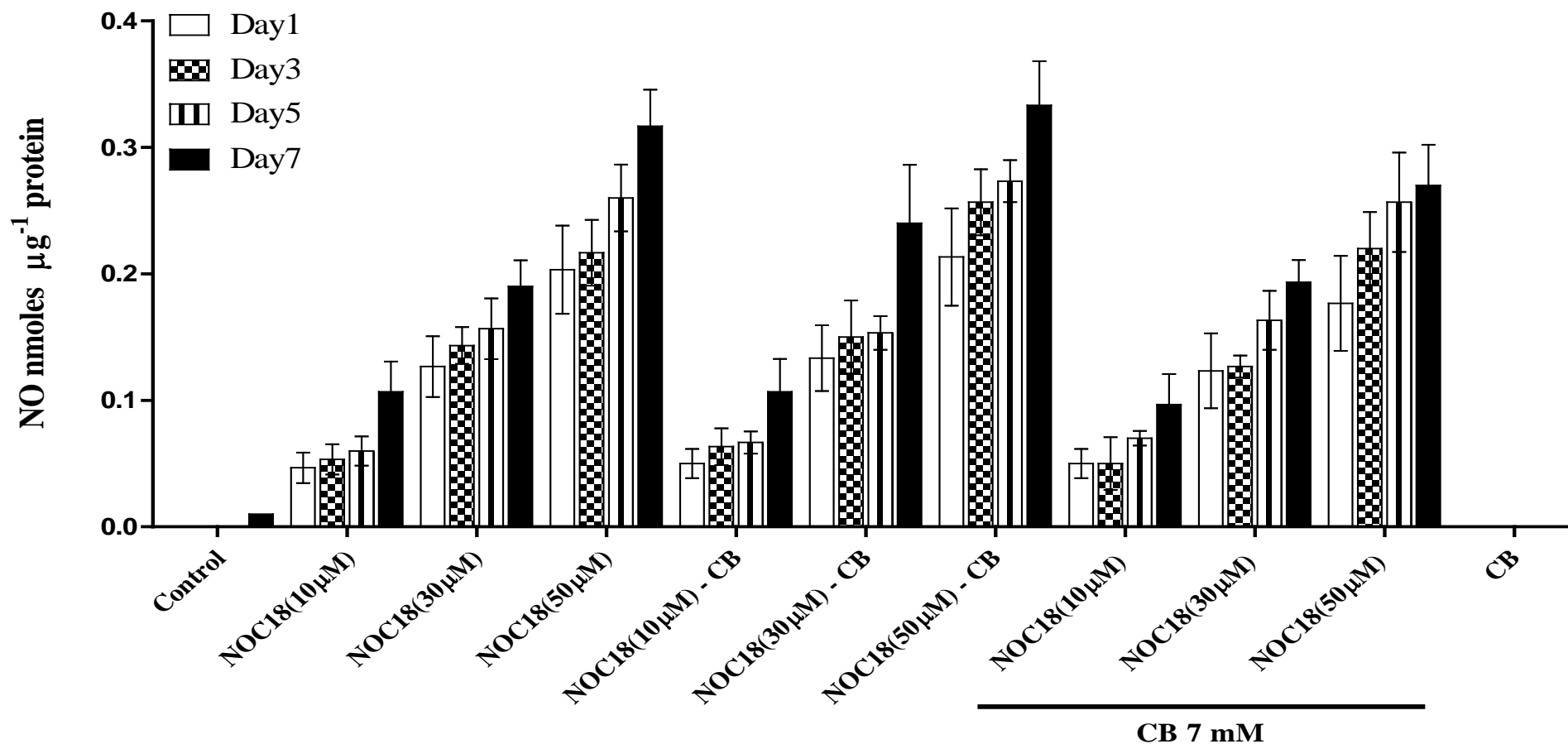
Figure 5.6 B: Summary data of the time dependent generation of NO from NOC 18 in RASMCs.

Cells cultured to ~90% confluency were incubated either with culture medium alone (control) or treated with NOC 18 at different concentrations in the presence or absence of CB (7mM CaCl$_2$, 7mM β-GP). NOC 18-CB represents data from cells pretreated with the NO donor for 1 hour before adding CB, and NOC 18+CB represents coincubation of both for 1, 3, 5, and 7 days. Total NO was quantified by the Griess assay as described in methods (section 2.3). The data represents means ± S.E.M. from 3 experiments.
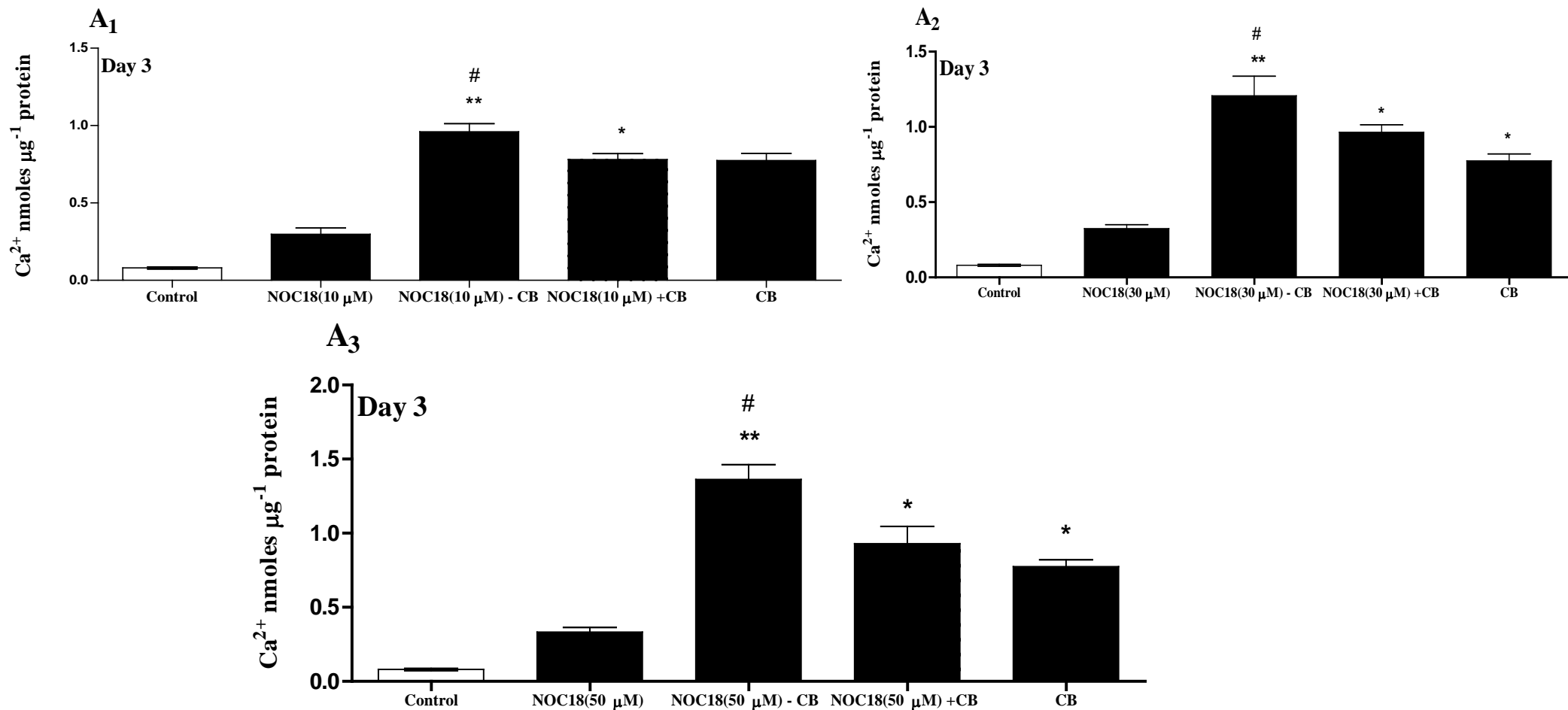
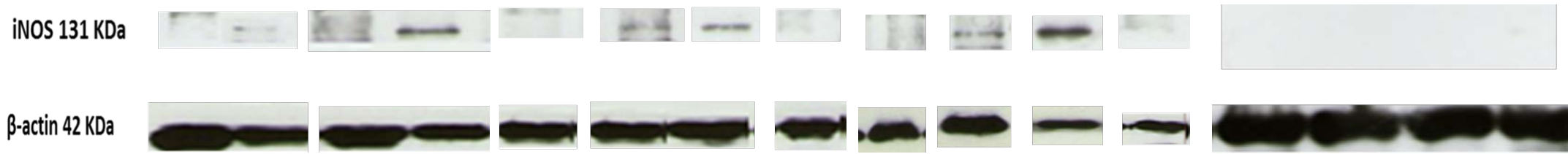**Figure 5.7 A: Effect of NOC 18 on calcification of RASMCs.**

Cells were cultured to ~90% confluency and incubated either with culture medium alone (control) or treated with NOC 18 at different concentrations in the presence or absence of CB (7mM $CaCl_2$, 7mM β-GP). NOC 18-CB represents data from cells pretreated with the NO donor for 1 hour before adding CB, and NOC 18+CB represents coincubation of both for 3 days. Total calcium was quantified as described in methods (section 2.6). The data represents means ± S.E.M. from 3 experiments. * denotes $p < 0.05$ and ** denotes $p < 0.01$ compared to control cells while # denotes $p < 0.05$ compared to CB alone.

225
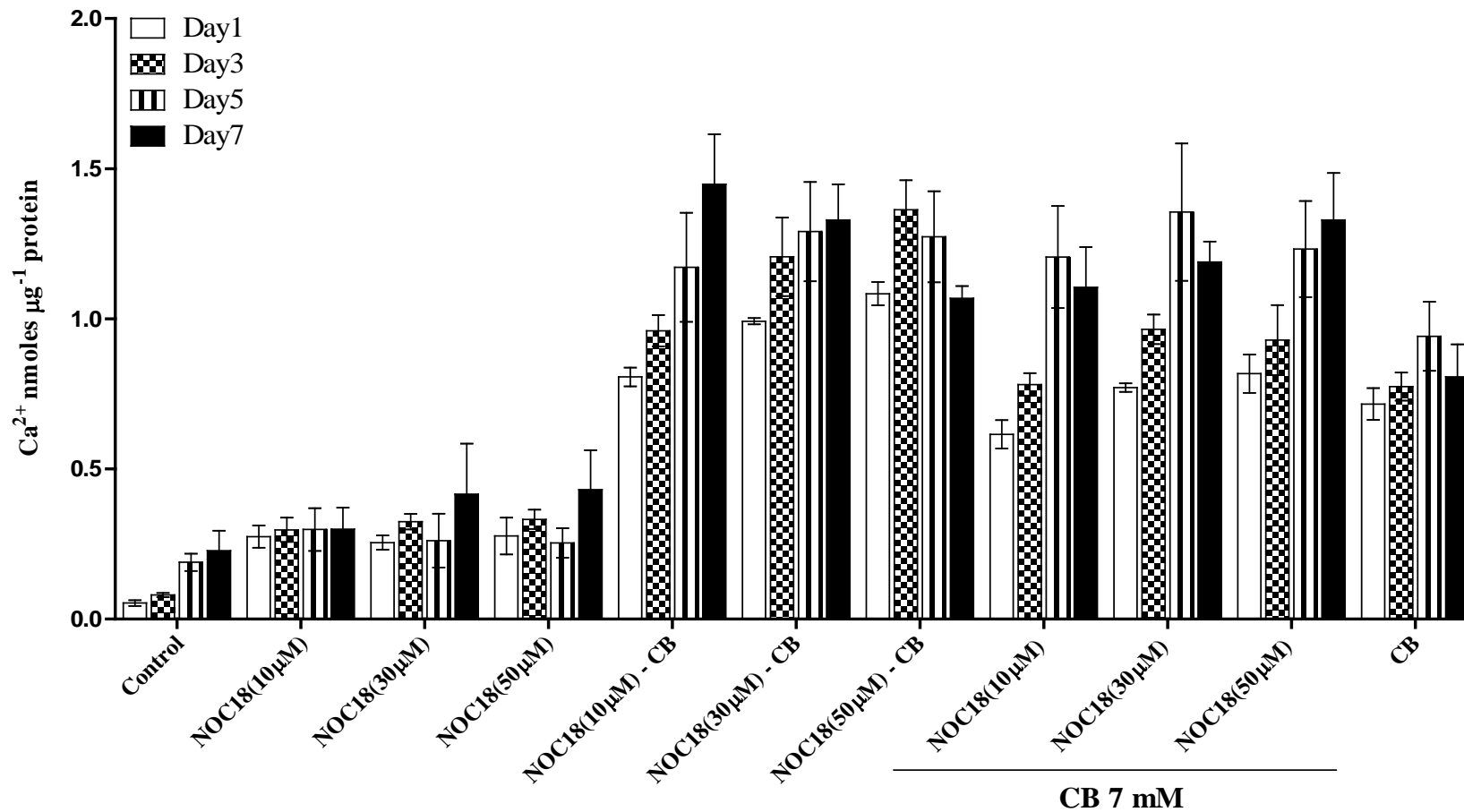
Figure 5.7 B: Summary data of the effects of NOC 18 on calcification of RASMCs.

Cells were cultured to ~90% confluency and incubated either with culture medium alone (control) or treated with NOC 18 at different concentrations in the presence or absence of CB (7mM $CaCl_2$, 7mM β-GP). NOC 18-CB represents data from cells pretreated with the NO donor for 1 hour before adding CB, and NOC 18+CB represents coincubation of both for 1, 3, 5, and 7 days. Total calcium was quantified as described in methods (section 2.6). The data represents means ± S.E.M. from 3 experiments.

5.3.4- Staining of calcific plaques with ARS:

As shown in Figure 5.8, plaques representative of calcification were not detectable in cells incubated with medium alone; NOC18 at 10, 30 and 50 μM alone; NOC 18 10, 30 and 50 μM +CB. Plaques were only detected in cells pretreated with 30 and 50 μM NOC 18 prior to CB. Coincubation of NOC 18 and CB at the same time failed to show any staining suggesting perhaps the absence of calcification. This however contrasts with the data above showing that NOC 18 plus CB caused significant increases in calcium irrespective of whether the NO donor was preincubated or added together with CB. With preincubation of NOC18 the mineralisation of HA occurred in the cells when CB was added. However, the alternate protocol whereby NOC18 and CB were added together did not appear to promote mineralisation.
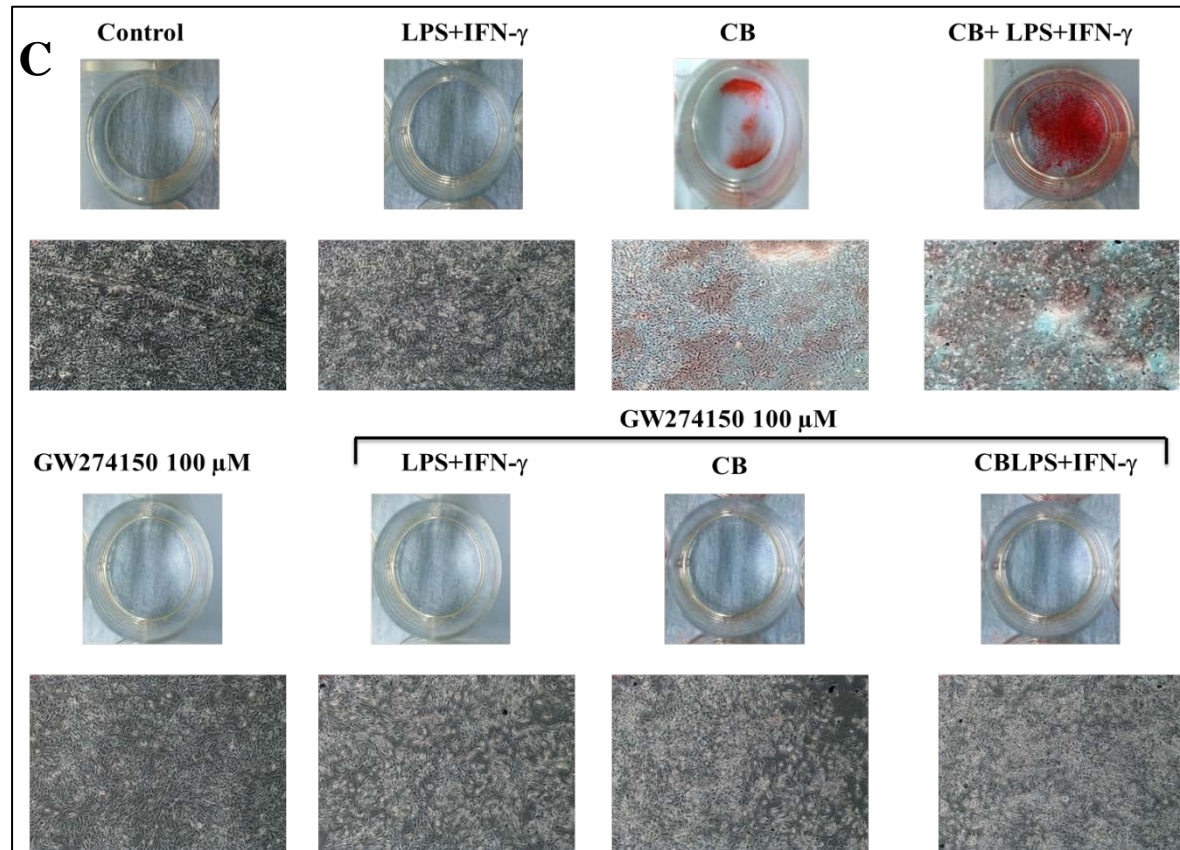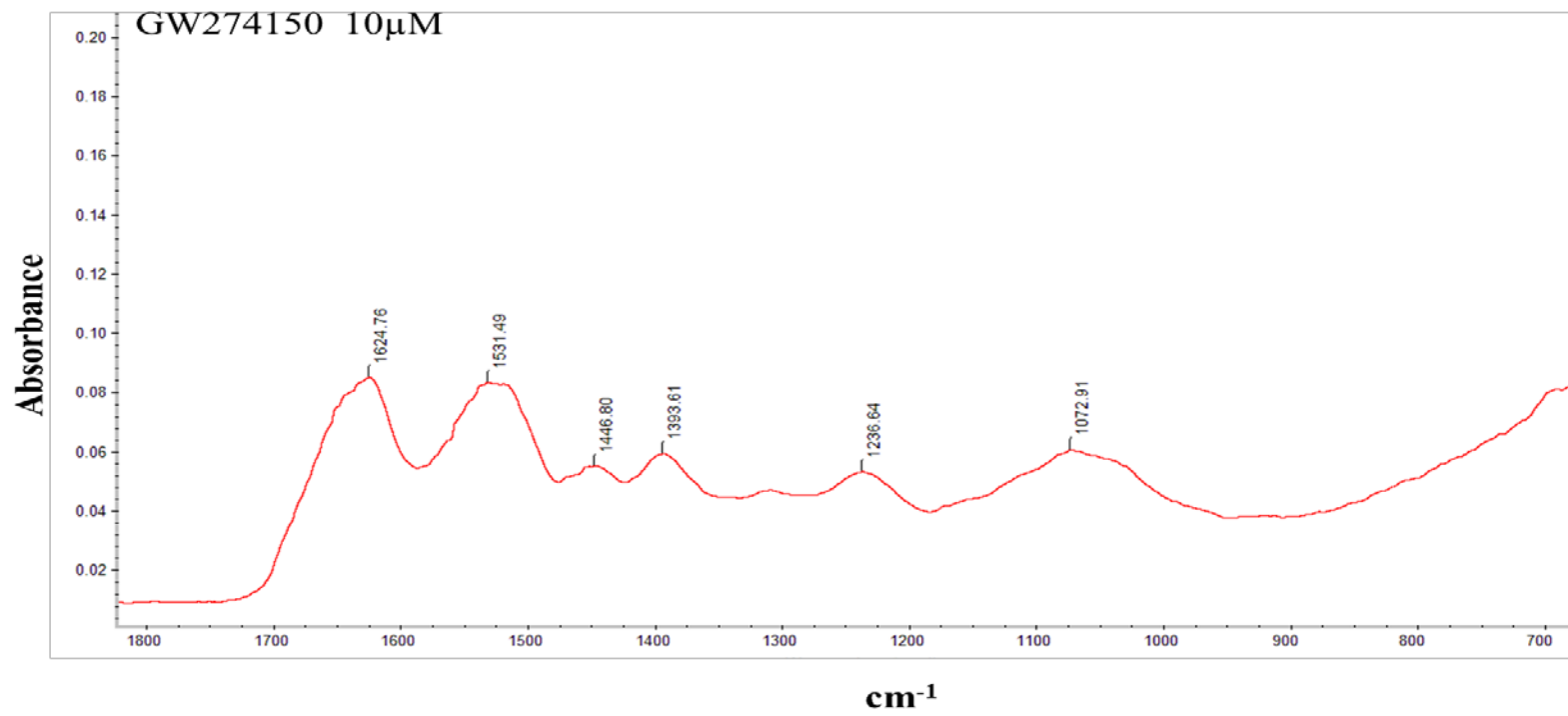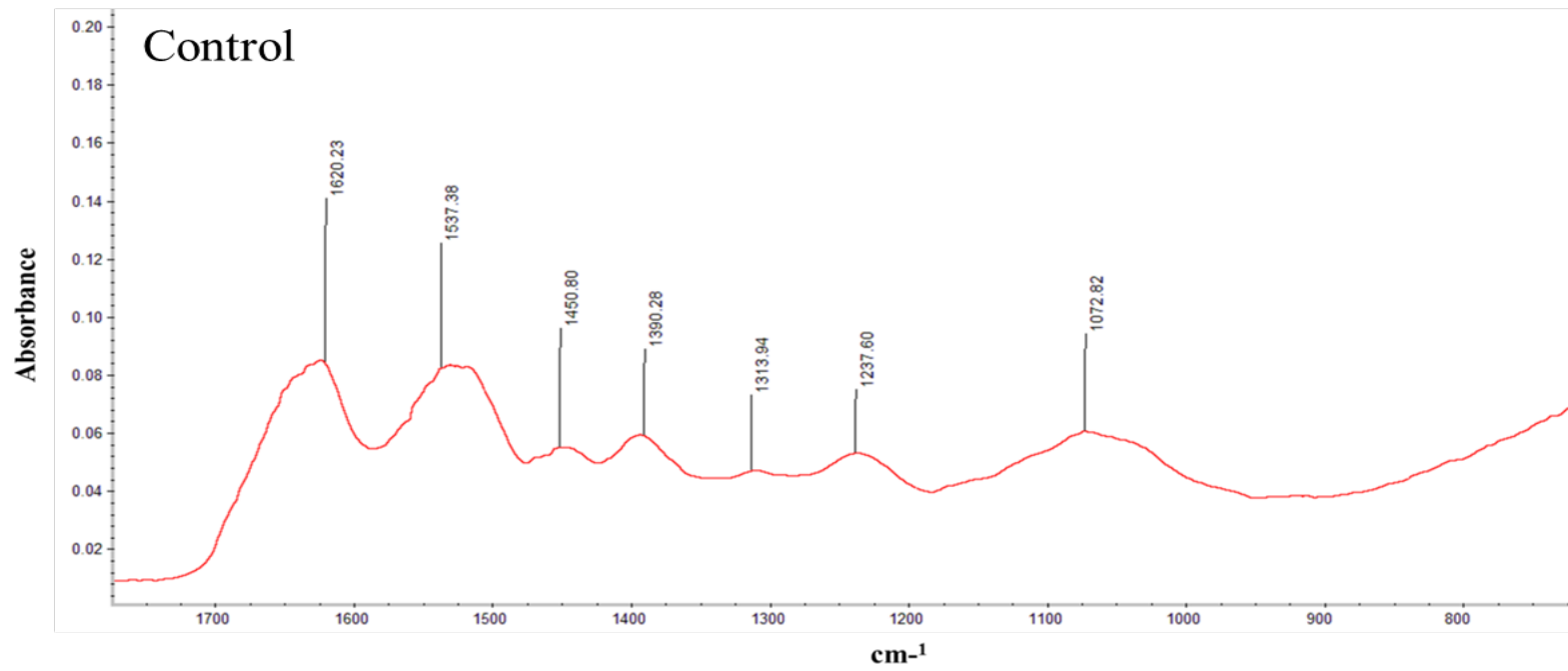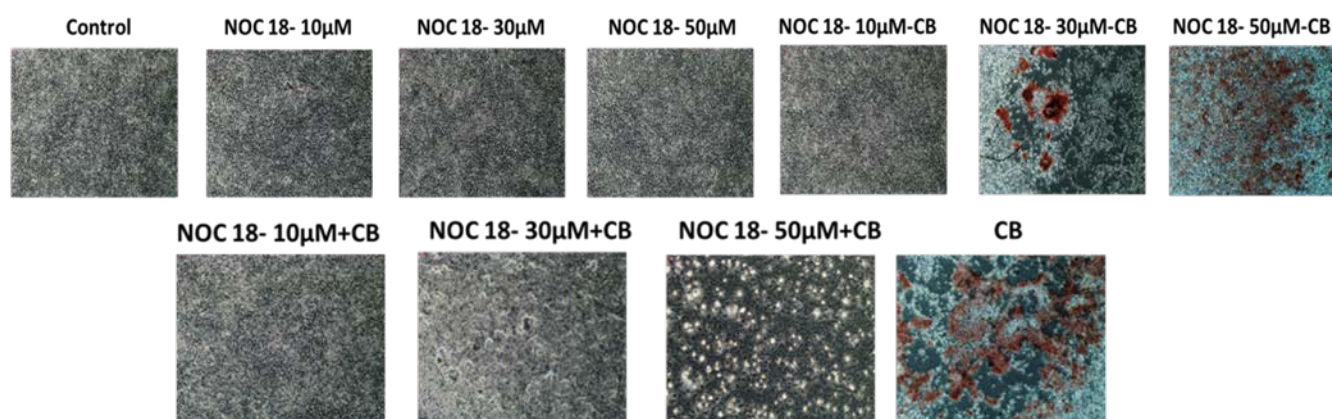

Figure 5.8: Alizarin red staining of calcified RASMCs.

Cells were cultured to ~90% confluency and incubated either with culture medium alone (control), CB. NOC 18-CB represents data from cells pretreated with the NO donor for 1 hour before adding CB, and NOC 18+CB represents coincubation of both for 5 days. Cells were treated with 1x of ARS (1: 10 stock solution) at the end of the treatment period as described in method (Section 2.8). The images are representative of 3 individual experiments which were taken with an inverted Olympus microscope at 10X magnification using GX capture programme.

5.3.5- Effects of Sodium nitroprusside (SNP) on calcification of RASMCs.

As with NOC 18, addition of SNP at concentrations of 10, 30 and 50 μM resulted in a concentration and time dependent increase in NO detected in the culture medium as nitrite (Figure 5.9 B). Addition of CB 1hour after SNP or in combination with did not cause any significant changes in NO production as seen in (Figure 5.9A$_{1, 2\ \&3}$). In the experiments carried out to detect changes in calcification, there were significant increases in calcium when cells were coincubated with different concentrations of SNP compared to control cells but the response did not show any concentration dependency. (Figure 5.10 A$_{1, 2\ \&3}$) at day3.

The addition of CB either an hour after or together with SNP marginally enhanced the calcium levels seen with CB alone but significantly enhanced that caused by SNP alone compared to the control, not to CB alone. The summary data of the trends observed is shown inFigure5.10B.
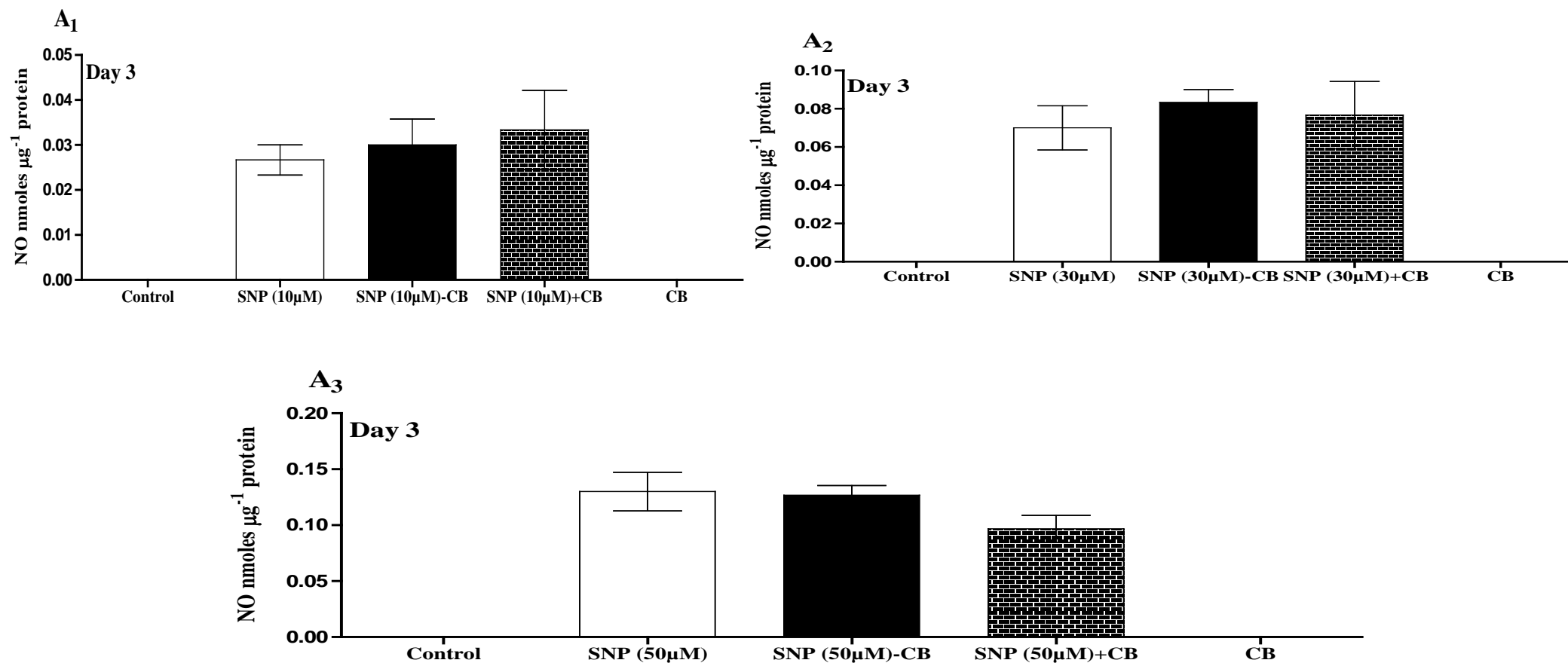
Figure 5.9 A: Effects generation of NO from SNP in RASMCs.

Cells were cultured to ~90% confluency and incubated either with culture medium alone (control) or treated with SNP at different concentrations in the presence or absence of CB (7mM $CaCl_2$, 7mM β-GP). SNP-CB represents data from cells pretreated with the NO donor for 1 hour before adding CB, and SNP+CB represents coincubation of both together for 3 days. Total NO was quantified by the Griess assay as described in methods (section 2.3). The data represents means ± S.E.M. from 3 experiments.
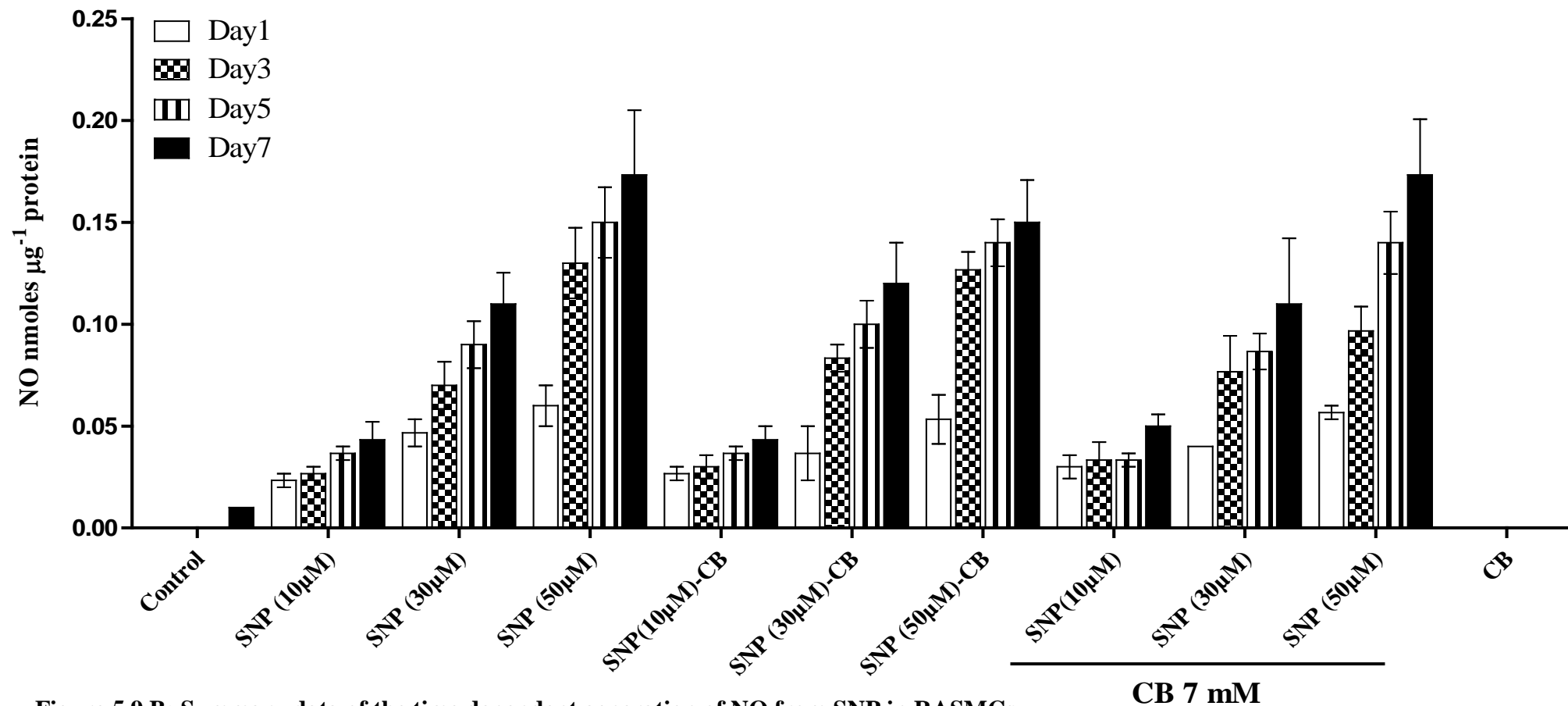
Figure 5.9 B: Summary data of the time dependent generation of NO from SNP in RASMCs.

Cells were cultured to ~90% confluency and incubated either with culture medium alone (control) or treated with SNP at different concentrations in the presence or absence of CB (7mM CaCl$_2$, 7mM β-GP). SNP-CB represents data from cells pretreated with the NO donor for 1 hour before adding CB, and SNP+CB represents coincubation of both for 1, 3, 5, and 7 days. Total NO was quantified by the Griess assay as described in methods (section 2.3). The data represents means ± S.E.M. from 3 experiments.
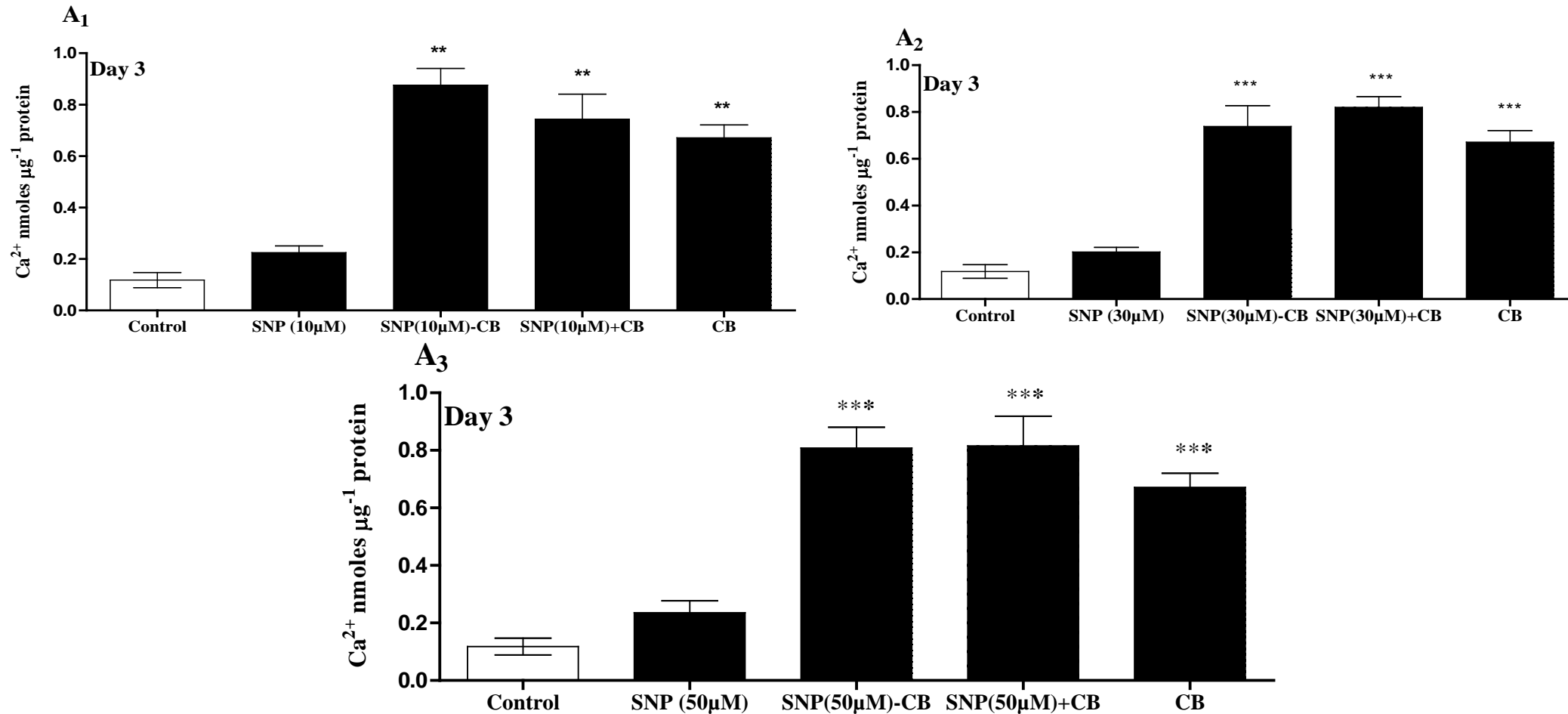
Figure 5.10 A: Effects of SNP on calcification of RASMCs.

Cells cultured to ~90% confluency were incubated either with culture medium alone (control) or treated with SNP at different concentrations in the presence or absence of CB (7mM CaCl$_2$, 7mM β-GP). SNP-CB represents data from cells pretreated with the NO donor for 1 hour before adding CB, and SNP+CB represents coincubation of both together. Total calcium was quantified as described in methods (section 2.6). The data represents means $\pm$ S.E.M. from 3 experiments. ** denotes $p<0.01$ and *** denotes $p< 0.001$ compared to control cells.
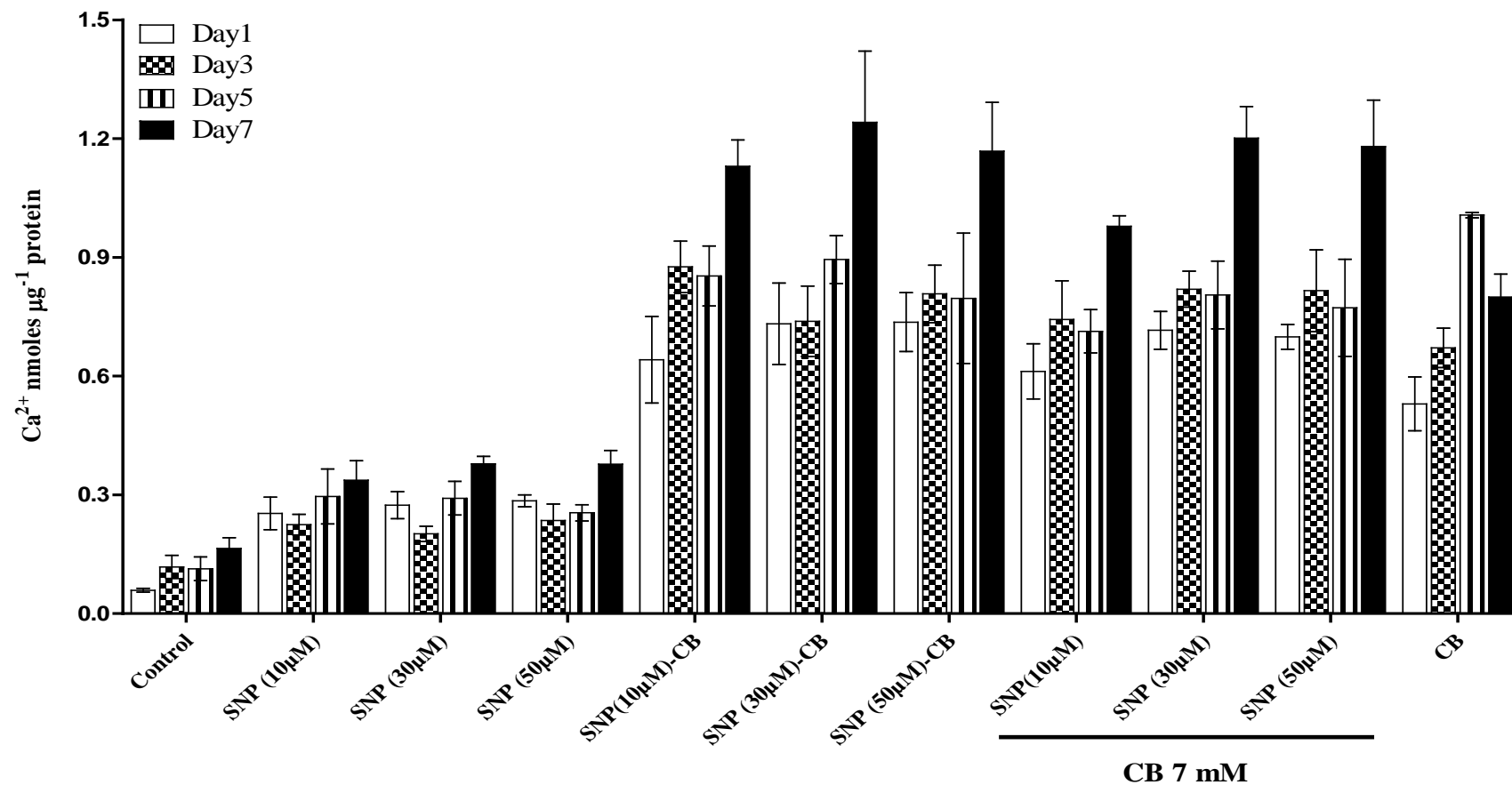
Figure 5.10 B: Summary data of the effects of SNP on calcification of RASMCs.

Cells cultured to ~90% confluency were incubated either with culture medium alone (control) or treated with SNP at different concentrations in the presence or absence of CB (7mM $CaCl_2$, 7mM β-GP). SNP-CB represents data from cells pretreated with the NO donor for 1 h before adding CB, and SNP+CB represents coincubation of both for 1, 3, 5, and 7days. Total calcium was quantified as described in methods (section 2.6). The data represents means ± S.E.M. from 3 experiments.

5.3.6- Staining of calcific plaques with ARS:

Coincubation of RASMCs with different concentrations of SNP did not form mineralised plaque as observed with cells incubated with CB alone. In addition, incubation of cells with SNP in the presence of CB did not cause the formation of HA crystal as no staining was observed with ARS (Figure 5.11). These results were unexpected especially as SNP plus CB cause similar elevations in calcium as CB alone. The reason for this discrepancy is unclear.
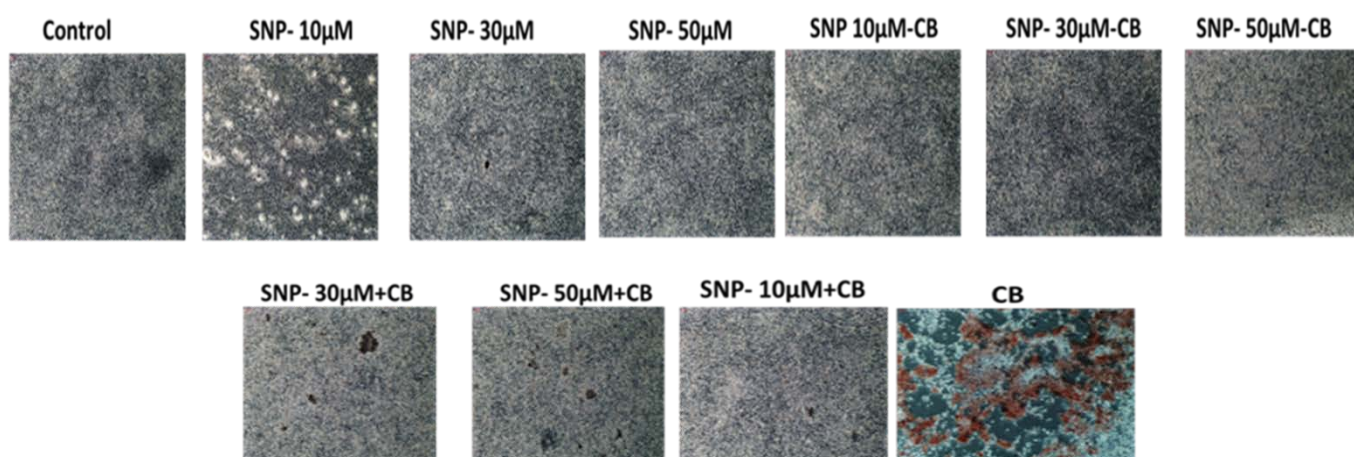
Figure 5.11: Alizarin red staining of calcified RASMCs.

Cells were cultured to ~90% confluency and incubated either with culture medium alone (control), CB. SNP-CB represents data from cells pretreated with the NO donor for 1 hour before adding CB, and SNP+CB represents coincubation of both for 5 days. Cells were treated with 1x of ARS (1: 10 stock solution) at the end of the treatment period as described in method (Section 2.8). The images are representative of 3 individual experiments which were taken with an inverted Olympus microscope at 10X magnification using GX capture programme.

5.3.7 - Effects of different concentrations of GW274150, NOC 18, and SNP on cell viability:

Figure 5.12 shows that RASMCs incubated with a concentration range of GW274150 (3, 10, 20, 50, and 100 µM) in presence or absence of CB and/or LPS+IFN-γ did not cause any significant change in cell viability except at day 7 where marginal decreases (28%) in viability were observed and surprisingly this was more pronounced when GW274150 was used alone. Similar trends were also seen with NOC 18 and with SNP (Figure 5.13) which all goes to support that all compounds and conditions were well tolerated at the earlier time points.
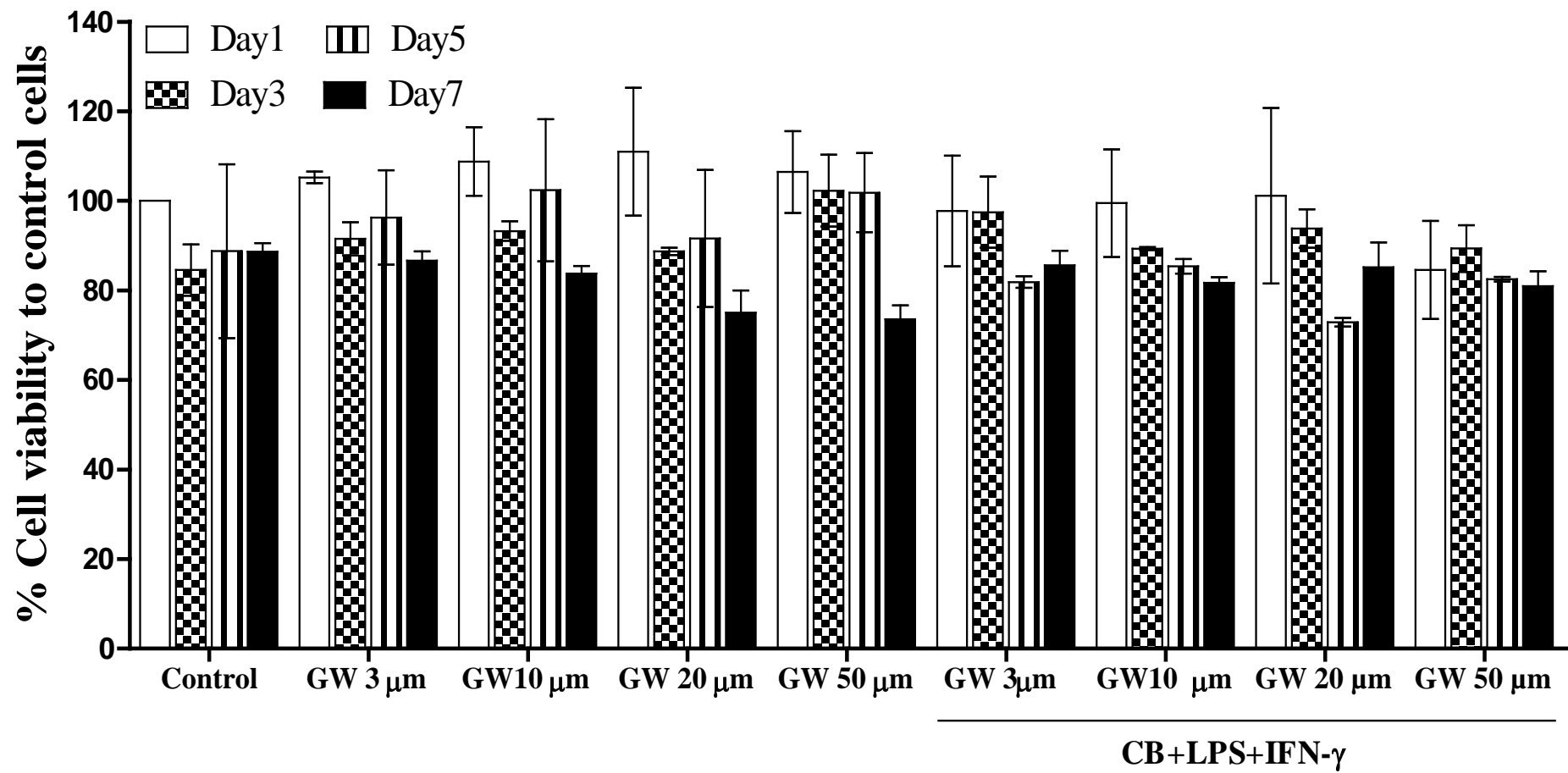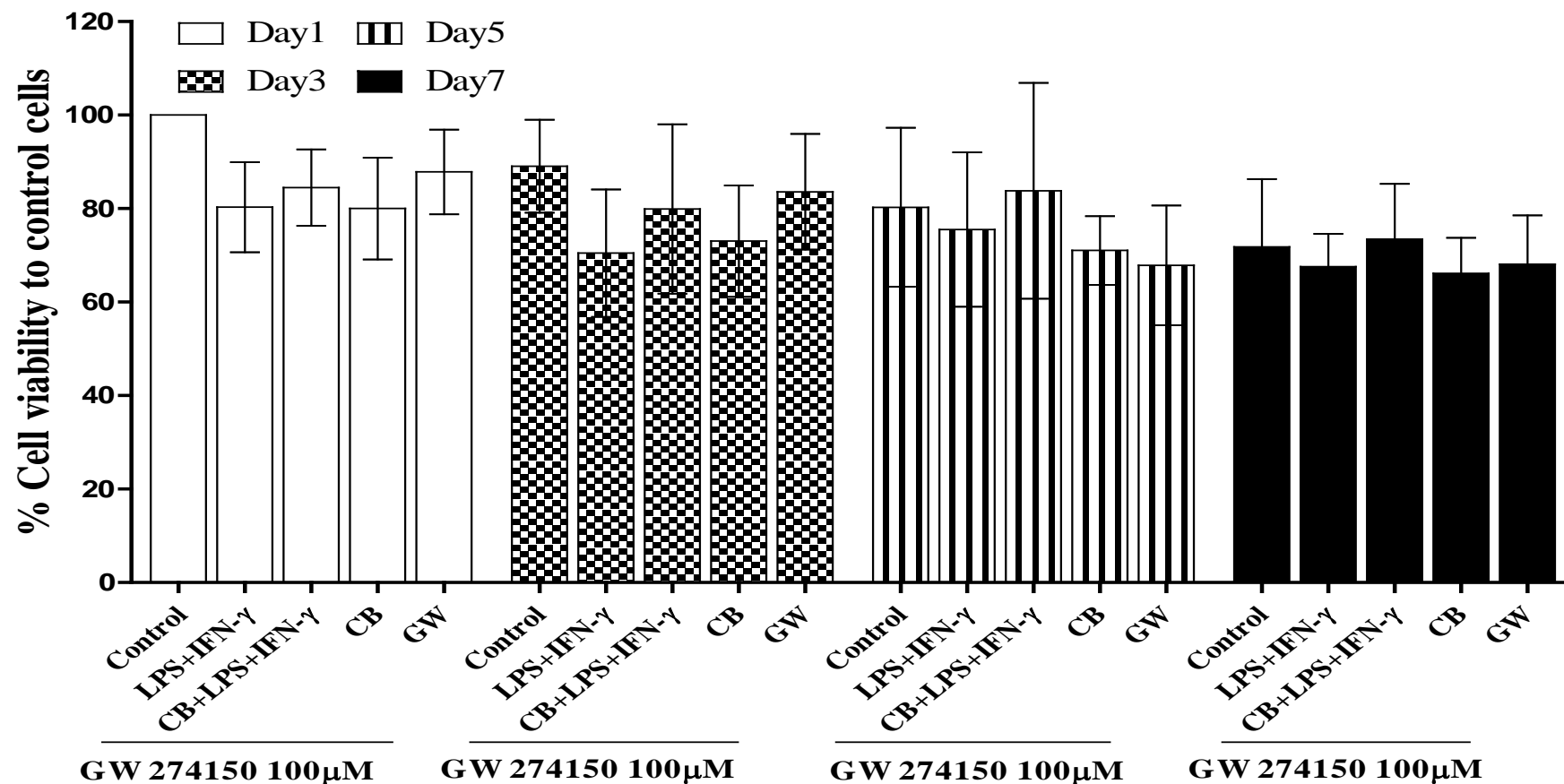
Figure 5.12: Effects of different concentrations of GW274150 with/without LPS+IFN-γ + CB on cell viability

Cells were plated in 96 well plates to ~90% confluency and incubated with either medium alone or with increasing concentrations of GW274150 in the presence of LPS+IFN-γ and CB. When used, GW 274150 (GW) was added to cells for 30 minutes prior to the addition of CB+LPS+IFN-γ for 1, 3, 5 and 7 days. The medium was subsequently removed from each well and the cells incubated with 0.5mg ml^{-1} MTT in complete culture medium as described on method (Section 2.7). The data is represented as % change of cell viability taking controls as 100%. The values represent the mean ± SEM from 3 experiments.

236
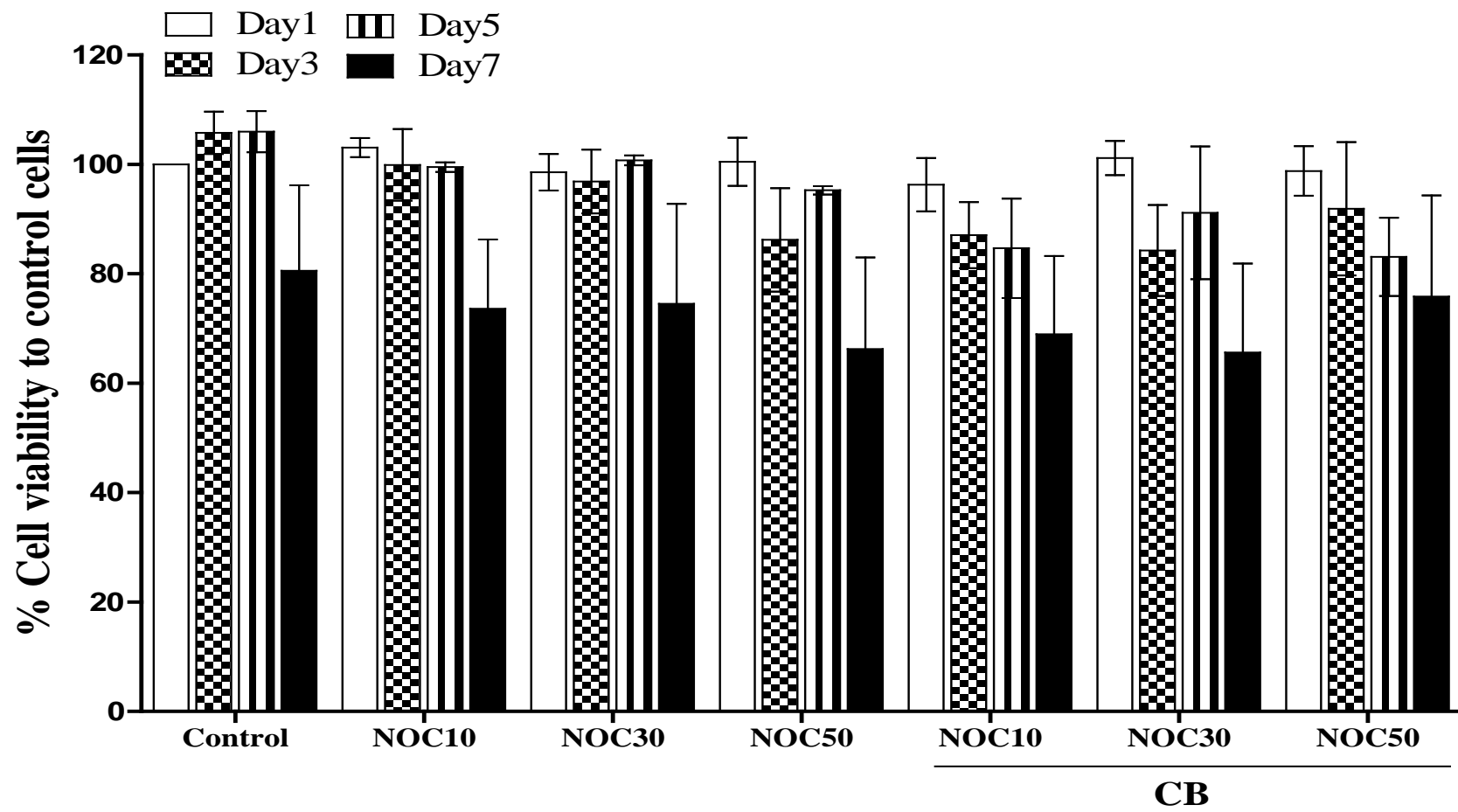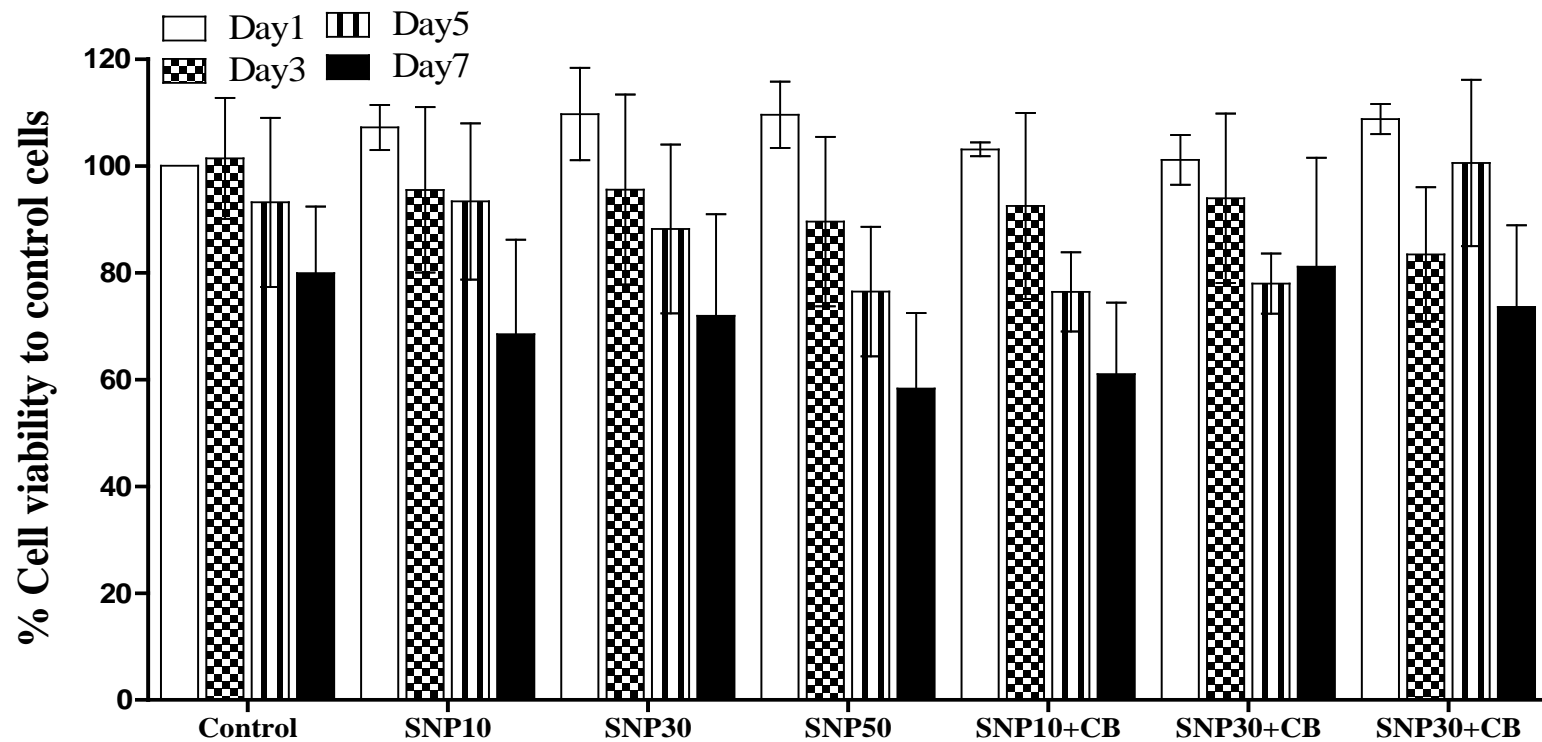
Figure 5.13: Effects different concentrations of NOC 18/ SNP with or without CB on cell viability.

Cells were plated in 96 well plates to ~90% confluency and incubated with either medium alone or with increasing concentrations of NOC18/SNP or in combination with CB for 1, 3, 5, 7 days. The medium was subsequently removed from each well and the cells incubated with 0.5mg ml^{-1} MTT in complete culture medium as described on method (Section 2.7). The data is represented as % change of cell viability taking controls as 100%. The values represent the mean $\pm$ SEM from 3 experiments.

5.4-Discussion:

It was demonstrated in the previous chapters that activation of RASMCs with $CaCl_2$ or CB in absence of NO production enhanced calcium levels. Furthermore, LPS or together with IFN-γ were used in order to stimulate the pathway of NO production resulting in potentiation of this process. Interestingly, these inflammatory mediators induced increases in calcium level even in the absence of calcification inducers. The incubation of RASMCs with LPS + IFN-γ in the presence of calcification inducers caused further induction of NO by iNOS and was associated with elevations in calcium levels. In term of iNOS expression, the protein was found to be significantly expressed compared to the response to the LPS + IFN-γ alone.

The previous chapter also detailed the levels of iNOS expression determined in different conditions. Interestingly, when the cells were incubated in a combination of LPS and IFN-γ the production of NO by iNOS was induced. The addition of CB to the media with LPS+IFN-γ significantly enhanced the production of NO/iNOS, which was sustained at day 3 compared to LPS+IFN-γ alone. This elevation of NO production and iNOS expression may be because LPS induces, while IFN-γ stabilises the iNOS mRNA (Raghavan *et al.*, 2001) and this could explain why NO was produced by iNOS in response to LPS and IFN-γ in RASMCs. While the addition of CB and LPS+IFN-γ caused more elevation of NO/iNOS and this reason might be referred to the CB leading to sustainable effect of NO/iNOS compared to LPS+IFN-γ

Further investigations detailed in chapter 4 used ARS and FT-IR analysis to determine HA crystals formation indicating calcification. Using ARS, it was found that mineralisation required the presence of $CaCl_2$ either with both LPS and IFN-γ or when *β*-GP was present. Furthermore, the mineralisation was greater when CB and both inflammatory mediators were

also present. Thus, when the cells were incubated in the media containing a combination of CB +LPS and IFN-γ the mineralisation was greatest compared to that seen with CB alone.

On the other hand, FT-IR analysis showed the characteristic vibrational molecule peak for the HA crystal was present only in samples from RASMCs incubated in either LPS+CB, IFN-γ+CB, LPS+ IFN-γ + CaCl$_2$ or LPS+ IFN-γ + CB. Thus, most of these results confirmed the induction of NO production by iNOS, and the elevation of calcium levels were linked to the formation of HA crystals detected via ARS staining and FT-IR analysis.

The investigations detailed in this chapter aimed to test how the presence of NO in the cell media was related to calcification. The protocol used for these experiments was adjusted in order to ensure that no nitric oxide was present in the cell culture before calcifying conditions were introduced. This was achieved by pre-incubating cells with the selective iNOS inhibitor GW274150.Coincubation of cells with GW274150 at 10, 50, and 100 µM either in the presence of LPS+IFN-γ or with CB inhibited NO production significantly, which is to be expected as GW274150 blocks the activity of iNOS and has been demonstrated by other studies to be a selective competitive inhibitor of iNOS (De Alba *et al.*, 2006). Furthermore, minimal levels of endogenous NO were detected in the cell culture, which is to be expected under the control conditions. In addition, the use of CB in combination with LPS+IFN-γ again caused a significant expression of iNOS compared to that seen with LPS+IFN-γ. As already discussed in chapter 4 iNOS mRNA is stabilised and expression sustained under these conditions (CB+LPS+IFN-γ). However, the occurrence of such results in RASMCs has not yet been published, thus this represents a novel mechanism established in RASMCs.

While the presence of GW274150 either at 10 or 50 µM concentrations appeared not to affect the expression of iNOS at day 3 in comparison to when it was absent, the production of NO by iNOS was significantly inhibited. This is to be expected as GW274150 reduces iNOS

activity rather than expression itself (Chatterjee *et al.*, 2003). In contrast, with the use of 100 μM of GW274150 in the presence of LPS+IFN-γ with/without CB resulted in both the inhibition of iNOS activity and the inhibition of iNOS expression and this was an unexpected observation. No other studies have demonstrated GW274150 altering iNOS expression. This is the first study showing this result and therefore unique in the literature. This result may be due to one of several reasons including the following: a) GW274150 at 100 μM could be acting to reduce the amount of NF-kB available and thus reduce the amount of iNOS mRNA transcribed, in turn reducing the amount of iNOS protein produced; b) at the high concentration of 100 μM GW274150 may be acting non-selectively. It may be blocking the pathway which leads to generation of iNOS without direct interaction with the iNOS enzyme itself. This is based on the observation that at lower concentration of GW274150 iNOS expression is enhanced rather than repressed; c) at this concentration GW274150 may be acting translationally by reducing the half-life of iNOS mRNA, and thus reducing the amount of iNOS protein produced. Other studies have found drugs such as dexamethasone and rapamycin acting in this manner (Korhonen *et al.*, 2002; Lisi *et al.*, 2011); d) GW274150 competes with L-arginine via inhibition of iNOS activity resulting in reduced NO production for the active site. Therefore, at this concentration GW274150 may be involved in activation of negative feedback mechanisms controlling expression of iNOS, in order to minimise the level of NO produced.

Previous studies have demonstrated that concentrations of 5 μM were able to inhibit iNOS by 50% (Chatterjee *et al.* 2003). However, concentrations used *in vitro* have varied widely between 1nM (Chatterjee *et al.* 2003), 1 μM (Baydoun *et al.*, 2006),10 μM (Schurgers *et al.* 2010) and 100 μM (Alderton *et al.* 2005). The range used in our study covered the extremes of these concentrations, being between 10 and 100 μM. However, GW274150 has been never

shown to inhibit expression of any protein *in vivo* or *in vitro* at any concentration. This mechanism of reduced expression needs to be determined.

In relation to calcification cells coincubated with CB+LPS+IFN-γ had a significant elevation of calcium compared to the control or LPS+IFN-γ or CB alone. LPS may trigger expression of pro-calcific proteins such BMP 2 and ALP by stimulating TLR2 and 4 which in turn result in acceleration of the transition of VSMCs into osteoblast like cells (Tintut *et al.*, 2002; Zehnder *et al.*, 2002). IFN-γ has a role in inducing calcification through the activation of 1alpha-OHase (Stoffels *et al.*, 2006) and this converts $25\text{-(OH)}_2\text{D}_2$ (Calcidiol) to $1,25\ \text{(OH)}_2$ D_3(Calcitriol), resulting in elevated calcium level leading to hypercalcemia (Somjen *et al.,* 2005). The studies detailed in previous chapters demonstrated mineralisation with IFN-γ, LPS and CB combined; and elevated calcium with IFN-γ with $CaCl_2$ from day 1 and CB day 3 onwards. NO production appears to be stimulated and sustained by the combined presence of LPS and IFN-γ, however there is a significant reduction in NO when GW274150 was present at all the concentrations used. GW274150 by itself did not cause calcification but instead significantly blocked calcification caused by LPS and IFN-γ without altering the effect of CB. The fact that GW274150 is a selective inhibitor of iNOS activity suggests that 10 and 50 µM of GW274150 inhibit NO and enhanced calcium levels marginally compared to LPS+IFN-γ alone, and this was not led to enhance of HA crystal formation possibly caused through NO production, e.g. the presence of NO may promote crystal nucleation. Moreover, there may be the possibility that NO reacts with alizarin thus blocking the staining of the HA or it could be the limitation of calcium presence in the medium. However, there is no proof for this. Further the result of the FT-IR was also negative, so this possibility can be disregarded. Moreover, it may also be a non-selective effect of GW274150 at the highest concentration of 100 µM could potentially block other pathways that mediate calcification

therefore inhibition of calcification that may be seen but this may not be related to NO. However, there are no studies that demonstrate that GW274150 may cause changes in cell signalling and this would need to be investigated in the future in order to understand the mechanism that mediates the suppression of iNOS expression and calcification by high concentrations of GW274250. Previous studies have demonstrated that GW274150 reduced the inflammation in synovial fluid caused by inflammatory mediators which stimulated NO production by iNOS. In the model of osteoarthritis the disease mechanism involved the formation of HA crystals between the cartilage in the knees and arms (Genovese *et al*., 2005; Víteček *et al*., 2012). Thus, the inhibition of HA formation by GW274150 supports the latter observations.

The levels of calcium were enhanced when 10 and 50 μM of GW274150 were used in the presence of LPS+IFN-γ or with CB alone, however at the same concentrations GW274150 appeared to partially suppressing the level of calcium significantly when LPS+IFN-γ+CB were all present. The experiments in the previous chapters demonstrated that CB and inflammatory mediators together had an additive effect on increasing iNOS expression and NO production. Thus, the effect of GW274150 may be related to its influence on calcium levels rather than its effect on NO production directly.

It is important to clarify why GW274150 had different effects at different concentrations and it may be helpful to conduct further experiments using alternative selective inhibitors of iNOS activity such as Byk 191023 (Su *et al.*, 2010) to understand whether the blockade of iNOS activity might regulate calcification of smooth muscle cells. Further studies examining the effect of GW274150 on the vascular calcification would help to determine the mechanism of GW274150 action on smooth muscle cells in order to support potential therapeutic use in the future.

To investigate the effects of NO on calcification RASMCs were incubated with two different NO donors, NOC 18 and SNP. These have different NO release profiles and therefore can help to identify whether the induction of calcification may be regulated directly by the NO molecule. Two set of experiments were carried out in which cells were exposed to either NOC 18 or SNP together with CB; added either simultaneously, or after the cells were pre-incubated in media containing the NO producers for one hour before addition of CB.

As shown in previous chapters the presence of CB in the media resulted in significantly elevated calcium level at day 5 as well as HA crystal formation. The result was the same when the cells were preincubated with 30μM and 50μM of NOC18 prior to addition of CB. In contrast, at the lower concentration of 10μM NOC18 while the level of calcium was also elevated significantly at day 3, HA crystals were not formed in this condition. This suggests that the lower level of slow released NO may be the limiting factor in HA formation. When comparing this to the results when both NOC18 and CB were added to the media together, calcium was more significantly elevated, and no HA crystals were observed via ARS. This indicates that the NO needs to be elevated prior to the influx of extracellular calcium for HA formation.

However, when both NOC 18 and CB were added to the cells together there may be a delay the activation of the calcification by the spontaneous release of NO and the results of this method should be further investigated in future. These results could contribute to the determination of the role of pro-calcific factor such as Runx2 in calcification.

NOC 18 did not appear to have any pharmacological effect on RASMCs as the NO levels were not significantly elevated in most conditions, apart from when the highest concentration of 50μM was used on its own, or used to preincubate the cell culture prior to adding CB. At this higher concentration it may be that NO in the media released by NOC18 is entering the

cells to increase NO levels above the basal level. This result supports the possibility that NOC18 or indeed NO may contribute to calcification and agrees with previous studies demonstrating that NOC 18 elevates mRNA level of osteocalcin and may therefore contribute to the mineralisation process (Otsuka *et al.*, 1998). A further study has demonstrated that NOC 7 or NOC 18 caused the induction of intracellular cGMP in rat calvarial osteoblastic cells (ROB) and this in turn promotes mineralisation. This study aimed to establish whether the induction of cGMP could be linked to the induction of mineralisation of ROB. Interestingly, NOC 7/NOC 18 induced an increase in levels of osteocalcin mRNA, the pro-calcific marker, but did not affect ALP and may therefore not be involved in the mechanism of mineralisation caused by ALP (Otsuka *et al.*, 1998). The authors suggested that NO plays a pivotal role in the formation of mineralised nodules in the osteoblast cells.

Furthermore, a study was done by Yasuhara and coworker which showed that NO could be considered to participate in mineralisation and differentiation of pulp cell growth. Their results showed that incubation of cells with β-GP, ascorbic acid, dexamethasone, and $KH(2)PO(4)$ in the presence of NOC 18 caused formation of mineralisation plaques (Yasuhara *et al.*, 2007). The result could be explain by the fact that continuous release of NO by NOC 18 could support a reaction of NO and free molecular oxygen (O_2) present into cells resulting in formation of $ONOO^-$ which in turn induced increases in calcium levels into the cells. Another possibility could be that NOC 18 activates the calcium-sensing receptor (CaSR) which potentiates the mechanism of VC.

Studies have demonstrated that NOC 18 may cause stimulation of c-GMP production leading to prevention of the activity of calcification inducers via signalling to induce NO production by reducing TGF-β expression. This in turn elevates the phosphorylation of Smad2/3, which is involved in calcifying smooth muscle cells (Kanno *et al.*, 2008). The same pathway might

be used by NOC 18 in the current experiment, meaning HA crystallisation did not occur. This needs further clarification.

With regards to SNP, incubation of the cells with this compound for an hour prior to addition of CB, or addition together with CB did result in slight inhibition of NO. Furthermore, when both CB and SNP are present together the levels of calcium at day 7 are higher than when CB was present by itself. The increase maybe be because SNP has a short half-life and over the 3 day incubation period there may no longer be any NO available to suppress calcification thus the increases seen albeit marginal. The study by Huitema *et al.* (2006a) supports this as it shows that SNP inhibited the progression of calcification in the ATDC5 cell and suggested that it could also inhibit calcification in VSMCs (Huitema *et al.*, 2006a).

Unlike NOC 18, the incubation of cells with SNP did not cause any significant changes in calcification. It seems that the short half-life of SNP and its profile of releasing NO could not result in the induction of mineralisation. This result goes in parallel with other studies illustrating that SNP inhibits the mineralisation of ATDC5 cells. This inhibition occurred when cells were coincubated with β-GP or inorganic phosphate in the presence of SNP for 21 days. The results suggested that the addition of SNP within the range of 1-1000 µM resulted in significant inhibition of calcification process and that is why no plaques were observed by ARS. SNP may act via c-GMP independently and this was confirmed by incubating cells with 1 H-[1,2,4]Oxadiazolo[4,3-a]quinoxalin-1-one (ODQ), an inhibitor of the soluble guanylyl cyclase (sGC) in presence of SNP, which inhibited elevation of calcium levels when compared to the analog of cGMP (Huitema *et al.*, 2006a; Huitema *et al.*, 2006b). Therefore, the incubation of cells with SNP would play a beneficial role as target for treating VC.

The cell viability studies conducted demonstrated that while the cells tolerate most of the agents used in the experiments well, CB does have an impact on cell viability as well as combined with GW274150, or NOC 18/SNP. At day 7 the presence of CB reduced cell viability by approximately 20%. It is interesting to note that a loss of RASMCs viability has been linked to VC under atherosclerotic conditions (Shin and Kwun, 2014). Further the elevation of extracellular calcium has been linked in increased intramitochondrial production of ROS, which can lead to apoptosis (Voccoli *et al.* 2014). The results of this study are therefore supported by previously published work.

In summary, the studies carried out to date show that inhibition of NO/iNOS by GW274150 caused reduction of calcium levels in a calcifying environment and this might be a pivotal link between NO/iNOS and calcification. Moreover, increased extracellular NO appears to enhance calcium levels, when a slow NO releasing agent NOC18 is used rather than fast releasing SNP; especially with the CB after NO increase. However with the fast release of NO by SNP no effect on calcium level is observed.

CHAPTER VI

RESULTS

Signal transduction mechanisms that regulate iNOS expression, NO production and calcification in cultured RASMCs

6.1- Introduction:

Data presented in chapter 3 showed that activation of RASMCs by LPS + IFN-γ caused the elevation of calcium levels above control and further elevation was determined when cells were coincubated with CB/CaCl$_2$ which lead to the formation of HA crystal indicative of calcification. These effects were observed together with increases in NO production /iNOS expression as shown in chapter 4 and suggest that various signalling processes may be activated in the cells to cause calcification and/or NO production through the induction of iNOS.

The pathway that activates the formation of iNOS causing NO production in RASMCs is well known and is reported to occur through different signalling molecules including the p38 MAPK (Hattori *et al.*, 2003;Yamakawa *et al.*, 1999) and Akt (Rzucidlo *et al.*, 2007) amongst others. Similarly, there has also been considerable studies carried out to establish the signal transduction mechanism that regulate calcification and the pathways identified include AMP-activated protein kinase (AMPK) (Cao *et al.*, 2013), and p 38 MAPK (Li *et al.*, 2002). Currently, it is not clear whether there is overlap between these pathways in regulating iNOS expression and calcification nor has it been established whether the regulation of activation of any of these pathways using pharmacological interventions simultaneously alters the process of calcification and induction of iNOS. This has therefore been investigated as part of this thesis.

In addition, further experiments were carried out investigating changes in expression of the pro-calcific marker Runx2 by western blotting in order to understand whether the regulation of calcification and/or NO/iNOS is also associated with changes in expression of Runx2. This transcription factor was selected because previous studies have demonstrated evidence of a link between activation of Erks and Runx2 in osteoblast cells.

Ge and coworkers found that incubation of MC3T3-E1 cells with ascorbic acid containing BMP2/7 regulates mineralisation through activation of the Erk pathway leading to increased expression of Runx2. Furthermore, induction of Runx2 is associated with phosphorylated Erk expression, but without changes in p38 MAPK in osteoblast cells. This was thought to contribute to the induction of the calcification process (Ge *et al.*, 2012). In contrast, a study by Lee and coworker found that the p38 MAPK pathway together with Smad caused the induction of Runx2, which in turn resulted in the release of TGF-β and BMP2 in the mouse myoblast cell lines (C2C12 cells). These effects contributed to triggering osteoblast differentiation (Li *et al.*, 2002).

Furthermore, inflammatory cytokines such as TGF-β cause activation of Tak1, which significantly reduces the formation of osteoblast cells, resulting in severe osteopenia. This activity leads to the regulation of Runx2 through p38 MAPK phosphorylation. Therefore, the phosphorylation of p38 MAPK plays a significant role in the activation of Runx2 into osteoblast cells (Greenblatt *et al.*, 2013). However, it is not clear whether calcified smooth muscle cells are regulated by p38 MAPK leading to the induction of Runx2.

In this thesis two different time courses were used; as the activation of some signalling molecules may occur earlier or later. Regarding this, cells were activated with LPS alone, or together with IFN-γ, in the presence or absence of calcification inducers over a time course ranging from 1- 48 hours or 1-5 days. For instance, cells were preactivted with LPS alone, or LPS+CB; or in another set of experiments LPS+IFN-γ by themselves or together with CB over 1-48 hours. A second time course used LPS+IFN-γ, either alone or together with either $CaCl_2$, $β$-GP or CB over 1-5 days. This time range was identified following the results of previous experiments to determine the time point of induction of maximal calcification.

The main objective was to establish whether signalling molecules including p 38 MAPK, Akt, and Erk1/2 are phosphorylated in RASMCs in response to calcifying agents, in either the absence or presence of LPS+IFN-γ.

6.2- Experimental protocol:

Cells were cultured and quantification of total protein and identification of protein expression by western blotting were performed as described in chapter 2, section 2.6 and 2.10 respectively. The protease inhibitors cocktail (the dilution factor is 1:200 1x lysis buffer explained in chapter 2 at section 2.4 and this product contains; AEBSF, Aprotinin, Bestatin, E-64, Leupeptin, and Pepstatin A). The phosphatase inhibitors was diluted by 1:100 lysis 1x buffer containing; Sodium orthovanadate, Sodium molybdate, Sodium tartrate, and Imidazole. Both products were used for extracting cells after incubating with LPS + IFN-γ/calcification inducers, or in combination. The effect of SB203580 or LY294002 at 10 µM of both were involved in this study in order to understand the role of p 38 MAPK or PI3K and see whether play a role as down or upstream molecule in calcified RASMCs.

6.2.1- Expression of Runx2 and p 38 MAPK in cells incubated with calcification inducers with or without LPS/ LPS+IFN-γ.

RASMCs were cultured to ~90% confluence and incubated with LPS alone / LPS + IFN-γ , CB alone or together with CB. The activation of p38 MAPK was measured at 1, 6, 12, 18, 24 and 48 hours. Another set of experiment activated cells with LPS+IFN-γ followed by the addition of calcification inducers and the p 38 MAPK measured during 1, 3, and 5 days. In Akt phosphorylation, it was determined during 1, 6, 12, 18, 24 and 48 hours of activation. At the same time calcification and iNOS protein (and thus NO production) were simultaneously induced, as in previous experiments (chapter 4), in order to determine whether Akt regulates this induction. Detection and quantification of Runx2 was also determined by western blotting over the time course of 1, 3, and 5, days. This time point was identified by a previous experiment to identify the point of maximal calcification induction.

6.2.2- The effect of GW2742150 on Runx2 expression in RASMCs:

RASMCs were cultured to ~90% confluence and incubated with LPS and IFN-γ, CB , or in combination in presence or absence of GW274150. Quantification of Runx2 was determined by western blotting at 3 days and this was the time point found previously from the first experiment to induce maximal calcification.

6.3-Results:

6.3.1- Effect of LPS/IFN-γ with/ without CaCl₂, β-GP, or CB on the p38 MAPK phosphorylation in RASMCs:

Incubation of cells with medium only (control) did not result in the activation by phosphorylation of p38 MAPK activation, as no phosphoprotein was detected in the western blots obtained using the phospho-p38 antibody (Figure 6.1). Compared to the response of the control cells, the use of LPS alone showed significant induction of p38 MAPK phosphorylation, which peaked at 12 hours, and was sustained until the last time point; 48 hours. When CB alone was used for cell incubation, the phosphorylation of p38 MAPK was activated at 6 hours, followed by further increase until a maximum at 24 hours, followed by a sustain thereafter (48 hours). This result is comparable to the response seen with LPS alone (18-24 hours) as shown in Figure 6.1. The combination of CB and LPS did not enhance the phosphorylation of p38 MAPK compared the response to CB alone. It is notable that using the p38 MAPK specific inhibitor SB203580, and Akt specific inhibitor LY294002, significantly reduced ($p<0.01$) phosphorylation of p38 MAPK at 24 hours. This indicates that these perhaps have the either same or diverse upstream targets which are neither p38 MAPK nor Akt.

Figure 6.2 shows the measurement of p38 MAPK phosphorylation over a 48 hour time period. The use of both LPS+IFN-γ with and without CB, resulted in the significant induction of p38 MAPK phosphorylation, compared to the responses seen with either CB alone or CB with LPS, at 18 hours and 24 hours. The maximum induction with LPS+IFN-γ by themselves occurred at 48 hours, and this was designated as 100%. CB alone also induced p38 MAPK phosphorylation, and levels of phosphorylation were marginally higher to responses with LPS+IFN-γ at all time periods. The peak of phosphorylation was seen at 24h and there was

no further potentiation when LPS+IFN-γ were present together, or present together with CB. Again, using either the p38 MAPKs specific inhibitor, SB203580, or the Akt specific inhibitor LY294002 partially reduced expression of p38 MAPK.

The phosphorylation of p38 MAPK, was also followed over a longer time period, up to 5 days. For these studies, cells were incubated with LPS+IFN-γ in either the presence or the absence of $CaCl_2$ Figure 6.3 A, β-GP Figure 6.3 B, or CB Figure 6.3 C. Activation of cells by LPS+IFN-γ followed by the continuous addition of LPS+IFN-γ for next 24 hours resulted in induction phosphorylation of p38 MAPK at day 1, which rapidly declined thereafter. In contrast with the use of $CaCl_2$ alone, an elevation of phosphorylated p38 MAPK was found at day 1, which increased over time and was sustained over the whole 5 days. While, when incubated with $CaCl_2$ and LPS+IFN-γ together, the induction of p38 MAPK phosphorylation was close to that of $CaCl_2$ alone, but declined rapidly to control levels at day 3.

Similarly, with the use of β-GP and LPS+IFN-γ together, phosphorylation of p38 MAPK peaked at day 1, and declined rapidly over the time course. While with β-GP alone phosphorylation of p38 MAPK resulted in the elevation from day 1, peaking at day 3 following by sustained levels at day 5. The same results were also seen when CB alone was used, however when placed together with LPS+IFN-γ the peak of phosphorylation was at day 1 followed by a decline. This was significantly reduced thereafter, compared to the response with CB alone.
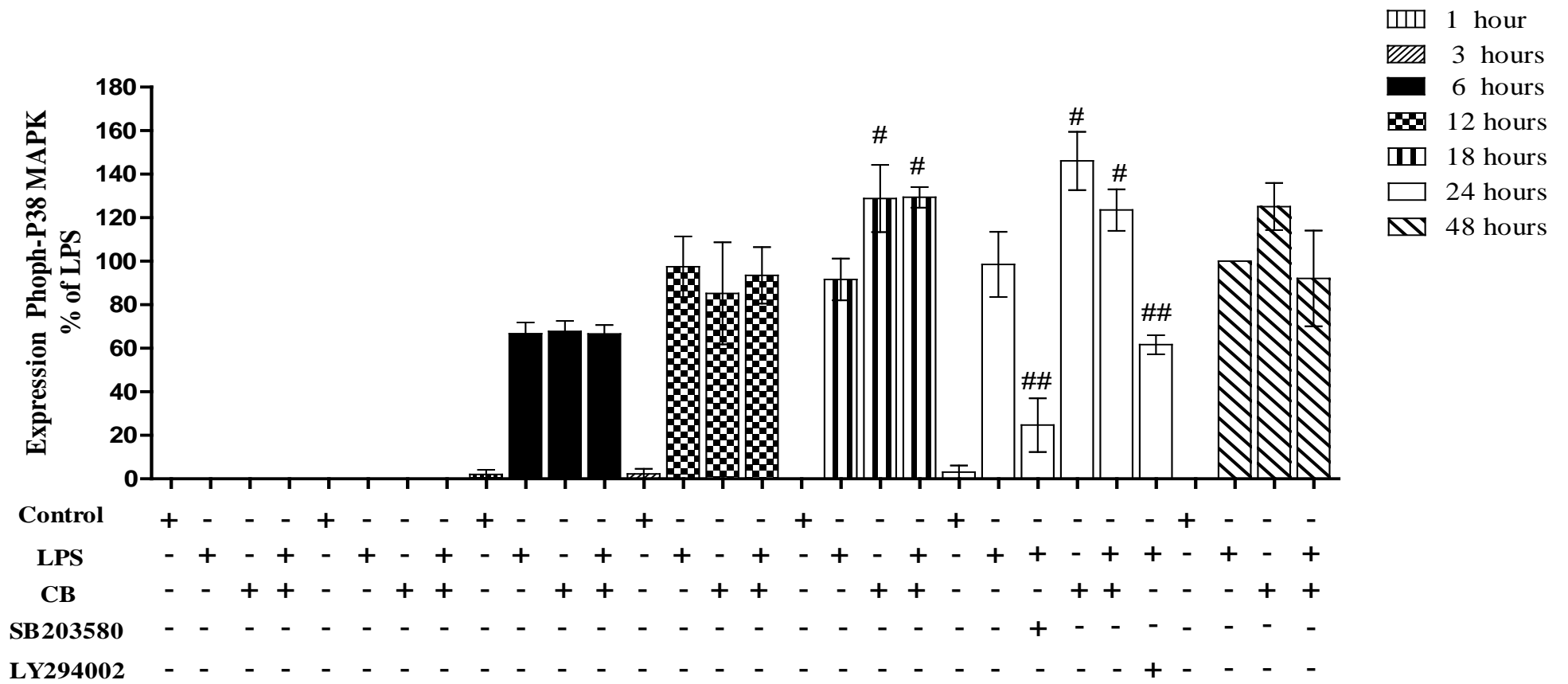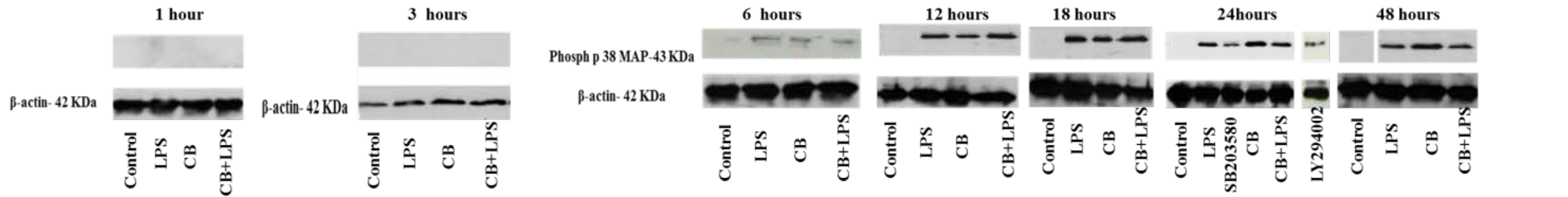
Figure 6.1: Effects LPS, CB or in combination on p 38 MAPK phosphorylation in RASMCs.

Cells were cultured to ~90% confluency and incubated with culture medium alone (control), LPS (100 μg.ml^{-1}), CB (7mM CaCl$_2$+7mM β-GP) or in combination for 1, 3, 6, 12, 18, 24, 48 hours. Phospho p38 expression was determined by western blotting using a phosphor-specific p38 monoclonal antibody as described in the methods (Section 2.10). The data is represented as % change of p 38 MAPK taking the LPS response at 48 hours as 100%. The values represent means ± S.E.M. from 3 individual experiments. # denotes $p<0.05$ and ## denotes $p<0.01$ compared to LPS.

Figure 6.2: Effects LPS+ IFN-γ, CB or in combination on p 38 MAPK phosphorylation in RASMCs.

Cells were cultured to ~90% confluency and incubated with culture medium alone (control), LPS (100 µg.ml^{-1})+ IFN-γ (100 U ml^{-1}), CB (7mM CaCl$_2$+7mM β-GP) or in combination for 1, 3, 6, 12, 18, 24, 48 hours. Phospho p38 expression was determined by western blotting using a phosphor-specific p38 monoclonal antibody as described in the methods (Section 2.10). The data is represented as % change of p 38 MAPK taking the LPS+IFN-γ response at 48 hours as 100%. The values represent means ± S.E.M. from 3 individual experiments. # denotes $p<0.05$ and ## denotes $p<0.01$ compared to LPS+IFN-γ alone.

A

	Day 1				Day 3				Day 5			
Phosph p 38 MAP-43 KDa												
β-actin- 42 KDa												

	Control	LPS+IFN-γ	CaCl₂	CaCl₂+LPS+IFN-γ	Control	LPS+IFN-γ	CaCl₂	CaCl₂+LPS+IFN-γ	Control	LPS+IFN-γ	CaCl₂	CaCl₂+LPS+IFN-γ
Control	+	-	-	-	+	-	-	-	+	-	-	-
LPS+IFN-γ	-	+	-	+	-	+	-	+	-	+	-	+
CaCl₂	-	-	+	+	-	-	+	+	-	-	+	+

Legend: ■ Day1 ▥ Day3 ☐ Day5

260

B

Day 1   **Day 3**   **Day 5**

Phosph p 38 MAP-43 KDa

β-actin- 42 KDa

C

Day 1   Day 3   Day 5

Phosph p 38 MAP-43 KDa

β-actin- 42 KDa

Figure 6.3: Effects CaCl$_2$, *β*-GP, or CB with/without LPS+IFN-γ on p 38 MAPK phosphorylation in RASMCs.

Cells were cultured to ~90% confluency and incubated with culture medium alone (control), LPS (100 μg ml^{-1}) + IFN-γ(100 U ml^{-1}) for 24 hours followed the addition of CaCl$_2$ (7mM; Panel A), *β*-GP (7mM; Panel B) or CB (Panel C) in the continued presence of LPS and IFN-γ and incubated for a further period of 1, 3, and 5 days. The data is represented as % change of p 38 MAPK taking the LPS+IFN-γ response at day 1 as 100%. Phospho p38 expression was determined by western blotting using a phosphor-specific p38 monoclonal antibody as described in the methods (Section 2.10).The values represent means ± S.E.M. from 3 individual experiments. # denotes *p*<0.05 and ## denotes *p*<0.01 compared to LPS + IFN-γ.

6.3.2- Effect of LPS+IFN-γ with/ without CB on phosphorylation of Akt in RASMCs:

Pretreating cells with LPS+IFN-γ in the presence or absence of calcifying agents did not cause phosphorylation of the Akt protein after 1, 3, and 6 hours of incubation. The control cells showed no phosphorylation of Akt, while incubation of cells with either LPS+IFN-γ, CB or in combination, did produce the phosphoprotein at 12 hours, but the peak was observed at 24 hours, but declined thereafter (Figure 6.4). The induction of Akt phosphorylation was more significant with CB alone at 24 hours, and this was not further enhanced when LPS + IFN-γ were coadministered (Figure6.4).
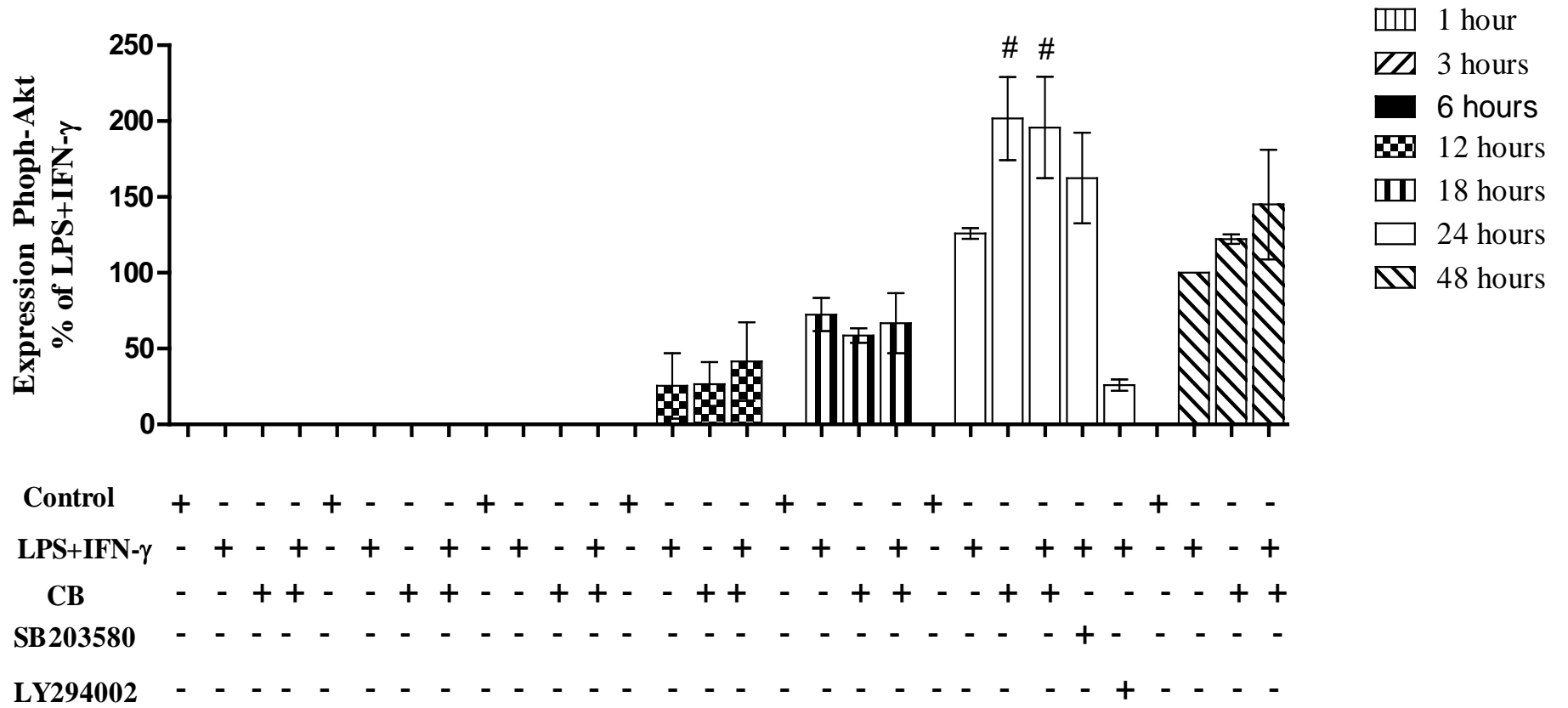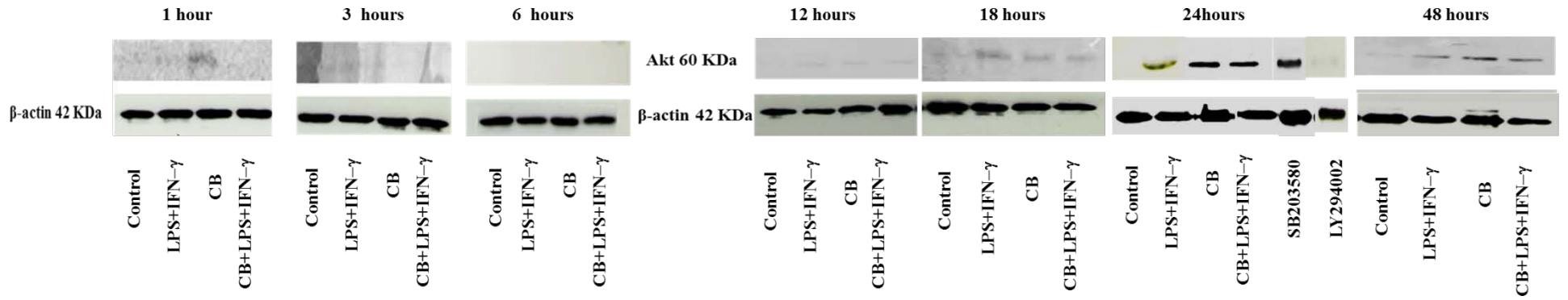
Figure 6.4: Effects LPS+IFN-γ, CB, or in combination on the Akt phosphorylation in RASMCs

Cells were cultured to ~90% confluency and incubated with culture medium alone (control), LPS (100 µg.ml^{-1})+ IFN-γ (100 U ml^{-1}), CB (7mM; CaCl$_2$+7mM; β-GP) or in combination for 1, 3, 6, 12, 18, 24, 48 hours. Phospho Akt expression was determined by western blotting using a phosphor-specific Akt monoclonal antibody as described in the methods (Section 2.10). The data is represented as % change of Akt taking the LPS+IFN-γ response at 48 hours as 100%. The values represent means ± S.E.M. from 3 individual experiments. # denotes $p<0.05$ and compared to LPS + IFN-γalone

6.3.3- Effect of LPS+IFN-γ with/ without CaCl₂, β-GP, or CB on the phosphorylation of p44/42 MAPKs (Erk-1/2) in RASMCs:

In parallel with the studies above, additional experiments were carried out to establish whether other signalling molecule such as p44/42 MAPKs may also be activated under the conditions that induce iNOS expression and/or calcification in RASMCs. Cells incubated with medium only did not show any phosphorylation of the Erks while cells activated by LPS+IFN-γ or in combination with CaCl₂, β-GP, or with CB caused induction of the phosphorylation of Erks (Figure 6.5). The level of phosphorylated Erks was marginally higher with the presence of calcification inducers when compared to LPS+IFN-γ alone. Coincubations of calcification inducers with LPS+IFN-γ did not further enhance the phosphorylations and in fact appear to suppress the process (Figure 6.5). The level of Erk's phosphorylation was more than 200% at day 3 when either CaCl₂ or β-GP, or CB were present by themselves. This time period was selected as previous experiments had indicated that maximum calcification in RASMCs was achieved at day 3 but the time constrain to follow as p 38 MAPK experiments.
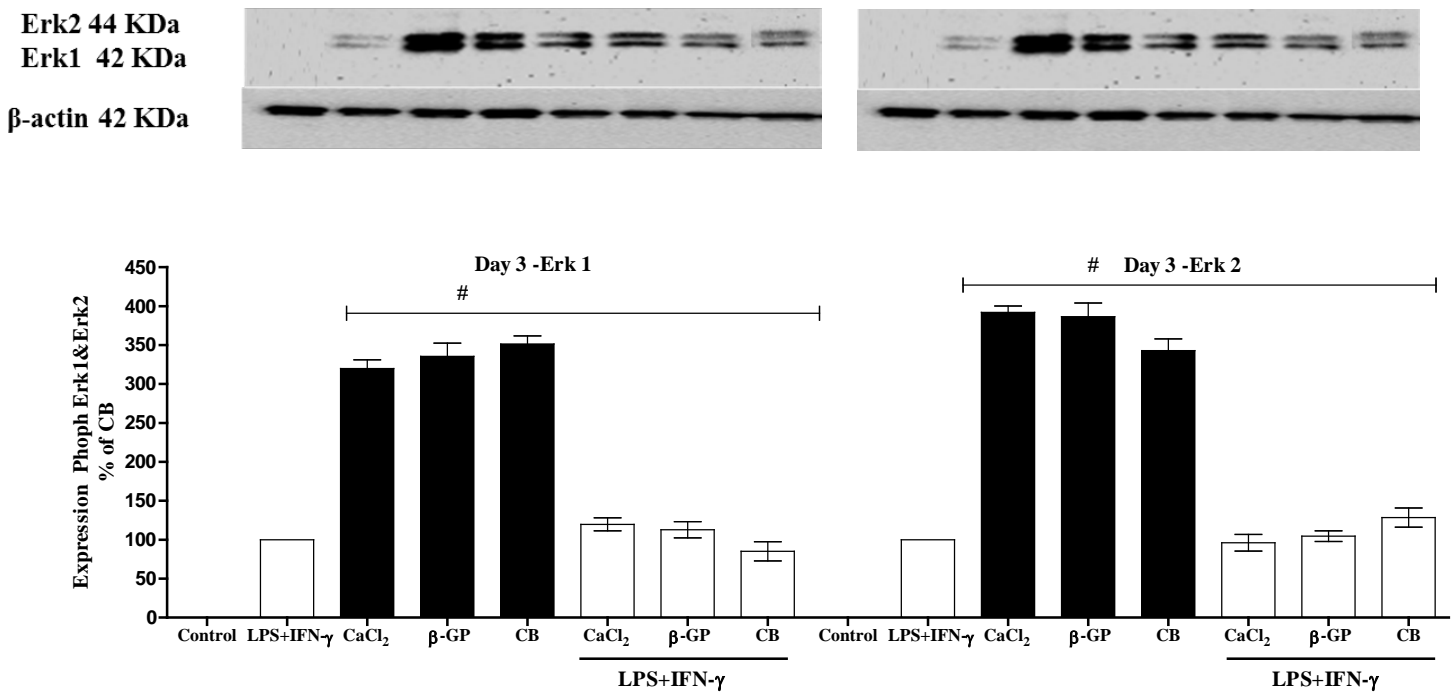
Figure 6.5: Effects LPS+IFN-γ with and without CaCl₂, β-GP, or CB on phosphorylation of Erk1/2 in RASMCs.

Cells were cultured to ~90% confluency and incubated with culture medium alone (control), LPS (100 μg ml⁻¹) + IFN-γ(100 U ml⁻¹) for 24 hours followed the addition of CaCl₂ (7mM), β-GP (7mM) or CB in the continued presence of LPS plus IFN-γ and incubated for a further period of 3 days. The data is represented as % change of Erks taking the LPS+ IFN-γ response as 100%. Phospho Erks expression were determined by western blotting using a phosphor-specific Erks monoclonal antibody as described in the methods (Section 2.10).The values represent means ± S.E.M. from 3 individual experiments. # denotes $p<0.05$ and compared to calcification inducers with LPS+ IFN-γ .

6.3.4-Effects CaCl₂, *β*-GP, CB with/without LPS+IFN-γ on Runx2 expression in RASMCs:

Cells coincubated with medium alone did not show significant expression of Runx2. However, activation of cells with LPS+IFN-γ resulted in expression of Runx2 at day 1 followed by a declined thereafter day 3 and 5 as shown in Figure 6.6. The use of the calcification inducers independently induced Runx2 expressions which were higher than the levels seen with LPS+IFN-γ. Moreover, the responses unlike those seen with LPS+IFN-γ, were sustained over the time course of the experiments. Coincubation of CaCl₂, *β*-GP or CB with LPS+IFN-γ resulted in a suppression in levels of Runx2 at days 3 and 5 which were well below the levels seen even with LPS+IFN-γ alone (Figure 6.6).

.
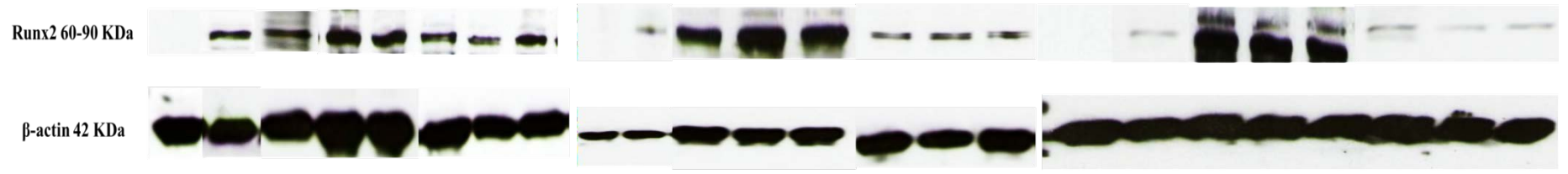
Control	+	-	-	-	-	-	-	-	+	-	-	-	-	-	-	-	+	-	-	-	-	-	-
LPS+IFN-γ	-	+	-	-	-	+	+	+	-	+	-	-	-	+	+	+	-	+	-	-	-	+	+
CaCl$_2$	-	-	+	-	-	+	-	-	-	-	+	-	-	+	-	-	-	-	+	-	-	+	-
β-GP	-	-	-	+	-	-	+	-	-	-	-	+	-	-	+	-	-	-	-	+	-	-	+
CB	-	-	-	-	+	-	-	+	-	-	-	-	+	-	-	+	-	-	-	-	+	-	-
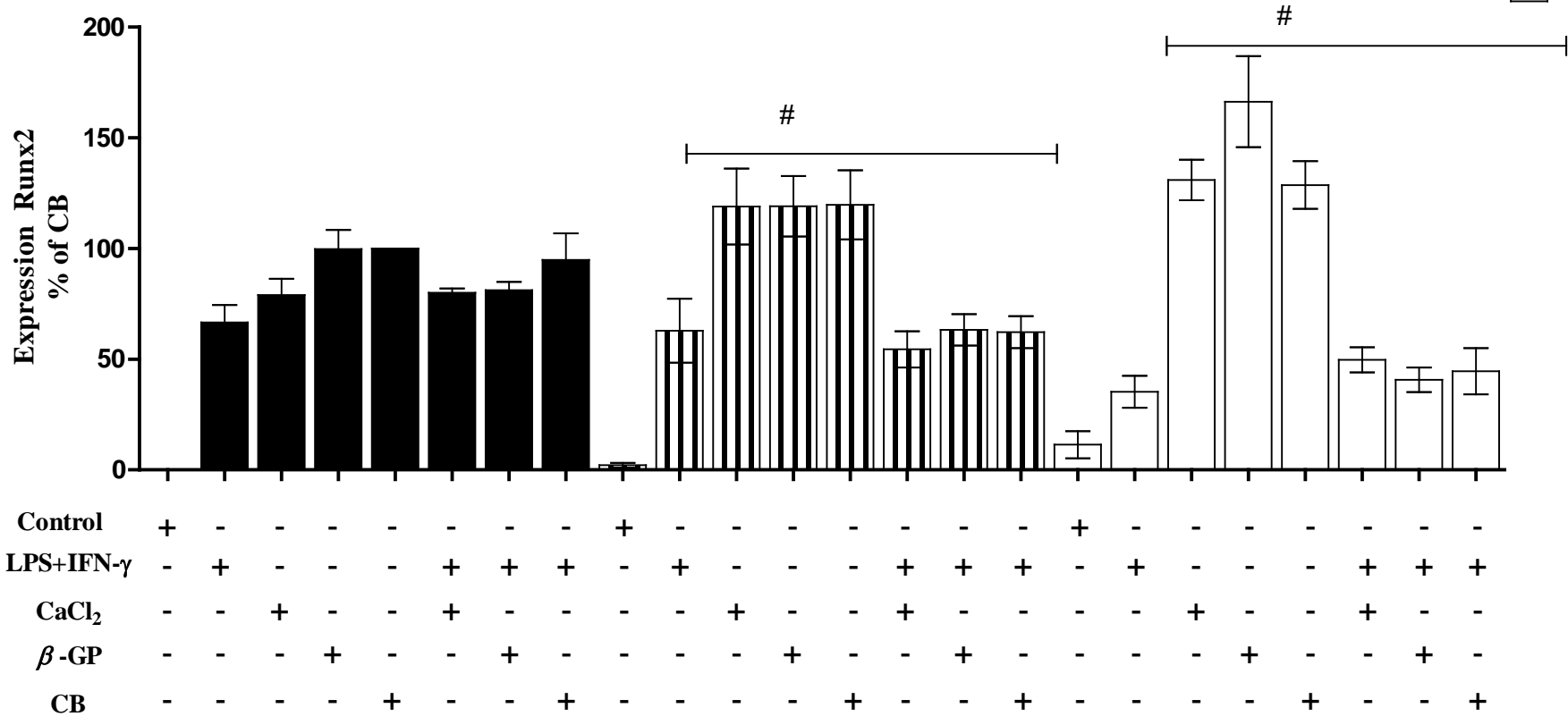
Figure 6.6: Effects LPS+IFN-γ with and without CaCl₂, *β*-GP, or CB on Runx2 in RASMCs.

Cells were cultured to ~90% confluency and incubated with culture medium alone (control), LPS (100 µg ml^{-1}) + IFN-γ(100 U ml^{-1}) for 24 hours followed the addition of CaCl$_2$ (7mM), *β*-GP (7mM) or CB in the continued presence of LPS and IFN-γ and incubated for a further period of 1, 3, and 5 days. The data is represented as % change of Runx2 taking the CB response at day 1 as 100%. Runx2 expression were determined by western blotting using Runx2 monoclonal antibody as described in the methods (Section 2.10).The values represent means ± S.E.M. from 3 individual experiments. # denotes *p*<0.05 and compared to CB alone.

6.3.5- Effect of GW274150 on LPS+IFN-γ, CB or in combination on Runx2 expression in RASMCs:

Our previous results showed that incubation of cells with GW274150 at 100μM caused significant inhibition of calcification especially when cells were treated with CB+LPS+IFN-γ at day 3 and this time period was selected as previous experiments had indicated that maximum calcification in RASMCs was achieved at day 3.Further experiments have therefore been carried out to establish whether GW274150 regulated Runx2 expression.

As can be seen from Figure 6.7, the control cells did not showed any expression of Runx2. However, activation of cells with LPS+IFN-γ with/ without inhibiting the activity of iNOS using GW274150 resulted in no changes in the expression of Runx2 (Figure 6.7). Furthermore, GW274150 did not caused any significant changes in Runx2 in cells treated with CB or with CB in the presence of LPS+IFN-γ (Figure 6.7). Thus, it seems GW274150 does not have any significant effect on Runx2 expression induced by LPS+IFN-γ or by CB and may therefore not regulate calcification through suppression of this transcription factor.
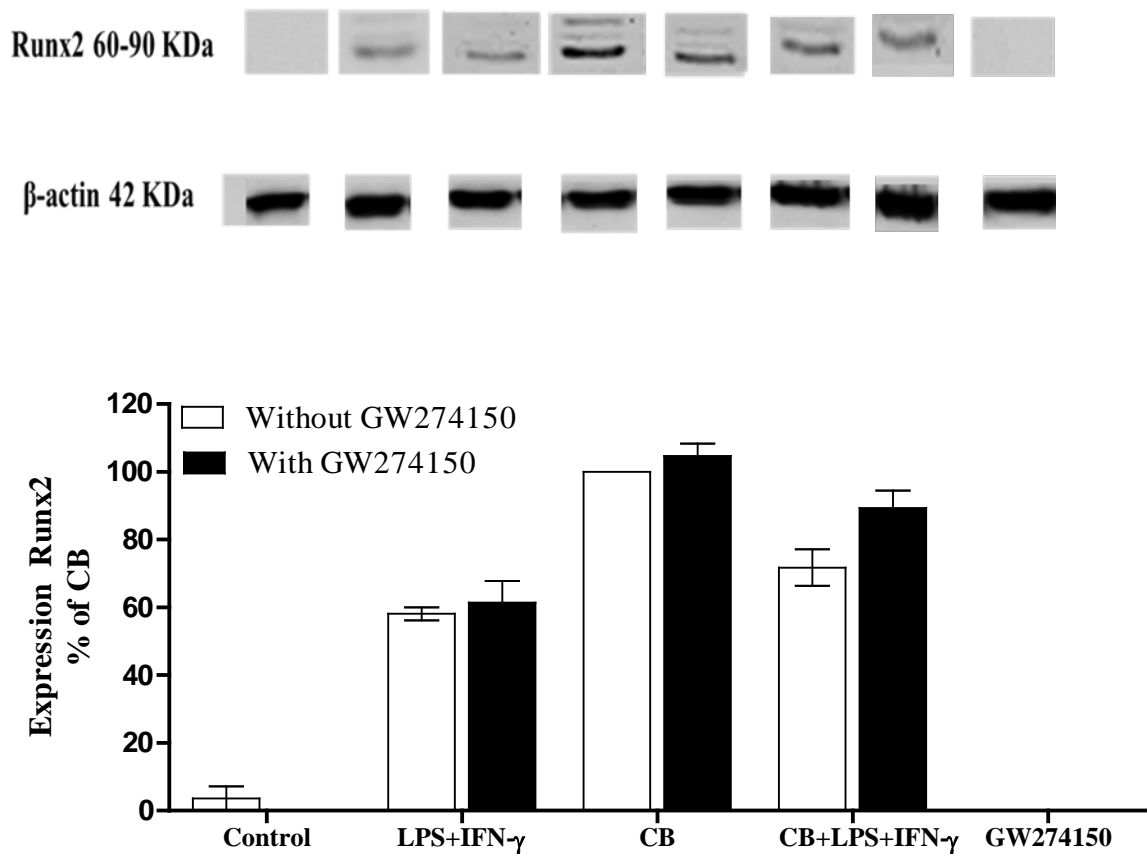
Figure 6.7: Effect of LPS + IFN-γ, CB with/ without GW274150 on Runx2 in RASMCs

Cells were cultured to ~90% confluency and incubated with culture medium alone (control), LPS (100 μg ml^{-1}) + IFN-γ(100 U ml^{-1}) for 24 hours followed the addition of CB (7mM; CaCl$_2$+ 7mM; *β*-GP) in the continued presence of LPS and IFN-γ with/without GW274150 at 100μM and incubated for a further period of 3 days. The data is represented as % change of Runx2 taking the CB response as 100%. Runx2 expression were determined by western blotting using Runx2 monoclonal antibody as described in the methods (Section 2.10).The values represent means ± S.E.M. from 3 individual experiments.

6.4- Discussion:

As discussed in the previous chapters, inflammatory mediators such as LPS and IFN-γ play a critical role in the induction of calcium levels leading to enhanced VC. The experiments in this chapter were conducted to understand the signalling mechanisms that may regulate calcification and establish whether these overlap with those that regulate iNOS expression and thus NO production. Several studies have considered the phosphorylation of p38 MAPK, Akt and Erks to be among the primary targets for activation leading to iNOS expression (Chan *et al.*, 2001; Liao *et al.*, 2008; Zhao *et al.*, 2012).

Experiments in chapter 5 investigated the importance of NO on calcification of RASMCs incubated with different NO donors such as NOC 18 and SNP. The results showed that cells concinubated with the slow NO producer NOC 18, especially in the presence of CB caused elevations of calcium levels, as well as plaque formation, which was confirmed by positive staining with ARS. The selective iNOS inhibitors, GW274150, was subsequently used to confirm whether the NO derived from iNOS regulated calcification, and the results showed that concentrations lower than 100μM of GW274150 suppressed NO production, which in turn enhanced calcium levels. This suggests that NO may suppress calcification. Further experiments may however be needed to conclusively demonstrate this. There may be a threshold concentration of NO, below which calcification is inhibited, while above this level calcification may be promoted by NO.

The current study demonstrates that cells incubated with LPS and IFN-γ resulted in induction of p38 MAPK. Interestingly, inducers of calcification also induced phosphorylation of p38 MAPK. Of these, the highest level of activation was with $CaCl_2$ or *β*-GP by themselves, although this was not dissimilar to the level seen when they were combined in CB.

However, with CB the levels of p38 MAPK were sustained over 5 days at over 120% of that induced by LPS+IFN-γ. In combination with any of the calcifying agents, when observed over 5 days, the presence of LPS+IFN-γ modulated the effect of the agents to reduce the level of p38 MAPK activation. Thus, NO production via iNOS may reduce p38 MAPK activation through an unknown mechanism. Moreover, when observed over 48 hours the highest level of p38 MAPK activation was noted with CB alone at 24 hours, which was greater than that with LPS or LPS+IFN-γ.

Using the Akt inhibitor LY294002 in the presence of LPS+IFN-γ had a significant effect of p38 MAPK phosphorylation, while the use of the inhibitor SB203580 with LPS+IFN-γ which blocks both of p38 MAPK and Akt; had the greatest reduction effect in activating p38 MAPK. Identifying the reason for this needs further investigation, as it cannot be attributed only to an increase of iNOS/NO production.

As this coincides with the induction of iNOS, it is reasonable to speculate that calcification inducers regulated iNOS expression and NO production, which was reported in chapter 4 through phosphorylation of p38 MAPK. It is clear now that NO promotes the progression of calcification in RASMCs, as the experimental evidence shows that when RASMCs were activated by LPS + IFN-γ and when either CB or $CaCl_2$ was present, an elevation of NO through iNOS was obtained. This in turn induced increases in calcium levels above the control, and these increases led to the formation of HA crystals, which were indicative of calcification.

From the literature, it is known that LPS and IFN-γ have signal transduction at the cell surface. LPS binds the LPS binding protein which ligands the CD14, and this stimulates intracellular signalling via TAK1-Binding Protein-1 to activate downstream phosphorylation of p38 MAPK (Choi *et al.*, 2012).

Cross talk at the TLR4 activates NF-kB downstream which induces expression of iNOS. On the other hand, IFN-γ binding to the IFN receptor stimulates the downstream expression of IRF1. This in turn increases the half-life of iNOS mRNA. However, the mechanism of LPS and IFN-γ promotion of calcification in RASMCs is still undetermined. Nevertheless it is known that an in alternative pathway involving the NF-kB ligand RANKL, binding of RANKL to its receptor at the cell surface activates downstream signalling to promote calcification via increased BMP4 expression (Panizo *et al.*, 2009; Walsh *et al.*, 2014). Furthermore, there may be another unknown pathway which is yet to be identified that produces the synergistic effects observed. Several factors are possible for having a role in linking iNOS expression/NO production with calcification. These include p38 MAPK, Akt and Runx2. The phosphorylation of p38 MAPK activates its signal pathway which can result in increased iNOS expression. This can be blocked by a specific inhibitor in smooth muscle cells (Jin *et al.*, 2014).

Activation of the p38 MAPK pathway has also been found to be involved in the calcification of smooth muscle cells. These evidences together provide a good case for investigating a link between NO and calcification via p38 MAPK phosphorylation. It is important to state that conclusions about the role of p38 MAPK in inducing iNOS cannot be made as the levels of iNOS and calcification were not quantified in this study. This work is recommended for the future. One way to investigate this would be to compare the calcification achieved when p38 MAPK is inhibited.

The induction of p38 MAPK may also contribute to the calcification process and in support of this, studies have found that calcifying agents and IL-6 contribute to the stimulation of the p38 MAPK and Akt but not to the Erk1/2 signalling molecules, especially at 24 hours of incubation. This may directly enhance matrix mineralisation (Abedin *et al*, 2006).

In addition, the calcification aortic valve interstitial cells (AVICs) has been reported to involve p38 MAPK (Cortizo *et al.*, 2006) and inhibiting p38 MAPK caused a reduction of the calcification process in osteoblast cells (Deng *et al.*, 2014). In contrast, the mineralisation of smooth muscle cells has been shown to be regulated through Akt at an earlier time course (24 hours) followed by a decline at later time, although this may not be related. The selection of this earlier time course was based on the findings of previous study (Abedin *et al.,* 2006).

Our study found that the phosphorylation of Akt was highest at 24 hours with CB alone, this being greater than when LPS+IFN-γ and CB were together in the media or LPS+IFN-γ alone. It appears at 24 hours that iNOS/NO by LPS+IFN-γ may be modulating Akt phosphorylation. However, at 48 hours the greatest phosphorylation of Akt was due to LPS+IFN-γ and CB together. Thus, it may be that CB activates phosphorylation of Akt earlier than LPS+IFN-γ. Using the inhibitor SB203580 activity of Akt was reduced with LPS+IFN-γ present, but using LYS294002 gave the greatest reduction to approximately 25% of that seen with LPS+IFN-γ. Again due to the actions of these inhibitors identifying the reason for this needs further investigation. Comparing p38 MAPK activation with Akt activation, both had a peak at 24 hours. Both were also most activated by calcification inducers alone. Put together these suggest a common upstream activation point.

Our data has demonstrated that the treatment of cells with LPS+IFN-γ lead to the activation of phosphorylation p38 MAPK, causing the iNOS protein in smooth muscle cells to reach a maximum at 48 hours. Moreover, cells coincubated with LPS + IFN-γ caused activation of Akt at earlier time course (24 hours). The amount of calcium detected with inflammatory mediators was also significantly induced compared to the response of control cells. These results are in agreement with previous studies in which IL-6, LPS and TNF-α also exerted similar effects through phosphorylated p38 MAPK (Chan *et al.*, 2001).

Moreover, cells incubated with LPS + IFN-γ in the presence of calcification inducers promoted the induction of the extracellular matrix mineralisation with much more elevated levels of calcium than measured with the calcifying agents only. Significant phosphorylation of p38 MAPK was detected at an earlier incubation time point, especially at 18 and 24 hours, but was not detected at days 3, and 5. This could mean that p38 MAPK was stimulated at an earlier time course in which its activation potentiates the action of calcification performed on iNOS expression during a longer period of time. However, beyond 3 days the mineralisation on RASMCs is not regulated by p38 MAPK, but rather another pathway is involved. In addition, Abedin and coworker indicated that Erk1/2 was not phosphorylated at 24 hours. Therefore, the activation of Erk1/2 by phosphorylation only at day 3 was investigated. From our results in the case of Erk1/2, the regulation of calcification induced in RASMCs via NO release by iNOS did not appear to be regulated via the phosphorylation of Erk1/2. Following Erk1 and Erk2 over 3 days indicated that the CB alone induced the greatest level of phosphorylation, which were all very similar. When combined with LPS+IFN-γ the levels of phosphorylation were reduced to around one third. This suggests that iNOS/NO reduced the activation of Erk1 and Erk2 in RASMCs, while calcium levels and calcification increases this.

The phosphorylation of Erk1/2 occurred independently of NO using of $CaCl_2$ or β-GP alone, or in combination. This suggests a role for Erk1/2 in the regulation of calcium levels in the cell. The role of Erk1/2 has been investigated in other disease pathologies (Rodríguez-Peña *et al.*, 2008) not related to VSMCs, where they appear to have a role in initiating the apoptotic cascade. Moreover, Erk1/2 has been shown to activate transcription factors involved in early gene responses (Roskoski, 2012). Erk1/2 activation is inhibited by U0126.Therefore, future studies should further investigate whether Erk1/2 is activated earlier than 3 days, whether the involvement of Erk1/2 in regulation of calcium is related to calcification and what is the

effect of using the inhibitor U0126 to block Erk1/2 phosphorylation on the calcification of RASMCs.

Considering the link between Runx2 and calcification, Runx2 was investigated in this study to see whether it contributes to the induction of calcification in our studies. As identified in studies detailed in previous chapters calcification was evident at day 1, peaked at day 3, and declined thereafter. Therefore, this time course was selected to determine whether Runx2 was active during the period, and whether a trend in activation matched the trend of calcification of RASMCs induced via iNOS production of NO. It is clear from the results that RASMCs incubated with calcification inducers alone activate the signalling pathways of p38 MAPK, Erk1/2, and Akt. However, no evidence was found for the involvement of Runx2 in linking iNOS induction/NO to calcification in VSMCs. The presence of inflammatory mediators with calcifying agents did not cause any significant changes either with p38 MAPK or Runx2 at longer time intervals. This action does not seem to be regulated through p38 MAPK or Runx2, a finding not consistent with other studies for various cell lines, bone cells, and stem cells, excluding smooth muscle cells. Based on these finding, Artigas and coworker explains that the activation of p38 MAPK results in an interaction between ostrix and Runx2, which in turn causes calcification in C2C12, Saos-2, and HEK-293T cell lines (Artigas *et al.*, 2014). Furthermore, the activation of receptors of BMP9 stimulate the pathways of p38 MAPK and Erk1/2, which further potentiate pro-calcific markers such as ALP and OC into C3H10T1/2, C2C12, HEK293, and HCT116 cell lines (Mesenchymal Progenitor Cells) (Li *et al.*, 2002). Interestingly, Lin and colleagues recently published their findings that Runx2 is necessary for the calcification of smooth muscle cells in mouse arteries, induced via vitamin D overload. Here Runx2 alters the cell phenotype to become osteogenic (Lin *et al.*, 2015). However, its action does not involve altering either serum calcium or phosphate. Our study seems to agree with these findings. Thus, the Runx2 pathway does not feed directly into the pathway by

which iNOS expression is induced. Future studies could be conducted to determine the role of Runx2 in the rat using the methods described from Lin and colleagues. It was also found that the inhibitors of p38 MAPK can reduce the expression of Runx2 and Smads signalling molecules (Franceschi *et al.*, 2003; Zhao *et al.*, 2012). Thus, the calcified smooth muscle cell is regulated through p38 MAPK, which in turn significantly activates Runx2 in different cell line involving smooth muscle cells. Whether the release of NO by iNOS induced calcification needs to be determined in RASMCs.

A recent study has highlighted a possible meeting point on the p38 MAPK, Akt, Erk1/2 and Runx2 pathways. The enzyme vascular peroxidase 1 appears to be necessary for downstream activation of these pathways, as knocking down the gene in VSMCs inhibited calcification. It is thought that the production of hypochlorous acid by this enzyme activates the pathways identified above (Tang *et al.*, 2015). However, the role of iNOS in this process has not been determined.

Based on the observations in this study, RASMCs coincubated with calcification inducers in the absence of LPS+IFN-γ were found to produce a significantly greater amount of Runx2, while the cells incubated with calcification inducers and LPS+IFN-γ produced less Runx2. The amount of calcium/calcification was however significant in RASMCs coincubated with calcification inducers and LPS+IFN-γ. The relevance of the reduction in Runx2 remains to be established. For example, cells incubated with calcification inducers only showed a significant induction of Runx2, and this supports the claim that RASMCs differentiate into osteoblast-like cells upon induction of artheroma. If Runx2 is not expressed, cells may develop into chondrocyte-like cells instead, although the amount of calcium and the formation of HA crystal were also extensively detected in the results for chapter 4.

A literature review has demonstrated that calcification of mesenchymal progenitor cells could differentiation into hypertrophic chondrocyte caused by chondrogensis marker [sex determining region Y (Sox9)], considered to be a negative regulator, whereas the activity of Runx2 controlled calcification acting as a positive regulator (Ikegami *et al.*, 2011; Zhou *et al.*, 2006). Another suggestion that may be of relevance in our study is that incubation of cells with calcification inducers in the presence of LPS+IFN-γ might potentiate Sox9 leading to calcification. This suggestion needs to be confirmed, but agrees with a study demonstrating that *β*-GP resulted in the induction of Cbfa1, Msx2, and Sox9, but was inhibited by magnesium in BVSMCs (Kircelli *et al.*, 2011). This also raises the possibility that in our *in vitro* model cells may be differentiating to chondrocytes like cells and not to osteoblast like cells. Thus, Runx2 may not play a significant role in calcification of smooth muscle cells activated by inflammatory mediators and calcification inducers.

As mentioned before, high concentration of GW274150 inhibited the expression of iNOS and it has been at 100 μM, meaning that GW274150 possibly acts upstream of iNOS induction in a manner non selective for iNOS. Interestingly, GW274150 did not cause any significant changes to Runx2 expression in RASMCs when the cells were activated with CB+LPS+IFN-γ in the presence of GW274150 compared to the presence of CB+LPS+IFN-γ alone. Furthermore, when the cells were incubated with CB in the presence of GW274150 there was no effect on Runx2 expression compared to CB alone. Thus, it may be possible to conclude that there is no link between NO/iNOS and Runx2. Therefore, there may be another transcription factor, which binds another gene, that it has not been identified by this study through which GW274150 achieves a reduction of smooth muscle calcification which is independent of Runx2.

Conclusions can be drawn from the work detailed in this chapter. Firstly, calcifying agents alone were able to induce phosphorylation of p38 MAPK, Akt, and Erk1/2. Together, these results indicate that these signalling molecule may be involved in the induction of calcification by the calcifying agents; $CaCl_2$, β-GP and CB leading to activate Runx2. Secondly, iNOS/NO induced calcification by the presence of inflammatory mediators and calcifying agents appears to be involved in reducing the activation of p38 MAPK, Akt, and Erk1/2 via unknown mechanism. Lastly, Runx2 does not appear to be involved in the calcification of RASMCs specifically by iNOS/NO which another alternative pathway may be involved in this. Figure 6.8 illustrates the mechanistic of action for calcified smooth muscle cells in the presence or absence of inflammatory mediators.
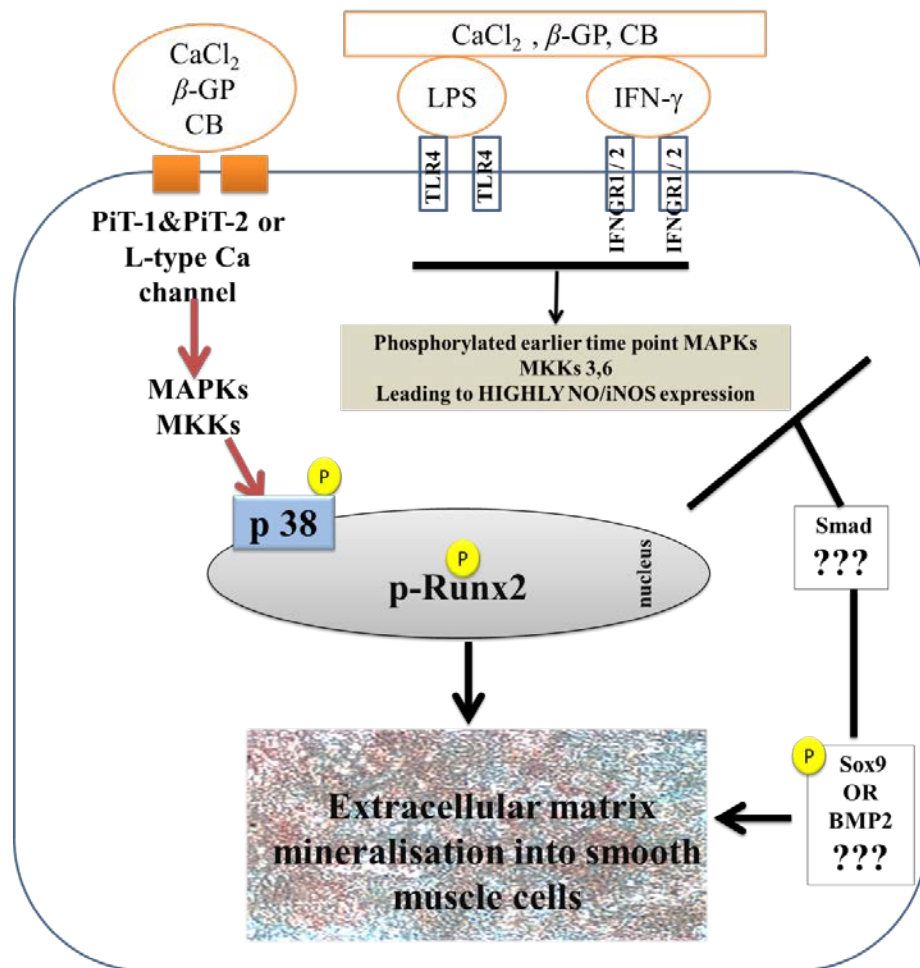
Figure 6.8: Potential mechanism of VC is caused with/without NO production /iNOS in RASMCs.

CHAPTER VII

General discussion, Conclusion, and Limitations & future work

7.1-Discussion:

The studies described in this thesis were conducted in order to understand the role of NO/iNOS in relation to the potential mechanisms that may mediate the induction of calcification in RASMCs. In addition, parallel studies were carried out to establish whether the iNOS pathway may be regulated under conditions that induce VC in RASMCs, with a view to determining whether under the latter condition iNOS expression and thus NO production may be regulated in such a way that it in turn regulates the process of calcification. These studies in their entirety were initiated to clarify whether NO protects against or promotes VC. Indeed, as already highlighted, there are reports that NO production by iNOS protects against VC (Cao *et al.*, 2013; Kanno *et al.*, 2008) but these findings do not agree with other research, in various other cell types that suggests NO may enhance the mechanism of VC (Zaragoza *et al.*, 2006; Yasuhara *et al.*, 2007).

The table below summarises the findings of the current research:

Table 7.1: The Importance of findings in the current study

Aim/research question	Factor tested	Result	Conclusion or inference
Validation of *in vitro* calcification model (Patidar *et al.*, 2013)	Calcification model	There are differences in the absolute (no NO produced) versus cumulative levels of NO (by inflammatory mediators) in experiments	Changing the cell culture media daily may represent a better model of the *in vivo* environment i.e. a constant flow of blood/fluid through the artery.
Can calcification be induced using $CaCl_2$ and/or *β*-GP?	$CaCl_2$	• Elevated calcium. • No plaque formation. • No HA.	$CaCl_2$ independently induced mineralisation.
	β-GP	Little change in calcium.	*β*-GP alone showed little effect
	CB	• Elevated calcium. • Plaque formation. • HA crystals.	• Both $CaCl_2$ and *β*-GP required for calcification. • Low calcium limits calcification *in vivo*. • Low *β*-GP limits calcification *in vivo*.
Does NO production regulate calcification?	LPS	• Marginal induction of iNOS accompanied by NO production. • Elevated calcium. • No HA.	• Other factors required for HA formation are missing.
	IFN-γ	• Limited iNOS/NO. • Elevated calcium. • No HA .	• IFN-γ stabilises iNOS mRNA in the cell. • Other factors required for HA formation are missing.
	LPS + IFN-γ	• Significant induction of iNOS peaking at day 3 accompanied by elevated NO production. • Elevated calcium.	• Other factors required for HA formation are missing.

	LPS + CaCl$_2$, or β-GP	• Induction of iNOS accompanied by NO production. • No HA	• iNOS/NO do not cause mineralisation of VSMCs. • iNOS/NO increase may be due to calcium enhancement.
	LPS + CB	• Induction of iNOS accompanied by NO production. • HA crystals.	
	IFN-γ + CaCl$_2$, or β-GP	• iNOS not produced. • marginal increase in NO. • Greater elevation of calcium compared to CaCl$_2$, or β-GP alone. • Significantly higher than LPS alone or in combination with CaCl$_2$,/β-GP/CB.	• Source of NO may be iNOS- limit of detection by Western blot. • Future work to confirm no iNOS mRNA using qPCR analysis. • IL-1 levels too low for iNOS induction.
	IFN-γ + CB	• Induction of iNOS/NO produced. • HA crystals.	• IFN-γ may cause hypercalcemia by direct action on 1alpha-OHase.
	LPS + IFN-γ + β-GP	• Induction of iNOS/NO produced. • No HA crystals • β-GP modulates elevation of calcium.	• Extracellular calcium required for HA mineralisation of VSMCs. • β-GP modulates elevation of calcium.
	LPS + IFN-γ +CaCl$_2$ or CB	• Induction of iNOS/NO produced. • Faster rate of calcification compared to CB alone. • HA crystals.	• Induction of iNOS linked to levels of calcium • LPS + IFN-γ enhance rate of calcification.

Does preincubation with LPS and/or IFN-γ before addition of calcifying agents induce mineralisation?	The effect of preincubation with LPS and/or IFN-γ.	• Elevated levels of calcium.	• iNOS causes increase in calcium levels. This is an 'additive effect'.
Does preincubation with CaCl$_2$ / β-GP / CB before addition of inflammatory mediators induce iNOS?	The effect of preincubation with CaCl$_2$ / β-GP / CB.	• iNOS only present at 18 – 48 hours post incubation.	• calcium induces iNOS expression via a different pathway to LPS and IFN-γ.
Does the induction of iNOS/NO regulate calcification?	The effect of LPS and IFN-γ on calcification.	• A significant increase in iNOS/NO. • A significant increase in calcium.	• CB may modulate NO and iNOS production in RASMCs. • Either, LPS+IFN-γ modulates the activity of plasma membrane calcium channels indirectly, or causes the release of calcium stores in VSMCs, via an alternative pathway. • NO may enhance mineralisation of VSMCs. • Expression of iNOS enhanced under calcifying conditions – may lead to increased risk of plaque formation *in vivo* • Further *in vivo* investigation needed in animal model.
What is the effect of GW274150?	Presence of NO on calcium levels	• NO production inhibited at 10, 50 and 100µM. iNOS expression inhibited at 100 µM except 10 and 50 µM • Calcium elevated marginally at 10 µM and 50 µM when either LPS +IFN-γ or CB	• At high concentration GW274150 may non-selectively inhibit iNOS expression.

		alone not LPS +IFN-γ+CB significantly inhabited elevation of calcium. • Calcium levels lower with 100 µM GW274150 when either LPS +IFN-γ or CB alone. • Lower elevation of calcium when LPS +IFN-γ+CB at all concentrations of GW274150.	• Unknown cause of lower calcium levels.
Does inhibition of iNOS effect mineralisation of VSMCs?	Effect of NO on mineralisation	• GW274150 eliminated HA formation.	Lower levels of NO linked to elimination of HA formation. • NO is necessary for mineralisation.
What is the effect of the presence of NO from NO donors?	Presence of NO without iNOS	• Significant elevation of calcium. • HA crystals in presence of slow releasing donor NOC 18 (30 and 50 µM) prior to addition of CB. • No HA crystals in presence of fast releasing donor SNP.	• Elevation of NO when CB + LPS +IFN-γ are present is due to some interaction effect in RASMCs. • Sustained release of NO may contribute to increased mineralisation. • Fast NO release had on effect on calcium level.
Is p38 MAPK involved in the signalling pathway for NO production?	Effect of inflammatory mediators on p38 MAPK activation.	• Significant increase in p38 MAPK phosphorylation due to LPS at 18 hours onwards.	• There is common point for p38 MAPK pathway and the iNOS induction pathway at 18 hours.
Is p38 MAPK involved in the signalling pathway involving elevation of calcium?	Effect of calcifying agents p38 MAPK activation	• Increase in p38 MAPK phosphorylation by CB only	• Calcium involved in activation of p38 MAPK pathway by calcifying agent only in absence of NO via iNOS

Is Akt involved in the signalling pathway for NO production?	Effect of inflammatory mediators on Akt activation.	• No significant increase in Akt phosphorylation with inflammatory mediators.	• No evidence for convergence of NO production and Akt pathway.
	Effect of calcifying agents on Akt activation	• Significant increase in Akt phosphorylation when CB present at early time point (12-24 hours)	• There is common point for the Akt pathway and the pathway elevating calcium
Is Erk1/2 involved in the signalling pathway for NO production?	Effect of inflammatory mediators or calcifying agents on Erk1/2 activation.	• calcifying agents only caused significant induction of phosphorylation at day 3	• Calcium modulates activation of Erk1/2 signalling pathway in VSMCs
Is Runx2 involved in the signalling pathway for NO production?	Effect of inflammatory mediators or calcifying agents on Runx2 levels	• calcifying agents only caused significant induction of Runx2 at day 3 and 5 • Runx2 lower with LPS+ IFN-γ compared to calcifying agents.	• No link could be established between the activation of p38 MAPK or Akt and Runx2 when NO presence via iNOS • Calcium promotes Runx2 levels linked to activation of p 38 MAPK when absence of NO via iNOS
Is the inhibitory effect of GW274150 on iNOS expression via Runx2?	Effect of NO on Runx2	• Levels not significantly altered at day 3	• NO/iNOS does not have a role in the Runx2 induction pathway.

The findings of the research suggest that LPS activates the expression of iNOS and hence the levels of NO increase. In terms of IFN-γ, by itself this can cause elevation of calcium levels but does not increase expression of iNOS. Previous studies have shown IFN-γ to stabilise iNOS mRNA (Wileman *et al.*, 1995). However elevated phosphate and calcium also activate the iNOS expression, via an alternate uncharacterised route. Thus, the presence of just the calcifying agents is sufficient to induce mineralisation of VSMCs. Furthermore, the experiments where VSMCs were preincubated with calcifying agents showed iNOS

expression from 18 hours post incubation, again suggesting that calcifying agents induce iNOS expression by an alternative pathway to LPS, and modulate the level of NO.

This increased expression of iNOS may contribute to an increased risk of plaque formation *in vivo*. This phenomenon needs further exploration in the animal model to confirm the biological action in organs.

When one or both inflammatory mediators and both calcifying agents, i.e. calcium and phosphate are present in the vascular smooth muscle environment, the effect of these substances is additive such that the level of NO is enhanced. This in turn accelerates the mineralisation process. A low level of calcium can limit the formation of HA crystals. The inflammatory mediators in combination can also increase the level of calcium in the VSMCs. Without the presence of IFN-γ, LPS and calcifying agents can cause mineralisation of cells, but both calcium and phosphate need to be elevated. Thus, even though NO is elevated, no HA is observed when either calcium or phosphate is low. This provides support for the idea that NO by does not cause mineralisation of VSMCs, rather it can contribute to increased mineralisation.

Without LPS there appeared to be no induction of iNOS, despite NO being elevated. This may be because the limit of detection by Western blot could not confirm the presence of iNOS mRNA. This can be confirmed in the future using qPCR analysis. However again a suggestion of an alternate source of iNOS generation, e.g. another enzyme may be possible. This needs to be further explored. There may also be other unidentified limiting factors for iNOS expression.

When both LPS and IFN-γ are present without any calcifying agents being added, the levels of calcium are elevated either by their indirect action on calcium channels of by in induction of release of calcium stores in VSMCs, via an alternative pathway. This however does not

result in HA crystal formation, despite NO being elevated; again supporting the idea that NO by itself is insufficient to cause vascular mineralisation.

Using the iNOS inhibitor GW274150 produced a significant novel result. While at 10 and 50 µM, its effect was inhibition of enzyme activity; at 100 µM its action involved possible upstream reduction of iNOS expression as a reduction of calcium elevation. Thus suggest a complex effect on the cell at physiologically high concentrations. GW274150 also eliminated mineralisation, suggesting that in contrast to previous experiments NO may an essential requirement for HA formation. However, using the donor of NO suggested that the level of NO may be less important than the speed of NO release. A slow sustained release of NO by NOC18 produced HA crystals in contrast to a fast release by SNP. The slow release is similar to what occurs in chronic inflammation, whereas fast release is acute, similar to an injury that is repaired by the immune system and cell repair mechanisms. Thus, the nature of NO release becomes the key factor. In fact, fast release of NO may be protective against mineralisation of VSMCs due absence of HA crystal even when CB was present. The literature survey suggests that evidence points towards NO being protective against vascular mineralisation (Kanno *et al*.,2008), as NO acts as a secondary messenger in the cell molecule. However, due to the toxic nature of NO, prolonged elevation of NO specifically inhibits mitochondrial respiration via the electron transport chain. This contributes to the cytotoxicity of NO.

Lastly, when examining selected secondary messenger signalling pathways, the results suggested that NO and calcifying agents both enhance mineralisation, with additive effect, possibility independent on the activation of the p38 MAPK and Akt signalling pathways. Although, these two pathways are already well established in the literature in relation to other phenomenon. In terms of vascular calcification, Akt appears to be activated during smooth muscle injury (Fitzgerald *et al.,* 2008, Stabile *et al.,* 2003), or by inflammatory mediators (Hattori *et al.,* 2003, Okazaki *et al.,* 2009), which promotes expression of iNOS and

calcification. Akt involvement is also implicated in VSMC apoptosis (Allard *et al.,* 2008). Mitogen activated protein p38 MAPK is activation is linked to promotion of vascular calcification (Abedin *et al*., 2006), and increases in apoptosis (Liao *et al.,* 2013, Yang *et al.,* 2000, Loidl *et al.,* 2004). Furthermore, activation of p38 MAPK regulates expression of amino acid transporter such as the L-arginine transporter in vascular endothelium (Huang *et al.,* 2004), and this links to an increase in NO production via iNOS.

No involvement of Erk1/2 or Runx2 pathway activation was observed in the mineralisation process via NO produced /iNOS in the current study. A review of the literature indicates only a limited number of studies involved the study of Erk1/2 or Runx2 in VSMCs. Liao et al., 2008 found that *β*-GP induced osteoblastic differentiation of VSMCs possibly through the activation of Erk1/2. Osteogenic differentiation was also linked to Erk1/2 by Huang and colleagues (2013b). While Tang *et al.,* (2015) identified vascular peroxidase 1 production of hypochlorous acid being responsible for promoting activation of Akt, Erk1/2 and p38 MAPK, as well as expression of Runx2. In mice Runx2 deficiency has been linked to protection against vascular calcification (Sun *et al.,* 2012), and that Runx2 regulates change of smooth muscle phenotype to osteoclast phenotype during atherosclerosis (Byon *et al*., 2011, Xia *et al.,* 2015, Zhang *et al.,* 2014).

A deeper exploration of signalling pathways and other pro-calcific factor (such as BMP2) could show a novel mechanism in VSMCs. Table 7.2 below summarised the changes in signalling molecule activity over time course in VSMCs.

Table 7.2: The effect changes of signalling molecule activity by inflammatory mediators during time course in VSMCs.

Inflammatory mediators	Signalling molecule	Start and peaked time point (minutes)	Citation
LPS	p 38 MAPK	activated at30 minutes then declined thereafter	(Jacob *et al.*, 2005)
	p 38 MAPK	15 minutes and returning to the baseline at 120 minutes.	(Ohashi *et al.*, 2000; Jiang *et al.*, 2010)
	p 38 MAPK	30 minutes and sustained up to 240 minutes.	(Yamakawa *et al.*, 1999)
LPS+IFN-γ	p 38 MAPK	Start at 30 minutes and peaked at 60 minutes following the declined thereafter between 120 -240 minutes.	(Lamon *et al.*,2010)
LPS	Erk1/2	30 minutes and sustained up to 240 minutes.	(Yamakawa *et al.*, 1999)
LPS+IFN-γ	Erk1/2	30 minutes to peaked at 60 and sustained at 240 minutes.	(Lamon *et al.*,2010)
LPS	Akt	Begins at 15 minutes and peaked to 60 minutes followed by a declined thereafter (120 minutes)	(Jiang *et al.*, 2014)
LPS+IFN-γ	Akt	Begins at 15 mins and sustained up to 240 minutes tested	Hattori, Hattori & Kasai, 2003

7.2-Conclusion:

It has been found that the induction of iNOS and the subsequent production of NO under defined conditions may cause elevation of calcium level leading to HA crystal formation in RASMCs, observed by ARS staining and FT-IR. It appears that inflammatory mediators and calcification inducers may cause activation of the cellular calcification process not through MAPKs and Akt. It may be that production of NO generated by iNOS is regulated by another pro-calcific factor, which is not Runx2. This transforms factors in cells which in turn activate various the processes associated with VC. These findings confirmed that iNOS plays a modulatory role in the calcification of RASMCs. NO may significantly exacerbate calcification when produced within a calcifying environment. These together may contribute to enhanced calcification with potential detrimental consequences in *vivo*.

7.3- Limitations and Future work:

Translating research science from the bench into medicines for use in clinical settings is a difficult and complex process. The current study used cell culture. Despite this being a sufficient model to explore deposition of HA crystals at the cellular level, this could be not the same as an organ or whole organism animal. Furthermore, the use of rat cells may not adequately model how the human VSMCs behave physiologically. The levels of substances tested can be toxic to the organism. In fact, the results did suggest a level of cytotoxicity due to the concentrations of substances tested. Thus, in physiological conditions, the toxicity itself may be sufficient to cause cellular dysfunction and vascular calcification. This could serve as a limitation to the study.

In the investigations the concentrations of the calcium in the calcifying agents and the concentration of phosphate was kept the same, however future work may benefit from exploration of the effect of a range of concentrations. For example, the normal range of human plasma and tissue fluid calcium concentration is 2.2 - 2.6mM (Ihmoda, 2005), while in rats the level is 2.5mM (Lewin et al., 2002). Thus, 3mM concentration of extracellular calcium is considered to be hypercalcemic, whereas the concentration used in these studies was more than 2x higher, at 7mM. Furthermore, the levels of β-GP could also be varied, as this too had the fixed concentration of 7mM. Therefore, the methods used could be modified to explore a wider variety of concentrations of calcium, phosphate, etc.

It is interesting to note that in VSMCs free calcium concentrations vary, and intracellular signalling is partly achieved by waves of elevated calcium (Hill-Eubank *et al.,* 2011). Altering extracellular calcium levels could disrupt the intracellular signalling as calcium enters the cell, for example through voltage gated channels. This is itself may contribute to cytotoxicity, and thus promote vascular calcification.

L-arginine is a requirement of iNOS for the synthesis of NO. The cells used were not supplemented with L-arginine. Therefore, any potential effect on the level of NO could be diminished if the level of L-arginine becomes limiting. The study could be extended by supplementing with L-arginine in a range of concentrations.

GW2741250 has been shown to suppress iNOS expression, it would be interesting to establish whether this effect is mediated through regulation of iNOS gene expression using qPCR in parallel with the studies above. In this case cells will be activated with LPS and IFN-γ in the absence and presence of GW274150 at different concentrations. iNOS mRNA expression will be analysed using iNOS specific primers. Parallel studies could induce iNOS, and then GW274150 added in a concentration dependent manner to see if the compound affects both the transcription of the iNOS gene, and the stability of the iNOS mRNA.

It has been found that incubation of cells with IFN-γ in the presence of calcification inducers resulted in a significant increase of NO production, therefore it may be worth exploring whether this is due to induction of iNOS expression through enhanced gene transcription or whether IFN-γ as reported by others, acts to stabilise the iNOS gene. These studies could be carried out by probing for the stability of the iNOS gene using qPCR analysis of total mRNA isolate form cells treated with IFN-γ. Alternatively, cells could be activated with LPS and IFN-γ added to see if the gene stability was increased.

The literature indicates that other signalling molecules such as IL-6 (Abedin *et al.,* 2006) IL-2 are also involved in vascular calcification. Therefore, the study could be extended to explore how variations in these can affect vascular calcification. This could also explore how

variations in cytokines and inflammatory mediators effect phosphorylation of p38 MAPK or Akt, as well as levels of Runx2 or BMP2, in VSMCs.

The compound Carboxy-PTIO is a NO scavenger. It will be used in experiments to examine whether the absence of NO may inhibit or promote of calcification.

Transfecting iNOS cDNA into RASMCs in future work will determine whether the expression of the enzyme and thus subsequent production of NO is in itself critical for calcification to occur in the absence of any potential inflammatory processes.

The effect of other specific iNOS inhibitors (such as Byk 191023) on VSMC mineralisation could be explored and compared to the effect of GW274150, to confirm the effect of variations in NO levels. In addition, as stated above, the level of iNOS expression could be quantified via qPCR, to give an accurate picture of variations in expression in a specific time course.

The current study used RASMCs as a model for mineralisation. However, a human cell line may show differences in the level of protein expression or ion levels, etc. Therefore, extension of the current research in this direction is recommended.

The MTT assay used indicated cytotoxicity when the cells were incubated continuously for longer time periods in inflammatory mediators/calcifying agents. In these conditions the levels of NO were measured. While it is likely that cytotoxicity may interfere with NO levels, in chronic conditions such as cardiovascular disease involving vascular mineralisation, it is also likely that cytotoxicity is a phenomenon due to continuous inflammation (Willerson and Ridker, 2004). Furthermore, varying the replenishment of media allowed comparison of the effect continuous incubation periods, and as has been mentioned above continuous replenishment may serve as a better model for the continuous blood flow *in vivo.*

Bench based research provides a starting point for clinical research. It elucidates signalling pathways and identifies potential target for drug therapies. It also provides some indication of toxicity levels for tested substances. However, the physiological and biological effects can be complicated and based on a myriad of interactions, therefore continuous research is essential to refine any model, especially when complicated intracellular signalling networks are involved, and slight changes to concentrations can have a significant effect. In the case of NO for example, the study found the speed of release was important. Thus, any future work would need to focus on refining and pinpointing the length of time of chronic NO exposure which leads to calcification.

REFERENCES

Abedin, M., Lim, J., Tang, T. B., Park, D., Demer, L. L., & Tintut, Y. (2006). N-3 fatty acids inhibit vascular calcification via the p38-mitogen-activated protein kinase and peroxisome proliferator-activated receptor-γ pathways.*Circulation research*, *98*(6), 727-729.

Abedin, M., Tintut, Y., & Demer, L. L. (2004). Vascular calcification mechanisms and clinical ramifications. *Arteriosclerosis, thrombosis, and vascular biology*, *24*(7), 1161-1170.

Adams, J. S., & Hewison, M. (2012). Extrarenal expression of the 25-hydroxyvitamin D-1-hydroxylase. *Archives of biochemistry and biophysics*,*523*(1), 95-102.

Addison, W. N., Azari, F., Sørensen, E. S., Kaartinen, M. T., & McKee, M. D. (2007). Pyrophosphate inhibits mineralization of osteoblast cultures by binding to mineral, up-regulating osteopontin, and inhibiting alkaline phosphatase activity. *Journal of Biological Chemistry*, *282*(21), 15872-15883.

Adeney, K. L., Siscovick, D. S., Ix, J. H., Seliger, S. L., Shlipak, M. G., Jenny, N. S., & Kestenbaum, B. R. (2009). Association of serum phosphate with vascular and valvular calcification in moderate CKD. *Journal of the American Society of Nephrology*, *20*(2), 381-387.

Ahmed, S., Hood, A. F., Evan, A. P., & Moe, S. M. (2001). Calciphylaxis is associated with hyperphosphatemia and increased osteopontin expression by vascular smooth muscle cells. *American journal of kidney diseases*,*37*(6), 1267-1276.

Al-Aly, Z. (2008). Metabolic acidosis and vascular calcification: using blueprints from bone to map a new venue for vascular research. *Kidney international*, *73*(4), 377-379.

Al-Aly, Z., Shao, J. S., Lai, C. F., Huang, E., Cai, J., Behrmann, A., ... & Towler, D. A. (2007). Aortic Msx2-Wnt calcification cascade is regulated by TNF-α–dependent signals in diabetic Ldlr−/− mice. *Arteriosclerosis, thrombosis, and vascular biology*, *27*(12), 2589-2596.

Alderton, W. K., Cooper, C. H., & Knowles, R. (2001). Nitric oxide synthases: structure, function and inhibition. *Biochem. j*, *357*, 593-615.

Alderton, W. K., Angell, A. D., Craig, C., Dawson, J., Garvey, E., Moncada, S., ... & Schwartz, S. (2005). GW274150 and GW273629 are potent and highly selective inhibitors of inducible nitric oxide synthase in vitro and in vivo. *British journal of pharmacology*, *145*(3), 301-312.

Allard, D., Figg, N., Bennett, M. R., & Littlewood, T. D. (2008). Akt regulates the survival of vascular smooth muscle cells via inhibition of FoxO3a and GSK3. *Journal of Biological Chemistry*, *283*(28), 19739-19747.

Alò, F., Conti, C., Ferraris, P., Giorgini, E., Rubini, C., Sabbatini, S., & Tosi, G. (2009). Micro-FTIR imaging spectroscopy of calcified atheromatous carotid plaques. Part IV. *Journal of Molecular Structure*, *922*(1), 58-63.

Amann, K. (2008). Media calcification and intima calcification are distinct entities in chronic kidney disease. *Clinical Journal of the American Society of Nephrology*, *3*(6), 1599-1605.

Anderson, H. C., Sipe, J. B., Hessle, L., Dhamyamraju, R., Atti, E., Camacho, N. P., & Millán, J. L. (2004). Impaired calcification around matrix vesicles of growth plate and bone in alkaline phosphatase-deficient mice. *The American journal of pathology*, *164*(3), 841-847.

Angelis, M., Wong, L. L., Myers, S. A., & Wong, L. M. (1997). Calciphylaxis in patients on hemodialysis: a prevalence study. *Surgery*, *122*(6), 1083-1090.

Antonia, O. R. S. I., Beltrán, B., Clementi, E., Hallén, K., Feelisch, M., & Moncada, S. (2000). Continuous exposure to high concentrations of nitric oxide leads to persistent inhibition of oxygen consumption by J774 cells as well as extraction of oxygen by the extracellular medium. *Biochemical Journal*, *346*(2), 407-412.

Arihiro, S., Ohtani, H., Hiwatashi, N., Torii, A., Sorsa, T., & Nagura, H. (2001). Vascular smooth muscle cells and pericytes express MMP-1, MMP-9, TIMP-1 and type I procollagen in inflammatory bowel disease.*Histopathology*, *39*(1), 50-59.

Artigas, N., Ureña, C., Rodríguez-Carballo, E., Rosa, J. L., & Ventura, F. (2014). Mitogen-activated Protein Kinase (MAPK)-regulated Interactions between Osterix and Runx2 Are Critical for the Transcriptional Osteogenic Program. *Journal of Biological Chemistry*, *289*(39), 27105-27117.

Aslam, F., Haque, A., Haque, J., & Joseph, J. (2010). Heart failure in subjects with chronic kidney disease: best management practices. *World journal of cardiology*, *2*(5), 112.

Aviram, M. (1995). LDL-platelet interaction under oxidative stress induces macrophage foam cell formation. *Thrombosis and haemostasis*, *74*(1), 560-564.

Azenabor, A. A., Kennedy, P., & York, J. (2009). Free intracellular Ca 2+ regulates bacterial lipopolysaccharide induction of iNOS in human macrophages. *Immunobiology*, *214*(2), 143-152.

Balligand, J. L., Ungureanu-Longrois, D., Simmons, W. W., Pimental, D., Malinski, T. A., Kapturczak, M., ... & Kelly, R. A. (1994). Cytokine-inducible nitric oxide synthase (iNOS) expression in cardiac myocytes. Characterization and regulation of iNOS expression and detection of iNOS activity in single cardiac myocytes in vitro. *Journal of Biological Chemistry*,*269*(44), 27580-27588.

Bates, J. N., Baker, M. T., Guerra, R., & Harrison, D. G. (1991). Nitric oxide generation from nitroprusside by vascular tissue: evidence that reduction of the nitroprusside anion and cyanide loss are required. *Biochemical pharmacology*, *42*, S157-S165.

Baydoun, A., Wileman, S., Wheeler-jones, C., Marber, M., Mann, G., Pearson, J., & Closs, E. (1999). Transmembrane signalling mechanisms regulating expression of cationic amino acid transporters and inducible nitric oxide synthase in rat vascular smooth muscle cells.*Biochem. J*, *344*, 265-272.

Baydoun, A. R., Bertran, J., Thakur, S., Dawson, J., Palacín, M., & Knowles, R. G. (2006). y+ LAT-1 mediates transport of the potent and selective iNOS inhibitor, GW274150, in control J774 macrophages. *Amino acids*, *31*(2), 101-109.

Baylis, C. (2006). Arginine, arginine analogs and nitric oxide production in chronic kidney disease. *Nature Clinical Practice Nephrology*, *2*(4), 209-220.

Bellasi, A., Kooienga, L., Block, G. A., Veledar, E., Spiegel, D. M., & Raggi, P. (2009). How long is the warranty period for nil or low coronary artery calcium in patients new to hemodialysis. *J Nephrol*, *22*(2), 255-262.

Beltrán, B., Orsi, A., Clementi, E., & Moncada, S. (2000). Oxidative stress and S-nitrosylation of proteins in cells. *British journal of pharmacology*,*129*(5), 953-960.

Berridge, M. J. (1998). Neuronal calcium signaling. *Neuron*, *21*(1), 13-26.

Bi, X., Yang, X., Bostrom, M. P., & Camacho, N. P. (2006). Fourier transform infrared imaging spectroscopy investigations in the pathogenesis and repair of cartilage. *Biochimica et Biophysica Acta (BBA)-Biomembranes*,*1758*(7), 934-941.

Billiar, T. R., Curran, R. D., Steuhr, D. J., Hoffmann, K., & Simmons, R. L. (1990). Inhibition of L-arginine metabolism by NG-monomethyl-L-arginine in vivo promotes hepatic damage in response to lipopolysaccharide. *Nitric oxide from L-arginine: A bioregulatory system. Moncada S, Higgs EA (eds). Amesterdam, Elsevier*, 275-80.

Blacher, J., Guerin, A. P., Pannier, B., Marchais, S. J., & London, G. M. (2001). Arterial calcifications, arterial stiffness, and cardiovascular risk in end-stage renal disease. *Hypertension*, *38*(4), 938-942.

Blackmore, R. S., Greenwood, C., & Gibson, Q. H. (1991). Studies of the primary oxygen intermediate in the reaction of fully reduced cytochrome oxidase. *Journal of Biological Chemistry*, *266*(29), 19245-19249.

Boelens, R., Wever, R., Van Gelder, B. F., & Rademaker, H. (1983). An EPR study of the photodissociation reactions of oxidised cytochrome c oxidase-nitric oxide complexes. *Biochimica et Biophysica Acta (BBA)-Bioenergetics*,*724*(2), 176-183.

Bogdan, C. (2001). Nitric oxide and the immune response. *Nature immunology*, *2*(10), 907-916.

Borutaité, V., & Brown, G. C. (1996). Rapid reduction of nitric oxide by mitochondria, and reversible inhibition of mitochondrial respiration by nitric oxide. *Biochemical Journal*, *315*(1), 295-299.

Boyce, B. F., & Xing, L. (2007). The RANKL/RANK/OPG pathway. *Current osteoporosis reports*, *5*(3), 98-104.

Brandenburg, V. M., Sinha, S., Specht, P., & Ketteler, M. (2014). Calcific uraemic arteriolopathy: a rare disease with a potentially high impact on chronic kidney disease–mineral and bone disorder. *Pediatric Nephrology*,*29*(12), 2289-2298.

Brini, M., Ottolini, D., Calì, T., & Carafoli, E. (2013). Calcium in health and disease. In *Interrelations between Essential Metal Ions and Human Diseases*(pp. 81-137). Springer Netherlands.

Brookes, P. S., Land, J. M., Clark, J. B., & Heales, S. J. (1998). Peroxynitrite and brain mitochondria: evidence for increased proton leak.*Journal of neurochemistry*, *70*(5), 2195-2202.

Brown, G. C., & Cooper, C. (1994). Nanomolar concentrations of nitric oxide reversibly inhibit synaptosomal respiration by competing with oxygen at cytochrome oxidase. *FEBS letters*, *356*(2-3), 295-298.

Brown, G. C. (2001). Regulation of mitochondrial respiration by nitric oxide inhibition of cytochrome c oxidase. *Biochimica et Biophysica Acta (BBA)-Bioenergetics*, *1504*(1), 46-57.

Browner, N. C., Sellak, H., & Lincoln, T. M. (2004). Downregulation of cGMP-dependent protein kinase expression by inflammatory cytokines in vascular smooth muscle cells. *American Journal of Physiology-Cell Physiology*, *287*(1), C88-C96.

Browner, W. S., Lui, L. Y., & Cummings, S. R. (2001). Associations of Serum Osteoprotegerin Levels with Diabetes, Stroke, Bone Density, Fractures, and Mortality in Elderly Women 1. *The Journal of Clinical Endocrinology & Metabolism*, *86*(2), 631-637.

Brownlee, M. (2001). Biochemistry and molecular cell biology of diabetic complications. *Nature*, *414*(6865), 813-820.

Byon, C. H., Javed, A., Dai, Q., Kappes, J. C., Clemens, T. L., Darley-Usmar, V. M., ... & Chen, Y. (2008). Oxidative stress induces vascular calcification through modulation of the osteogenic transcription factor Runx2 by AKT signaling. *Journal of Biological Chemistry*, *283*(22), 15319-15327.

Byon, C. H., Sun, Y., Chen, J., Yuan, K., Mao, X., Heath, J. M., ... & Chen, Y. (2011). Runx2-upregulated receptor activator of nuclear factor κB ligand in calcifying smooth muscle cells promotes migration and osteoclastic differentiation of macrophages. *Arteriosclerosis, thrombosis, and vascular biology*, *31*(6), 1387-1396.

Cai, T. B., Wang, P. G., & Holder, A. A. (2005). NO and NO donors. *Nitric oxide donors for pharmaceutical and biological applications. Wang PG, Cai TB, Taniguchi N, eds. Weinheim: Wiley VCH.*

Cao, X., Li, H., Tao, H., Wu, N., Yu, L., Zhang, D., ... & Zhu, Q. (2013). Metformin inhibits vascular calcification in female rat aortic smooth muscle cells via the AMPK-eNOS-NO pathway. *Endocrinology*, *154*(10), 3680-3689.

Chae, H. J., Park, R. K., Chung, H. T., Kang, J. S., Kim, M. S., Choi, D. Y., ... & Kim, H. R. (1997). Nitric oxide is a regulator of bone remodelling. *Journal of pharmacy and pharmacology*, *49*(9), 897-902.

Chakrabarty, P., Ceballos-Diaz, C., Lin, W. L., Beccard, A., Jansen-West, K., McFarland, N. R., & Golde, T. E. (2011). Interferon-[gamma] induces progressive nigrostriatal degeneration and basal ganglia calcification. *Nature neuroscience*, *14*(6), 694-696.

Chan, E. D., & Riches, D. W. (2001). IFN-γ+ LPS induction of iNOS is modulated by ERK, JNK/SAPK, and p38 mapk in a mouse macrophage cell line. *American Journal of Physiology-Cell Physiology*, *280*(3), C441-C450.

Chatterjee, P. K., Patel, N. S., Sivarajah, A., Kvale, E. O., Dugo, L., Cuzzocrea, S., ... & Yaqoob, M. M. (2003). GW274150, a potent and highly selective inhibitor of iNOS, reduces experimental renal ischemia/reperfusion injury. *Kidney international*, *63*(3), 853-865.

Chen, H. H., & Wang, D. L. (2004). Nitric oxide inhibits matrix metalloproteinase-2 expression via the induction of activating transcription factor 3 in endothelial cells. *Molecular pharmacology*, *65*(5), 1130-1140.

Chen, N. X., & Moe, S. M. (2003). Arterial calcification in diabetes. *Current diabetes reports*, *3*(1), 28-32.

Chen, N. X., O'Neill, K. D., Chen, X., Kiattisunthorn, K., Gattone, V. H., & Moe, S. M. (2011). Activation of arterial matrix metalloproteinases leads to vascular calcification in chronic kidney disease. *American journal of nephrology*, *34*(3), 211-219.

Chester, A. H., Borland, J. A., Buttery, L. D., Mitchell, J. A., Cunningham, D. A., Hafizi, S., ... & Yacoub, M. H. (1998). Induction of nitric oxide synthase in human vascular smooth muscle: interactions between proinflammatory cytokines. *Cardiovascular research*, *38*(3), 814-821.

Chiou, H. J., Hung, S. C., Lin, S. Y., Wei, Y. S., & Li, M. J. (2009). Correlations among mineral components, progressive calcification process and clinical symptoms of calcific tendonitis. *Rheumatology*, kep359.

Choi, M. E., Ding, Y., & Kim, S. I. (2012, May). TGF-β signaling via TAK1 pathway: Role in kidney fibrosis. In *Seminars in nephrology* (Vol. 32, No. 3, pp. 244-252). WB Saunders.

Chyu, K. Y., Dimayuga, P. C., Zhao, X., Nilsson, J., Shah, P. K., & Cercek, B. (2004). Altered AP-1/Ref-1 redox pathway and reduced proliferative response in iNOS-deficient vascular smooth muscle cells. *Vascular Medicine*, *9*(3), 177-183.

Clapham, D. E. (2007). Calcium signaling. *Cell*, *131*(6), 1047-1058.

Cleeter, M. W. J., Cooper, J. M., Darley-Usmar, V. M., Moncada, S. A., & Schapira, A. H. V. (1994). Reversible inhibition of cytochrome c oxidase, the terminal enzyme of the mitochondrial respiratory chain, by nitric oxide. *FEBS letters*, *345*(1), 50-54.

Clementi, E., Brown, G. C., Feelisch, M., & Moncada, S. (1998). Persistent inhibition of cell respiration by nitric oxide: crucial role of S-nitrosylation of mitochondrial complex I and protective action of glutathione. *Proceedings of the National Academy of Sciences*, *95*(13), 7631-7636.

Collins, A. J., Kasiske, B., Herzog, C., Chavers, B., Foley, R., Gilbertson, D., ... & Matas, A. (2005). Excerpts from the United States Renal Data System 2004 annual data report: atlas of end-stage renal disease in the United States. *American Journal of Kidney Diseases*, *45*, A5-A7.

Cortizo, A. M., Molinuevo, M. S., Barrio, D. A., & Bruzzone, L. (2006). Osteogenic activity of vanadyl (IV)–ascorbate complex: Evaluation of its mechanism of action. *The international journal of biochemistry & cell biology*, *38*(7), 1171-1180.

Covic, A., Kanbay, M., Voroneanu, L., Turgut, F., Serban, D., Serban, I., & Goldsmith, D. (2010). Vascular calcification in chronic kidney disease. *Clinical science*, *119*, 111-121.

Cozzolino, M., Brancaccio, D., Gallieni, M., & Slatopolsky, E. (2005). Pathogenesis of vascular calcification in chronic kidney disease. *Kidney international*, *68*(2), 429-436.

Creager, M. A., Lüscher, T. F., Cosentino, F., & Beckman, J. A. (2003). Diabetes and vascular disease pathophysiology, clinical consequences, and medical therapy: part I. *Circulation*, *108*(12), 1527-1532.

Crouthamel, M. H., Lau, W. L., Leaf, E. M., Chavkin, N. W., Wallingford, M. C., Peterson, D. F., ... & Giachelli, C. M. (2013). Sodium-dependent phosphate cotransporters and phosphate-induced calcification of vascular smooth muscle cells redundant roles for PiT-1 and PiT-2. *Arteriosclerosis, thrombosis, and vascular biology*, *33*(11), 2625-2632.

Dalmeijer, G. W., van der Schouw, Y. T., Magdeleyns, E. J., Vermeer, C., Verschuren, W. M., Boer, J. M., & Beulens, J. W. (2013). Matrix Gla protein species and risk of cardiovascular events in type 2 diabetic patients. *Diabetes care*, *36*(11), 3766-3771.

De Alba, J., Clayton, N. M., Collins, S. D., Colthup, P., Chessell, I., & Knowles, R. G. (2006). GW274150, a novel and highly selective inhibitor of the inducible isoform of nitric oxide synthase (iNOS), shows analgesic effects in rat models of inflammatory and neuropathic pain. *Pain*, *120*(1), 170-181.

Deedwania, P., & Srikanth, S. (2008). Diabetes and vascular disease.

Deng, X. S., Meng, X., Zeng, Q., Fullerton, D., Mitchell, M., & Jaggers, J. (2015). Adult Aortic Valve Interstitial Cells Have Greater Responses to Toll-Like Receptor 4 Stimulation. *The Annals of thoracic surgery*, *99*(1), 62-71.

Destainville, A., Champion, E., Bernache-Assollant, D., & Laborde, E. (2003). Synthesis, characterization and thermal behavior of apatitic tricalcium phosphate. *Materials Chemistry and Physics*, *80*(1), 269-277.

Di Bartolo, B. A., Chan, J., Bennett, M. R., Cartland, S., Bao, S., Tuch, B. E., & Kavurma, M. M. (2011). TNF-related apoptosis-inducing ligand (TRAIL) protects against diabetes and atherosclerosis in Apoe−/− mice. *Diabetologia*,*54*(12), 3157-3167.

Ding, Y., & Vaziri, N. D. (1998). Calcium channel blockade enhances nitric oxide synthase expression by cultured endothelial cells. *Hypertension*, *32*(4), 718-723.

Dubey, R. K., Jackson, E. K., & Lüscher, T. F. (1995). Nitric oxide inhibits angiotensin II-induced migration of rat aortic smooth muscle cell. Role of cyclic-nucleotides and angiotensin1 receptors. *Journal of Clinical Investigation*, *96*(1), 141.

Du, X. L., Edelstein, D., Rossetti, L., Fantus, I. G., Goldberg, H., Ziyadeh, F., ... & Brownlee, M. (2000). Hyperglycemia-induced mitochondrial superoxide overproduction activates the hexosamine pathway and induces plasminogen activator inhibitor-1 expression by increasing Sp1 glycosylation.*Proceedings of the National Academy of Sciences*, *97*(22), 12222-12226.

Drapier, J. C., & Hibbs, J. B. (1988). Differentiation of murine macrophages to express nonspecific cytotoxicity for tumor cells results in L-arginine-dependent inhibition of mitochondrial iron-sulfur enzymes in the macrophage effector cells. *The Journal of Immunology*, *140*(8), 2829-2838.

Dritsa, V. (2012). *FT-IR spectroscopy in medicine*. INTECH Open Access Publisher.

Ea, H. K., Uzan, B., Rey, C., & Lioté, F. (2005). Octacalcium phosphate crystals directly stimulate expression of inducible nitric oxide synthase through p38 and JNK mitogen-activated protein kinases in articular chondrocytes. *Arthritis research & therapy*, *7*(5), R915.

Eddington, H., Sinha, S., & Kalra, P. A. (2009). Vascular calcification in chronic kidney disease: a clinical review. *Journal of renal care*, *35*(s1), 45-50.

Ehnes, D. D., Geransar, R. M., Rancourt, D. E., & Zur Nieden, N. I. (2015). Exogenous nitric oxide enhances calcification in embryonic stem cell-derived osteogenic cultures. *Differentiation*.

El Asmar, M. S., Naoum, J. J., & Arbid, E. J. (2014). Vitamin k dependent proteins and the role of vitamin k2 in the modulation of vascular calcification: a review. *Oman medical journal*, *29*(3), 172.

ELDesoky, E. S., Derendorf, H., & Klotz, U. (2006). Variability in response to cardiovascular drugs. *Current clinical pharmacology*, *1*(1), 35-46.

Ewence, A. E., Bootman, M., Roderick, H. L., Skepper, J. N., McCarthy, G., Epple, M., ... & Proudfoot, D. (2008). Calcium phosphate crystals induce cell death in human vascular smooth muscle cells a potential mechanism in atherosclerotic plaque destabilization. *Circulation research*, *103*(5), e28-e34.

Faury, G., Usson, Y., Robert-Nicoud, M., Robert, L., & Verdetti, J. (1998). Nuclear and cytoplasmic free calcium level changes induced by elastin peptides in human endothelial cells. *Proceedings of the National Academy of Sciences*, *95*(6), 2967-2972.

Félétou, M. (2011). The endothelium: Part 1: multiple functions of the endothelial cells—focus on endothelium-derived vasoactive mediators.

Fitzgerald, T. N., Shepherd, B. R., Asada, H., Teso, D., Muto, A., Fancher, T., ... & Dardik, A. (2008). Laminar shear stress stimulates vascular smooth muscle cell apoptosis via the Akt pathway. *Journal of cellular physiology*,*216*(2), 389-395.

Flade, K., Lau, C., Mertig, M., & Pompe, W. (2001). Osteocalcin-controlled dissolution-reprecipitation of calcium phosphate under biomimetic conditions.*Chemistry of materials*, *13*(10), 3596-3602.

Floege, J., & Ketteler, M. (2004). Vascular calcification in patients with end-stage renal disease. *Nephrology Dialysis Transplantation*, *19*(suppl 5), v59-v66.

Foley, R. N., Parfrey, P. S., & Sarnak, M. J. (1998). Epidemiology of cardiovascular disease in chronic renal disease. *Journal of the American Society of Nephrology: JASN*, *9*(12 Suppl), S16-23.

Förstermann, U., Boissel, J. P., & Kleinert, H. (1998). Expressional control of the 'constitutive'isoforms of nitric oxide synthase (NOS I and NOS III).*The FASEB Journal*, *12*(10), 773-790.

Förstermann, U., Gath, I., Schwarz, P., Closs, E. I., & Kleinert, H. (1995). Isoforms of nitric oxide synthase: properties, cellular distribution and expressional control. *Biochemical pharmacology*, *50*(9), 1321-1332.

Franceschi, R. T., & Xiao, G. (2003). Regulation of the osteoblast-specific transcription factor, Runx2: Responsiveness to multiple signal transduction pathways. *Journal of cellular biochemistry*, *88*(3), 446-454.

Fukumoto, S. (2009). Phosphatidylinositol 3-kinase/Akt pathway regulates inflammatory mediators-induced calcification of human vascular smooth muscle cells. *Osaka City Med. J*, *55*, 71-80.

Galat, A. (1980). Study of the Raman scattering and infrared absorption spectra of branched polysaccharides. *Acta Biochimica Polonica*, *27*(2), 135-142.

Garg, U. C., & Hassid, A. (1989). Nitric oxide-generating vasodilators and 8-bromo-cyclic guanosine monophosphate inhibit mitogenesis and proliferation of cultured rat vascular smooth muscle cells. *Journal of Clinical Investigation*, *83*(5), 1774.

Ge, C., Yang, Q., Zhao, G., Yu, H., Kirkwood, K. L., & Franceschi, R. T. (2012). Interactions between extracellular signal-regulated kinase 1/2 and P38 Map kinase pathways in the control of RUNX2 phosphorylation and transcriptional activity. *Journal of Bone and Mineral Research*, *27*(3), 538-551.

Genovese, T., Cuzzocrea, S., Di Paola, R., Failla, M., Mazzon, E., Sortino, M. A., ... & Vancheri, C. (2005). Inhibition or knock out of inducible nitric oxide synthase result in resistance to bleomycin-induced lung injury. *Respir Res*, *6*(58), 1-17.

Giacco, F., & Brownlee, M. (2010). Oxidative stress and diabetic complications. *Circulation research*, *107*(9), 1058-1070.

Giachelli, C. M. (2009). The emerging role of phosphate in vascular calcification. *Kidney international*, *75*(9), 890-897.

Giachelli, C. M. (2004). Vascular calcification mechanisms. *Journal of the American Society of Nephrology*, *15*(12), 2959-2964.

Gómez-Ordóñez, E., & Rupérez, P. (2011). FTIR-ATR spectroscopy as a tool for polysaccharide identification in edible brown and red seaweeds. *Food Hydrocolloids*, *25*(6), 1514-1520.

Gow, A. J., & Ischiropoulos, H. (2001). Nitric oxide chemistry and cellular signaling. *Journal of cellular physiology*, *187*(3), 277-282.

Granger, D. L., & Lehninger, A. L. (1982). Sites of inhibition of mitochondrial electron transport in macrophage-injured neoplastic cells. *The Journal of Cell Biology*, *95*(2), 527-535.

Green, L. C., Wagner, D. A., Glogowski, J., Skipper, P. L., Wishnok, J. S., & Tannenbaum, S. R. (1982). Analysis of nitrate, nitrite, and [15 N] nitrate in biological fluids. *Analytical biochemistry*, *126*(1), 131-138.

Greenblatt, M. B., Shim, J. H., & Glimcher, L. H. (2013). Mitogen-activated protein kinase pathways in osteoblasts. *Annual review of cell and developmental biology*, *29*, 63-79.

Gross, M. L., Meyer, H. P., Ziebart, H., Rieger, P., Wenzel, U., Amann, K., ... & Ritz, E. (2007). Calcification of coronary intima and media: immunohistochemistry, backscatter imaging, and x-ray analysis in renal and nonrenal patients. *Clinical Journal of the American Society of Nephrology*,*2*(1), 121-134.

Guerrero, F., de Oca, A. M., Aguilera-Tejero, E., Zafra, R., Rodríguez, M., & López, I. (2011). The effect of vitamin D derivatives on vascular calcification associated with inflammation. *Nephrology Dialysis Transplantation*, gfr555.

Gundberg, C. M., Lian, J. B., & Booth, S. L. (2012). Vitamin K-dependent carboxylation of osteocalcin: friend or foe?. *Advances in Nutrition: An International Review Journal*, *3*(2), 149-157.

Guo, F. H., Uetani, K., Haque, S. J., Williams, B. R., Dweik, R. A., Thunnissen, F. B., ... & Erzurum, S. C. (1997). Interferon gamma and interleukin 4 stimulate prolonged expression of inducible nitric oxide synthase in human airway epithelium through synthesis of soluble mediators.*Journal of Clinical Investigation*, *100*(4), 829.

Guzik, T. J., West, N. E., Pillai, R., Taggart, D. P., & Channon, K. M. (2002). Nitric oxide modulates superoxide release and peroxynitrite formation in human blood vessels. *Hypertension*, *39*(6), 1088-1094.

Han, J. K., Song, H. Y., Saito, F., & Lee, B. T. (2006). Synthesis of high purity nano-sized hydroxyapatite powder by microwave-hydrothermal method. *Materials chemistry and physics*, *99*(2), 235-239.

Hattori, Y., Hattori, S., & Kasai, K. (2003). Lipopolysaccharide activates Akt in vascular smooth muscle cells resulting in induction of inducible nitric oxide synthase through nuclear factor-kappa B activation. *European journal of pharmacology*, *481*(2), 153-158.

Hattori, Y., Campbell, E. B., & Gross, S. S. (1994). Argininosuccinate synthetase mRNA and activity are induced by immunostimulants in vascular smooth muscle. Role in the regeneration or arginine for nitric oxide synthesis. *Journal of Biological Chemistry*, *269*(13), 9405-9408.

Hattori, Y., Matsumura, M., & Kasai, K. (2003). Vascular smooth muscle cell activation by C-reactive protein. *Cardiovascular research*, *58*(1), 186-195.

Hattori, Y., Nakanishi, N., & Kasai, K. (2002). Statin enhances cytokine-mediated induction of nitric oxide synthesis in vascular smooth muscle cells. *Cardiovascular research*, *54*(3), 649-658.

Hayashino, Y., Okamura, S., Matsunaga, S., Tsujii, S., Ishii, H., & Tenri Cohort Study Group. (2012). The association between problem areas in diabetes scale scores and glycemic control is modified by types of diabetes therapy: diabetes distress and care registry in Tenri (DDCRT 2). *Diabetes research and clinical practice*, *97*(3), 405-410.

Henry, Y., Lepoivre, M., Drapier, J. C., Ducrocq, C., Boucher, J. L., & Guissani, A. (1993). EPR characterization of molecular targets for NO in mammalian cells and organelles. *The FASEB Journal*, *7*(12), 1124-1134.

Heo, S. K., Yun, H. J., Noh, E. K., Park, W. H., & Park, S. D. (2008). LPS induces inflammatory responses in human aortic vascular smooth muscle cells via Toll-like receptor 4 expression and nitric oxide production. *Immunology letters*, *120*(1), 57-64.

Hibbs, J. B., Taintor, R. R., Vavrin, Z., & Rachlin, E. M. (1988). Nitric oxide: a cytotoxic activated macrophage effector molecule. *Biochemical and biophysical research communications*, *157*(1), 87-94.

Hill-Eubanks, D. C., Werner, M. E., Heppner, T. J., & Nelson, M. T. (2011). Calcium signaling in smooth muscle. *Cold Spring Harbor perspectives in biology*, *3*(9), a004549.

Ho, W. P., Chan, W. P., Hsieh, M. S., & Chen, R. M. (2009). Runx2-mediated bcl-2 gene expression contributes to nitric oxide protection against hydrogen peroxide-induced osteoblast apoptosis. *Journal of cellular biochemistry*, *108*(5), 1084-1093.

Høivik, H. O., Laurijssens, B. E., Harnisch, L. O., Twomey, C. K., Dixon, R. M., Kirkham, A. J., ... & Lunnon, M. W. (2010). Lack of efficacy of the selective iNOS inhibitor GW274150 in prophylaxis of migraine headache. *Cephalalgia*, *30*(12), 1458-1467.

Huang, J., Huang, H., Wu, M., Li, J., Xie, H., Zhou, H., ... & Peng, Y. (2013). Connective tissue growth factor induces osteogenic differentiation of vascular smooth muscle cells through ERK signaling. *International journal of molecular medicine*, *32*(2), 423-429.

Huang, H., Rose, J. L., & Hoyt, D. G. (2004). p38 Mitogen-activated protein kinase mediates synergistic induction of inducible nitric-oxide synthase by lipopolysaccharide and interferon-γ through signal transducer and activator of transcription 1 Ser727 phosphorylation in murine aortic endothelial cells. *Molecular pharmacology*, *66*(2), 302-311.

Huang, R. L., Yuan, Y., Zou, G. M., Liu, G., Tu, J., & Li, Q. (2013). LPS-stimulated inflammatory environment inhibits BMP-2-induced osteoblastic differentiation through crosstalk between TLR4/MyD88/NF-κB and BMP/Smad signaling. *Stem cells and development*, *23*(3), 277-289.

Huhtakangas, J. A., Olivera, C. J., Bishop, J. E., Zanello, L. P., & Norman, A. W. (2004). The vitamin D receptor is present in caveolae-enriched plasma membranes and binds 1α, 25 (OH) 2-vitamin D3 in vivo and in vitro. *Molecular Endocrinology*, *18*(11), 2660-2671.

Huitema, L. F., Vaandrager, A. B., van Weeren, P. R., Barneveld, A., Helms, J. B., & van de Lest, C. H. (2006 a). The nitric oxide donor sodium nitroprusside inhibits mineralization in ATDC5 cells. *Calcified tissue international*, *78*(3), 171-177.

Huitema, L. F., van Weeren, P. R., Barneveld, A., van de Lest, C. H., Helms, J. B., & Vaandrager, A. B. (2006 b). Iron ions derived from the nitric oxide donor sodium nitroprusside inhibit mineralization. *European journal of pharmacology*, *542*(1), 48-53.

Hung, A., Vernet, D., Xie, Y., Rajavashisth, T., Rodríguez, J. A., Rajfer, J., & González-cadavid, N. F. (1995). Expression of inducible nitric oxide synthase in smooth muscle cells from rat penile corpora cavernosa. *Journal of andrology*, *16*(6), 469-481.

Hunter, G. K., & Goldberg, H. A. (1993). Nucleation of hydroxyapatite by bone sialoprotein. *Proceedings of the National Academy of Sciences*, *90*(18), 8562-8565.

Iadecola, C., Zhang, F., Casey, R., Clark, H. B., & Ross, M. E. (1996). Inducible nitric oxide synthase gene expression in vascular cells after transient focal cerebral ischemia. *Stroke*, *27*(8), 1373-1380.

Ihmoda, I. A., & Turner, N. (2005). What I tell my patients about blood and urine tests. *BRITISH JOURNAL OF RENAL MEDICINE*, *10*(2), 15.

Ikeda, K., Souma, Y., Akakabe, Y., Kitamura, Y., Matsuo, K., Shimoda, Y., ... & Matsubara, H. (2012). Macrophages play a unique role in the plaque calcification by enhancing the osteogenic signals exerted by vascular smooth muscle cells. *Biochemical and biophysical research communications*, *425*(1), 39-44.

Ikegami, D., Akiyama, H., Suzuki, A., Nakamura, T., Nakano, T., Yoshikawa, H., & Tsumaki, N. (2011). Sox9 sustains chondrocyte survival and hypertrophy in part through Pik3ca-Akt pathways. *Development*, *138*(8), 1507-1519.

Irving, J. (2012). *Calcium and phosphorus metabolism*. Elsevier.

Jacob, T., Ascher, E., Alapat, D., Olevskaia, Y., & Hingorani, A. (2005). Activation of p38MAPK signaling cascade in a VSMC injury model: role of p38MAPK inhibitors in limiting VSMC proliferation. *European journal of vascular and endovascular surgery*, *29*(5), 470-478.

Jiang, D., Li, D., Cao, L., Wang, L., Zhu, S., Xu, T., ... & Pan, D. (2014). Positive feedback regulation of proliferation in vascular smooth muscle cells stimulated by lipopolysaccharide is mediated through the TLR 4/Rac1/Akt pathway. *PloS one*, *9*(3), e92398.

Jiang, P., Xu, J., Zheng, S., Huang, J., Xiang, Q., Fu, X., & Wang, T. (2010). 17β-estradiol down-regulates lipopolysaccharide-induced MCP-1 production and cell migration in vascular smooth muscle cells. *Journal of molecular endocrinology*, *45*(2), 87-97.

Jin, C., Guo, J., Qiu, X., Ma, K., Xiang, M., Zhu, X., & Guo, J. (2014). IGF-1 induces iNOS expression via the p38 MAPK signal pathway in the anti-apoptotic process in pulmonary artery smooth muscle cells during PAH.*Journal of Receptors and Signal Transduction*, *34*(4), 325-331.

Johnson, F. K., Johnson, R. A., Peyton, K. J., & Durante, W. (2005). Arginase inhibition restores arteriolar endothelial function in Dahl rats with salt-induced hypertension. *American Journal of Physiology-Regulatory, Integrative and Comparative Physiology*, *288*(4), R1057-R1062.

Johnson, K., Jung, A., Murphy, A., Andreyev, A., Dykens, J., & Terkeltaub, R. (2000). Mitochondrial oxidative phosphorylation is a downstream regulator of nitric oxide effects on chondrocyte matrix synthesis and mineralization.*Arthritis & Rheumatism*, *43*(7), 1560.

Johnson, R. C., Leopold, J. A., & Loscalzo, J. (2006). Vascular calcification pathobiological mechanisms and clinical implications. *Circulation research*,*99*(10), 1044-1059.

Jones, R. J., Jourd'heuil, D., Salerno, J. C., Smith, S. M., & Singer, H. A. (2007). iNOS regulation by calcium/calmodulin-dependent protein kinase II in vascular smooth muscle. *American Journal of Physiology-Heart and Circulatory Physiology*, *292*(6), H2634-H2642.

Jono, S., McKee, M. D., Murry, C. E., Shioi, A., Nishizawa, Y., Mori, K., ... & Giachelli, C. M. (2000). Phosphate regulation of vascular smooth muscle cell calcification. *Circulation research*, *87*(7), e10-e17.

Jono, S., Nishizawa, Y., Shioi, A., & Morii, H. (1998). 1, 25-Dihydroxyvitamin D3 increases in vitro vascular calcification by modulating secretion of endogenous parathyroid hormone–related peptide. *Circulation*, *98*(13), 1302-1306.

Jono, S., Nishizawa, Y., Shioi, A., & Morii, H. (1997). Parathyroid Hormone–Related Peptide as a Local Regulator of Vascular Calcification Its Inhibitory Action on In Vitro Calcification by Bovine Vascular Smooth Muscle Cells.*Arteriosclerosis, thrombosis, and vascular biology*, *17*(6), 1135-1142.

Kanazawa, I., Yamaguchi, T., Tada, Y., Yamauchi, M., Yano, S., & Sugimoto, T. (2011). Serum osteocalcin level is positively associated with insulin sensitivity and secretion in patients with type 2 diabetes. *Bone*, *48*(4), 720-725.

Kanno, Y., Into, T., Lowenstein, C. J., & Matsushita, K. (2008). Nitric oxide regulates vascular calcification by interfering with TGF-β signalling.*Cardiovascular research*, *77*(1), 221-230.

Knipp, B. S., Ailawadi, G., Ford, J. W., Peterson, D. A., Eagleton, M. J., Roelofs, K. J., ... & Graziano, K. D. (2004). Increased MMP-9 expression and activity by aortic smooth muscle cells after nitric oxide synthase inhibition is associated with increased nuclear factor-κB and activator protein-1 activity. *Journal of Surgical Research*, *116*(1), 70-80.

Kapustin, A. N., Davies, J. D., Reynolds, J. L., McNair, R., Jones, G. T., Sidibe, A., ... & Shanahan, C. M. (2011). Calcium regulates key components of vascular smooth muscle cell–derived matrix vesicles to enhance mineralization. *Circulation research*, *109*(1), e1-e12.

Kapustin, A. N., & Shanahan, C. M. (2011). Osteocalcin A Novel Vascular Metabolic and Osteoinductive Factor?. *Arteriosclerosis, thrombosis, and vascular biology*, *31*(10), 2169-2171.

Katakami, N., Sakamoto, K., Kaneto, H., Matsuhisa, M., Shimizu, I., Ishibashi, F., ... & Yamasaki, Y. (2009). Combined effect of oxidative stress-related gene polymorphisms on atherosclerosis. *Biochemical and biophysical research communications*, *379*(4), 861-865.

Kelpke, S. S., Reiff, D., Prince, C. W., & Thompson, J. A. (2001). Acidic Fibroblast Growth Factor Signaling Inhibits Peroxynitrite-Induced Death of Osteoblasts and Osteoblast Precursors. *Journal of Bone and Mineral Research*, *16*(10), 1917-1925.

Kendrick, J., Kestenbaum, B., & Chonchol, M. (2011). Phosphate and cardiovascular disease. *Advances in chronic kidney disease*, *18*(2), 113-119.

Kessler, P., Kronemann, N., Hecker, M., Busse, R., & Schini-Kerth, V. B. (1997). Effects of barbiturates on the expression of the inducible nitric oxide synthase in vascular smooth muscle. *Journal of cardiovascular pharmacology*, *30*(6), 802-810.

Ketteler, M., Bongartz, P., Westenfeld, R., Wildberger, J. E., Mahnken, A. H., Böhm, R., ... & Floege, J. (2003). Association of low fetuin-A (AHSG) concentrations in serum with cardiovascular mortality in patients on dialysis: a cross-sectional study. *The Lancet*, *361*(9360), 827-833.

Ketteler, M., Wolf, M., Hahn, K., & Ritz, E. (2013). Phosphate: a novel cardiovascular risk factor. *European heart journal*, *34*(15), 1099-1101.

Kim, K. M. (1994). Apoptosis and calcification. *Scanning microscopy*, *9*(4), 1137-75.

Kim, K. Y., Kim, B. G., Kim, S. O., Yoo, S. E., Kwak, Y. G., Chae, S. W., & Hong, K. W. (2002). Prevention of Lipopolysaccharide-Induced Apoptosis by (2S, 3S, 4R)-N"-Cyano-N-(6-amino-3, 4-dihydro-3-hydroxy-2-methyl-2-dimethoxymethyl-2H-benzopyran-4-yl)-N′-benzylguanidine, a Benzopyran Analog, in Endothelial Cells. *Journal of Pharmacology and Experimental Therapeutics*, *300*(2), 535-542.

Kircelli, F., Peter, M. E., Ok, E. S., Celenk, F. G., Yilmaz, M., Steppan, S., ... & Passlick-Deetjen, J. (2011). Magnesium reduces calcification in bovine vascular smooth muscle cells in a dose-dependent manner. *Nephrology Dialysis Transplantation*, gfr321.

Kockx, M. M., De Meyer, G. R., Muhring, J., Jacob, W., Bult, H., & Herman, A. G. (1998). Apoptosis and related proteins in different stages of human atherosclerotic plaques. *Circulation*, *97*(23), 2307-2315.

Korhonen, R., Lahti, A., Hämäläinen, M., Kankaanranta, H., & Moilanen, E. (2002). Dexamethasone inhibits inducible nitric-oxide synthase expression and nitric oxide production by destabilizing mRNA in lipopolysaccharide-treated macrophages. *Molecular pharmacology*, *62*(3), 698-704.

Kreutz, M., Andreesen, R., Krause, S. W., Szabo, A., Ritz, E., & Reichel, H. (1993). 1, 25-dihydroxyvitamin D3 production and vitamin D3 receptor expression are developmentally regulated during differentiation of human monocytes into macrophages. *Blood*, *82*(4), 1300-1307.

Kwon, S. H., Jun, Y. K., Hong, S. H., & Kim, H. E. (2003). Synthesis and dissolution behavior of β-TCP and HA/β-TCP composite powders. *Journal of the European Ceramic Society*, *23*(7), 1039-1045.

Lam, C. F., Lan, R. S., Van Heerden, P. V., Ilett, K. F., & Henry, P. J. (2003). Diethylenetriamine NITRIC oxide adduct relaxes precontracted mouse tracheal smooth muscle*. *Clinical and experimental pharmacology and physiology*, *30*(9), 709-711.

Lamawansa, M. D., Wysocki, S. J., House, A. K., & Norman, P. E. (1996). Vitamin D3 exacerbates intimal hyperplasia in balloon-injured arteries. *British journal of surgery*, *83*(8), 1101-1103.

Lancaster, J. R., & Hibbs, J. B. (1990). EPR demonstration of iron-nitrosyl complex formation by cytotoxic activated macrophages. *Proceedings of the National Academy of Sciences*, *87*(3), 1223-1227.

Lee, D. C., Stenland, C. J., Hartwell, R. C., Ford, E. K., Cai, K., Miller, J. L., ... & Petteway, S. R. (2000). Monitoring plasma processing steps with a sensitive Western blot assay for the detection of the prion protein. *Journal of virological methods*, *84*(1), 77-89.

Leopold, J. A. (2014). MicroRNAs regulate vascular medial calcification.*Cells*, *3*(4), 963-980.

Lewin, E., Garfia, B., Recio, F. L., Rodriguez, M., & Olgaard, K. (2002). Persistent downregulation of calcium-sensing receptor mRNA in rat parathyroids when severe secondary hyperparathyroidism is reversed by an isogenic kidney transplantation. *Journal of the American Society of Nephrology*, *13*(8), 2110-2116.

Li, X., Udagawa, N., Itoh, K., Suda, K., Murase, Y., Nishihara, T., ... & Takahashi, N. (2002). p38 MAPK-mediated signals are required for inducing osteoclast differentiation but not for osteoclast function. *Endocrinology*,*143*(8), 3105-3113.

Li, X., Yang, H. Y., & Giachelli, C. M. (2008). BMP-2 promotes phosphate uptake, phenotypic modulation, and calcification of human vascular smooth muscle cells. *Atherosclerosis*, *199*(2), 271-277.

Liao, L., Zhou, Q., Song, Y., Wu, W., Yu, H., Wang, S., ... & Lu, L. (2013). Ceramide mediates Ox-LDL-induced human vascular smooth muscle cell calcification via p38 mitogen-activated protein kinase signaling. *PloS one*,*8*(12), e82379.

Liao, X. B., Zhou, X. M., Li, J. M., Yang, J. F., Tan, Z. P., Hu, Z. W., ... & Yuan, L. Q. (2008). Taurine inhibits osteoblastic differentiation of vascular smooth muscle cells via the ERK pathway. *Amino acids*, *34*(4), 525-530.

Libby, P., & Ridker, P. M. (2006). Inflammation and atherothrombosis: from population biology and bench research to clinical practice. *Journal of the American College of Cardiology*, *48*(9s1), A33-A46.

Lim, K., Lu, T. S., Molostvov, G., Lee, C., Lam, F. T., Zehnder, D., & Hsiao, L. L. (2012). Vascular Klotho deficiency potentiates the development of human artery calcification and mediates resistance to fibroblast growth factor 23. *Circulation*, *125*(18), 2243-2255.

Lin, C. Y., Tsai, P. S., Hung, Y. C., & Huang, C. J. (2009). L-type calcium channels are involved in mediating the anti-inflammatory effects of magnesium sulphate. *British journal of anaesthesia*, aep336.

Lin, F. Y., Chen, Y. H., Tasi, J. S., Chen, J. W., Yang, T. L., Wang, H. J., ... & Lin, S. J. (2006). Endotoxin induces toll-like receptor 4 expression in vascular smooth muscle cells via NADPH oxidase activation and mitogen-activated protein kinase signaling pathways. *Arteriosclerosis, thrombosis, and vascular biology*, *26*(12), 2630-2637.

Lin, M. E., Chen, T., Leaf, E. M., Speer, M. Y., & Giachelli, C. M. (2015). Runx2 Expression in Smooth Muscle Cells Is Required for Arterial Medial Calcification in Mice. *The American journal of pathology*.

Lin, S. Y., Li, M. J., & Cheng, W. T. (2007). FT-IR and Raman vibrational microspectroscopies used for spectral biodiagnosis of human tissues.*Journal of Spectroscopy*, *21*(1), 1-30.

Lisi, L., Navarra, P., Feinstein, D. L., & Dello Russo, C. (2011). The mTOR kinase inhibitor rapamycin decreases iNOS mRNA stability in astrocytes. *J Neuroinflammation*, *8*(1), 1.

Liu, H., Lu, Q., & Huang, K. (2010). Selenium suppressed hydrogen peroxide-induced vascular smooth muscle cells calcification through inhibiting oxidative stress and ERK activation. *Journal of cellular biochemistry*, *111*(6), 1556-1564.

Loidl, A., Claus, R., Ingolic, E., Deigner, H. P., & Hermetter, A. (2004). Role of ceramide in activation of stress-associated MAP kinases by minimally modified LDL in vascular smooth muscle cells. *Biochimica et Biophysica Acta (BBA)-Molecular Basis of Disease*, *1690*(2), 150-158.

Lu, K. C., Wu, C. C., Yen, J. F., & Liu, W. C. (2014). Vascular calcification and renal bone disorders. *The Scientific World Journal*, *2014*.

Luo, G., Ducy, P., McKee, M. D., Pinero, G. J., Loyer, E., Behringer, R. R., & Karsenty, G. (1997). Spontaneous calcification of arteries and cartilage in mice lacking matrix GLA protein.

McCullough, P. A., Agrawal, V., Danielewicz, E., & Abela, G. S. (2008). Accelerated atherosclerotic calcification and Mönckeberg's sclerosis: a continuum of advanced vascular pathology in chronic kidney disease.*Clinical Journal of the American Society of Nephrology*, *3*(6), 1585-1598.

McFadzean, I., & Gibson, A. (2002). The developing relationship between receptor-operated and store-operated calcium channels in smooth muscle.*British journal of pharmacology*, *135*(1), 1-13.

Meejoo, S., Maneeprakorn, W., & Winotai, P. (2006). Phase and thermal stability of nanocrystalline hydroxyapatite prepared via microwave heating.*Thermochimica Acta*, *447*(1), 115-120.

Meng, Z., Yan, C., Deng, Q., Gao, D. F., & Niu, X. L. (2013). Curcumin inhibits LPS-induced inflammation in rat vascular smooth muscle cells in vitro via ROS-relative TLR4-MAPK/NF-κB pathways. *Acta Pharmacologica Sinica*, *34*(7), 901-911.

Milkiewicz, M., Kelland, C., Colgan, S., & Haas, T. L. (2006). Nitric oxide and p38 MAP kinase mediate shear stress-dependent inhibition of MMP-2 production in microvascular endothelial cells. *Journal of cellular physiology*,*208*(1), 229-237.

Mizobuchi, M., Towler, D., & Slatopolsky, E. (2009). Vascular calcification: the killer of patients with chronic kidney disease. *Journal of the American Society of Nephrology*, *20*(7), 1453-1464.

Mobasherpour, I., Heshajin, M. S., Kazemzadeh, A., & Zakeri, M. (2007). Synthesis of nanocrystalline hydroxyapatite by using precipitation method.*Journal of Alloys and Compounds*, *430*(1), 330-333.

Moe, S. M., & Chen, N. X. (2008). Mechanisms of vascular calcification in chronic kidney disease. *Journal of the American Society of Nephrology*,*19*(2), 213-216.

Mohler, E. R., Gannon, F., Reynolds, C., Zimmerman, R., Keane, M. G., & Kaplan, F. S. (2001). Bone formation and inflammation in cardiac valves.*Circulation*, *103*(11), 1522-1528.

Moncada, S., Higgs, E. A., Hodson, H. F., Knowles, R. G., López-Jaramillo, P., McCall, T., ... & Schulz, R. (1991). The l-Arginine: Nitric Oxide Pathway.*Journal of Cardiovascular Pharmacology*, *17*, S1-hyhen.

Mosmann, T. (1983). Rapid colorimetric assay for cellular growth and survival: application to proliferation and cytotoxicity assays. *Journal of immunological methods*, *65*(1), 55-63.

Napoli, C., & Ignarro, L. J. (2001). Nitric oxide and atherosclerosis. *Nitric oxide*, *5*(2), 88-97.

Naschberger, E., Werner, T., Vicente, A., Guenzi, E., Topolt, K., Leubert, R., ... & Sturzl, M. (2004). Nuclear factor-kappaB motif and interferon-alpha-stimulated response element co-operate in the activation of guanylate-binding protein-1 expression by inflammatory cytokines in endothelial cells.*Biochem. J*, *379*, 409-420.

Nishikawa, T., Edelstein, D., Du, X. L., Yamagishi, S. I., Matsumura, T., Kaneda, Y., ... & Giardino, I. (2000). Normalizing mitochondrial superoxide production blocks three pathways of hyperglycaemic damage. *Nature*,*404*(6779), 787-790.

Nitta, K., Akiba, T., Uchida, K., Otsubo, S., Otsubo, Y., Takei, T., ... & Nihei, H. (2004). Left ventricular hypertrophy is associated with arterial stiffness and vascular calcification in hemodialysis patients. *Hypertension research*, *27*(1), 47-52.

Nordin, B. E. C. (1997). Calcium in health and disease. *Food nutrition and agriculture*, 13-26.

Norman, A. W. (2006). Vitamin D receptor: new assignments for an already busy receptor. *Endocrinology*, *147*(12), 5542-5548.

Norman, P. E., & Powell, J. T. (2014). Vitamin D and cardiovascular disease. *Circulation research*, *114*(2), 379-393.

Ohashi N, Matsumori A, Furukawa Y, Ono K, Okada M, Iwasaki A*, et al.* (2000). Role of p38 mitogen-activated protein kinase in neointimal hyperplasia after vascular injury. *Arteriosclerosis, thrombosis, and vascular biology* **20**(12)**:** 2521-2526.

Olsztyńska-Janus, S., Szymborska-Małek, K., Gąsior-Głogowska, M., Walski, T, Komorowska, M., Witkiewicz, W., ... & Szotek, S. (2012). Spectroscopic techniques in the study of human tissues and their components. Part I: IR spectroscopy. *Acta Bioeng Biomech*, *14*, 101-115.

O'N, K. (2005). Role of calcification inhibitors in the pathogenesis of vascular calcification in chronic kidney disease (CKD). *Kidney international*, *67*(6), 2295-2304.

Ortolani, F., Rigonat, L., Bonetti, A., Contin, M., Tubaro, F., Rattazzi, M., & Marchini, M. (2010). Pro-calcific responses by aortic valve interstitial cells in a novel in vitro model simulating dystrophic calcification. *Italian Journal of Anatomy and Embryology*, *115*(1/2), 135-139.

Otsuka, E., Hirano, K., Matsushita, S., Inoue, A., Hirose, S., Yamaguchi, A., & Hagiwara, H. (1998). Effects of nitric oxide from exogenous nitric oxide donors on osteoblastic metabolism. *European journal of pharmacology*,*349*(2), 345-350.

Otsuka, F., Sakakura, K., Yahagi, K., Joner, M., & Virmani, R. (2014). Has our understanding of calcification in human coronary atherosclerosis progressed?. *Arteriosclerosis, thrombosis, and vascular biology*, *34*(4), 724-736.

Pacher, P., Beckman, J. S., & Liaudet, L. (2007). Nitric oxide and peroxynitrite in health and disease. *Physiological reviews*, *87*(1), 315-424.

Pan, W., Quarles, L. D., Song, L. H., Yu, Y. H., Jiao, C., Tang, H. B., ... & Xiao, Z. S. (2005). Genistein stimulates the osteoblastic differentiation via NO/cGMP in bone marrow culture. *Journal of cellular biochemistry*, *94*(2), 307-316.

Pan, W. Q., Ruan, X., Wheeler, D. C., Norman, J., Moorhead, J. F., Varghese, Z., ... & Unwin, R. (2007). FGF23 inhibits inflammation-induced calcification in human vascular smooth muscle cells.

Panda, K., Ghosh, S., & Stuehr, D. J. (2001). Calmodulin activates intersubunit electron transfer in the neuronal nitric-oxide synthase dimer.*Journal of biological chemistry*, *276*(26), 23349-23356.

Panizo, S., Cardus, A., Encinas, M., Parisi, E., Valcheva, P., López-Ongil, S., ... & Valdivielso, J. M. (2009). RANKL increases vascular smooth muscle cell calcification through a RANK-BMP4–dependent pathway.*Circulation research*, *104*(9), 1041-1048.

Pardali, E., & Ten Dijke, P. (2012). TGFβ signaling and cardiovascular diseases. *International journal of biological sciences*, *8*(2), 195.

Parikh, S. J., & Chorover, J. (2006). ATR-FTIR spectroscopy reveals bond formation during bacterial adhesion to iron oxide. *Langmuir*, *22*(20), 8492-8500.

Patidar, A., Singh, D. K., Winocour, P., Farrington, K., & Baydoun, A. R. (2013). Human uraemic serum displays calcific potential in vitro that increases with advancing chronic kidney disease. *Clinical Science*, *125*(5), 237-245.

Pereira, L., Lee, S. Y., Gayraud, B., Andrikopoulos, K., Shapiro, S. D., Bunton, T., ... & Ramirez, F. (1999). Pathogenetic sequence for aneurysm revealed in mice underexpressing fibrillin-1. *Proceedings of the National Academy of Sciences*, *96*(7), 3819-3823.

Poderoso, J. J., Carreras, M. C., Lisdero, C., Riobó, N., Schöpfer, F., & Boveris, A. (1996). Nitric oxide inhibits electron transfer and increases superoxide radical production in rat heart mitochondria and submitochondrial particles. *Archives of biochemistry and biophysics*, *328*(1), 85-92.

Poderoso, J. J., Peralta, J. G., Lisdero, C. L., Carreras, M. C., Radisic, M., Schöpfer, F., ... & Boveris, A. (1998). Nitric oxide regulates oxygen uptake and hydrogen peroxide release by the isolated beating rat heart. *American Journal of Physiology-Cell Physiology*, *274*(1), C112-C119.

Persy, V. P., & McKee, M. D. (2011). Prevention of vascular calcification: is pyrophosphate therapy a solution&quest. *Kidney international*, *79*(5), 490-493.

Price, P. A., Faus, S. A., & Williamson, M. K. (2001). Bisphosphonates alendronate and ibandronate inhibit artery calcification at doses comparable to those that inhibit bone resorption. *Arteriosclerosis, thrombosis, and vascular biology*, *21*(5), 817-824.

Proudfoot, D., & Shanahan, C. M. (2001). Biology of calcification in vascular cells: intima versus media. *Herz*, *26*(4), 245-251.

Proudfoot, D., Skepper, J. N., Shanahan, C. M., & Weissberg, P. L. (1998). Calcification of human vascular cells in vitro is correlated with high levels of matrix Gla protein and low levels of osteopontin expression. *Arteriosclerosis, thrombosis, and vascular biology*, *18*(3), 379-388.

Qiu, L. Q., Sinniah, R., Stephen, I., & Hsu, H. (2004). Coupled induction of iNOS and p53 upregulation in renal resident cells may be linked with apoptotic activity in the pathogenesis of progressive IgA nephropathy.*Journal of the American Society of Nephrology*, *15*(8), 2066-2078.

Raghavan, S. A., & Dikshit, M. (2001). L-citrulline mediated relaxation in the control and lipopolysaccharide-treated rat aortic rings. *European journal of pharmacology*, *431*(1), 61-69.

Rajamannan, N. M., Subramaniam, M., Rickard, D., Stock, S. R., Donovan, J., Springett, M., ... & Spelsberg, T. (2003). Human aortic valve calcification is associated with an osteoblast phenotype. *Circulation*, *107*(17), 2181-2184.

Raynaud, S., Champion, E., Bernache-Assollant, D., & Thomas, P. (2002). Calcium phosphate apatites with variable Ca/P atomic ratio I. Synthesis, characterisation and thermal stability of powders. *Biomaterials*, *23*(4), 1065-1072.

Rees, S. G., Wassell, D. T. H., Shellis, R. P., & Embery, G. (2004). Effect of serum albumin on glycosaminoglycan inhibition of hydroxyapatite formation. *Biomaterials*, *25*(6), 971-977.

Reynolds, J. L., Joannides, A. J., Skepper, J. N., McNair, R., Schurgers, L. J., Proudfoot, D., ... & Shanahan, C. M. (2004). Human vascular smooth muscle cells undergo vesicle-mediated calcification in response to changes in extracellular calcium and phosphate concentrations: a potential mechanism for accelerated vascular calcification in ESRD. *Journal of the American Society of Nephrology*, *15*(11), 2857-2867.

Richards, J., El-Hamamsy, I., Chen, S., Sarang, Z., Sarathchandra, P., Yacoub, M. H., ... & Butcher, J. T. (2013). Side-specific endothelial-dependent regulation of aortic valve calcification: interplay of hemodynamics and nitric oxide signaling. *The American journal of pathology*, *182*(5), 1922-1931.

Riemer, E. C. (2003). Inflammatory Atherosclerosis: Characteristics of the Injurious Agent. *Archives of Pathology & Laboratory Medicine*, *127*(11), 1533.

Rodríguez-Peña, A. B., Grande, M. T., Eleno, N., Arévalo, M., Guerrero, C., Santos, E., & López-Novoa, J. M. (2008). Activation of Erk1/2 and Akt following unilateral ureteral obstruction. *Kidney international*, *74*(2), 196-209.

Roskoski, R. (2012). ERK1/2 MAP kinases: structure, function, and regulation. *Pharmacological research*, *66*(2), 105-143.

Rzucidlo, E. M., Martin, K. A., & Powell, R. J. (2007). Regulation of vascular smooth muscle cell differentiation. *Journal of Vascular Surgery*, *45*(6), A25-A32.

Sabbatini, M., Pisani, A., Uccello, F., Fuiano, G., Alfieri, R., Cesaro, A., ... & Andreucci, V. E. (2003). Arginase inhibition slows the progression of renal failure in rats with renal ablation. *American Journal of Physiology-Renal Physiology*, *284*(4), F680-F687.

Sage, A. P., Tintut, Y., & Demer, L. L. (2010). Regulatory mechanisms in vascular calcification. *Nature Reviews Cardiology*, *7*(9), 528-536.

Saifan, C. (2013 a). Calciphylaxis: case report. *Reactions*, *1470*, 41-42.

Saifan, C., Saad, M., El-Charabaty, E., & El-Sayegh, S. (2013 b). Warfarin-induced calciphylaxis: a case report and review of literature. *International journal of general medicine*, *6*, 665.

Sano, M., Fujita, H., Morita, I., Uematsu, H., & Murota, S. I. (1999). Vitamin K2 (Menatetrenone) Induces iNOS in Bovine Vascular Smooth Muscle Cells. No Relationship between Nitric Oxide Production and. GAMMA.-Carboxylation. *Journal of nutritional science and vitaminology*,*45*(6), 711-723.

Sarig, S., Weiss, T. A., Katz, I., Kahana, F., Azoury, R., Okon, E., & Kruth, H. S. (1994). Detection of cholesterol associated with calcium mineral using confocal fluorescence microscopy. *Laboratory investigation; a journal of technical methods and pathology*, *71*(5), 782-787.

Satou, Y., Al-Shawafi, H. A., Sultana, S., Makita, S., Sohda, M., & Oda, K. (2012). Disulfide bonds are critical for tissue-nonspecific alkaline phosphatase function revealed by analysis of mutant proteins bearing a C 201-Y or C 489-S substitution associated with severe hypophosphatasia.*Biochimica et Biophysica Acta (BBA)-Molecular Basis of Disease*, *1822*(4), 581-588.

Schiffrin, E. L., Lipman, M. L., & Mann, J. F. (2007). Chronic kidney disease effects on the cardiovascular system. *Circulation*, *116*(1), 85-97.

Schmidt, R. J., & Baylis, C. (2000). Total nitric oxide production is low in patients with chronic renal disease1. *Kidney international*, *58*(3), 1261-1266.

Schmidt, R. J., Yokota, S., Tracy, T. S., Sorkin, M. I., & Baylis, C. (1999). Nitric oxide production is low in end-stage renal disease patients on peritoneal dialysis. *American Journal of Physiology-Renal Physiology*,*276*(5), F794-F797.

Schurgers, E., Kelchtermans, H., Mitera, T., Geboes, L., & Matthys, P. (2010). Discrepancy between the in vitro and in vivo effects of murine mesenchymal stem cells on T-cell proliferation and collagen-induced arthritis. *Arthritis Research and Therapy*, *12*(1), R31.

Schutte, R., Huisman, H. W., Malan, L., Van Rooyen, J. M., Smith, W., Glyn, M. C. P., ... & Schutte, A. E. (2013). Alkaline phosphatase and arterial structure and function in hypertensive African men: the SABPA study.*International journal of cardiology*, *167*(5), 1995-2001.

Segersten, U., Correa, P., Hewison, M., Hellman, P., Dralle, H., Carling, T., ... & Westin, G. (2002). 25-hydroxyvitamin D3-1α-hydroxylase expression in normal and pathological parathyroid glands. *The Journal of Clinical Endocrinology & Metabolism*, *87*(6), 2967-2972.

Shanahan, C. M., Cary, N. R., Metcalfe, J. C., & Weissberg, P. L. (1994). High expression of genes for calcification-regulating proteins in human atherosclerotic plaques. *Journal of Clinical Investigation*, *93*(6), 2393.

Shanahan, C. M. (2007). Inflammation Ushers in Calcification A Cycle of Damage and Protection?. *Circulation*, *116*(24), 2782-2785.

Shanahan, C. M., Crouthamel, M. H., Kapustin, A., & Giachelli, C. M. (2011). Arterial calcification in chronic kidney disease: key roles for calcium and phosphate. *Circulation research*, *109*(6), 697-711.

Shanahan, C. M., Proudfoot, D., Farzaneh-Far, A., & Weissberg, P. L. (1998). The role of Gla proteins in vascular calcification. *Critical Reviews™ in Eukaryotic Gene Expression*, *8*(3-4).

Shroff, R. C., & Shanahan, C. M. (2007, March). Vascular calcification in patients with kidney disease: the vascular biology of calcification. In *Seminars in dialysis* (Vol. 20, No. 2, pp. 103-109). Blackwell Publishing Ltd.

Shao, J. S., Aly, Z. A., Lai, C. F., Cheng, S. L., Cai, J. U. N., Huang, E., ... & Towler, D. A. (2007). Vascular Bmp–Msx2–Wnt signaling and oxidative stress in arterial calcification. *Annals of the New York Academy of Sciences*, *1117*(1), 40-50.

Sharpe, M. A., & Cooper, C. E. (1998). Interaction of peroxynitrite with mitochondrial cytochrome oxidase catalytic production of nitric oxide and irreversible inhibition of enzyme activity. *Journal of Biological Chemistry*,*273*(47), 30961-30972.

Shin, M. Y., & Kwun, I. S. (2014). Zinc Restored the Decreased Vascular Smooth Muscle Cell Viability under Atherosclerotic Calcification Conditions.*Preventive nutrition and food science*, *19*(4), 363.

Shioi, A., Katagi, M., Okuno, Y., Mori, K., Jono, S., Koyama, H., & Nishizawa, Y. (2002). Induction of bone-type alkaline Phosphatase in human vascular smooth muscle cells roles of tumor necrosis factor-α and oncostatin M derived from macrophages. *Circulation research*, *91*(1), 9-16.

Shioi, A., Mori, K., Jono, S., Wakikawa, T., Hiura, Y., Koyama, H., ... & Morii, H. (2000). Mechanism of atherosclerotic calcification. *Zeitschrift für Kardiologie*, *89*(2), S075-S079.

Shioi, A., Nishizawa, Y., Jono, S., Koyama, H., Hosoi, M., & Morii, H. (1995). β-Glycerophosphate accelerates calcification in cultured bovine vascular smooth muscle cells. *Arteriosclerosis, thrombosis, and vascular biology*, *15*(11), 2003-2009.

Schweizer, M., & Richter, C. (1994). Nitric oxide potently and reversibly deenergizes mitochondria at low oxygen tension. *Biochemical and biophysical research communications*, *204*(1), 169-175.

Simon, A., & Levenson, J. (1993). Early detection of subclinical atherosclerosis in asymptomatic subjects at high risk for cardiovascular disease. *Clinical and Experimental Hypertension*, *15*(6), 1069-1076.

Singh, D. K., Winocour, P., Summerhayes, B., Kaniyur, S., Viljoen, A., Sivakumar, G., & Farrington, K. (2012). Prevalence and progression of peripheral vascular calcification in type 2 diabetes subjects with preserved kidney function. *Diabetes research and clinical practice*, *97*(1), 158-165.

Sklepkiewicz, P., Schermuly, R. T., Tian, X., Ghofrani, H. A., Weissmann, N., Sedding, D., ... & Pullamsetti, S. S. (2011). Glycogen synthase kinase 3beta contributes to proliferation of arterial smooth muscle cells in pulmonary hypertension. *PLoS One*, *6*(4), e18883-e18883.

Smith, P. K., Krohn, R. I., Hermanson, G. T., Mallia, A. K., Gartner, F. H., Provenzano, M., ... & Klenk, D. C. (1985). Measurement of protein using bicinchoninic acid. *Analytical biochemistry*, *150*(1), 76-85.

Somjen, D., Weisman, Y., Kohen, F., Gayer, B., Limor, R., Sharon, O., & Stern, N. (2005). 25-Hydroxyvitamin D3-1α-hydroxylase is expressed in human vascular smooth muscle cells and is upregulated by parathyroid hormone and estrogenic compounds. *Circulation*, *111*(13), 1666-1671.

Stabile, E., Zhou, Y. F., Saji, M., Castagna, M., Shou, M., Kinnaird, T. D., ... & Fuchs, S. (2003). Akt controls vascular smooth muscle cell proliferation in vitro and in vivo by delaying G1/S exit. *Circulation research*, *93*(11), 1059-1065.

Steitz, S. A., Speer, M. Y., Curinga, G., Yang, H. Y., Haynes, P., Aebersold, R., ... & Giachelli, C. M. (2001). Smooth muscle cell phenotypic transition associated with calcification upregulation of cbfa1 and downregulation of smooth muscle lineage markers. *Circulation research*,*89*(12), 1147-1154.

Stephens, A. S., & Morrison, N. A. (2014). Novel Target Genes of RUNX2 Transcription Factor and 1, 25-Dihydroxyvitamin D3. *Journal of cellular biochemistry*, *115*(9), 1594-1608.

Stoffels, K., Overbergh, L., Giulietti, A., Verlinden, L., Bouillon, R., & Mathieu, C. (2006). Immune Regulation of 25-Hydroxyvitamin-D3-1α-Hydroxylase in Human Monocytes. *Journal of Bone and Mineral Research*,*21*(1), 37-47.

Stuehr, D. J., & Nathan, C. F. (1989). Nitric oxide. A macrophage product responsible for cytostasis and respiratory inhibition in tumor target cells. *The Journal of experimental medicine*, *169*(5), 1543-1555.

Su, F., Huang, H., Akieda, K., Occhipinti, G., Donadello, K., Piagnerelli, M., ... & Vincent, J. L. (2010). Effects of a selective iNOS inhibitor versus norepinephrine in the treatment of septic shock. *Shock*, *34*(3), 243-249.

Sun, Y., Byon, C. H., Yuan, K., Chen, J., Mao, X., Heath, J. M., ... & Chen, Y. (2012). Smooth muscle cell–specific Runx2 deficiency inhibits vascular calcification. *Circulation research*, *111*(5), 543-552.

Tang, Y., Xu, Q., Peng, H., Liu, Z., Yang, T., Yu, Z., ... & Shi, R. (2015). The role of vascular peroxidase 1 in ox-LDL-induced vascular smooth muscle cell calcification. *Atherosclerosis*, *243*(2), 357-363.

Tintut, Y., Patel, J., Parhami, F., & Demer, L. L. (2000). Tumor necrosis factor-α promotes in vitro calcification of vascular cells via the cAMP pathway. *Circulation*, *102*(21), 2636-2642.

Tintut, Y., Patel, J., Territo, M., Saini, T., Parhami, F., & Demer, L. L. (2002). Monocyte/macrophage regulation of vascular calcification in vitro. *Circulation*, *105*(5), 650-655.

Trion, A., Schutte-Bart, C., Bax, W. H., Jukema, J. W., & van der Laarse, A. (2008). Modulation of calcification of vascular smooth muscle cells in culture by calcium antagonists, statins, and their combination. *Molecular and cellular biochemistry*, *308*(1-2), 25-33.

Trion, A., & van der Laarse, A. (2004). Vascular smooth muscle cells and calcification in atherosclerosis. *American heart journal*, *147*(5), 808-814.

Tsutsumi, S., Zhang, X., Takata, K., Takahashi, K., Karas, R. H., Kurachi, H., & Mendelsohn, M. E. (2008). Differential regulation of the inducible nitric oxide synthase gene by estrogen receptors 1 and 2. *Journal of Endocrinology*, *199*(2), 267-273.

Ucla, C., Roux-Lombard, P., Fey, S., Dayer, J. M., & Mach, B. (1990). Interferon gamma drastically modifies the regulation of interleukin 1 genes by endotoxin in U937 cells. *Journal of Clinical Investigation*, *85*(1), 185.

Valdivielso, J. M. (2011). Vascular calcification: types and mechanisms. *Nefrologia*, *31*(2), 142-147.

Vallance, P., & Charles, I. (1998). Nitric oxide in sepsis: of mice and men. *Sepsis*, *1*(2), 93-100.

van der Wal, A. C., & Becker, A. E. (1999). Atherosclerotic plaque rupture–pathologic basis of plaque stability and instability. *Cardiovascular research*, *41*(2), 334-344.

Víteček, J., Lojek, A., Valacchi, G., & Kubala, L. (2012). Arginine-based inhibitors of nitric oxide synthase: therapeutic potential and challenges. *Mediators of inflammation*, *2012*.

Voccoli, V., Tonazzini, I., Signore, G., Caleo, M., & Cecchini, M. (2014). Role of extracellular calcium and mitochondrial oxygen species in psychosine-induced oligodendrocyte cell death. *Cell death & disease*, *5*(11), e1529.

Walsh, M. C., & Choi, Y. (2014). Biology of the RANKL–RANK–OPG system in immunity, bone, and beyond. *Frontiers in immunology*, *5*.

Wang, R. N., Green, J., Wang, Z., Deng, Y., Qiao, M., Peabody, M., ... & Idowu, O. (2014). Bone Morphogenetic Protein (BMP) signaling in development and human diseases. *Genes & diseases*, *1*(1), 87-105.

Wagner, L., Klein, J. D., Sands, J. M., & Baylis, C. (2002). Urea transporters are distributed in endothelial cells and mediate inhibition of L-arginine transport. *American Journal of Physiology-Renal Physiology*, *283*(3), F578-F582.

Welter, R., Yu, L., & Yu, C. A. (1996). The effects of nitric oxide on electron transport complexes. *Archives of biochemistry and biophysics*, *331*(1), 9-14.

Wever, R. M., Lüscher, T. F., Cosentino, F., & Rabelink, T. J. (1998). Atherosclerosis and the two faces of endothelial nitric oxide synthase.*Circulation*, *97*(1), 108-112.

Wileman, S. M., Mann, G. E., & Baydoun, A. R. (1995). Induction of L-arginine transport and nitric oxide synthase in vascular smooth muscle cells: synergistic actions of pro-inflammatory cytokines and bacterial lipopolysaccharide. *British journal of pharmacology*, *116*(8), 3243.

Wileman, S. M., Mann, G. E., Pearson, J. D., & Baydoun, A. R. (2003). Role of L-citrulline transport in nitric oxide synthesis in rat aortic smooth muscle cells activated with LPS and interferon-γ. *British journal of pharmacology*,*140*(1), 179-185.

Willerson, J. T., & Ridker, P. M. (2004). Inflammation as a cardiovascular risk factor. *Circulation*, *109*(21 suppl 1), II-2.

Wirrig, E. E., & Yutzey, K. E. (2014). Conserved transcriptional regulatory mechanisms in aortic valve development and disease. *Arteriosclerosis, thrombosis, and vascular biology*, *34*(4), 737-741.

Wong, K. K., Thavornpattanapong, P., Cheung, S. C., Sun, Z., & Tu, J. (2012). Effect of calcification on the mechanical stability of plaque based on a three-dimensional carotid bifurcation model. *BMC cardiovascular disorders*,*12*(1), 7.

Xiao, S., Wagner, L., Mahaney, J., & Baylis, C. (2001). Uremic levels of urea inhibit L-arginine transport in cultured endothelial cells. *American Journal of Physiology-Renal Physiology*, *280*(6), F989-F995.

Xia, Z. Y., Hu, Y., Xie, P. L., Tang, S. Y., Luo, X. H., Liao, E. Y., ... & Xie, H. (2015). Runx2/miR-3960/miR-2861 positive feedback loop is responsible for osteogenic transdifferentiation of vascular smooth muscle cells. *BioMed research*

international, 2015.

Yamakawa, T., Eguchi, S., Matsumoto, T., Yamakawa, Y., Numaguchi, K., Miyata, I., ... & Inagami, T. (1999). Intracellular Signaling in Rat Cultured Vascular Smooth Muscle Cells: Roles of Nuclear Factor-κB and p38 Mitogen-Activated Protein Kinase on Tumor Necrosis Factor-α Production 1.*Endocrinology*, *140*(8), 3562-3572.

Yang, C. M., Chiu, C. T., Wang, C. C., Chien, C. S., Hsiao, L. D., Lin, C. C., ... & Pan, S. L. (2000). Activation of mitogen-activated protein kinase by oxidized low-density lipoprotein in canine cultured vascular smooth muscle cells. *Cellular signalling*, *12*(4), 205-214.

Yang, X., Fullerton, D. A., Su, X., Ao, L., & Meng, X. (2009). Pro-osteogenic phenotype of human aortic valve interstitial cells is associated with higher levels of Toll-like receptors 2 and 4 and enhanced expression of bone morphogenetic protein 2. *Journal of the American College of Cardiology*,*53*(6), 491-500.

Yasuhara, R., Suzawa, T., Miyamoto, Y., Wang, X., Takami, M., Yamada, A., & Kamijo, R. (2007). Nitric oxide in pulp cell growth, differentiation, and mineralization. *Journal of dental research*, *86*(2), 163-168.

Zaragoza, C., López-Rivera, E., García-Rama, C., Saura, M., Martínez-Ruíz, A., Lizarbe, T. R., & Lamas, S. (2006). Cbfa-1 mediates nitric oxide regulation of MMP-13 in osteoblasts. *Journal of cell science*, *119*(9), 1896-1902.

Zebger-Gong, H., Müller, D., Diercke, M., Haffner, D., Hocher, B., Verberckmoes, S., ... & Querfeld, U. (2011). 1, 25-Dihydroxyvitamin D3-induced aortic calcifications in experimental uremia: up-regulation of osteoblast markers, calcium-transporting proteins and osterix. *Journal of hypertension*, *29*(2), 339-348.

Zehnder, D., Bland, R., Chana, R. S., Wheeler, D. C., Howie, A. J., Williams, M. C., ... & Hewison, M. (2002). Synthesis of 1, 25-dihydroxyvitamin D3 by human endothelial cells is regulated by inflammatory cytokines: a novel autocrine determinant of vascular cell adhesion. *Journal of the American Society of Nephrology*, *13*(3), 621-629.

Zelzer, E., & Olsen, B. R. (2003). The genetic basis for skeletal diseases.*Nature*, *423*(6937), 343-348.

Zeng, Q., Song, R., Ao, L., Xu, D., Venardos, N., Fullerton, D. A., & Meng, X. (2014). Augmented Osteogenic Responses in Human Aortic Valve Cells Exposed to oxLDL and TLR4 Agonist: A Mechanistic Role of Notch1 and NF-κB Interaction.

Zhang, J., Zheng, B., Zhou, P. P., Zhang, R. N., He, M., Yang, Z., & Wen, J. K. (2014). Vascular calcification is coupled with phenotypic conversion of vascular smooth muscle cells through Klf5-mediated transactivation of the Runx2 promoter. *Bioscience reports*, *34*(6), e00148.

Zhang, C., Hein, T. W., Wang, W., Miller, M. W., Fossum, T. W., McDonald, M. M., ... & Kuo, L. (2004). Upregulation of vascular arginase in hypertension decreases nitric oxide–mediated dilation of coronary arterioles. *Hypertension*,*44*(6), 935-943.

Zhao, Y., Song, T., Wang, W., Wang, J., He, J., Wu, N., ... & Luo, J. (2012). P38 and ERK1/2 MAPKs act in opposition to regulate BMP9-induced osteogenic differentiation of mesenchymal progenitor cells. *PLoS One*, *7*(8), e43383.

Zhou, G., Zheng, Q., Engin, F., Munivez, E., Chen, Y., Sebald, E., ... & Lee, B. (2006). Dominance of SOX9 function over RUNX2 during skeletogenesis.*Proceedings of the National Academy of Sciences*, *103*(50), 19004-19009.

Zhu, Y., Farrehi, P. M., & Fay, W. P. (2001). Plasminogen activator inhibitor type 1 enhances neointima formation after oxidative vascular injury in atherosclerosis-prone mice. *Circulation*, *103*(25), 3105-3110.

APPENDIX

Table: Products name and supplier

Product name	Supplier
Membrane filter Immobilon-P transfer membranes 0.45µm pore size 265mm x 3.75 m Millipore	Fisher Scientific
Tris(hydroxymethyl) methylamine 'Tris buffer' 99.8%	Fisher Scientific
Tween 20	Fisher Scientific
p-Coumaric acid-10G	Sigma-Aldrich
Biotinylated Protein Ladder Detection Pack	cell signaling
Kodak® processing chemicals for autoradiography films GBX developer/replenisher	Sigma-Aldrich
BCA protein Assay Reagent B, Thermo Scientific Pierce	Fisher Scientific
D-PBS Dulbecco's Phosphate Buffered Saline (10X) liquid	Fisher scientific
BCA protein Assay Reagent A, Thermo Scientific Pierce	Fisher scientific
Hyperfilm ECL 18x24cm GE Healthcare	Fisher scientific
Glycine	Fisher scientific
Tris (hydroxymethyl) methylamine	Fisher scientific
Sodium dodecyl sulfate - 1KG	Sigma-Aldrich
Hyperfilm ECL 18x24cm GE Healthcare	Fisher scientific
450ML PROTOGEL 30% SOLUTION AT 37.5:1 RATIO Acrylamide:methylene Bis Acrylamide solution, National Diagnostics	Fisher scientific
100 ML Penicillin-streptomycin solution	Fisher scientific
1 Kg Tris (hydroxymethyl) methylamine, Biological buffer	Sigma-Aldrich
Ammonium persulphate	Acros Organics
Anti-Rabbit IgG (whole molecule)–Peroxidase antibody produced in goat	Sigma Aldrich
Biotinylated protein ladder detection pack	New England Biolabs
1 Kg Glycine	Fisher scientific

Table: Ingredients of DEME

Ingredients (Amino acid, vitamins, inorganic salts and other components)	Molecular weight	Concentration (g/L)	(mM)
Glycine	75	0.03	0.4
L-Arginine hydrochloride	211.0	0.084	0.398
L-Cystine 2HCl	313.0	0.063	0.201
L-Glutamine	146.0	0.58	3.972
L-Histidine hydrochloride-H2O	210.0	0.042	0.2
L-Isoleucine	131.0	0.105	0.802
L-Leucine	131.0	0.105	0.802
L-Lysine hydrochloride	183	0.146	0.798
L-Methionine	149	0.03	0.201
L-Phenylalanine	165	0.066	0.4
L-Serine	105	0.042	0.4
L-Threonine	119	0.095	0.798
L-Tryptophan	204	0.016	0.078
L-Tyrosine	181	0.072	0.398
L-Valine	117	0.094	0.803
Choline chloride	140	0.004	0.0286
D-Calcium pantothenate	477	0.004	0.008
Folic Acid	441	0.004	0.009
Niacinamide	122	0.004	0.033
Pyridoxine hydrochloride	206	0.004	0.019
Riboflavin	376	0.0004	0.001

Thiamine hydrochloride	337	0.004	0.012
i-Inositol	180	0.0072	0.04
Magnesium Sulfate (MgSO4-7H2O)	246	0.2	0.813
Potassium Chloride (KCl)	75	0.4	5.333
Sodium Bicarbonate (NaHCO3)	84	3.7	44.047
Sodium Chloride (NaCl)	58	6.4	110.345
Sodium Phosphate monobasic (NaH2PO4-2H2O)	154	0.141	0.916
D-Glucose (Dextrose)	180	0.1	5.555
Phenol Red	376.4	0.015	0.0399
Sodium Pyruvate	110	0.11	1